NeuroRegulation

The Official Journal of

ISNR
INTERNATIONAL SOCIETY FOR NEUROREGULATION & RESEARCH

Volume 13, Number 1, 2026

NeuroRegulation

NeuroRegulation (ISSN: 2373-0587) is published quarterly by the International Society for Neuroregulation and Research (ISNR), 2146 Roswell Road, Suite 108, PMB 736, Marietta, GA 30062, USA.

Aim and Scope

NeuroRegulation is a peer-reviewed journal providing an integrated, multidisciplinary perspective on clinically relevant research, treatment, and public policy for neurofeedback, neuroregulation, and neurotherapy. The journal reviews important findings in clinical neurotherapy, biofeedback, and electroencephalography for use in assessing baselines and outcomes of various procedures. The journal draws from expertise inside and outside of the International Society for Neuroregulation and Research to deliver material which integrates the diverse aspects of the field. Instructions for submissions and Author Guidelines can be found on the journal website (http://www.neuroregulation.org).

NeuroRegulation

ISNR INTERNATIONAL SOCIETY FOR NEUROREGULATION & RESEARCH

Volume 13, Number 1

2026

Contents

RESEARCH PAPERS

PERSPECTIVES

CLINICAL CORNER

TECHNICAL NOTES

NeuroRegulation

ISNR INTERNATIONAL SOCIETY FOR NEUROREGULATION & RESEARCH

The Effectiveness of Neurofeedback Training on Cognitive Function Improvement and Quantitative Electroencephalography Features in Poststroke Cognitive Impairment

Rini Nindela[*]*, Yohanes Febrianto, Yusril Yusril, Muhammad H. Haddani, Sri Handayani, Dya Anggraeni, and Mgs. Irsan Saleh*

Sriwijaya University, Mohammad Hoesin Hospital, Palembang, Indonesia

Abstract

Background. Poststroke cognitive impairment (PSCI) involves cognitive deficits emerging within 3 months after stroke. Quantitative EEG (qEEG) in PSCI typically shows changes in relative power, delta-alpha ratio, and peak alpha frequency. Neurofeedback training (NFT) is a promising intervention to improve cognitive function and qEEG patterns, though findings remain inconsistent. Nonetheless, even brief NFT interventions may yield meaningful benefits. **Methods.** This study assessed the effectiveness of five individualized qEEG-guided NFT sessions (30 min each) in 24 PSCI patients, focusing on changes in MoCA-INA scores and qEEG parameters. **Results.** NFT significantly improved MoCA-INA scores ($Z = -4.106$, $p < .001$, effect size = 0.839), particularly in visuospatial/executive and delayed recall domains, with sustained effects 1 month later. QEEG analysis revealed increased temporal alpha ($t = -1.875$, $p = .037$, effect size = 0.23) and parietal beta relative power ($t = -1.827$, $p = .040$, effect size = 0.11). Greater cognitive gains were observed in patients aged ≤60 years. **Conclusion.** These findings support the clinical utility of short-term, qEEG-guided NFT in improving cognitive outcomes and modulating neural activity in PSCI patients. The sustained benefits observed suggest potential for long-term therapeutic impact.

Keywords: Poststroke cognitive impairment; neurofeedback training; quantitative electroencephalography; MoCA-INA

Citation: Nindela, R., Febrianto, Y., Yusril, Y., Haddani, M. H., Handayani, S., Anggraeni, D., & Saleh, M. I. (2026). The effectiveness of neurofeedback training on cognitive function improvement and quantitative electroencephalography features in poststroke cognitive impairment. *NeuroRegulation, 13*(1), 2–19. https://doi.org/10.15540/nr.13.1.2

***Address correspondence to**: Rini Nindela, Jendral Sudirman St. KM 3.5, Palembang, 30126, Indonesia. Email: rini_nindela@unsri.ac.id

Edited by:
Rex L. Cannon, PhD, Currents, Knoxville, Tennessee, USA

Reviewed by:
Rex L. Cannon, PhD, Currents, Knoxville, Tennessee, USA
Randall Lyle, PhD, Mount Mercy University, Cedar Rapids, Iowa, USA

Introduction

Poststroke cognitive impairment (PSCI) is defined as cognitive deficits occurring within the first 3 months after a stroke, unrelated to other medical conditions such as metabolic, endocrine, vasculitis, or depressive disorders. PSCI can be classified into cognitive impairment no dementia (CIND) and poststroke dementia (PSD; Tugasworo et al., 2023). This condition is often underrecognized and overshadowed by the more prominent motor deficits (McDonald et al., 2019). Indonesia Stroke Registry Data showed that 60.59% of stroke patients experienced cognitive impairment in 2013 (Ong et al., 2015).

Quantitative electroencephalography (qEEG) is a low-cost, noninvasive tool with high temporal resolution for assessing brain function, particularly in dementia. It directly measures functional brain status (Hadiyoso et al., 2022; Petrovic et al., 2017). Spectral power analysis has demonstrated that PSCI patients exhibit increased delta relative power, decreased alpha and beta power, globally elevated theta activity, increased frontal delta/alpha ratio (DAR), and delta+theta/alpha+beta ratio (DTABR),

as well as a reduction in peak alpha frequency (PAF), a known indicator of cognitive function (Babiloni et al., 2021; Hadiyoso et al., 2022).

Currently, no traditional cognitive rehabilitation method is recommended as the mainstay therapy with proven effectiveness in improving cognitive function poststroke (Merriman et al., 2019). Limitations of conventional rehabilitation include repetitive tasks and evaluations, reliance on clear patient responses, dependence on complex verbal instructions, and the considerable cognitive effort required. An alternative approach involves adaptive use of brain-computer interface (BCI) technologies. A prominent BCI modality for poststroke cognitive rehabilitation is electroencephalography-based neurofeedback training (EEG-NFT; Kober et al., 2015).

NFT aims to enhance cognitive function through mechanisms such as implicit learning, operant conditioning, self-regulation, and neuroplasticity. It trains individuals to modulate their brain's electrical activity, either by enhancing or inhibiting specific patterns. This process can induce long-term neural changes that support the recovery or enhancement of neurocognitive, emotional, and overall brain function. NFT is also believed to help prevent progression from mild cognitive impairment (MCI) to dementia and may accelerate or enable functional recovery previously thought unattainable (Ali et al., 2020; Tosti et al., 2024).

EEG-NFT is considered a novel and off-label therapeutic approach for cognitive disorders, particularly in stroke patients, and remains understudied. Most studies have reported cognitive improvements following NFT, but these findings are not always consistent or statistically significant. Interestingly, the number and frequency of sessions do not appear to significantly influence EEG-NFT effectiveness (Tosti et al., 2024; Vilou et al., 2023).

Anggraeni et al. (2024) reported a 2.63-point improvement in the Montreal Cognitive Assessment-Indonesian Version (MoCA-INA) scores (p = .019, effect size = −0.828) after 10 sessions of NFT in eight PSCI-ND patients using individualized qEEG protocols, though without significant domain-specific changes. Hohenfeld et al. (2017) found that three MRI-based NFT sessions in healthy individuals led to a 1.187-point increase in MoCA scores (p = .002), whereas Alzheimer's disease patients in the same study exhibited a decline. Jang et al. (2017) conducted an NFT study on MCI patients and observed significant improvements in the Montreal Cognitive Assessment -Korean Version (MoCA-K) scores after both 8 and 16 sessions (p = .042). Marlats et al. (2020) demonstrated improvements in MoCA scores following 3 to 20 sessions of NFT, especially in executive and memory domains. Lavy et al. (2018) reported sustained memory function improvements 1-month postintervention, although Marlats et al. (2020) noted that MoCA scores returned to baseline after 1 month. QEEG improvements following NFT have also been documented, including increased power in targeted frequency bands, enhanced peak alpha frequency, and shifts from slower (theta and delta) to faster (alpha and beta) brain waves, which correlate with cognitive gains (Andrade et al., 2022; Hohenfeld et al., 2017; Wigton & Krigbaum, 2015).

Given the inconsistent findings regarding EEG-NFT impact on cognitive function, the limited evidence on its effectiveness in PSCI patients, particularly over the long term, and the limitations of conventional rehabilitation, further research is warranted to explore NFT as a rehabilitative option for PSCI. Considering the high prevalence and significant burden of PSCI on patients and their families, this study represents the first in Indonesia to assess the efficacy of NFT in improving cognitive function and modifying qEEG parameters both posttreatment and over a longer follow-up period.

Methods

Study Design and Setting

This study employed an analytical quasi-experimental design with a one-group pretest-posttest approach. The research was conducted at the Memory and Neurofeedback Clinic of Mohammad Hoesin Hospital (RSMH), Palembang, between July and December 2024.

Participants

The study involved patients diagnosed with PSCI, encompassing both individuals with PSCI without dementia (PSCI-ND) and those with PSD. Participants were recruited through consecutive sampling at the memory outpatient clinic, where diagnoses were established using comprehensive neuropsychological assessments.

The inclusion criteria were patients aged 18 years or older, with poststroke duration of more than 3 months, a confirmed diagnosis of PSCI, residing in Palembang, and willing to participate in the study. Exclusion criteria included individuals with visual and auditory impairments, moderate to severe depression, aphasia, a history of epilepsy or

seizures, or other neurological brain disorders such as Parkinson's disease, brain tumors, multiple sclerosis, neuromyelitis optica spectrum disorder (NMOSD), and congenital abnormalities. Patients who had previously or were currently undergoing other neurorestorative therapies, such as transcranial magnetic stimulation (TMS) or transcranial direct current stimulation (tDCS), were also excluded. Dropout criteria included patients who withdrew before completing the study or passed away before study completion.

All participants received explanations about the potential benefits and adverse effects of the intervention and provided informed consent before enrollment. This study was approved by the Ethics Committee of RSMH Palembang (Approval No: DP.04.03/D.XVIII.06.08/ETIKRSMH/14/2024).

Procedure and Intervention

Diagnosed PSCI patients underwent baseline assessment of cognitive function using the MoCA-INA (T0), followed by baseline qEEG recordings. The qEEG assessment included relative power measurements in the frontal (F3, F4, F7–F8), central (C3, C4), parietal (P3, P4), temporal (T3, T4, T5, T6), occipital (O1, O2), and global regions, along with frontal DAR and PAF in frontal, central, parietal, temporal, occipital, and global areas.

Each patient then underwent five consecutive daily neurofeedback training (NFT) sessions using the Neurosoft-Neuron-Spectrum-61 system, with each session lasting approximately 30 min. The room setup, preparation, and execution of these sessions are illustrated in Figure 1. The NFT protocol was tailored to each patient's baseline qEEG profile and incorporated audiovisual feedback.

Thirteen patients followed the alpha protocol, receiving visual feedback in the form of a mushroom graphic that enlarged upon achieving the alpha threshold. Seven patients followed the beta protocol, with feedback delivered via a car racing animation in which the car accelerated when the beta target was reached. Four patients followed the alpha-theta protocol, receiving feedback through a Millennium Falcon spaceship animation that increased speed when the training target was met. The visual feedback used in each protocol is illustrated in Figure 2.

Following the completion of the five NFT sessions, a postintervention assessment (T1) was conducted using MoCA-INA and qEEG. One month after the intervention, MoCA-INA was reassessed (T2) to evaluate long-term effectiveness. All MoCA-INA assessments were performed by individuals not directly involved in the study to minimize potential assessment bias.

Figure 1. *Room Setup, Preparation, and Execution of NFT Sessions.*

Figure 2A. *Visual Feedback Used in Each Protocol: Mushroom Video for Alpha Protocol.*

Figure 2B. *Visual Feedback Used in Each Protocol: Car Racing Video for Beta Protocol.*

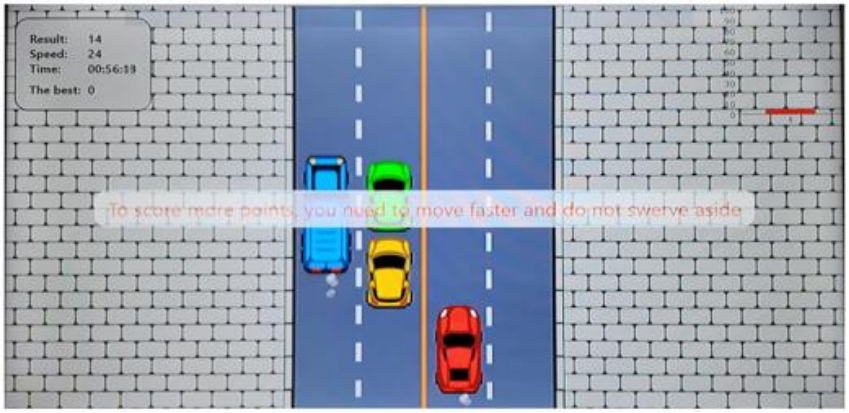

Figure 2C. *Visual Feedback Used in Each Protocol: Millennium Falcon Video for Alpha-Theta Protocol.*

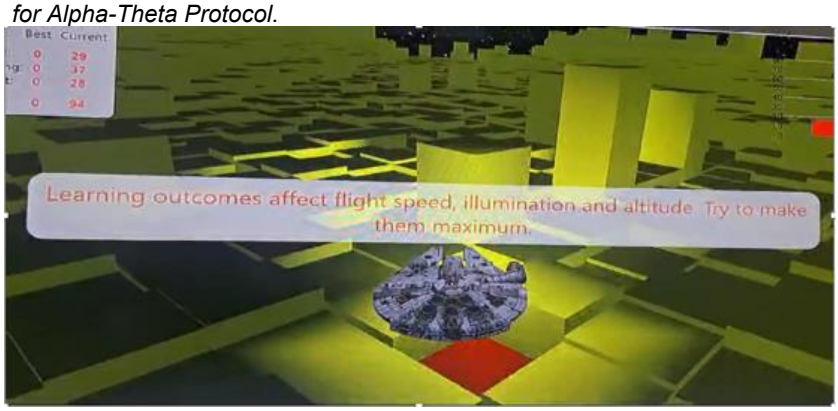

Data Analysis

Data analysis was performed using SPSS version 30. Comparisons of MoCA-INA scores at T0–T1, T1–T2, and T0–T2 were conducted using paired sample *t*-tests for normally distributed data or Wilcoxon tests for non-normally distributed data. Changes in qEEG components—including increased fast-wave relative power, decreased slow-wave relative power, reduced frontal DAR, and increased PAF—were also analyzed using paired sample *t*-tests or Wilcoxon tests, as appropriate. Differences between PSCI-ND and PSD groups were assessed

using independent *t*-tests or Mann-Whitney U tests. Multivariate analysis was conducted using logistic regression to identify factors influencing improvements in MoCA-INA scores.

Results

As shown in Figure 3, a total of 56 PSCI patients were identified through comprehensive neuropsychological testing. However, 26 patients were excluded: 11 declined to participate, 6 presented with depressive symptoms, 4 had aphasia, 2 had seizure disorders, 2 were diagnosed with Parkinson's disease, and 1 had previously received TMS therapy. An additional 6 patients dropped out: 3 did not complete NFT, 1 failed to undergo qEEG evaluation, and 2 missed the 1-month post-NFT follow-up. Ultimately, 24 patients met the inclusion criteria and completed all stages of the study. No adverse effects were reported during the intervention. The clinical and sociodemographic characteristics of the patients are presented in Table 1.

Among the participants, 54.17% were over 60 years old, 62.50% were male, 91.67% had ischemic strokes, 83.34% had subcortical lesions, 62.50% had a stroke onset longer than 6 months, and 66.67% were classified as PSCI-ND. The cognitive domains most commonly impaired based on MoCA-INA results were visuospatial/executive function and delayed memory. The five most affected domains identified through comprehensive neuropsychological testing were delayed memory (83.34%), executive function (75.00%), recognition (75.00%), working memory (70.83%), and language (62.50%).

The average interval between the baseline (T0) and immediate postintervention (T1) assessments was 81.83 days. This relatively long interval was due to several factors, including patient scheduling after initial memory testing, delays in receiving official qEEG reports, and the initiation of NFT sessions. The mean interval between T1 and the 1-month follow-up (T2) was 33.42 days, and the mean total duration from T0 to T2 was 115.25 days.

Figure 3. *Flow Chart of the Study.*

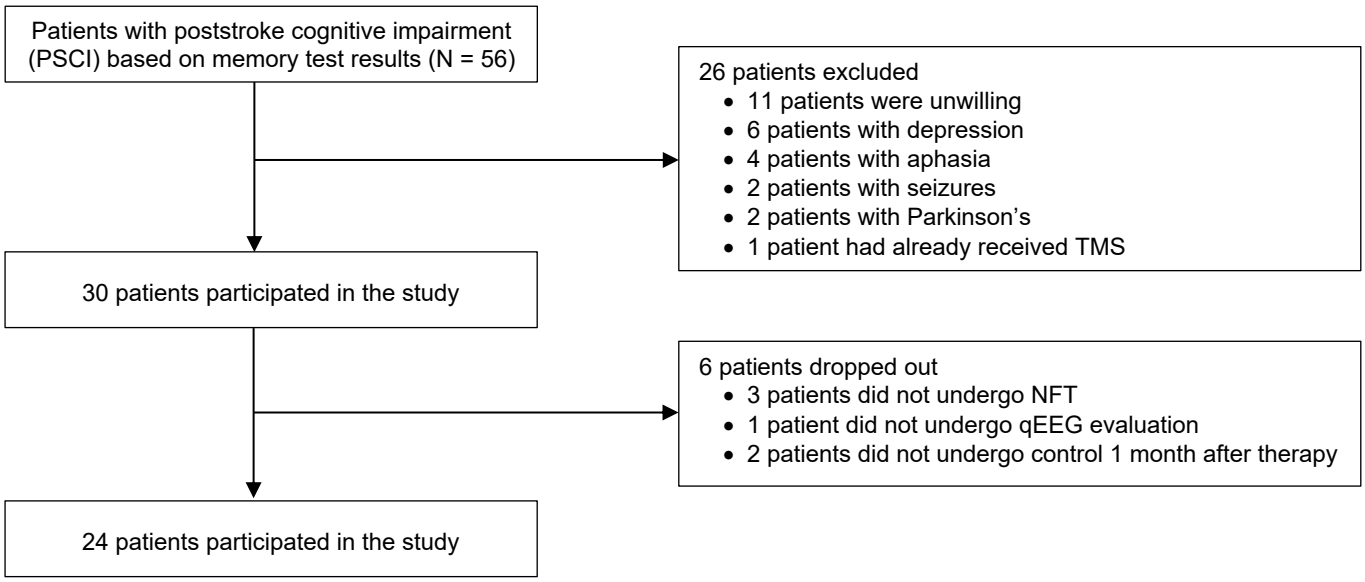

Table 1
Sociodemographic and Clinical Characteristics, and Categorical Analysis of MoCA-INA Score Improvements

Variable	Frequency (*n*)/(%)	*P* T0–T1	*P* T1–T2	*P* T0–T2
Age		0.033[a]	1.000[a]	0.014[c]
≤60 years old	11 (45.83%)			
>60 years old	13 (54.17%)			

Table 1
Sociodemographic and Clinical Characteristics, and Categorical Analysis of MoCA-INA Score Improvements

Variable	Frequency (*n*)/(%)	*P* T0–T1	*P* T1–T2	*P* T0–T2
Sex		1.000[a]	0.533[a]	0.089[a]
Male	15 (62.50%)			
Female	9 (37.50%)			
Education		0.412[a]	1.000[a]	1.000[a]
Higher education (>12 years)	15 (62.50%)			
Lower education (≤12 years)	9 (37.50%)			
Stroke Type		1.000[a]	0.239[a]	1.000[a]
Ischemic	22 (91.67%)			
Hemorrhagic	2 (8.33%)			
Lesion Location		0.390[b]	0.555[b]	1.000[b]
Cortical	2 (8.33%)			
Subcortical	20 (83.34%)			
Corticosubcortical	2 (8.33%)			
Stroke Onset		0.099[a]	0.533[a]	0.400[a]
≤6 months	9 (37.50%)			
>6 months	15 (62.50%)			
Stroke Frequency		1.000[a]	0.437[a]	1.000[a]
1x	20 (83.34%)			
>1x	4 (16.66%)			
Hypertension		1.000[a]	0.343[a]	1.000[a]
No	3 (12.50%)			
Yes	21 (87.50%)			
Diabetes		1.000[a]	1.000[a]	1.000[a]
No	3 (12.50%)			
Yes	21 (87.50%)			
NIHSS at Memory Test		0.631[a]	0.521[a]	0.317[a]
Minor stroke (0–4)	19 (79.17%)			
Moderate stroke (5–15)	5 (20.83%)			
Acethylcholinesterase Inhibitor Treatment		1.000[a]	0.530[a]	1.000[a]
Yes	7 (29.17%)			
No	17 (70.83%)			
PSCI Subtype		1.000[a]	0.526[a]	1.000[a]
PSCI-ND	16 (66.67%)			
PSD	8 (33.33%)			
NFT Protocol		0.160[b]	0.554[b]	0.041[b]
Alpha	13 (54.17%)			
Alpha-theta	4 (16.67%)			
Beta	7 (29.16%)			

[a] = Fisher's exact test; [b] = Likelihood ratio; [c] = Pearson chi-square with continuity correction.

Cognitive Profile

Table 2 and Figure 4 illustrate the comparison of overall and domain-specific MoCA-INA scores before (T0), immediately after NFT (T1), and 1-month postintervention (T2). At baseline, the mean MoCA-INA score was 19.04 ± 6.13, with a median of 20.00 (range: 7.00–25.00). At T1, there was a mean increase of 2.63 points (T1 = 21.67) and a median increase of 3 points (T1 = 23). At T2, the mean decreased slightly by 0.46 points (T2 = 21.21), while the median remained unchanged. The results demonstrated significant improvements in total MoCA-INA scores following the five NFT sessions. Between T0 and T1, the improvement was statistically significant ($Z = -4.106$, $p < 0.001$, effect size = 0.839), as was the change from T0 to T2 ($Z = -3.471$, $p < 0.001$, effect size = 0.709). The comparison between T1 and T2 (long-term effect) showed sustained cognitive improvement, with no significant difference ($Z = -1.331$, $p = 0.183$).

Table 2

Bivariate Analysis of MoCA-INA Median Scores at T0, T1, and T2

	T0	T1	T2	*p* (T0–T1)	*p* (T1–T2)	*p* (T0–T2)
MoCA-INA Total				**<0.001[a]**	0.183[a]	**<0.001[a]**
Mean ± *SD*	19.04 ± 6.13	21.67 ± 6.24	21.21 ± 6.92			
Median (Min–Max)	20.00 (7–25)	23.00 (9–30)	23.00 (7–29)			
Visuospatial/executive				**0.025[a]**	0.763[a]	**0.032[a]**
Mean ± *SD*	3.21 ± 1.72	3.79 ±1.35	3.83 ± 1.52			
Median (Min–Max)	4.00 (0–5)	4.00 (0–5)	4.50 (0–5)			
Naming				0.052[a]	1.000[a]	0.070[a]
Mean ± *SD*	2.50 ± 0.72	2.79 + 0.51	2.79 + 0.51			
Median (Min–Max)	3.00 (1–3)	3.00 (1–3)	3.00 (1–3)			
Attention				0.232[a]	**0.022[a]**	0.294[a]
Mean ± *SD*	4.46 ± 1.50	4.75 ± 1.45	4.17 ± 1.37			
Median (Min–Max)	5.00 (1–6)	5.00 (1–6)	5.00 (1–6)			
Language				0.593[a]	0.593[a]	1.000[a]
Mean ± *SD*	1.88 ± 0.95	1.79 ± 0.98	1.88 ± 1.11			
Median (Min–Max)	2.00 (0–3)	2.00 (0–3)	2.00 (0–3)			
Abstraction				**0.029[a]**	0.480[a]	0.052[a]
Mean ± *SD*	1.08 ± 0.65	1.46 ± 0.78	1.38 ± 0.82			
Median (Min–Max)	1.00 (0–2)	2.00 (0–3)	2.00 (0–3)			
Delayed Recall				**0.015[a]**	0.917[a]	**0.025[a]**
Mean ± *SD*	1.04 ± 1.30	1.96 ± 1.85	2.00 ± 2.15			
Median (Min–Max)	0.00 (0–4)	2.00 (0–5)	1.00 (0–5)			
Orientation				0.327[a]	0.557[a]	0.144[a]
Mean ± *SD*	4.83 ± 1.71	5.04 ± 1.33	5.13 ± 1.39			
Median (Min–Max)	6.00 (1–6)	6.00 (2–6)	6.00 (2–6)			

[a] = Wilcoxon test.

Figure 4. *Comparison of Mean and Median MoCA-INA Scores at T0 (Baseline), T1 (Post-NFT), and T2 (1-Month Post-NFT).*

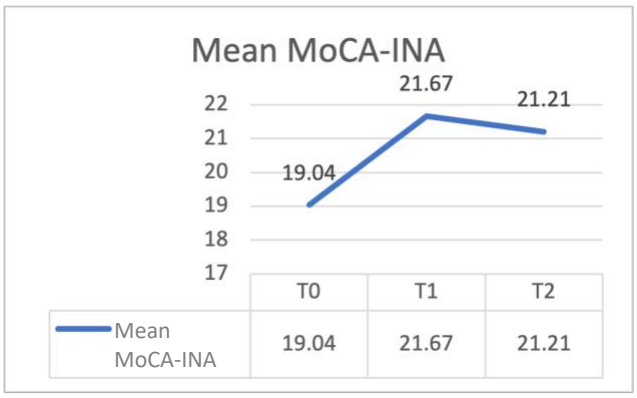

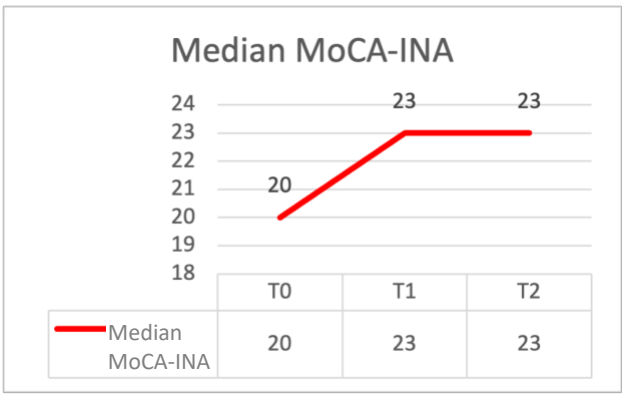

Domain-specific analysis showed statistically significant improvements in the visuospatial/executive domain between T0–T1 ($Z = -2.236$, $p = .025$, effect size: 0.457) and T0–T2 ($Z = -2.142$, $p = .032$, effect size: 0.438); abstraction domain at T0–T1 ($Z = -2.183$, $p = .029$, effect size: 0.446); and delayed recall domain at both T0–T1 ($Z = -2.341$, $p = .015$, effect size: 0.497) and T0–T2 ($Z = -2.242$, $p = .025$, effect size: 0.458). The attention domain showed a minor increase at T1, though not statistically significant, followed by a significant decrease at T2 ($p = .022$), but without a significant difference compared to baseline (T0–T2, $p = .294$).

Quantitative Electroencephalography Components

Table 3 and Figure 5 illustrate the comparison of relative power values (both regionally and globally) before and after NFT. At baseline, alpha and beta waves were found to be more dominant than delta and theta waves. This pattern may be attributed to several factors, including a stroke onset of more than 6 months in most participants (mean = 14.75 ± 11.97 months), a majority of subjects classified as PSCI-ND, and the predominance of subcortical lesions. These factors are believed to influence qEEG patterns, where fast waves (alpha and beta) remain more dominant than slow waves (delta and theta).

Following NFT (post-NFT), reductions were observed in the median relative power of occipital delta (13.92% → 11.96%), central delta (15.23% → 14.29%), global theta (13.97% → 13.33%), frontal theta (14.11% → 13.49%), central theta (14.62% → 13.57%), parietal theta (12.98% → 12.48%), and temporal theta (15.16% → 14.99%). In contrast, improvements were seen in fast-wave components, including increased mean frontal alpha (22.50% → 22.61%), median central alpha (19.79% → 22.68%), mean temporal alpha (30.24% → 32.96%), and mean occipital alpha (39.13% → 40.04%). For beta waves, increases were observed in mean central beta (25.49% → 26.52%), mean parietal beta (26.58% → 28.00%), and mean occipital beta (21.15% → 22.56%).

Statistically significant improvements were identified in temporal alpha relative power ($t = -1.875$, $p = .037$, effect size = 0.23) and parietal beta relative power ($t = -1.827$, $p = .040$, effect size = 0.11). Other spectral components did not show statistically significant differences between pre- and postintervention measurements ($p > .05$).

Table 4 presents the comparisons of frontal DAR and PAF before and after therapy. No statistically significant difference was found in the median frontal DAR values ($p = .577$). Similarly, no significant differences were observed in PAF across all brain regions or in global median values ($p > .05$), indicating that these components remained relatively stable following NFT.

Table 3
Comparison of Relative Power Values Pre- and Post-NFT

	Pre-NFT (%)		Post-NFT (%)		
	M*ean ± *SD	**Median (Min–Max)**	**Mean ± *SD***	**Median (Min–Max)**	***p***
Relative power					
Delta					
Global	17.62 ± 8.00	16.13 (4.64–39.55)*	17.85 ± 7.30	17.11 (5.21–40.54)*	.558[a]
Frontal	23.11 ± 6.92*	21.23 (10.34–35.15)	24.77 ± 8.08*	23.75 (12.96–40.54)	.065[b]
Central	16.91 ± 7.98	15.23 (5.97–34.10)*	16.81 ± 5.81	14.29 (8.37–28.08)*	.689[a]
Parietal	15.02 ± 7.56	12.09 (5.73–33.47)*	15.26 ± 5.97	12.93 (7.17–24.69)*	.689[a]
Temporal	17.15 ± 5.80*	16.52 (8.36–31.37)	17.80 ± 6.14*	16.85 (5.21–29.40)	.250[b]
Occipital	15.89 ± 9.28	13.92 (4.63–39.55)*	14.60 ± 6.79	11.96 (6.98–26.53)*	.241[a]
Theta					
Global	16.69 ± 9.66	13.97 (5.58–47.83)*	16.39 ± 9.45	13.33 (5.97–58.36)*	.401[a]
Frontal	17.16 ± 9.83	14.11 (6.35–46.37)*	16.59 ± 8.93	13.49 (7.81–50.84)*	.732[a]
Central	15.94 ± 7.41	14.62 (5.58–34.78)*	15.63 ± 7.59	13.57 (6.42–38.34)*	.648[a]
Parietal	15.14 ± 8.45	12.98 (5.91–29.28)*	15.11 ± 9.06	12.48 (5.97–43.35)*	.549[a]
Temporal	18.23 ± 10.95	15.16 (7.34–46.69)*	18.16 ± 10.59	14.99 (8.63–58.36)*	.841[a]
Occipital	17.00 ± 11.56	12.83 (6.80–47.83)*	16.45 ± 11.65	13.31 (6.26–53.72)*	.466[a]
Alpha					
Global	30.15 ± 14.46	28.29 (7.45–63.06)*	30.69 ± 13.93	28.12 (6.94–67.29)*	.570[a]
Frontal	22.50 ± 10.00*	20.80 (7.45–42.49)	22.61 ± 9.97*	21.84 (6.94–49.41)	.451[b]
Central	24.46 ± 11.47	19.79 (8.63–43.97)*	24.53 ± 10.16	22.68 (7.47–47.12)*	.797[a]
Parietal	34.40 ± 14.55	36.92 (7.89–56.26)	33.28 ± 14.06	32.70 (9.59–58.59)	.259[b]
Temporal	30.24 ± 11.81*	29.79 (11.46–51.88)	32.96 ± 11.52*	36.25 (12.40–49.89)	**.037[b]**
Occipital	39.13 ± 17.37*	42.16 (9.56–63.06)	40.04 ± 16.10*	45.09 (10.64–67.28)	.314[b]
Beta					
Global	22.71 ± 9.41	23.29 (4.22–54.35)*	23.37 ± 10.86	22.50 (4.07–62.31)*	.539[a]
Frontal	20. 61 ± 6.65*	21.63 (7.34–33.67)	20.53 ± 8.15*	21.92 (6.09–40.69)	.451[b]
Central	25.49 ± 8.83*	26.07 (10.12–42.48)	26.52 ± 10.24*	27.68 (9.25–52.77)	.169[b]
Parietal	26.58 ± 11.77*	26.92 (7.41–54.35)	28.00 ± 13.36*	31.13 (5.96–62.31)	**.040[b]**
Temporal	19.73 ± 7.13*	19.43 (6.39–31.60)	19.28 ± 7.58*	20.41 (5.39–39.71)	.238[b]
Occipital	21.15 ± 10.31*	20.98 (4.22–54.35)	22.56 ± 11.96*	22.60 (4.07–53.03)	.090[b]

[a] = Wilcoxon test; [b] = Paired sample *T*-Test; * = Data analyzed.

Figure 5. *Comparison of Relative Power Values Pre- and Post-NFT.*

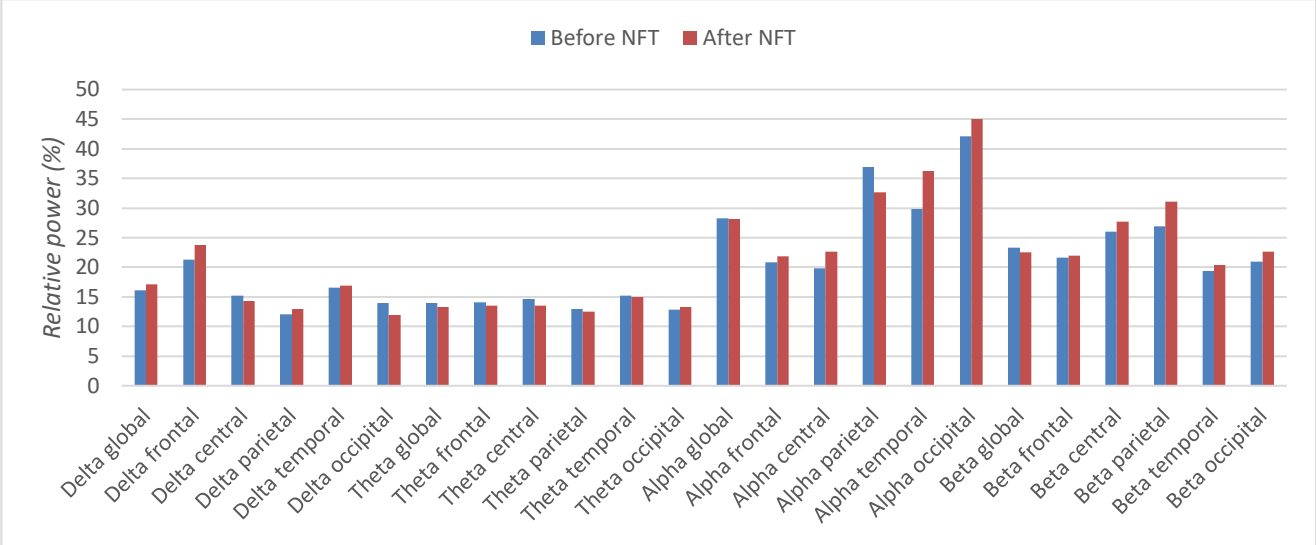

Table 4
Differences in Frontal DAR and PAF Before and After NFT

	Pre-NFT	Post-NFT	*p*
Frontal delta/alpha ratio (DAR)			0.577[a]
Mean ± *SD*	1.41 ± 1.04	1.50 ± 1.07	
Median (Min–Max)	1.06 (0.37–4.74)*	1.15 (0.27–4.72)*	
Peak alpha frequency (PAF)			
Frontal			0.345[b]
Mean ± *SD*	9.54 ± 0.36*	9.55 ± 0.37*	
Median (Min–Max)	9.63 (8.85–10.09)	9.66 (8.89–10.28)	
Central			0.254[b]
Mean ± *SD*	9.61 ± 0.33*	9.59 ± 0.30*	
Median (Min–Max)	9.66 (9.03–10.08)	9.67 (8.96–10.10)	
Parietal			0.488[b]
Mean ± *SD*	9.75 ± 0.40*	9.75 ± 0.45*	
Median (Min–Max)	9.73 (9.12–10.53)	9.79 (9.04–10.77)	
Temporal			0.480[b]
Mean ± *SD*	9.44 ± 0.38*	9.44 ± 0.37*	
Median (Min–Max)	9.40 (8.82–10.13)	9.46 (8.81–9.99)	
Occipital			0.237[b]
Mean ± *SD*	9.67 ± 0.54*	9.64 ± 0.47*	
Median (Min–Max)	9.69 (8.86–10.61)	9.73 (8.84–10.42)	
Global			0.076[a]
Mean ± *SD*	9.60 ± 0.41	9.59 ± 0.40	
Median (Min–Max)	9.63 (8.82–10.62)*	9.63(8.82–10.42)*	

[a] = Wilcoxon test; [b] = Paired sample *T*-Test; * = Data analyzed.

Factors Influencing MoCA-INA Score Improvement

A categorical analysis was conducted to evaluate cognitive improvement by grouping variables based on defined categories. In this analysis, the criterion for improvement was based on previous literature, which defines a clinically meaningful change in MoCA-INA scores as an increase of more than 2 points (Zuo et al., 2022). The analysis compared score changes across three time points: T0–T1, T1–T2, and T0–T2. The distribution of MoCA-INA improvement is illustrated in Figure 6. At T0–T1 (baseline to postintervention), 16 patients (66.67%) demonstrated improvement, while 8 patients (33.33%) showed no improvement.

Cross-tabulation analysis of potential sociodemographic and clinical predictors of MoCA-INA score improvement is presented in Table 1, covering comparisons at T0–T1, T1–T2, and T0–T2. In the T0–T1 analysis, among all the variables assessed, only age was significantly associated with cognitive improvement. Patients under 60 years of age showed statistically significant improvement in MoCA-INA scores (p = .033).

In the T1–T2 analysis, no sociodemographic or clinical variables were found to significantly influence MoCA-INA score changes (p > .05). However, in the T0–T2 comparison (baseline to 1-month postintervention), two variables were significantly associated with improvement in mean MoCA-INA scores: age (p = .014) and the type of NFT protocol applied (p = .041).

PSCI Subtypes Analysis

A subgroup analysis was conducted by stratifying patients based on the severity of cognitive impairment into PSCI-ND and PSD groups. The analysis assessed changes in average MoCA-INA scores and qEEG wave patterns in both groups.

Table 5 shows that the PSCI-ND group had higher median MoCA-INA scores than the PSD group at all three time points (T0, T1, and T2). However, no statistically significant differences were observed in the change scores (Δ MoCA-INA) across the time intervals T0–T1, T1–T2, and T0–T2, indicating that the effectiveness of NFT did not differ significantly between the PSCI-ND and PSD groups at any measurement point.

Figure 6. *Categories of Mean MoCa-INA Score Improvement.*

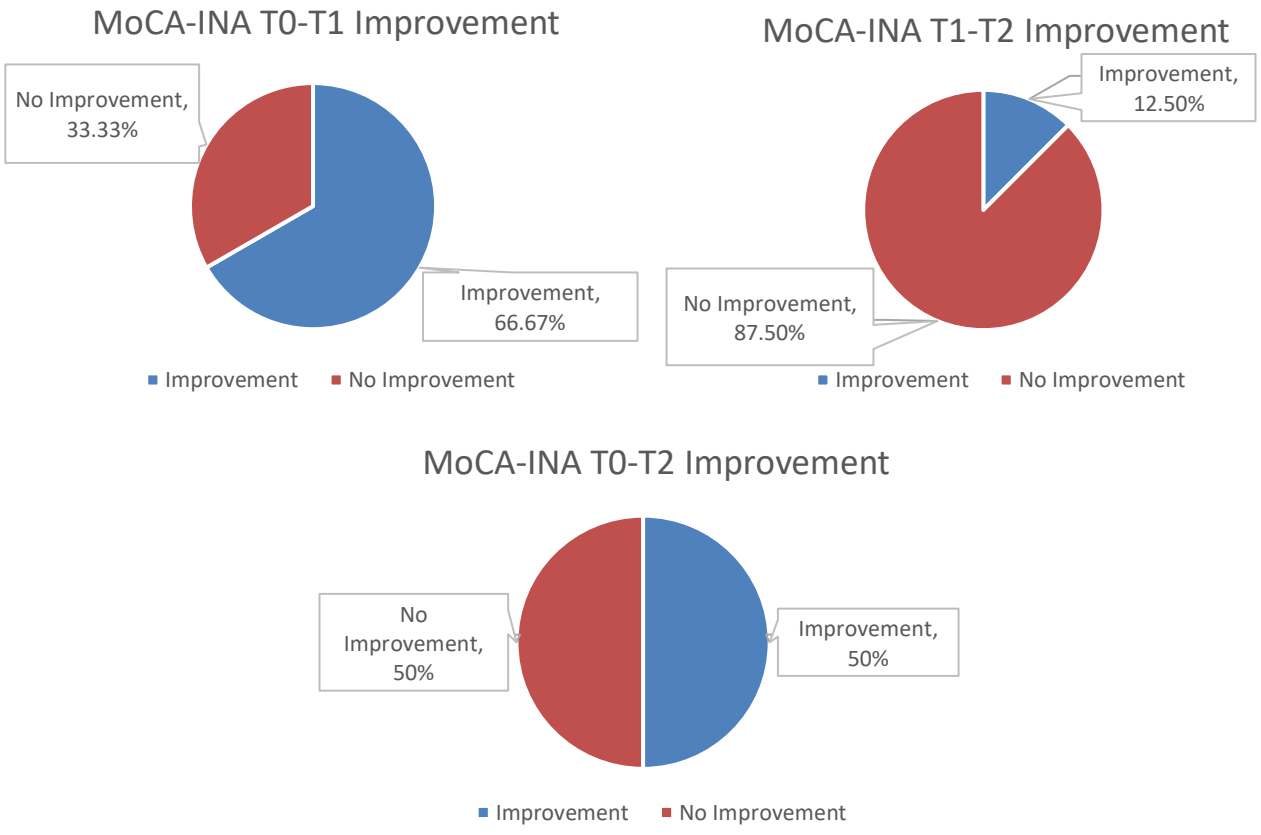

Table 5
Bivariate Analysis of Differences Between PSCI-ND and PSD Groups

Variable	PSCI-ND		PSD		p
	Mean ± *SD*	Median (Min–Max)	Mean ± *SD*	Median (Min–Max)	
MoCA-INA					
MoCA-INA T0	20.75 ± 5.67	23.50 (7–25)*	15.63 + 5.88	15.50 (8–25)*	.063[a]
MoCA-INA T1	23.56 ± 5.93	26.00 (9–30)*	17.88 + 5.28	17.00 (12–25)*	**.034[a]**
MoCA-INA T2	23.25 + 6.37	25.00 (7–29)*	17.13 + 6.44	17.50 (8–25)*	**.027[a]**
∆ MoCA-INA T0–T1	2.81 ± 2.26*	2.50 (−1–(8))	2.25 ± 1.58*	2.50 (0–5)	.536[b]
∆ MoCA-INA T1–T2	−0.31 ± 1.53	0.00 (−3–(2))*	-0.75 ± 0.88	0.00 (−4–(1))*	.445[a]
∆ MoCA-INA T0–T2	2.50 ± 2.16	3.00 (0–6)*	1.50 ± 2.26*	2.00 (−3–(4))*	.508[a]

[a] = Mann-Whitney test; [b] = Independent *T*-Test; * = Data analyzed.

Subgroup analysis revealed that both groups showed significant improvement from T0 to T1 (PSCI-ND: p < .001, effect size = 0.845; PSD: p = .003, effect size = 0.40). From T0 to T2, only the PSCI-ND group showed a statistically significant improvement (p = .002, effect size = 0.7725). At the domain level, significant improvements were observed primarily in the visuospatial/executive and delayed recall domains, especially among the PSCI-ND group.

Regarding qEEG, the PSCI-ND group exhibited increases in nearly all fast-wave spectra (alpha and beta), with significant changes in median global alpha (26.04% → 27.90%, *p* = .032), mean temporal alpha (29.18% → 32.97%, *p* = .037), and mean occipital beta (23.08% → 25.66%, *p* = .039). No significant changes were observed in DAR or PAF. In contrast, the PSD group displayed inconsistent delta wave patterns with no statistical significance (*p* > .05), a significant decrease in global theta (20.51% → 19.33%, *p* = .043), and reductions in global alpha (30.84% → 29.97%, *p* = .027) and central alpha (18.37% → 26.13%, *p* = .019). Although beta power increased, the changes were not statistically significant (*p* > .05).

Kendall's Tau correlation analysis (Table 6) showed no significant associations between the timing of MoCA-INA assessments and the magnitude of score changes. Additionally, no significant correlations were found between post-NFT qEEG components and MoCA-INA scores at T1.

Table 6
Kendall's Tau Correlation Analysis

Variable	Correlation Coefficients	p
Time Interval T0–T1*Mean MoCA-INA T1	0.315	.018
Time Interval T1–T2*Mean MoCA-INA T2	0.004	.490
Time Interval T0–T2*Mean MoCA-INA T2	0.296	.024
Time Interval T0–T1* ∆ MoCA- INA T0–T1	0.172	.136
Time Interval T1–T2* ∆ MoCA- INA T1–T2	−0.025	.438
Time Interval T0–T2* ∆ MoCA- INA T0–T2	0.251	.054
Absolute Power Global Delta*Mean MoCA-INA T1	−0.082	.292
Absolute Power Global Teta*Mean MoCA-INA T1	−0.112	.227
Absolute Power Global Alpha*Mean MoCA-INA T1	−0.015	.460
Absolute Power Global Beta*Mean MoCA-INA T1	−0.097	.258
Relative Power Global Delta*Mean MoCA-INA T1	0.067	.327

Table 6
Kendall's Tau Correlation Analysis

Variable	Correlation Coefficients	p
Relative Power Global Teta*Mean MoCA-INA T1	−0.126	.198
Relative Power Global Alpha *Mean MoCA-INA T1	0.082	.292
Relative Power Global Beta*Mean MoCA-INA T1	−0.022	.441
Frontal DAR*Mean MoCA-INA T1	−0.108	.235
Global PAF*Mean MoCA-INA T1	0.037	.402

Multivariate Analysis

In the multivariate analysis for T0–T1, age <60 years was identified as the most influential factor associated with improvement in MoCA-INA scores at T1, with an Exp(B) value of 20.045, p = .035, and a 95% confidence interval (CI) of 1.241–323.771. Similarly, in the T0–T2 analysis, age <60 years remained the most significant factor, with an Exp(B) of 22.778, p = .014, and a 95% CI of 1.876–276.572.

Discussion

The findings of this study demonstrate that after five sessions of NFT using individualized qEEG-based protocols, cognitive function improved significantly, and the effect persisted for up to 1-month postintervention. A statistically significant increase in MoCA-INA scores was observed at T1 (p = .001) with a large effect size (0.839). No decline in MoCA-INA scores was noted 1 month after NFT, and comparison between T0 and T2 also revealed significant improvement (p < .001; effect size = 0.709). At the domain level, significant improvements were found, particularly in visuospatial/executive function and delayed recall.

Improvements were also observed in fast-wave EEG spectra, alongside reductions in slow-wave activity. These findings indicate that NFT may serve as a beneficial adjunctive therapy for patients with PSCI, including both PSCI-ND and PSD, showing both immediate and sustained effects 1-month posttreatment. Based on these results, NFT appears to be an effective cognitive rehabilitation modality, potentially superior to conventional approaches, even with only five sessions.

These findings are consistent with a study by Anggraeni et al. (2024), which reported a 2.63-point improvement in MoCA-INA scores (14.75 → 17.38; p = .019) after 10 NFT sessions over 2 weeks in PSCI-ND patients. A comparable result was observed in the PSCI-ND subgroup of the present study, with a 2.81-point increase in mean MoCA-INA scores (20.75 → 23.56; p < .001). However, unlike the 2024 study by Anggraeni et al., which found no significant domain-level differences, the current study reported significant improvements in the visuospatial/executive, abstraction, and delayed recall domains, possibly due to the larger sample size (Anggraeni et al., 2024).

Similar results were reported by Jang et al. (2019) in Korea, who studied five MCI patients (aged 40–80 years, baseline MoCA <22) receiving 16 NFT sessions. MoCA scores increased by 4.4 points after eight sessions (week 4; 19.4 → 23.8, p = .042), and by 6.2 points after 16 sessions (week 8; 19.4 → 25.6, p = .042). Improvements were also noted in complex memory, cognitive flexibility, attention, reaction time, and executive function. The larger increase in MoCA scores in Jang's study may be due to the higher number of sessions and the differing study population. These findings suggest that greater session frequency may yield greater improvements.

Madijova et al. (2024) similarly, reported significant improvements in MoCA scores among poststroke patients following 30 days of NFT combined with pharmacological therapy. In Group 1 (NFT + Cytoflavin), MoCA scores increased by 3.9 points (20.3 → 24.2); in Group 2 (NFT + Memantine), by 4.6 points (19.9 → 24.5); and in Group 3 (NFT + Cytoflavin + Memantine), by 4.9 points (20.2 → 25.1). Another study supporting these findings is Marlats et al. (2020), which investigated 20 MCI patients undergoing 20 sessions of SMR/theta NFT. The study reported a mean MoCA increase of 1.9 points (23.2 → 25.1; p = .007), which was lower than the improvement observed in the present study. This lower gain may be attributable to the older age of participants (mean age 76.1 years) compared to this study (mean age 61.17 years).

Comparable cognitive improvements were also reported by Kober et al. (2015), who found that among 11 poststroke patients (>1 month) receiving

NFT with SMR protocols and six patients receiving upper alpha protocols, there were enhancements in both short-term and long-term verbal memory. Specifically, SMR training led to improvements in short-term visuospatial memory, while upper alpha protocols were more effective in enhancing working memory compared to no intervention. Similarly, Cho et al. (2016) found improved visual discrimination and visual memory among 13 poststroke patients who underwent six sessions of NFT using the SMR-beta protocol.

Various theories have been proposed to explain how NFT can improve cognitive function in patients. First, the initial phase of learning is dominated by the frontal brain regions, supported by the striatum, which generates distinct representations (e.g., increased SMR activity) and reinforces those that yield positive feedback signals (e.g., visual feedback). Second, the most efficient frontal representations are activated and modulate connections to and within the thalamus. Third, the targeted brain state and the associated subjective experiences act as secondary reinforcers that help close the interoceptive homeostatic loop. The synergistic interaction between brain structure and function lies at the core of NFT. By targeting functional changes, NFT may induce structural modifications in the brain, which in turn support more persistent functional reorganization (Pinter et al., 2021).

The primary goal of NFT is to enable individuals to become aware of specific cortical activity patterns associated with more optimal behavioral or cognitive states. NFT can induce changes in brain electrical activity that synergize with cognitive enhancement through the patient's ability to self-modulate brainwave activity. Increases in alpha waves are associated with improvements in working memory and short-term memory. Alpha activity also plays a role in suppressing irrelevant or distracting processes, thereby enhancing attention and memory by inhibiting disruptive stimuli. Accordingly, NFT may accelerate functional recovery or even achieve improvements that are not possible through other therapies. These insights support the recommendation of NFT as a viable cognitive rehabilitation modality for poststroke patients (Anggraeni et al., 2024). The results of this study suggest that even with fewer sessions than other comparative studies (only five sessions in this study), a statistically significant improvement was observed in both the mean and median MoCA-INA total scores. Although not all cognitive domains showed significant improvement, this domain-specific variation in response may be influenced by factors such as differences in brain structure, individual neuropsychological and psychological profiles, limitations of the MoCA-INA tool, baseline domain scores that were not low enough, cognitive strategies employed, and the NFT protocol used (Anggraeni et al., 2024).

To date, relatively few studies have assessed the long-term effectiveness of NFT on cognitive function. Furthermore, there remains debate regarding the durability of NFT effects after the intervention ends. No clear cut-off criteria have been established, and specific categorizations based on different disease types remain lacking (Weber et al., 2020).

In this study, a slight decrease of 0.46 points was observed in the mean MoCA-INA total score 1-month posttherapy (21.67 → 21.21), with the same median value of 20.00, and this difference was not statistically significant (p = .183). However, the T0−T2 comparison still showed a significant increase in mean score by 2.17 points and in median by 3 points (p < .001). These findings suggest that the cognitive improvement resulting from NFT remains relatively stable over 1 month. This aligns with the study by Lavy et al. (2018), which involved 11 MCI patients who received 10 sessions of NFT using the upper alpha protocol. Improvements in memory scores (both verbal and nonverbal immediate memory) were sustained for up to 30 days postintervention (p = .441; Lavy et al., 2018).

These findings differ from those reported by Marlats et al. (2020), who studied 20 MCI patients receiving 30 sessions of SMR/theta NFT. One month after the intervention, a statistically significant decrease of 1.5 points was found in mean MoCA scores (25.1 → 23.6; p = .015), and there was no significant difference between baseline and 1-month posttherapy scores (23.2 → 23.6; p = .0937). However, performance on other memory tests (e.g., Logical Memory, RAVLT, TMT-A, and TMT-B) remained stable and comparable to posttreatment levels. The decline in MoCA scores in Marlat et al.'s study may be attributed to the older participant age range (65–90 years, mean age 76.1 years), in contrast to the younger mean age of 61.17 years in the present study. Bivariate analysis in our study also showed that younger age (<60 years) was significantly associated with improved MoCA-INA scores.

The persistence of clinical improvements following NFT may be explained by neuronal-level effects. As

NFT is a form of learning, it involves consolidation and reconsolidation processes that continue over time. Gradual improvements observed in the weeks following NFT may reflect slow but ongoing consolidation, regardless of the extent of practice. At the network level, NFT has been shown to affect brain structure postintervention. According to the Hebbian principle of neuroplasticity, "fire together, wire together," neurons' structural changes become more pronounced over time, and the regions engaged during NFT show increased synchronization, strengthening their functional connectivity (Rance et al., 2018).

This study also found statistically significant changes in specific regions of the fast-wave spectrum. In particular, mean temporal alpha relative power increased by 2.72% (p = .037), and parietal beta relative power increased by 1.42% (p = .040). Although no global changes were observed, the relative power results, which provide a more accurate representation of brainwave dynamics, tended to show increases in fast-wave activity (alpha and beta) and decreases in slow-wave activity (theta) post-NFT. Median relative theta power decreased in all regions except occipital theta, while alpha and beta waves generally increased, though not all reached statistical significance.

These results are consistent with the study by Cho et al. (2016), which reported increased relative beta power in the frontal and parietal regions of poststroke patients with cognitive impairment (MMSE scores 18–23) at 3 months post-onset. However, their intervention involved a longer duration of 30 NFT sessions using a beta-SMR protocol over 6 weeks. Cho suggested that NFT might promote the redistribution of brain activity to other regions, facilitating long-term improvements. Similarly, a study by Jang et al. (2019) reported a significant increase in average beta power after 16 NFT sessions over 8 weeks in patients with MCI (p = .001).

Marcos-Martínez et al. (2021) conducted a study on 11 cognitively healthy individuals over the age of 60 who received five sessions of motor imagery-based NFT. They observed increases in relative theta, alpha, and beta power (particularly alpha and beta), with statistically significant changes (p < .01). Specifically, mean relative alpha power increased by 3.7% (11.2% → 14.9%), and beta power by 4.3% (13.2% → 17.5%). Although similar trends were observed in the present study, the magnitude of increase was smaller (global alpha: 0.54%; global beta: 0.56%; p > .05).

A study by Marlats et al. (2020) involving 20 MCI patients who underwent 20 sessions of SMR/theta NFT also reported significant increases in log power of theta (p = .016) and alpha (p = .027) after treatment. The increase in alpha was hypothesized to reflect the effect of NFT in enhancing fast-wave brain activity while suppressing slow-wave spectra. Interestingly, a protocol designed to enhance beta instead led to increased alpha, supporting the hypothesis that the activation of specific frequency bands may influence others. The absence of global statistically significant changes in the present study—whether from overall or alpha/theta-specific protocols—may be attributed to the lower number of sessions.

In this study, no significant differences were found between pre- and postintervention values of frontal DAR and PAF. This contrasts with findings from Andrade et al. (2022) in cognitively impaired older adults undergoing 20 NFT sessions and from Lavy et al. (2018) in 11 MCI patients who received 10 NFT sessions. Both studies reported posttreatment improvements in PAF, although Lavy noted a decline after 30 days. These differences may stem from variations in the number of sessions and patient characteristics. To date, only a few studies have investigated the impact of NFT on DAR and PAF in PSCI patients.

The small and limited number of sessions in the present study (only five, compared to more than 10 in most other studies) may have contributed to the lack of significant changes in qEEG components. This aligns with findings by Zhou et al. (2024), who conducted a study involving five sessions of alpha-protocol NFT in 20 healthy individuals (mean age 23.83 years). No significant changes in alpha amplitude were found posttreatment. Zhou et al. (2024) suggested that unengaging feedback might lead to reduced motivation and diminished learning efficiency during NFT. Additionally, insufficient training sessions may contribute to the failure of long-term neurofeedback (NF) learning, which generally requires more than five sessions.

Other factors that may account for the absence of qEEG wave changes include interindividual differences such as variations in brain structure, neurophysiological and psychological characteristics, and cognitive strategies (Kober et al., 2017). Furthermore, the baseline power values in this study's participants were already close to normal topographic patterns—that is, dominance of fast-wave spectra (alpha and beta) over slow-wave spectra—due to several factors discussed earlier. As

a result, the range of posttreatment changes may have been limited, given that the initial patterns already resembled those of a healthy population. This near-normal baseline could be attributed to a longer stroke duration, a greater proportion of PSCI-ND cases, or the effects of pharmacologic treatment in the PSD group. Although the analysis did not reveal any significant effects of medication on MoCA-INA score improvement, such treatment may influence brainwave activity.

When analyzing the differences in NFT effectiveness between the PSCI-ND and PSD groups, both groups demonstrated improvements in total MoCA-INA scores—both mean and median—at T1, followed by a slight decline 1 month later, though scores remained higher than at baseline (T0). Statistically significant improvements at T1 were observed in both groups (PSCI-ND: $p < .001$; PSD: $p = .003$). No significant changes were found between T1 and T2. However, when comparing T0 and T2, the PSCI-ND group maintained a statistically significant improvement ($p = .002$), while the PSD group did not ($p = .052$). At the domain level, more cognitive domains showed improvement in the PSCI-ND group. No statistically significant differences were found in the delta MoCA-INA values between the two groups across T0–T1, T1–T2, or T0–T2, indicating that the magnitude of cognitive improvement was comparable between patients with MCI and those with dementia.

These findings align with the theoretical basis of NFT, which posits that the therapy can be effective in patients with cognitive impairments, including both MCI and dementia. Lujimes et al. (2016) evaluated NFT in 10 patients with Alzheimer's dementia who were already receiving cholinesterase inhibitors. Cognitive function was assessed using the Cambridge Cognitive Examination (CAMCOG), and 30 NFT sessions were conducted twice weekly. A 2% improvement in total CAMCOG scores was observed, with the memory subscale showing the most statistically significant gain. This suggests preserved neuroplasticity even in dementia patients.

Another study by Surmeli et al. (2016) involved nine patients with Alzheimer's dementia and 11 with vascular dementia who underwent 10–96 hours of NFT based on qEEG findings. Posttherapy MMSE scores improved significantly (overall: 18.8 → 24.5; Alzheimer's: 19.22 → 25.22; vascular: 18.45 → 23.0). The most notable improvements occurred in the orientation and recall domains. Cognitive gains were attributed to improved connectivity in the medial prefrontal cortex, medial temporal lobe, posterior cingulate cortex, precuneus, and the medial, lateral, and inferior parietal cortices. Notably, 19 out of 20 patients reportedly discontinued medication due to substantial symptom improvement (Surmeli et al., 2016; Trambaiolli et al., 2021). These findings support the use of NFT across a broad spectrum of patients, including those with dementia.

In terms of relative power, the PSCI-ND group showed significant increases in global and temporal alpha power as well as occipital beta power. In contrast, the PSD group exhibited decreases in theta, global alpha, and central alpha power. These findings support the theory that NFT promotes increased fast-wave (e.g., alpha and beta) activity while reducing slow-wave (e.g., theta) activity, thus enhancing cognitive function. Alpha activity in particular is known to increase significantly following EEG-based NFT (Marlats et al., 2020).

This suggests that, in terms of relative power—a more sensitive EEG measure—the PSCI-ND group demonstrated better self-regulation across qEEG parameters compared to the PSD group. Few studies have directly compared qEEG changes between MCI and dementia groups poststroke. Most available data are from single-group studies or case reports, especially among dementia populations, limiting direct comparisons. The lack of significant qEEG changes in this study compared to other research may be due to the lower number of sessions, as most studies use 10–30 sessions, or to relatively normal baseline values.

Multivariate analysis for both T0–T1 and T0–T2 indicated that age was a significant predictor of MoCA-INA score improvement (defined as a gain >2 points). Participants aged <60 years had a higher likelihood of cognitive improvement after NFT. This supports existing theories that age plays a crucial role in cognitive deficits, recovery, and NFT efficacy.

However, the influence of age on NFT effectiveness in PSCI patients could not be directly analyzed using comparable age-based subgroups, as no prior studies have made this comparison. The study by Anggraeni et al. (2024) used a different age cut-off (65 years) and had a smaller sample size. Another study, a meta-analysis by Lin et al. (2024) concluded that the impact of NFT on memory function differs between older and younger adults. Older age was associated with reduced NFT effectiveness for episodic memory, though working memory appeared unaffected. Nonetheless, NFT can enhance memory in older adults, especially with appropriate protocols and adequate training duration. It was noted that

over 300 min of training—roughly 10 sessions—is typically needed to achieve beneficial outcomes in older adults, which contrasts with the five-session design of the present study.

Neuroplasticity, the mechanism underlying post-NFT improvement, is also influenced by age. It is widely assumed that brain plasticity peaks in youth and gradually declines with age. Although new motor and cognitive skills can be acquired at any age, progress may be slower in older populations. Aging brains undergo characteristic neurodegenerative changes, including progressive loss of structure, function, or neuronal count. Neurodegeneration, to some extent, is a natural process in late life (Arcos-Burgos et al., 2019; Pauwels et al., 2018).

In older adults, no significant activation or modulation of the striatal system occurs during cognitive learning. This suggests that older individuals may require more extensive training to achieve the same neural and cognitive outcomes as younger individuals. Alternatively, it may reflect more limited behavioral and neural adaptability. Cognitive decline in older adults is often linked to diminished brain function, leading to reduced concentration, memory, and mental flexibility (Nguyen et al., 2019).

Limitations

This study has several limitations. First, it lacked a sham control or untreated comparison group, precluding direct conclusions about the effectiveness of NFT in avoiding placebo or learning effects. Second, scheduling difficulties for qEEG assessments and NFT sessions—often due to prolonged examination procedures—led to a relatively high dropout rate. Third, assessments could not be performed on patients with early stroke onset, as most posthospitalization stroke patients returned to type B referral hospitals, and only a few returned to RSMH. Consequently, most participants were chronic stroke patients with comorbidities or recurrent strokes. Finally, the follow-up period was limited to 1 month, which may not sufficiently reflect the long-term effects of NFT.

Conclusion

Five sessions of NFT using individualized qEEG-based protocols were effective in improving cognitive function, as measured by MoCA-INA, both immediately after training and 1-month postintervention. Improvements were also observed in qEEG relative power components. No significant differences in NFT effectiveness were found between the PSCI-ND and PSD groups. Younger age was associated with a greater likelihood of cognitive improvement.

Author Disclosure

The authors have no grants, financial interests, or conflicts to disclose. There was no use of AI in the preparation, creation, and completion of this manuscript. The researcher is responsible for the originality of the manuscript.

References

Ali, J. I., Viczko, J., & Smart, C. M. (2020). Efficacy of neurofeedback interventions for cognitive rehabilitation following brain injury: Systematic review and recommendations for future research. *Journal of the International Neuropsychological Society, 26*(1), 31–46. https://doi.org/10.1017/s1355617719001061

Andrade, K., Guieysse, T., Razafimahatratra, S., Houmani, N., Klarsfeld, A., Dreyfus, G., Dubois, B., Medani, T., & Vialatte, F. (2022). EEG-neurofeedback for promoting neuromodulation in the elderly: Evidence from a double-blind study. *bioRxiv,* Article 509227. https://doi.org/10.1101/2022.09.26.509227

Anggraeni, D., Haddani, M., Handayani, S., Nindela, R., & Febrianto, Y. (2024). Effectiveness of neurofeedback training in poststroke cognitive impairment. *NeuroRegulation, 11*(3), 296–303. https://doi.org/10.15540/nr.11.3.296

Arcos-Burgos, M., Lopera, F., Sepulveda-Falla, D., & Mastronardi, C. (2019). Neural plasticity during aging. *Neural Plasticity, 2019*, Article 6042132. https://doi.org/10.1155/2019/6042132

Babiloni, C., Arakaki, X., Bonanni, L., Bujan, A., Carrillo, M. C., Del Percio, C., Edelmayer, R. M., Egan, G., Elahh, F. M., Evans, A., Ferri, R., Frisoni, G. B., Güntekin, B., Hainsworth, A., Hampel, H., Jelic, V., Jeong, J., Kim, D. K., Kramberger, M., … Yener, G. (2021). EEG measures for clinical research in major vascular cognitive impairment: Recommendations by an expert panel. *Neurobiology of Aging, 103*, 78–97. https://doi.org/10.1016/j.neurobiolaging.2021.03.003

Cho, H.-Y., Kim, K.-T., & Jung, J.-H. (2016). Effects of neurofeedback and computer-assisted cognitive rehabilitation on relative brain wave ratios and activities of daily living of stroke patients: A randomized control trial. *Journal of Physical Therapy Science, 28*(7), 2154–2158. https://doi.org/10.1589/jpts.28.2154

Hadiyoso, S., Zakaria, H., Anam, P. A., & Rajab, T. L. E. (2022). EEG-based spectral dynamic in characterization of poststroke patients with cognitive impairment for early detection of vascular dementia. *Journal of Healthcare Engineering, 2022*(1), Article 5666229. https://doi.org/10.1155/2022/5666229

Hohenfeld, C., Nellessen, N., Dogan, I., Kuhn, H., Müller, C., & Papa, F., Ketteler, S., Goebel, R., Heinecke, A., Shah, N. J., Schulz, J. B., Reske, M., & Reetz, K. (2017). Cognitive improvement and brain changes after real-time functional MRI neurofeedback training in healthy elderly and prodromal Alzheimer's disease. *Frontiers in Neurology, 8*, Article 384. https://doi.org/10.3389/fneur.2017.00384

Jang, J.-H., Kim, J., Park, G., Kim, H., Jung, E.-S., Cha, J.-Y., Kim, C.-Y., Kim, S., Lee, J.-H., & Yoo, H. (2019). Beta wave enhancement neurofeedback improves cognitive functions in patients with mild cognitive impairment. *Medicine (Baltimore), 98*(50), Article e18357. https://doi.org/10.1097/md.0000000000018357

Kober, S. E., Schweiger, D., Witte, M., Grieshofer, P., Neuper, C., & Wood, G. (2017). Upper alpha based neurofeedback training in chronic stroke: Brain plasticity processes and

cognitive effects. *Applied Psychophysiology and Biofeedback, 42*(1), 69–83. https://doi.org/10.1007/s10484-017-9353-5

Kober, S. E., Schweiger, D., Witte, M., Reichert, J. L., Grieshofer, P., Neuper, C., & Wood, G. (2015). Specific effects of EEG based neurofeedback training on memory functions in post-stroke victims. *Journal of NeuroEngineering and Rehabilitation, 12*(1), Article 107. https://doi.org/10.1186/s12984-015-0105-6

Lavy, Y., Dwolatzky, T., Kaplan, Z., Guez, J., & Todder, D. (2018). Neurofeedback improves memory and peak alpha frequency in individuals with mild cognitive impairment. *Applied Psychophysiology and Biofeedback, 44*, 41–49. https://doi.org/10.1007/s10484-018-9418-0

Lin, Y.-R., Hsu, T.-W., Hsu, C.-W., Chen, P.-Y., Tseng, P.-T., & Liang, C.-S. (2024). Effectiveness of electroencephalography neurofeedback for improving working memory and episodic memory in the elderly: A meta-analysis. *Medicina, 60*(3), 369. https://doi.org/10.3390/medicina60030369

Lujimes, R. E., Pouwel, S., & Boonman, J. (2016). The effectiveness of neurofeedback on cognitive functioning in patients with Alzheimer's disease: Preliminary results. *Neurophysiologie Clinique, 46*(3), 179–187. https://doi.org/10.1016/j.neucli.2016.05.069

Madijova, Y. N., Azimoba, N. M., Xusenoa, N. T., & Salikhoa, S. M. (2024). Optimization of cognitive disorders in dementia using the neurofeedback therapy. *International Scientific Journal, 3*(2), 183–193. https://doi.org/10.5281/zenodo.10714723

Marcos-Martínez, D., Martínez-Cagigal, V., Santamaría-Vázquez, E., Pérez-Velasco, S., & Hornero, R. (2021). Neurofeedback training based on motor imagery strategies increases EEG complexity in elderly population. *Entropy, 23*(12), 1574. https://doi.org/10.3390/e23121574

Marlats, F., Bao, G., Chevallier, S., Boubaya, M., Djabelkhir-Jemmi, L., Wu, Y.-H., Lenoir, H., Rigaud, A.-S., & Azabou, E. (2020). SMR/theta neurofeedback training improves cognitive performance and EEG activity in elderly with mild cognitive impairment: A pilot study. *Frontiers in Aging Neuroscience, 12*, Article 147. https://doi.org/10.3389/fnagi.2020.00147

McDonald, M. W., Black, S. E., Copland, D. A., Corbett, D., Dijkhuizen, R. M., Farr, T. D., Jeffers, M. S., Kalaria, R. N., Karayanidis, F., Leff, A. P., Nithianantharajah, J., Pendlebury, S., Quinn, T. J., Clarkson, A. N., & O'Sullivan, M. J. (2019). Cognition in stroke rehabilitation and recovery research: Consensus-based core recommendations from the second stroke recovery and rehabilitation roundtable. *International Journal of Stroke, 14*(8), 774–782. https://doi.org/10.1177/1747493019873600

Merriman, N. A., Sexton, E., McCabe, G., Walsh, M. E., Rohde, D., Gorman, A., Jeffares, I., Donnelly, N.-A., Pender, N., Williams, D. J., Horgan, F., Doyle, F., Wren, M.-A., Bennett, K. E., & Hickey, A. (2019). Addressing cognitive impairment following stroke: Systematic review and meta-analysis of non-randomised controlled studies of psychological interventions. *BMJ Open, 9*(2), Article e024429. https://doi.org/10.1136/bmjopen-2018-024429

Nguyen, L., Murphy, K., & Andrews, G. (2019). Cognitive and neural plasticity in old age: A systematic review of evidence from executive functions cognitive training. *Ageing Research Reviews, 53*, Article 100912. https://doi.org/10.1016/j.arr.2019.100912

Ong, P. A., Muis, A., Rambe, A. S., Widjojo, F. S., Laksmidewi, A. A., & Pramono, A. (2015). *Panduan praktik klinik: Diagnosis dan penatalaksanaan demensia*. Perhimpunan Dokter Spesialis Saraf Indonesia.

Pauwels, L., Chalavi, S., & Swinnen, S. P. (2018). Aging and brain plasticity. *Aging, 10*(8), 1789–1790. https://doi.org/10.18632/aging.101514

Petrovic, J., Milosevic, V., Zivkovic, M., Stojanov, D., Milojkovic, O., Kalauzi, A., & Saponjic, J. (2017). Slower EEG alpha generation, synchronization and "flow"—possible biomarkers of cognitive impairment and neuropathology of minor stroke. *PeerJ*, *5*, Article e3839. https://doi.org/10.7717/peerj.3839

Pinter, D., Kober, S. E., Fruhwirth, V., Berger, L., Damulina, A., Khalil, M., Neuper, C., Wood, G., & Enzinger, C. (2021). MRI correlates of cognitive improvement after home-based EEG neurofeedback training in patients with multiple sclerosis: A pilot study. *Journal of Neurology, 268*(10), 3808–3816. https://doi.org/10.1007/s00415-021-10530-9

Rance, M., Walsh, C., Sukhodolsky, D. G., Pittman, B., Qiu, M., Kichuk, S. A., Wasylink, S., Koller, W. N., Bloch, M., Gruner, P., Scheinost, D., Pittenger, C., & Hampson, M. (2018). Time course of clinical change following neurofeedback. *NeuroImage, 181*, 807–813. https://doi.org/10.1016/j.neuroimage.2018.05.001

Surmeli, T., Eralp, E., Mustafazade, I., Kos, H., Özer, G. E., & Surmeli, O. H. (2016). Quantitative EEG neurometric analysis–Guided neurofeedback treatment in dementia. *Clinical EEG and Neuroscience, 47*(2), 118–133. https://doi.org/10.1177/1550059415590750

Tosti, B., Corrado, S., Mancone, S., Di Libero, T., Rodio, A., Andrade, A., & Diotaiuti, P. (2024). Integrated use of biofeedback and neurofeedback techniques in treating pathological conditions and improving performance: A narrative review. *Frontiers in Neuroscience, 18*, Article 1358481. https://doi.org/10.3389/fnins.2024.1358481

Trambaiolli, L. R., Cassani, R., Mehler, D. M. A., & Falk, T. H. (2021). Neurofeedback and the aging brain: A systematic review of training protocols for dementia and mild cognitive impairment. *Frontiers in Aging Neuroscience, 13*, Article 682683. https://doi.org/10.3389/fnagi.2021.682683

Tugasworo, D., Agung, L., Retnaningsih, R., Husni, A., Bintoro, A. C., & Wati, A. P. (2023). The correlation of glial fibrillary acid protein level to cognitive function outcome in acute lacunar ischemic stroke patient. *Open Access Macedonian Journal of Medical Sciences, 11*(B), 330–334. https://doi.org/10.3889/oamjms.2023.11393

Vilou, I., Varka, A., Parisis, D., Afrantou, T., & Ioannidis, P. (2023). EEG-neurofeedback as a potential therapeutic approach for cognitive deficits in patients with dementia, multiple sclerosis, stroke and traumatic brain injury. *Life, 13*(2), 365. https://doi.org/10.3390/life13020365

Weber, L. A., Ethofer, T., & Ehlis, A.-C. (2020). Predictors of neurofeedback training outcome: A systematic review. *NeuroImage: Clinical, 27*, Article 102301. https://doi.org/10.1016/j.nicl.2020.102301

Wigton, N., & Krigbaum, G. (2015). A review of qEEG-guided neurofeedback. *NeuroRegulation, 2*(3), 149–155. https://doi.org/10.15540/nr.2.3.149

Zhou, W., Nan, W., Xiong, K., & Ku, Y. (2024). Alpha neurofeedback training improves visual working memory in healthy individuals. *Npj Science of Learning, 9*(1), Article 32. https://doi.org/10.1038/s41539-024-00242-w

Zuo, L., Dong, Y., Liao, X., Pan, Y., Xiang, X., Meng, X., Li, H., Zhao, X., Wang, Y., Shi, J., & Wang, Y. (2022). Risk factors for decline in Montreal Cognitive Assessment (MoCA) scores in patients with acute transient ischemic attack and minor stroke. *The Journal of Clinical Hypertension, 24*(7), 851–857. https://doi.org/10.1111/jch.14453

Received: May 30, 2025
Accepted: July 3, 2025
Published: March 31, 2026

NeuroRegulation

ISNR INTERNATIONAL SOCIETY FOR NEUROREGULATION & RESEARCH

Developing and Applying a QEEG-Informed Transcranial Electrical Stimulation Protocol to Remediate Stuttering in Adults Who Stutter

Masoumeh Bayat[1], Reza Boostani[2], Mohammadreza Pirmoradi[3], Malihe Sabeti[4], Fariba Yadegari[5], Niloofar Fallahinia[6], and Mohammad Nami[7]*

[1]Iran University of Medical Sciences, School of Behavioral Sciences and Mental Health, Tehran, Iran
[2]Shiraz University, Shiraz, Iran
[3]Iran University of Medical Sciences, School of Behavioral Sciences and Mental Health, Tehran, Iran
[4]Islamic Azad University, Department of Computer Engineering, North-Tehran Branch, Tehran, Iran
[5]University of Social Welfare and Rehabilitation Sciences, Department of Speech and Language Pathology, Tehran, Iran
[6]Tehran University of Medical Sciences, Research Center for Cognitive and Behavioral Sciences, Tehran, Iran
[7]Shiraz University of Medical Sciences, School of Advanced Medical Sciences and Technologies, Shiraz, Iran

Abstract

Introduction. This study investigated whether personalized transcranial direct current stimulation (tDCS) protocols informed by quantitative EEG (qEEG) patterns could enhance treatment outcomes in adults who stutter (AWS), addressing individual variability in neural activity. **Methods.** Twenty male AWS participated in a double-blind, randomized controlled trial. EEG signals were recorded during speech tasks to differentiate neural substrates of fluent and stuttered speech. Over 10 days, participants received 10 sessions of speech therapy combined with tDCS. The experimental group received personalized tDCS (2 mA for 25 min per session) targeting regions identified through qEEG, while the control group received standard stimulation over FC5. Behavioral outcomes (SSI-4 scores) and EEG metrics were compared pretreatment, posttreatment, and at 3-month follow-up using repeated-measures ANOVA. **Results.** Both groups exhibited significant reductions in stuttering severity posttreatment. However, the study group maintained greater fluency at follow-up ($p < .001$). EEG analysis revealed that the study group demonstrated enhanced delta power in the FC5, reduced phase coherence in motor-auditory-somatosensory networks, and greater suppression of high-frequency bands in the personalized group. **Conclusion.** Personalized, qEEG-informed tDCS protocols yielded more sustainable fluency improvements than conventional tDCS, highlighting the potential of individualized neuromodulation strategies for treating stuttering.

Keywords: stuttering; qEEG; individualized tDCS; power spectrum; phase coherence

Citation: Bayat, M., Boostani, R., Pirmoradi, M., Sabeti, M., Yadegari, F., Fallahinia, N., & Nami, M. (2026). Developing and applying a qEEG-informed transcranial electrical stimulation protocol to remediate stuttering in adults who stutter. *NeuroRegulation, 13*(1), 20–42. https://doi.org/10.15540/nr.13.1.20

***Address correspondence to**: Mohammad Nami MD, PhD, Department of Neuroscience, School of Advanced Medical Sciences and Technologies, Shiraz University of Medical Sciences, Shiraz, Iran. Email: mohammad.nami@brainmappingfoundation.org

Edited by:
Rex L. Cannon, PhD, Currents, Knoxville, Tennessee, USA

Reviewed by:
Rex L. Cannon, PhD, Currents, Knoxville, Tennessee, USA
Randall Lyle, PhD, Mount Mercy University, Cedar Rapids, Iowa, USA

Introduction

Stuttering is a neurodevelopmental disorder (Smith & Weber, 2016) that affects nearly 5% of children and persists into adulthood in approximately 1% of cases (Yairi & Carrico, 1992). This condition is characterized by involuntary prolongations, repetitions, hesitations, and blocks at the sound, syllable, and word levels, which interfere with normal speech (Jiang et al., 2012). Despite its detrimental

effects on the quality of life, interpersonal relationships, and socioeconomic opportunities of adults who stutter (AWS; Craig et al., 2009; Farrahi et al., 2021; Yaruss, 2010), stuttering presents challenges from both clinical and pathological perspectives. Several neuroimaging studies investigating the neurological basis of stuttering suggest that it is a motor speech disorder with structural and functional abnormalities in specific brain subsystems. Although meta-analyses have yielded robust findings, several controversial issues remain (Etchell et al., 2017). These controversies are primarily due to group studies conducted on individuals who stutter. For example, Wymbs et al. (2013) conducted a study using functional magnetic resonance imaging (fMRI) while four AWS read single words. They found that while the level of within-subject agreement during the task was very high across two separate sessions, the level of between-subject agreement was low (Wymbs et al., 2013). This discrepancy is also evident in electrophysiological studies of stuttering. Research comparing the electroencephalogram (EEG) patterns of fluent and dysfluent states in AWS has indicated differences in brain regions, EEG frequency bands, and functional connections (Mersov et al., 2018; Sengupta et al., 2017; Vanhoutte et al., 2016). Stuttering research often distinguishes between those who stutter (the stuttering “trait”) and the behavior of stuttering (the stuttering “state”; Belyk et al., 2015). However, it provides limited insight into how brain activity in AWS may differ during episodes of stuttering compared to their brain activity during fluent speech.

Some studies on stuttering have introduced specific, different, and sometimes conflicting neurophysiological markers in the frequency ranges of theta (Ghaderi et al., 2018), alpha (Jenson et al., 2018; Saltuklaroglu et al., 2017; Wells & Moore, 1990), and beta (Jenson et al., 2018; Mersov et al., 2016; Saltuklaroglu et al., 2017). Alpha and beta oscillations have been examined more frequently than other frequency bands due to their roles in evaluating sensory feedback (alpha) and in the forward modeling of motor speech programs (beta; Korzeczek et al., 2022). Given the discriminative role of speech preparation in stuttering, many studies have compared the neural activities preceding fluent and disfluent utterances in AWS. Vanhoutte et al. (2016) found that the amplitudes of the contingent negative variation (CNV) before stuttered speech in AWS were not significantly different from the CNV amplitudes observed during fluent speech in fluent speakers. This finding suggests that the neural activity associated with stuttered speech in AWS exhibits similar signal properties to that of fluent speech, indicating the existence of compensatory mechanisms that support fluent speech despite the presence of stuttering (Vanhoutte et al., 2016). While some investigations have demonstrated poor alpha and beta suppression preceding speech in individuals with a stuttering trait (Bayat et al., 2024; Jenson et al., 2020; Jenson et al., 2018), Korzeczek et al. (2022) reported that stuttering severity in AWS is correlated with low beta power during prefluent speech preparation (Korzeczek et al., 2022). In a previous study from this lab on the same sample, the possibility of associating the delta band with the fluency state was also raised (Bayat et al., 2024).

Motor imagery (MI) is a condition examined within stuttering research. Imagined stuttering demonstrates a significant correlation with overt stuttering during a paragraph reading task in a positron emission tomography (PET) study (Ingham et al., 2000) and in a word production task during fMRI (Wymbs et al., 2013), particularly in terms of regional brain activation. Both imagined and overt stuttering display comparable neural activation patterns, especially within motor-related brain regions such as the supplementary motor area (SMA), anterior insula, and cerebellum (Ingham et al., 2000). This finding suggests that the neural underpinnings of stuttering involve these areas, regardless of whether the stuttering is real or imagined. Studies with high temporal resolution to investigate imagined speech indicate that, although covert (i.e., imagined) speech does not require movement or produce reafferent feedback, forward models of speech targets and anticipated sensory feedback are activated through a purely internal loop (Tian & Poeppel, 2010, 2012).

However, due to the neurological nature of the disorder, neural modulation, which is widely used in patients with neurological diseases (Paik, 2015), is an option being considered for stuttering. Applying transcranial electrical stimulation (tES) is one of these techniques that has shown remarkable results in speech and language disorders. Busan et al. (2021) presented noninvasive brain stimulation as a promising intervention to enhance brain function in individuals who stutter. In evaluating recent advancements in stuttering treatment, they explored how direct brain interventions can improve speech fluency (Busan et al., 2021). Brignell et al. (2020) included transcranial direct current stimulation (tDCS) among effective intervention approaches for stuttering (Brignell et al., 2020). The combination of neuromodulation techniques with more “conventional” interventions has been proposed as

an emerging strategy for treating stuttering (Busan et al., 2021). Several studies have investigated the use of tDCS in AWS. Some of these studies employed a single-session design (Chesters et al., 2017; Garnett et al., 2019; Karsan et al., 2022; Tezel-Bayraktaroglu et al., 2020; Yada et al., 2019), while others used a multisession design (Bakhtiar et al., 2023; Bashir & Howell, 2015; Chesters et al., 2018; Moein et al., 2022). Two of the single-session studies reported improvement in stuttering severity (Karsan et al., 2022; Yada et al., 2019). Chesters et al. (2018) succeeded in reducing the rate of stuttering during conversation and reading by performing five sessions of anodal stimulation on the FC5 electrode, although this fluency was not stable during conversation after 6 weeks (Chesters et al., 2018). Moein et al. (2022) and Bakhtiar et al. (2023) also reported promising results from using tDCS along with fluency shaping techniques (Bakhtiar et al., 2023; Moein et al., 2022).

The application of tDCS is grounded in a thorough understanding of the neurological basis of the disorder in question. Studies have shown that tDCS, particularly when administered over the left inferior frontal cortex, can significantly reduce stuttering in adults. This improvement is often noted when tDCS is combined with fluency-inducing techniques, such as choral and metronome-timed speech (Chesters et al., 2018; Moein et al., 2022; Taherifard et al., 2021). It demonstrates potential as an adjunctive treatment for stuttering by enhancing neural plasticity and modulating the brain networks, such as the left inferior frontal cortex, anterior insula, and SMA, which are involved in planning and initiating speech movement (Chesters et al., 2018; Chesters et al., 2021). Although tDCS can lead to significant improvements in speech fluency—especially when combined with behavioral therapies—(Garnett et al., 2019), additional research is necessary to optimize its application and understand its long-term benefits.

Quantitative EEG (qEEG) is a powerful and sensitive tool for identifying maladaptive brain activity patterns. Behavioral and mental states—such as reading, visualizing, or speaking—are assumed to be distinct yet uniform, involving similar perceptual and cognitive operations whenever they occur. It is also assumed that each mental operation presents a unique EEG and biochemical profile, reliably reproduced whenever the task or mental state occurs (Kaiser, 2007). QEEG employs advanced techniques for EEG signal feature extraction, including the analysis of specific frequency bands and connectivity (Popa et al., 2020). Implementation of qEEG in clinical practice has the potential to guide personalized medicine, which involves tailoring treatments to individual patients (Keizer, 2019). Since the effects of tDCS depend on the brain's baseline status at the time of application, individual patients exhibit considerable heterogeneity in treatment outcomes (Woods et al., 2016). Bjekić et al. (2022) reported that extracting the dominant theta-band frequency, based on associative memory-evoked EEG changes, can reliably be used to personalize oscillatory tES techniques (Bjekić et al., 2022). Personalized channel selection in brain-computer interfaces (BCI) based on EEG creates a direct pathway between the brain and external devices (Ma et al., 2023). Mastakouri et al. (2017) proposed personalized EEG-informed BCI training and tES to derive optimal tES parameters, such as stimulation site and frequency, as a novel intervention for motor performance rehabilitation in stroke patients (Mastakouri et al., 2017). Depending on the specific stimulation parameters, various tES paradigms can be differentiated, including tDCS and transcranial alternating current stimulation (tACS). Parameters such as intensity, duration, frequency, and the location and size of electrodes enable control over both the immediate effects and aftereffects of tES (Paulus et al., 2013). Brain imaging techniques are utilized to evaluate alterations in both the structure and function of specific brain regions prior to and following tDCS, in addition to measuring the propagation of the tDCS signal throughout the brain (Bashir & Howell, 2015). Garnett et al. (2019) examined the neural effects of high-definition tDCS (HD-tDCS) on the SMA employing fMRI.

Given the significant individual and group differences in relevant research results, we planned to develop personalized protocols based on the qEEG patterns of AWS to enhance the effectiveness and durability of the outcomes from the tDCS protocols. We hypothesized that AWS have distinct neural circuits underpinning fluent versus dysfluent states, prompting us to develop a protocol to differentiate the neural substrates of fluent and stuttered speech by analyzing EEG signals recorded during two speech tasks. Based on the findings of the previous study assessing the brain dynamics of speech preparation (SP) and imagined speech (IS) production in AWS (Bayat et al., 2024), we aimed to improve the quality and quantity of recorded signals by analyzing neural oscillations associated with both SP and IS. For each subject, we identified the areas that exhibited the most significant signal energy differences between the two fluency states. The corresponding areas were potentiated with anodal stimulation if their increased EEG activation was

associated with fluent speech, while they were inhibited with cathodal stimulation if their increased EEG activation was associated with stuttering. Participants in the study group received personalized stimulation, while those in the control group received conventional anodal stimulation of the FC5 electrode (Chesters et al., 2018). Since we utilized EEG to identify the area and modality of stimulation, we opted to investigate the effects of the intervention utilizing the same methodological approach. Due to the numerous parameters that must be controlled and conflicting data regarding the role of specific band frequencies in stuttering, we decided to limit the controlled parameters in the offline EEG to montages and current polarity, opting for tDCS instead of tACS.

We hypothesized that, consistent with previous studies, the study group would differ from the control group by exhibiting increased suppression of alpha and beta bands (Jenson et al., 2020; Korzeczek et al., 2022) and enhanced activation in the delta range (Bayat et al., 2024). One method of analyzing functional connectivity in the realm of frequency is measuring the degree of phase correlation. Phase coherence is the most common technique used to assess connectivity in studies related to language functions (Gaudet et al., 2020). To date, no study has examined the electrophysiological implications of treatment on functional connectivity. When comparing fluent and stuttered speech in AWS in terms of phase coherence, Sengupta et al. (2017) reported an increase in phase coherence across theta, alpha, and gamma bands at the left frontal electrodes while preparing for stuttered utterances. They attributed this increase in phase coherence during the preparation for stuttered utterances to heightened general activity associated with stuttering (Sengupta et al., 2017). Accordingly, successful treatment may modulate enhanced functional connectivity associated with the stuttering state, although the investigation of phase coherence in this research is primarily exploratory.

Therefore, we applied fast Fourier transform (FFT) relative band power and the FFT phase coherence algorithm in NeuroGuide to compare the two groups based on their posttreatment signal features. The study was a double-blind, randomized controlled trial with a pretest, posttest, and follow-up design.

Material and Methods

Participants

Twenty-two native Persian-speaking men (mean age: 35 ± 4 years, range 21–42) with persistent developmental stuttering participated in this study. They had no known history of hearing or other speech-language disorders, except for stuttering, and did not have any neurological disorders. Participants were screened for any safety contraindications for tDCS, particularly regarding a history of seizures. Subjects received compensation for their participation. Recruitment was conducted through convenience sampling among patients referred to our community mental health care setup who met the inclusion criteria. All subjects were right-handed (Oldfield, 1971), and their stuttering severity ranged from mild to very severe according to the Persian version of the Stuttering Severity Instrument, Fourth Edition (SSI-4; Tahmasebi et al., 2018). The signals of two subjects were excluded from the analysis due to technical issues, and the data from the remaining 20 subjects were analyzed. It should be noted that the initial qEEG data used in this study was the same as that from our previous study (Bayat et al., 2024), but this study focused on qEEG-informed tDCS, while the previous research speculated on qEEG features in a stuttering state. Written informed consent was obtained from all participants. The institutional ethical review board at Shiraz University of Medical Sciences (IR.SUMS.REC.1397.712) approved all experimental procedures.

Experimental Procedure

The flow diagram of the experimental design (Figure 1) provides an overview of the study procedure. Neural correlations of fluent and nonfluent speech were investigated and compared by analyzing EEG signals during speech tasks in two stages: first, at the beginning of the study to determine the regions of interest (ROIs) for tDCS, and second, at the end of the study to evaluate the intervention results. The speech tasks and signal acquisition process were similar in both stages. Figure 2 illustrates the process of obtaining, preprocessing, analyzing, and comparing the signals, as well as assigning subjects to the study and control groups.

Verbal Stimuli and Experimental Tasks

We employed 50 verbal stimuli (e.g., “Name your two friends” and “Say two fruits that start with the letter A”) as the outcome measure during the signal acquisition phase. This research represents a continuation of our previous studies, and the verbal stimuli as well as their presentation methodology are consistent with the procedures outlined by Bayat et al. (2023). The experimental design comprised five blocks, with 50 verbal stimuli presented in a random order within each block, resulting in 250 trial.

Figure 1. *Flow Diagram of Experimental Design.*

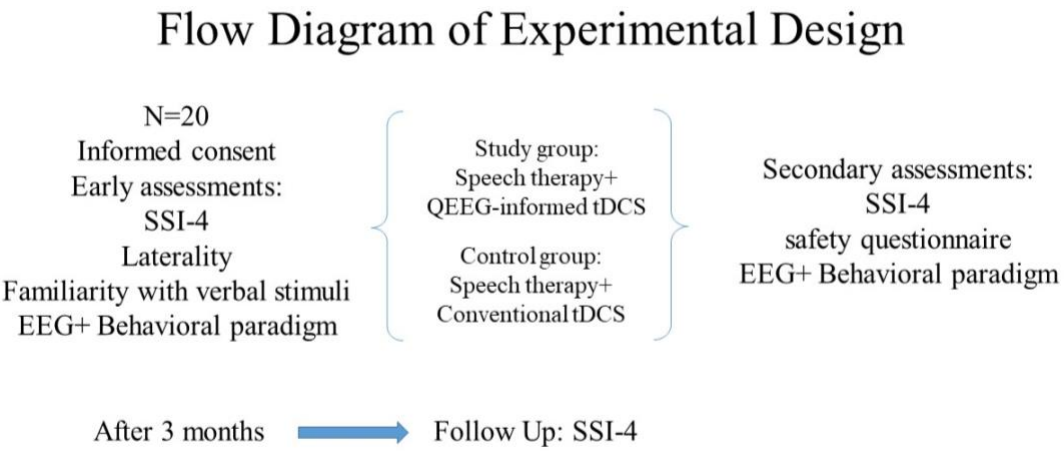

Figure 2. *A Snapshot From Experimental Design Regarding EEG Signal.*

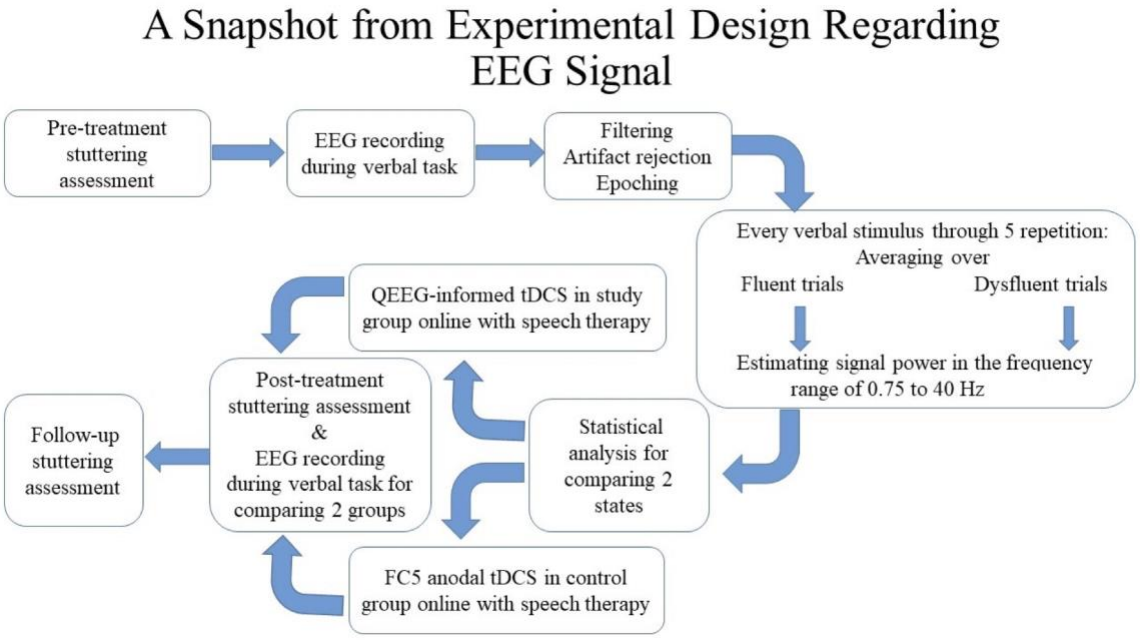

Each verbal stimulus was presented five times to increase the likelihood of achieving the desired conditions through adaptation or sensitization. This repetition aimed to elicit both fluent and disfluent responses from the participants. The adaptation or sensitization effect benefits our task by ensuring that the person experiences both stuttered and stutter-free trials during the five repetitions. Therefore, we do not want to control for this. A schematic representation of each trial and block is illustrated in Figure 3. This methodology enabled us to compare the signals of identical utterances while differentiating them based on fluency.

Initially, participants read a verbal stimulus in silence and prepared to answer it, after which they responded aloud. They were then required to determine whether they had stuttered. In the next two steps, they were asked to imagine and whisper their own utterance (the aloud answer) while maintaining the same fluency state (Figure 3). Each trial consisted of five icons representing five events presented on a PC screen using Psychtoolbox-3 through open-source MATLAB and GNU Octave functions for vision and neuroscience research (available at https://psychtoolbox.org/docs /DownloadPsychtoolbox). Details of the executive

procedure can be found in the study by Bayat et al. (2023).

To compensate for the low number of qualified trials, we decided to use the two conditions of SP and IS (among four speech-related tasks) in each trial to indirectly increase the number of available signals. This approach effectively doubled the opportunities to observe neural activity associated with both fluent and disfluent speech states. Although SP and IS tasks involve different cognitive and motor demands, they share overlapping neural mechanisms related to speech preparation and internal monitoring (Bayat et al., 2024). Two events associated with two tasks within specified time windows were selected for analysis and comparison: 2.5 s before the appearance of the speaker icon, designated as SP, and the middle 2 s of the imagining task, referred to as the IS.

During the IS condition, participants were instructed to visualize their responses from the previous step, using the same words and fluency (Figure 4). The first 500 ms of IS were excluded to reduce interference from the previous section. Similarly, the last 500 ms of IS were removed to ensure that the intended activity was captured before it finished. The sections of answering aloud and whispering were excluded from the final analyses. The whisper section (WH) was excluded at this stage due to insufficient evidence in the literature to support a correlation between the whispering condition and the other two conditions used. Additionally, because speech, especially stuttering, generates significant noise in the EEG, most studies prefer not to include parts of this section in signal analysis. A well-trained speech-language pathologist (SLP) supervised the procedure. If a participant responded with incorrect timing (e.g., answering before the relevant cues appeared) or exhibited excessive movement during task execution, the trial was classified as a rejected trial. The same protocol applied to trials in which questions were left unanswered by the examinees. A second SLP reviewed the recorded videos of the subjects during the task and assessed the trials based on their fluency offline. The video recordings were adjusted to ensure that the faces and upper bodies of the participants were visible to the SLP. A trial was considered dysfluent only if the subject and both SLPs agreed on this assessment. Similarly, trials were classified as fluent if the subject and both SLPs deemed them fluent. Participants' own assessments of the presence or absence of stuttering were effective in determining trial classifications. Before the test, participants were instructed to identify even an inaudible uncomfortable feeling as stuttering. Conversely, speech therapists were asked to label only those trials they were completely certain about as stuttering. This approach helped manage the common issues associated with stuttering-state studies. We accepted the risk of mistakenly rejecting some trials to ensure that trials in which the subject pressed the button incorrectly would not be classified as stuttered trials and would be excluded from the experiment. Participants were familiar with the verbal stimuli 1–3 weeks before the experiment. The signals from two subjects were not properly marked due to problems with the parallel port systems, resulting in their exclusion from the analysis. Consequently, the data from the remaining 20 subjects were analyzed.

Behavioral Evaluation

Stuttering severity was evaluated using the Persian version of the SSI-4 tool (Tahmasebi et al., 2018). This reliable and valid norm-referenced assessment tool is suitable for both clinical and research purposes (Riley & Bakker, 2009). The SSI-4 measures stuttering severity across four areas of speech behavior: frequency, duration, physical concomitants, and the naturalness of the individual's speech. Two qualified independent SLPs assessed the stuttering severity. The first SLP was trained by the second SLP, who developed the Persian version of the SSI-4, to evaluate and score stuttering severity and related behaviors. The stuttering evaluation process was conducted in three stages: 7–10 days before the intervention, 3–7 days after the intervention, and 3 months after the intervention during the follow-up stage.

Electrical Neuroimaging-EEG Acquisition

EEG data were recorded at a sampling rate of 512 Hz using a 64-channel BrainVision amplifier (Mulgrave, Australia). The active electrodes were arranged on an elastic cap according to the standard 10–10 electrode positioning system, and the electrical impedance of the scalp electrodes was maintained below 5 kΩ. Subjects were instructed to minimize eye blinks and body movements during the three events: SP, IS, and WH. Approximately 2-min pauses between blocks were implemented to prevent fatigue and muscle tension. The parallel port system delivered a marking pulse with the display of each icon to synchronize EEG signals for accurate offline analysis. The procedure of EEG recording was accomplished in two stages, 1–2 weeks before and 5–10 days after the intervention.

Figure 3. *The Study Design Representing a Trial and a Block. A) Timing of Tasks and Their Corresponding Icons B) Time Windows of Investigated Events.*

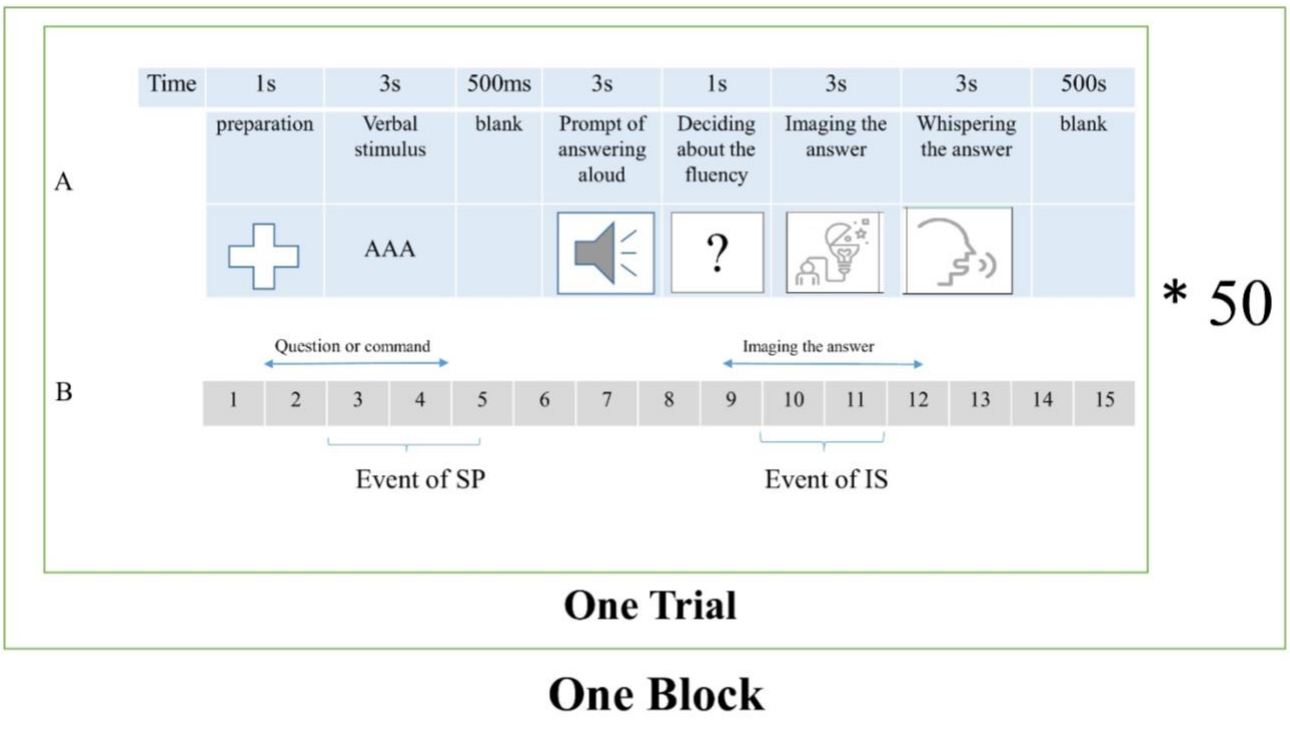

Quantitative Analysis of the EEG (qEEG)

Filtering, Artifact Rejection, and Separation of Fluent and Disfluent Trials. Once these trials were evaluated by SLPs and participants, MATLAB R2018b software was used to separate the signal and analyze its power for fluent versus disfluent conditions. These tasks were entirely separate, with human evaluation ensuring accuracy in classification and MATLAB providing precise, objective segmentation for signal analysis. EEG signals from each subject were imported into MATLAB-based EEGLAB_14_1_2b open-source software (Delorme & Makeig, 2004). The signals were then filtered using a fifth-order Butterworth bandpass filter with cut-off frequencies of 0.75 Hz and 45 Hz. The average montage for EEG acquisition was utilized.

Training for independent component analysis (ICA) was performed using the "Runica" algorithm in EEGLAB. This process resulted in 64 independent components corresponding to the number of recording electrodes. ICA is an effective tool for unmixing volume-conducted EEG signals, yielding components from both neural and nonneural sources, such as muscular and artifactual sources (Bell & Sejnowski, 1995; Olbrich et al., 2011). Training was stopped by default when the weight change was below 1×10^{-7} for more than 33 channels.

The ADJUST.1.1.1 tool (an open-source EEGLAB plugin available at https://sccn.ucsd.edu /wiki/Plugin_list_all), was employed to detect nonneural sources. ADJUST is a fully automated algorithm that identifies independent components of artifacts by combining stereotyped spatial and temporal features. These functions are optimized to capture blinks, eye movements, and frequent discontinuities in the feature selection dataset. The algorithm then provides a fast, efficient, and automated process for applying ICA to remove artifact (Mognon et al., 2011). After the removal of the detected components utilizing the ADJUST plug-in, an experienced neuroscientist performed a visual inspection to identify components resulting from muscle tension artifacts and faulty channels. Components associated with blinking or speaking tension were also eliminated. Channels identified by the neuroscientist as faulty were interpolated employing a spherical method for each participant.

Items for which responses across the five repetitions included both fluent and disfluent utterances were extracted, while those that were consistently fluent or disfluent across all five blocks were excluded. This approach allowed for a comparison of neural activation between two brain states differing by a singular feature (e.g., fluency vs. disfluency), while sharing linguistic aspects (e.g., the verbal stimulus

as well as the phonological and semantic components of the response). The signals accompanying fluent and stuttered responses were subsequently averaged separately for each verbal stimulus across the two tasks (i.e., SP and IS) at each electrode. This approach aimed to equalize the sample sizes of the fluent and stuttered utterances. The number of accepted verbal stimuli (items) for each participant is presented in Table 1.

ROIs, Current Types, and Signal Processing for Individualized Stimulation

In this stage, electrodes were allocated to 13 areas based on their involvement in speech and language. This allocation was accomplished using an algorithm introduced by Giacometti et al. (2014) for assigning scalp coordinates of EEG electrodes to cortical areas. We applied a reference table that correlates electrode proximity with cortical regions, consistent with our 64-channel system and the international 10–10 system. We then selected the ROIs for stimulation by comparing the signals associated with fluent and stuttered utterances from the electrodes in these 13 areas. This comparison was based on the accepted trial signals for each participant. The selected 13 areas along with their corresponding scalp electrodes are provided in Table 2. The average signal power in the frequency domain was computed for fluent versus dysfluent items between 0.75 and 40 Hz using FFT in MATLAB software. Band-power features, which represent the power of the EEG signal in specific frequency bands, are commonly used to identify and classify mental states. Kuremoto et al. (2017, 2018) proposed a feature extraction method using FFT and selected discriminant coefficients by maximizing the area under the curve (AUC) of the receiver operating characteristic (ROC) to differentiate among various classes of mental tasks. Variations in all EEG bands during both fluent and dysfluent speech production have been observed (Ghaderi et al., 2018; Jenson et al., 2020; Mersov et al., 2016; Piai & Zheng, 2019; Rimmele et al., 2018; Saltuklaroglu et al., 2017; Sengupta & Nasir, 2016). In this study, the power of all signals in the frequency range of 0.75 to 40 Hz was considered as the EEG feature, without separating them into specific frequency bands, which include delta, theta, alpha, beta, and gamma EEG bands. The power of EEG signals corresponding to fluent and dysfluent responses was compared for each participant using paired *t*-tests and the AUC of the ROC. This estimation was performed across 13 areas to identify ROIs. The procedure for selecting the ROIs involved finding the area with a) the lowest *p*-value resulting from the aforementioned *t*-test, provided there were significant differences ($p < .05$), and b) the highest AUC, if any measures exceeded 70% in the SP condition. An alternative option was to select an area that demonstrated both the lowest *p*-value and the highest AUC in the two conditions of SP and IS (a total of four measures) for participants who did not meet the two criteria. This area was determined based on a voting process among the specified measures, with the area receiving the most votes chosen as the ROI. The type of current applied in the study group (anodal or cathodal) was selected according to the sign of the difference in the measurement of fluent and dysfluent signal power in the selected ROI for each participant. In other words, participants in the study group received anodal stimulation if the sign of the difference indicated that the signal power associated with fluency was higher. Conversely, they received cathodal stimulation if the signal power associated with stuttering was higher. The control group received anodal stimulation over the FC5 electrode.

Table 1

The Number of Accepted Items of Verbal Stimuli From the Total of 50 Presented Verbal Stimuli in Each 20 Participants

Participant Number	1	2	3	4	5	6	7	8	9	10	11	12	13	14	15	16	17	18	19	20
Total Number of Accepted Verbal Stimuli	34	15	17	40	28	8	35	15	11	41	32	13	24	17	25	21	13	9	14	25

The priority of the SP condition was related to its determining role in stuttering (Mersov et al., 2018; Mersov et al., 2016; Vanhoutte et al., 2016). In determining the ROIs, when no area met the criteria of a significant paired *t*-test and an AUC above 70%, we used the signals from the two studied conditions, SP and IS. To compare the correlation between the two conditions, we separately calculated the differences in average signal power for fluent and dysfluent items across both conditions for all participants within their ROIs. The Pearson correlation coefficient was used to compare the obtained values and investigate the correlation between the two conditions of SP and IS. This procedure was completed for both pre- and posttreatment signals.

Stimulation and Online Speech Therapy

Participants were randomly assigned to study and control groups in this stage. Both groups received stimulation at 2 mA for 25 min using 5x5 cm electrodes while applying fluency shaping methods. Because the study was double-blind, each participant experienced both personal and conventional montages. This design ensured that neither the participants nor the SLP could identify which group the individuals were assigned to based on the montage used. By using NeuroStim 2 (made in Iran), the personalized tDCS protocol in the study group delivered real stimulation, while the control group received real anodal stimulation applied just over the FC5 area. While one montage delivered real stimulation, the other was set to sham. The cathode electrode was positioned on the right supraorbital ridge for conventional montages and on the opposite deltoid (extra cephalic) for individualized montages. No significant adverse effects were reported during or after the stimulation sessions. Participants were closely monitored, and while a few individuals reported minor discomfort, such as mild itching or tingling, this aligns with findings from previous studies on tDCS.

A certified SLP recorded the instructions and materials for fluency shaping methods, including easy onset and prolongation. In the first session, the subject watched a videotape in which the SLP explained these methods for 10 min. During the next 10 min, participants watched a prerecorded videotape of a speaker demonstrating the described techniques. In the final 10 min, the participant listened to a prerecorded voice and attempted to produce speech in unison with it. At this stage, an independent SLP corrected any issues related to the implementation of the method. From the second session to the end of the 10 sessions, prerecorded speech tasks containing the mentioned methods were used as therapeutic materials, and participants were asked to repeat the same patterns. The tasks began with single words and progressed to 8-word sentences. The SLP supervised the procedures and provided corrections as needed. Speech therapy was conducted online with tDCS.

Table 2

13 Selected Areas and Corresponding Scalp Electrodes According to 10–10 International System Consistent With 64-Channel EEG Recording According to the Algorithm Introduced by Giacometti et al. (2014)

Areas number	Laterality and name of the areas	Correspond electrodes
1	Right Pars Opercularis	32 & 9
2	Left Pars Opercularis	28 & 6
3	Right Triangularis	5 & 32
4	Left Triangularis	1 & 24
5	Right Superior Temporal Gyrus	14 & 41
6	Left Superior Temporal Gyrus	10
7	Right Inferior Parietal Cortex	22 & 45
8	Left Inferior Parietal Cortex	20 & 42
9	Right Banks Superior Temporal Sulcus	41 & 23
10	Left Banks Superior Temporal Sulcus	37
11	Right Precentral Gyrus	13 & 35
12	Left Precentral Gyrus	11 & 34
13	Paracentral Lobule	34, 12, & 35

Signal Analyses

NeuroGuide software compared FFT relative power and FFT phase coherence measures in the fluent state before and after the intervention between the study and control groups across the 19 default electrodes of the software, following the 10–20 system. The comparison at the pretreatment stage aimed to investigate the homogeneity of the two groups. NeuroGuide software (NG 3.0.9; Applied Neuroscience, St. Petersburg, FL, USA) is a sophisticated tool developed for analyzing frequency power and connectivity measures of EEG signals (available at https://appliedneuroscience.com /neuroguide/ and https://anineuroguide.com/; Cannon et al., 2012).

The FFT method employs mathematical techniques to analyze EEG data. Characteristics of the acquired EEG signal are computed using power spectral density (PSD) estimation to selectively represent the EEG samples signal (Al-Fahoum & Al-Fraihat, 2014). A phase correlation coefficient indicates the amount of variance in one signal that can be explained by another signal, and it is a normalized quantity ranging between 0 and 1 (Bastos & Schoffelen, 2016). Phase coherence is the most common technique used to measure connectivity in research on functional brain communication related to language functions (Gaudet et al., 2020). Since the study aims to select the appropriate type of individualized stimulation based on patterns of neural activity associated with fluent speech, we planned to compare the two groups in terms of neural activity during fluency. Subsequently, the posttreatment analysis compared the two groups in the fluent state to investigate the effects of the two protocols on the neural circuits involved in fluency.

Statistical Analyses

The homogeneity of the two groups was investigated regarding age, education, and stuttering severity using an independent *t*-test or its nonparametric equivalent before the intervention. The stuttering severity of the two groups was compared across three time points—pretreatment, posttreatment, and follow-up stages—using repeated measure ANOVA (rmANOVA). In this analysis, the three time points served as the within-subject factor with three levels, while the stimulation protocol was the between-subject factor, and the dependent variable was the severity of stuttering as measured by SSI-4 scores. The interaction between time and group was significant, $F(1) = 17.95$, $p < .001$, so a 2*2 rmANOVA was applied to compare the two groups at the pretreatment versus posttreatment and a 2*2 rmANOVA to compare pretreatment versus follow-up time points. A one-way repeated measures ANOVA (rmANOVA) for pairwise comparison of the three time points was performed to compare SSI-4 measures within each group separately. The correlation coefficient for the power difference of fluent and dysfluent signals between the SP and IS conditions was calculated using the Pearson correlation coefficient. Inter-rater reliability for stuttering severity scores rated by two SLPs was assessed using Cronbach's alpha coefficient. All of the aforementioned statistical analyses were conducted using SPSS-22 software. ROIs were determined using paired *t*-tests and AUC of the ROC method in MATLAB R2018b. The analysis and comparison of EEG signals between the two groups were conducted in NeuroGuide software, utilizing an independent *t*-test corrected for multiple comparisons.

Results

Homogeneity of Two Groups

Homogeneity of Behavioral and Demographic Features. The study and control groups were homogeneous in terms of education, $t(18) = 0.20$, $p = .739$, and age, $t(18) = 0.19$, $p = .315$. This homogeneity also applied to the severity of stuttering, as measured by the SSI-4, $t(18) = 0.185$, $p = .856$. Table 3 presents the mean and standard deviation for the demographic variables and stuttering severity from the early assessments.

Signal Homogeneity. Signals from the study and control groups did not reveal remarkable differences in FFT relative power and FFT phase coherence during the conditions of SP and IS in the fluent state. These results are depicted in Figures 2 and 3, respectively.

Table 3

Mean and Standard Deviation of Age, Education, and SSI4 Scores in Two Groups

	Age (Mean ± *SD*)	Education (Mean ± *SD*)	SSI-4 (Mean ± *SD*)
Study group	35.70 ± 1.94	14 ± 2.67	32.30 ± 8.96
Control group	32.5 ± 7.76	15 ± 1.94	31.60 ± 7.97

Figure 2. *Homogeneity of Two Groups According to Pretreatment through SP Condition.*

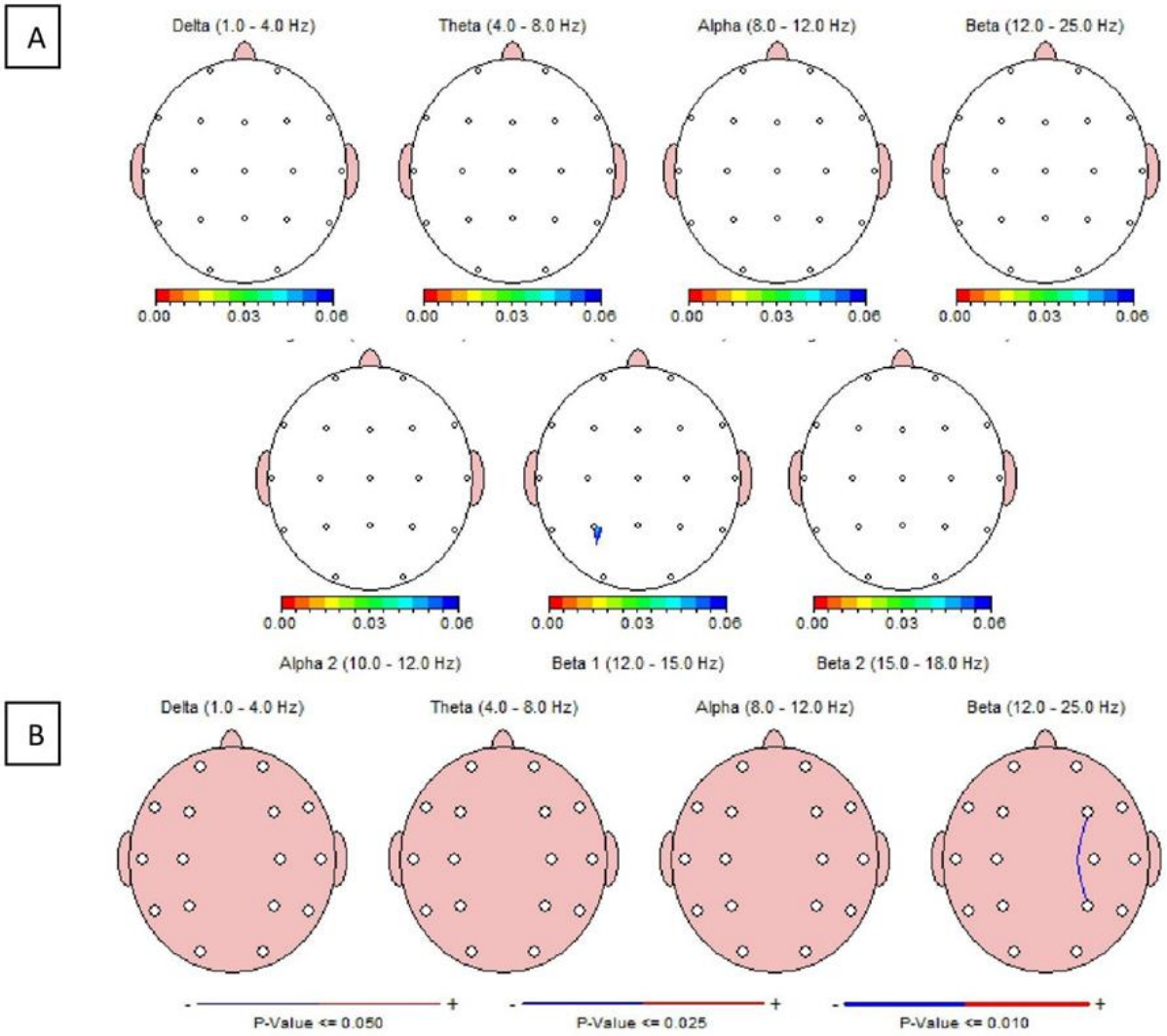

Note. Legend: A) FFT Relative Power and B) FFT Phase Coherence.

Figure 3. *Homogeneity of Two Groups According to Pretreatment Through IS Condition.*

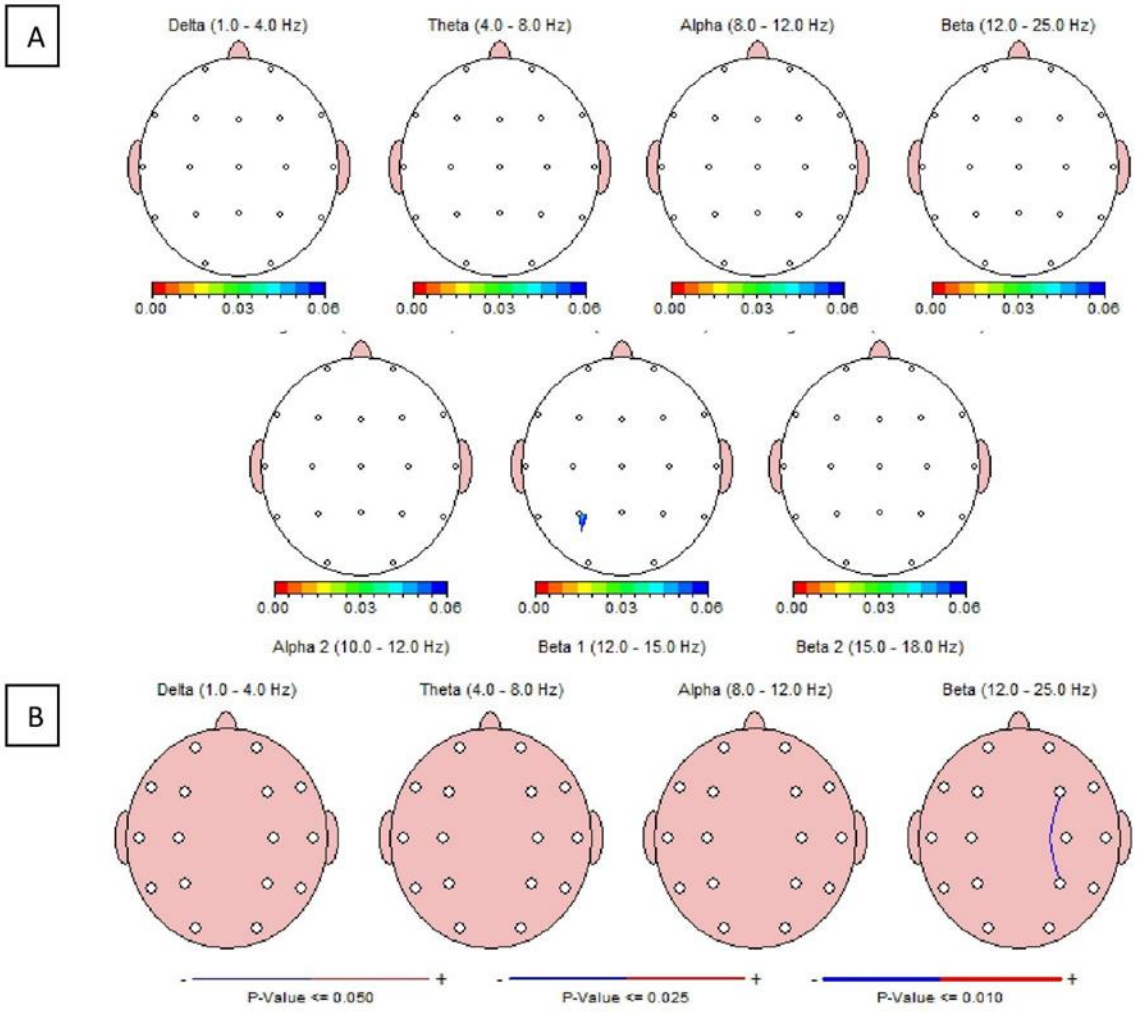

Note. Legend: A) FFT Relative Power and B) FFT Phase Coherence.

ROIs and Current Types

The ROIs, along with the measures of *p*-value and AUC for each participant, are presented in Table 4. Participants numbered 4, 5, and 7 met the first criteria: a) the lowest *p*-values indicating significant differences ($p < .05$), and b) the highest AUC of the ROC, with measures above 70% in the SP condition. The remaining seven participants were included based on the second criteria, which selected from the lowest *p*-values and the highest AUC measures in the SP and IS conditions. The types of current applied to each participant are shown in Table 5. Of the ten participants in the study group, six received anodal stimulation, while the remaining subjects received cathodal stimulation according to the difference in the measurement of fluent and dysfluent signal power in the selected ROI (Table 5). Since the study aimed to compare the effects of personalized stimulation with conventional stimulation, the impact of the type of stimulation (anodal vs. cathodal) was not investigated.

Additionally, the Pearson correlation test revealed a high correlation between the pretreatment power of EEG signals in the SP and IS conditions across the ROIs ($r = 0.87$, $n = 20$, $p < .001$). This correlation was also evident for the posttreatment power of EEG signals ($r = 0.900$, $n = 20$, $p < .001$).

Table 4

ROIs of Stimulation, the Areas With the Highest Measures of Area Under the Curve of the Receiver Operating Characteristic (AROC) and Their Detected Measures in SP and IS Conditions, the Areas With the Lowest P-Values and Their Detected Measures in SP and IS Conditions

Groups	Participants number	Area with the highest AROC according to SP	AROC measure according to SP	Area with the highest AROC according to SP	*p*-value measure according to SP	Area with the highest AROC according to IS	AROC measure according to IS	Area with the lowest *p*-value according to IS	*p*-value measure according to IS	ROI for stimulation
Study Group	1	9	0.6332	9	0.1439	9	0.7223	9	0.0118	9
	2	3	0.6978	1	0.1052	3	0.6267	3	0.3131	3
	3	3	0.8339	11	0.3555	6	0.9377	6	0.00026	6
	4	6	0.7075	6	0.022	6	0.6513	11	0.3251	6
	5	4	0.7015	4	0.0185	4	0.6359	4	0.3139	4
	6	4	0.5625	5	0.712	5	0.6094	5	0.3955	5
	7	12	0.7119	12	0.0081	12	0.8157	12	0.00083	12
	8	7	0.875	4	0.0879	13	0.9375	13	0.0517	13
	9	3	0.7591	3	0.1483	3	0.6275	3	0.09578	3
	10	6	0.6406	6	0.0616	6	0.6563	4	0.3624	6
Control Group	11	10	0.75	10	0.0028	8	0.7813	10	0.0024	2
	12	8	0.9586	8	0.0023	9	0.999	9	0.0021	2
	13	10	0.5937	10	0.3225	10	0.5781	10	0.3057	2
	14	4	0.9343	4	3.6E-05	9	0.9792	8	7.7E-05	2
	15	10	0.5603	10	0.3224	10	0.5781	10	0.3057	2
	16	13	1	2	0.0067	13	1	13	0.0301	2
	17	4	0.9941	4	6E-06	7	1	7	0	2
	18	4	0.5961	4	0.7129	1	0.6064	5	0.3955	2
	19	8	0.9586	8	0.0023	9	0.929	9	0.0021	2
	20	10	0.612	10	0.3224	12	0.5712	6	0.3433	2

Table 5
The Current Types According to the Difference Between the Signal Power Along With the Fluent and the Dysfluent States

Type of Applied Current	DS in the IS State	DS in the SP State	Participant Number
Anode	1.118100	1.524300	1
Cathode	−.037200	−.026400	2
Anode	.180200	.238100	3
Anode	.286000	.076500	4
Anode	.022800	.061500	5
Cathode	−.426800	−.171300	6
Cathode	−.234800	−.027500	7
Anode	.005000	.000900	8
Cathode	−.008400	−.021600	9
Anode	1.176400	.573000	10

Note. DS: Difference score, SP: speech preparation, IS: imagined speech; DS shows the difference between the signal power along with the fluent and the dysfluent states in the SP and IS states.

Behavioral Results

According to a 2*3 rmANOVA for SSI-4 measures, the main effect for the three levels of the within-group subject factor (pre, post, and follow-up) was significant, $F(2) = 76.96$, $p < .001$. However, no meaningful between-group subject effect was obtained, $F(1) = 3.53$, $p = .076$. The interaction between time and group was also significant, $F(1) = 17.95$, $p < .001$. A 2*2 rmANOVA was then applied to compare the two groups at the pretreatment versus posttreatment and pretreatment versus follow-up time points. The results indicated a preference for the study group during the follow-up stage (Table 6). Additionally, the results from a one-way rmANOVA for pairwise comparisons of the three time points are presented in Table 7 for SSI-4 measures. Stuttering severity significantly decreased after the intervention and increased 3 months later, yet remained significantly lower than the pretreatment level in both groups. The trend of stuttering severity across the three time points for the two groups according to the SSI-4 tool and scatter plots illustrating individual data points for the ANOVA results are illustrated in Figure 4A and Figure 4B, respectively. High inter-rater reliability was found (Kappa = 0.91, $p < .005$) for stuttering severity scores rated by two SLPs.

Table 6
Pairwise Comparisons of SSI-4 for Stuttering Severity scores of the Three Time Section in Two Groups

		Source	df	*F*	Sig.
2*2 rmANOVA	Comparing groups at pre vs. posttreatment	Time	1	95.31	$p < .001$*
		Group	1	0.21	$P = .65$
		Time*Group	1	0.86	$P = .37$
	Comparing groups at pretreatment vs. follow-up	Time	1	68.45	$p < .001$*
		Group	1	2.61	$P = .123$
		Time*Group	1	17.96	$p < .001$*

Note. Meaningful differences were shown with *in the column of Sig.

Table 7

Pairwise Comparisons of SSI-4 for Stuttering Severity Scores of the Three Time Point in Two Groups According to rm One-Way ANOVA

		Source	df	*F*	Sig.
2*2 rmANOVA	Comparing groups at pre vs. posttreatment	Time	1	95.31	$p < .001$*
		Group	1	0.21	$P = .65$
		Time*Group	1	0.86	$P = .37$
	Comparing groups at pretreatment vs. follow-up	Time	1	68.45	$p < .001$*
		Group	1	2.61	$P = .123$
		Time*Group	1	17.96	$p < .001$*

Note. Meaningful differences were shown with *in the column of Sig.

Figure 4. *A) Trend of Stuttering Severity Through the 3-Time Section in Two Groups. B) Scatter Plots Displaying Individual Data Points From the ANOVA Results.*

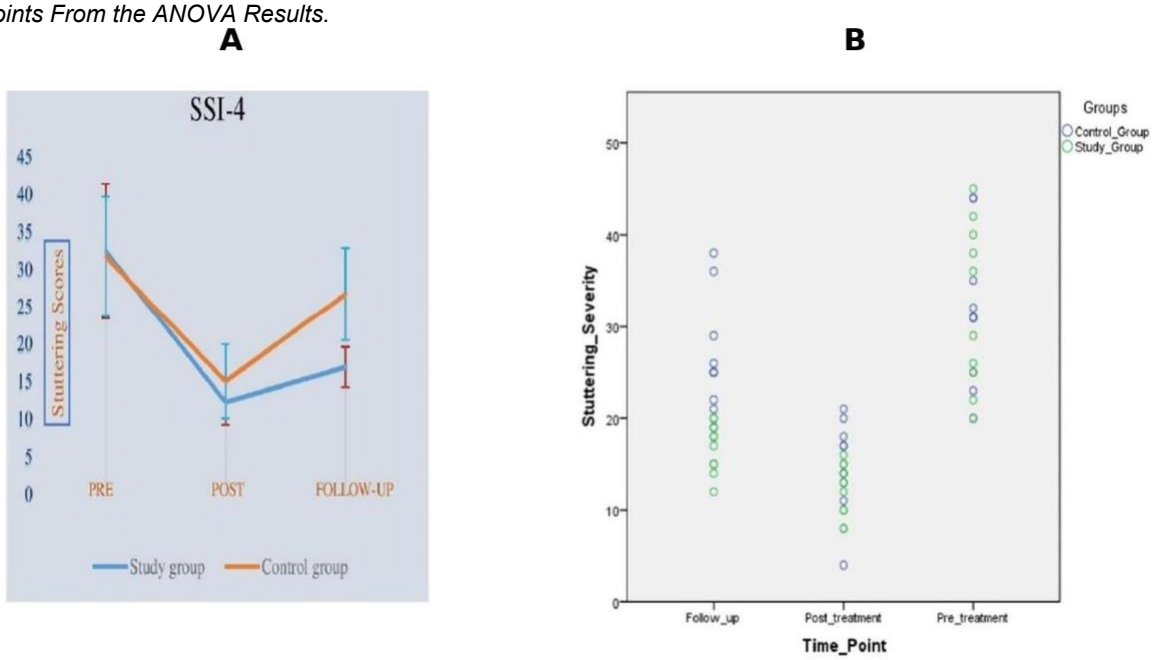

Note. Legend A: Pre: Pretreatment, Post: Posttreatment, and follow-up stage according to the Persian version of SSI-4.

Results of Signal Analyses

Red colors in the figures representing phase coherence indicate significant increases in the study group, while blue colors signify meaningful increases in the control group. The color maps for relative power highlight the areas with significant differences.

Results of Signal Analysis Through the Condition of SP. The study group showed a relative increase in delta band power at the FC5 electrode (equivalent to the Broca region) and an increase in beta band power over the occipital areas of the opposite hemisphere, compared to the control group. In the control group, the power of the low beta-frequency band showed a significant increase compared to the study group. Comparing the two groups in terms of phase coherence demonstrated that preparation for fluent speech in the control group was associated with enhanced inter- and intrahemispheric functional connectivity (FC) across the spectrum. In contrast, the study group exhibited increased left intrahemispheric FC through delta and theta band frequencies during preparation for fluent speech. The results are depicted in Figure 5.

Results on Signal Analysis Through the Condition of IS. In the IS condition, the difference between the two groups largely followed the pattern observed in the SP condition. In the study group,

fluency was associated with increasing delta band power over the F3 and C3 electrodes. In contrast, the control group exhibited fluency accompanied by increased beta band power over the F7, FC5, O1, FC6, C4, and Cz electrodes. Additionally, in the control group, imagined fluent speech was linked to greater inter- and intrahemispheric FCs connectivity across the spectrum. The results of the comparison between the two groups in the IS condition are illustrated in Figure 6.

Figure 5. *Posttreatment FFT Relative Power (RP) and FFT Phase Coherence Through SP Condition.*

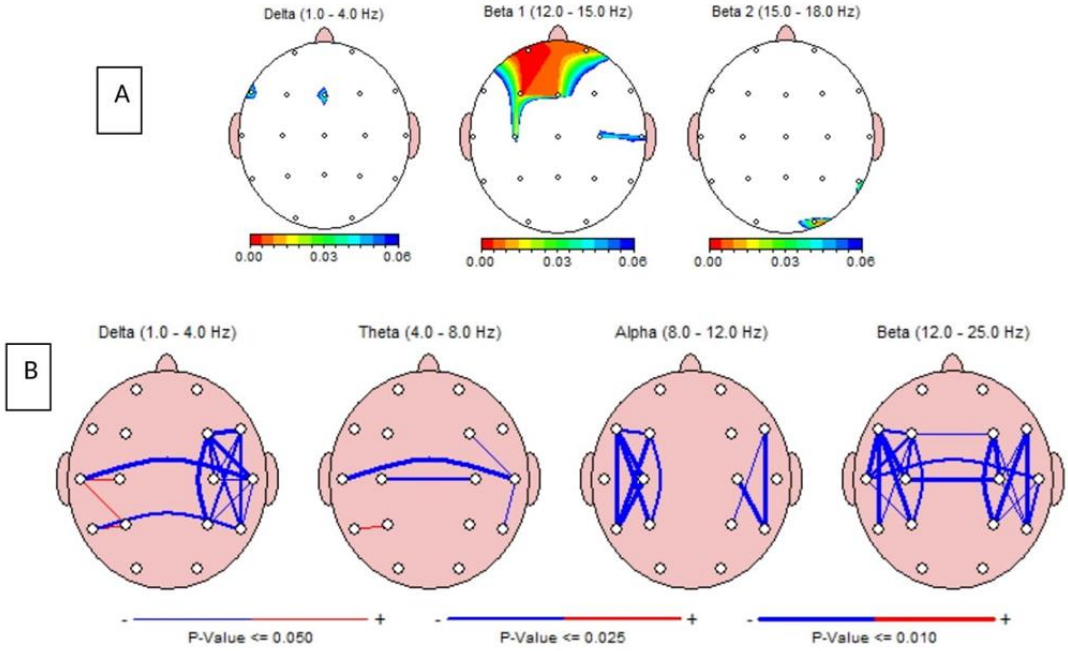

Figure 6. *Posttreatment FFT Relative Power and FFT Phase Coherence Through IS Condition.*

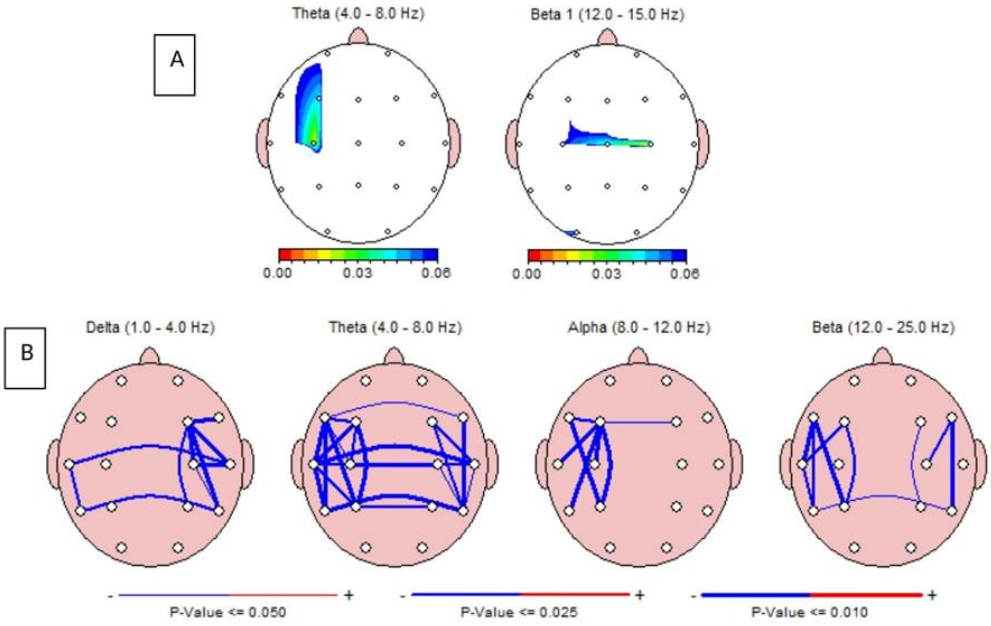

Note. Legend: A) increased theta relative power over F3 and C3 in the study group and increased beta relative power over F7, Fc5, Fc6, C4, Cz, and O1 in the control group. B) increased inter- and intrahemispheric phase coherence through the spectrum in the control group (blue lines).

Discussion

This study aims to investigate the effect of tDCS, optimized through EEG processing for each subject, on enhancing the effectiveness and maintenance of speech therapy outcomes in AWS. To achieve this, we compared two types of electrical stimulation in the study and control groups. The control group received anodal stimulation of the FC5 region according to a conventional pattern for stuttering, while the study group received stimulation based on a comparison of fluent and dysfluent signal power. The application of tDCS in both groups was integrated with speech therapy. We compared the two groups based on behavioral outcomes and changes in signal patterns, both immediately after 10 sessions of intervention and again after 3 months. We planned to monitor the persistence of behavioral outcomes, as relapse is a common complication in stuttering therapy following the cessation of treatment (Craig et al., 2002; Cream et al., 2009; DiLollo et al., 2002).

Behavioral Results

One of the main objectives of the present study was to investigate the effect of qEEG-based personalized tDCS protocols. This section compares the short-term and mid-term outcomes of the two types of stimulation patterns used. Comparing pretreatment and follow-up stage time points indicated a priority for the study group during the follow-up stage. This suggests that although personalized stimulation patterns may not enhance the effectiveness of the intervention, they may lead to a long-lasting effect. This finding is clinically significant for a disorder such as stuttering (Craig et al., 2009; Cream et al., 2009; DiLollo et al., 2002).

One common challenge in stuttering therapy is the time-consuming nature of behavioral interventions needed to achieve clinical results (Blomgren, 2013; Craig et al., 2002; Onslow et al., 1996). Therefore, any method associated with rapid remediation of stuttering will be highly regarded. In the present study, posttreatment outcomes showed a decrease in stuttering scores of 20.2 ± 0.94 in the study group and 16.7 ± 1.57 in the control group, according to the SSI-4. The effectiveness of tDCS increases when combined with behavioral interventions. This combination has demonstrated greater and more lasting fluency improvements than behavioral interventions alone. Chesters et al. (2018) conducted one of the first attempts to investigate the use of tDCS in AWS. They found that after 5 days of anodal stimulation of the left inferior frontal gyrus (IFG) combined with temporary fluency-inducing methods, stuttering scores were significantly reduced based on the SSI-4 tool in the study group (Chesters et al., 2018). Since the stimulation montage in the control group of our study was similar to that used by Chesters et al. (2018) in their study group, the significant difference in the results can be attributed to the variations in methodologies (Chesters et al., 2018; Chesters et al., 2017; Garnett et al., 2019). In addition, we designed a 10-session treatment over 2 weeks for our study, as opposed to the five sessions implemented by Chesters et al. (2018). Thus, the duration of the treatment and the methods used in fluency induction appear to be significant factors in remediating stuttering in the short term. One of the challenges in stuttering therapy is the relapse of the disorder after treatment cessation. A considerable amount of research has been conducted to investigate the causes and methods of prevention (Block et al., 2006; Miller & Guitar, 2009). In this context, follow-up on the results will be a crucial aspect of any treatment. While both our groups experienced a decrease in stuttering severity immediately after the intervention, the control group's stuttering severity significantly increased after 3 months but remained lower than baseline. In contrast, Chesters et al. (2018) reported that the mean stuttering scores of the study group in the SSI-4 test returned to baseline after 6 weeks. This difference may be attributed to the fluency-inducing method and/or the duration of our intervention. Moein et al. (2022) conducted another study that reported the effectiveness of tDCS in reducing the severity of stuttering. They found that 6 days of anodal stimulation of the left superior gyrus, combined with delayed auditory feedback (DAF), effectively reduced stuttered syllables immediately and up to 6 weeks postintervention. However, this study did not incorporate a follow-up design. This suggests that personalized tDCS may lead to more durable treatment effects.

Results of Signal Analyses

Signal Analyses Through the Condition of SP. IFG plays a crucial role in stuttering, particularly in relation to speech production and motor planning (Lu et al., 2010). Research indicates that individuals who stutter demonstrate atypical activation and connectivity patterns in the IFG, which may contribute to their speech dysfluency (Zhang et al., 2022). Studies reveal overactivation in the right IFG and underactivation in the left IFG among AWS, potentially indicating an increased demand for feedforward planning and dysfunction in auditory feedback systems (Cai et al., 2024). The right IFG is believed to function as a compensatory mechanism in stuttering, possibly as part of an expanded core

timing network that includes the basal ganglia and SMA (Etchell et al., 2014a). One of the expected changes after speech therapy for stuttering is increased activity in the IFG (Lu et al., 2017). Personalized tDCS targeting the IFG or its connected networks may help restore functional lateralization, thereby enhancing fluency. Our findings support this framework, as participants in the study group demonstrated greater suppression of maladaptive high-frequency activity in motor-related networks, likely reflecting improved neural coordination.

Furthermore, the study group showed an increase in the relative power of the delta band at the FC5 electrode during the SP condition (Figure 5). This increased activity at FC5 was observed in the study group, while the control group utilized anodal stimulation at FC5. One of the key advantages of personalized tDCS is its potential to optimize therapeutic outcomes by targeting specific neural circuits involved in stuttering. For example, our study found that stimulation aimed at enhancing delta-band activity in the motor preparation areas, specifically at the FC5 electrode during the SP condition, aligns with previous research indicating that delta oscillations play a role in facilitating error monitoring (Yordanova, Falkenstein, & Kolev, 2024). These delta oscillations produce error-specific signals that are essential for performance monitoring, enabling the distinction between correct and incorrect responses (Yordanova, Falkenstein, Hohnsbein, et al., 2004). In contrast, when comparing the control group to the study group during speech preparation, the relative power of the beta band in the electrodes corresponding to the left and right sensory-motor speech-related areas remained significantly higher in the control group. This suggests that despite achieving fluent speech, there has not yet been sufficient beta suppression necessary for an effective motor system (Bartolo et al., 2014; Etchell et al., 2014b; Mock et al., 2016). These results align with the theory regarding defective beta band suppression in stuttering. Accordingly, there are issues in specific brain areas of AWS, such as the basal ganglia and the SMA. These regions provide the internal timing substrate essential for planning and executing movements. Stuttering is considered an internal timing disorder characterized by modulations in the oscillatory power of the beta band (Etchell et al., 2014b). The sensitivity of beta oscillations to sensory-motor deficits resulting from stuttered speech has been well established (Jenson et al., 2020). In this context, a relapse of stuttering in this delicate and vulnerable network is predictable.

The role of the cerebellum, alongside the basal ganglia-thalamus-cortex circuit, has been demonstrated in internal timing for the smooth, rapid, and skillful execution of voluntary movements (Diedrichsen et al., 2003), speech production—especially at high speeds (Ackermann, 2008)—and in stuttering (Chang & Guenther, 2020; Neumann et al., 2018). However, opinions differ regarding the cerebellum's role in the treatment or improvement of stuttering. Kell et al. (2018) suggest that in cases where stuttering has recovered due to treatment, the cerebellum disconnects from the neocortical circuit. In contrast, Neumann et al. (2018) reported increased cerebellar activity following spontaneous stuttering recovery. The increased right cerebellar activity observed in our study group appears consistent with the findings of Neumann et al. (2018).

A few studies have explored the effect of therapy on functional brain communication, often using the fMRI technique (Kell et al., 2018; Korzeczek et al., 2021). To date, no study has examined the electrophysiological implications of treatment on functional connectivity, and only one study has compared fluent to stuttered speech in AWS in terms of phase coherence. Sengupta et al. (2017) reported an increase in the phase coherence of theta, alpha, and gamma bands at the left frontal electrodes while preparing for stuttered utterances. They attributed this increase to the heightened general activity associated with stuttering (Sengupta et al., 2017). Consequently, successful treatment may lead to a reduction in some measures of increased phase coherence. In comparing the two groups, the main feature associated with fluency in the study group was a significant decrease in greater phase coherence, which in the control group manifested in different bands and between electrodes related to motor-auditory-somatosensory areas of both hemispheres. Fluency in the control group was still associated with high phase coherence between different brain neural circuits, a characteristic of the dysfluency state (Sengupta et al., 2017). While the type and location of electrical stimulation were different and scattered across both hemispheres in the subjects of the study group, the control group had stimulation focused in the left inferior frontal region. Increased phase coherence in the delta band was observed in the left temporal-inferior parietal lobule (IPL) areas of the study group. One possible reason for the longer persistence of the behavioral results in the study group after 3 months may be the purposeful change in neural activities, leading to limited and targeted functional connectivity.

Signal Analyses Through the Condition of IS. In the study group, theta relative band power over the F3 and C3 regions was significantly higher than in the control group through the IS condition. Increases in power of frequencies below 10 Hz in the motor areas have been reported during both overt and covert normal speech (Bowers et al., 2019). In this context, the increase in theta band power may be interpreted as a successful strategy that has been reinforced in the study group. Although imagined speech does not involve any movement or generate re-afferent feedback, forward models of speech targets and expected sensory feedback are generated through a strictly internal loop (Tian & Poeppel, 2010, 2012). Since imagined speech engages the somatosensory and premotor areas, it is expected that these areas would differentiate between the two groups, shifting from the left IFG in the SP condition to coordination corresponding to the somatosensory cortex (C3) and the premotor area (F3) in the IS condition.

In the control group, an increase in beta relative power over the left and right IFG was observed during the Imagined stuttering (IS) condition. These findings align with the theory that defects in beta-band suppression are associated with stuttering. IS has been shown to correspond with overt stuttering in positron emission tomography (PET) studies (Ingham et al., 2000) and fMRI (Wymbs et al., 2013) in terms of regional brain activation. Additionally, Jenson et al. (2014) demonstrated that neural oscillations during syllable production and imagined speech are comparable. They later reported significantly decreased alpha and beta suppression in the left hemisphere in individuals with a stuttering trait during both overt and covert syllable production (Jenson et al., 2018). Consequently, the enhancement of beta suppression in the study group may be considered a marker of intervention success and is likely related to long-lasting outcomes in this group.

Regarding imagined speech, fluency was again associated with enhanced inter- and intrahemispheric FCs in the control group, similar to the SP condition. To our knowledge, no study has examined the effect of treatment on FC in the IS condition. However, the decrease in FC measures during the fluency state in this condition may also be interpretable within the framework of studies on speech preparation (Sengupta et al., 2017). Enhanced functional connectivity has been observed in various neurological disorders, such as autism (Mizuno et al., 2006) schizophrenia (Ding et al., 2019), and anxiety (Giménez et al., 2012). Considering the longer-lasting behavioral outcomes in the study group, the greater task-related FC in the control group suggests an open topic that requires further research.

Conclusion

Our findings suggest that individualized tDCS may be preferable to conventional tDCS, particularly regarding the maintenance of effects. Neural deficits associated with stuttering appear to be distributed across disparate networks. However, personalized intervention—through identification and stimulation of the individualized affected areas—likely led to similar activation patterns. We consider the increased activation of FC5, IFG, and the enhanced beta suppression over bihemispheric speech-related areas in the study group as evidence supporting this interpretation. Thus, the potentiated or inhibited neural networks may align with individual neural compensatory strategies or closely resemble expected and normal circuits. Nonetheless, we view this as a preliminary claim that requires further investigation.

Limitations and Future Directions

We recommend using a larger sample size to improve the accuracy of estimates. Additionally, we did not record a signal during the follow-up stage as per the predetermined study design. The current experimental design cannot separate the effects of tDCS from fluency-shaping training due to the absence of a sham group. Furthermore, we believe that utilizing the time-frequency spectrogram method, which takes advantage of the important benefits of EEG, may facilitate the exploration of protocols based on more efficient features. Our study acknowledges that EEG data can be contaminated during speaking tasks. Although we used the ADJUST algorithm for artifact removal, more advanced and better-validated methods, such as ASR, are now preferred. Furthermore, we did not assess the neural integrity of the components postcleaning with tools like IC_Label in EEGLAB, which is essential for ensuring data validity. Future studies should integrate these advancements to improve methodological rigor. In future studies, it is recommended that EMG traces be analyzed to effectively differentiate the components of the neural EEG signals, as this was not possible during the current study.

Author Declarations

This work was supported by the Shiraz University of Medical Sciences [grant numbers IR.SUMS.REC.1397.712, 2018]. This work was

funded by Shiraz University of Medical Sciences, School of Advanced Medical Sciences and Technologies. We are grateful to National Brain Mapping Laboratory for technical support. The authors declare that there is no conflict of interest regarding the publication of this article. Artificial intelligence (AI) tools were used solely for language-related assistance, specifically for grammar and clarity checking of the manuscript text. No AI tools were used for study design, data analysis, interpretation of results, or generation of scientific content. The authors take full responsibility for the accuracy, integrity, originality, and ethical compliance of the manuscript.

References

Ackermann, H. (2008). Cerebellar contributions to speech production and speech perception: Psycholinguistic and neurobiological perspectives. *Trends in Neurosciences, 31*(6), 265–272. https://doi.org/10.1016/j.tins.2008.02.011

Al-Fahoum, A. S., & Al-Fraihat, A. A. (2014). Methods of EEG signal features extraction using linear analysis in frequency and time-frequency domains. *International Scholarly Research Notices, 2014*(1), Article 730218. https://doi.org/10.1155/2014/730218

Bakhtiar, M., Wong, M. N., Shum, H. Y., & Lam, C. K. (2023). The effect of transcranial direct current stimulation on stuttering: A preliminary report. *Brain Stimulation, 16*(1), Article P227. https://doi.org/10.1016/j.brs.2023.01.332

Bartolo, R., Prado, L., & Merchant, H. (2014). Information processing in the primate basal ganglia during sensory-guided and internally driven rhythmic tapping. *The Journal of Neuroscience, 34*(11), 3910–3923. https://doi.org/10.1523/jneurosci.2679-13.2014

Bashir, N., & Howell, P. (2015). tDCS and stuttering. *Brain Stimulation, 8*(2), Article P429. https://doi.org/10.1016/j.brs.2015.01.369

Bastos, A. M., & Schoffelen, J.-M. (2016). A tutorial review of functional connectivity analysis methods and their interpretational pitfalls. *Frontiers in Systems Neuroscience, 9*, Article 175. https://doi.org/10.3389/fnsys.2015.00175

Bayat, M., Boostani, R., Sabeti, M., Yadegari, F., Pirmoradi, M., Rao, K., & Nami, M. (2024). Source localization and spectrum analyzing of EEG in stuttering state upon dysfluent utterances. *Clinical EEG and Neuroscience, 55*(3), 371–383. https://doi.org/10.1177/15500594221150638

Bayat, M., Boostani, R., Sabeti, M., Yadegari, F., Taghavi, M., Pirmoradi, M., Chakrabarti, P., & Nami, M. (2023). Speech related anxiety in adults who stutter. *Journal of Psychophysiology, 37*(1), 25–38. https://doi.org/10.1027/0269-8803/a000305

Bell, A. J., & Sejnowski, T. J. (1995). An information-maximization approach to blind separation and blind deconvolution. *Neural Computation, 7*(6), 1129–1159. https://doi.org/10.1162/neco.1995.7.6.1129

Belyk, M., Kraft, S. J., & Brown, S. (2015). Stuttering as a trait or state–An ALE meta-analysis of neuroimaging studies. *European Journal of Neuroscience, 41*(2), 275–284. https://doi.org/10.1111/ejn.12765

Bjekić, J., Živanović, M., Paunović, D., Vulić, K., Konstantinović, U., & Filipović, S. R. (2022). Personalized frequency modulated transcranial electrical stimulation for associative memory enhancement. *Brain Sciences, 12*(4), Article 472. https://doi.org/10.3390/brainsci12040472

Block, S., Onslow, M., Packman, A., & Dacakis, G. (2006). Connecting stuttering management and measurement: IV. Predictors of outcome for a behavioural treatment for stuttering. *International Journal of Language & Communication Disorders, 41*(4), 395–406. https://doi.org/10.1080/13682820600623853

Blomgren, M. (2013). Behavioral treatments for children and adults who stutter: A review. *Psychology Research and Behavior Management, 6*, 9–19. https://doi.org/10.2147/PRBM.S31450

Bowers, A., Saltuklaroglu, T., Jenson, D., Harkrider, A., & Thornton, D. (2019). Power and phase coherence in sensorimotor mu and temporal lobe alpha components during covert and overt syllable production. *Experimental Brain Research, 237*(3), 705–721. https://doi.org/10.1007/s00221-018-5447-4

Brignell, A., Krahe, M., Downes, M., Kefalianos, E., Reilly, S., & Morgan, A. T. (2020). A systematic review of interventions for adults who stutter. *Journal of Fluency Disorders, 64*, Article 105766. https://doi.org/10.1016/j.jfludis.2020.105766

Busan, P., Moret, B., Masina, F., Del Ben, G., & Campana, G. (2021). Speech fluency improvement in developmental stuttering using non-invasive brain stimulation: Insights from available evidence. *Frontiers in Human Neuroscience, 15*, Article 662016. https://doi.org/10.3389/fnhum.2021.662016

Cai, H., Dong, J., Mei, L., Feng, G., Li, L., Wang, G., & Yan, H. (2024). Functional and structural abnormalities of the speech disorders: a multimodal activation likelihood estimation meta-analysis. *Cerebral Cortex, 34*(3), Article bhae075. https://doi.org/10.1093/cercor/bhae075

Cannon, R. L., Baldwin, D. R., Shaw, T. L., Diloreto, D. J., Phillips, S. M., Scruggs, A. M., & Riehl, T. C. (2012). Reliability of quantitative EEG (qEEG) measures and LORETA current source density at 30 days. *Neuroscience Letters, 518*(1), 27–31. https://doi.org/10.1016/j.neulet.2012.04.035

Chang, S.-E., & Guenther, F. H. (2020). Involvement of the cortico-basal ganglia-thalamocortical loop in developmental stuttering. *Frontiers in Psychology, 10*, Article 3088. https://doi.org/10.3389/fpsyg.2019.03088

Chesters, J., Möttönen, R., & Watkins, K. E. (2018). Transcranial direct current stimulation over left inferior frontal cortex improves speech fluency in adults who stutter. *Brain, 141*(4), 1161–1171. https://doi.org/10.1093/brain/awy011

Chesters, J., Möttönen, R., & Watkins, K. E. (2021). Neural changes after training with transcranial direct current stimulation to increase speech fluency in adults who stutter. https://doi.org/10.31219/osf.io/8st3j

Chesters, J., Watkins, K. E., & Möttönen, R. (2017). Investigating the feasibility of using transcranial direct current stimulation to enhance fluency in people who stutter. *Brain and Language, 164*, 68–76. https://doi.org/10.1016/j.bandl.2016.10.003

Craig, A., Blumgart, E., & Tran, Y. (2009). The impact of stuttering on the quality of life in adults who stutter. *Journal of Fluency Disorders, 34*(2), 61–71. https://doi.org/10.1016/j.jfludis.2009.05.002

Craig, A., Hancock, K., & Cobbin, D. (2002). Managing adolescents who relapse following treatment for stuttering. *Asia Pacific Journal of Speech, Language and Hearing, 7*(2), 79–91. https://doi.org/10.1179/136132802805576490

Cream, A., O'Brian, S., Onslow, M., Packman, A., & Menzies, R. (2009). Self-modelling as a relapse intervention following speech-restructuring treatment for stuttering. *International Journal of Language & Communication Disorders, 44*(5), 587–599. https://doi.org/10.1080/13682820802256973

Delorme, A., & Makeig, S. (2004). EEGLAB: an open source toolbox for analysis of single-trial EEG dynamics including independent component analysis. *Journal of Neuroscience Methods, 134*(1), 9–21. https://doi.org/10.1016/j.jneumeth.2003.10.009

Diedrichsen, J., Ivry, R. B., & Pressing, J. (2003). Cerebellar and basal ganglia contributions to interval timing. In W. H. Meck (Ed.), *Functional and neural mechanisms of interval timing* (pp. 457–481). CRC Press.

DiLollo, A., Neimeyer, R. A., & Manning, W. H. (2002). A personal construct psychology view of relapse: Indications for a narrative therapy component to stuttering treatment. *Journal of Fluency Disorders, 27*(1), 19–42. https://doi.org/10.1016/S0094-730X(01)00109-7

Ding, Y., Ou, Y., Su, Q., Pan, P., Shan, X., Chen, J., Liu, F., Zhang, Z., Zhao, J., & Guo, W. (2019). Enhanced global-brain functional connectivity in the left superior frontal gyrus as a possible endophenotype for schizophrenia. *Frontiers in Neuroscience, 13*, Article 145. https://doi.org/10.3389/fnins.2019.00145

Etchell, A., Johnson, B., & Sowman, P. (2014a). Behavioral and multimodal neuroimaging evidence for a deficit in brain timing networks in stuttering: A hypothesis and theory. *Frontiers in Human Neuroscience, 8*, Article 467. https://doi.org/10.3389/fnhum.2014.00467

Etchell, A. C., Civier, O., Ballard, K. J., & Sowman, P. F. (2017). A systematic literature review of neuroimaging research on developmental stuttering between 1995 and 2016. *Journal of Fluency Disorders, 55*, 6–45. https://doi.org/10.1016/j.jfludis.2017.03.007

Etchell, A. C., Johnson, B. W., & Sowman, P. F. (2014b). Beta oscillations, timing, and stuttering. *Frontiers in Human Neuroscience, 8*, Article 1036. https://doi.org/10.3389/fnhum.2014.01036

Farrahi, H., Gharraee, B., Oghabian, M. A., Pirmoradi, M. R., Najibi, S. M., & Batouli, S. A. H. (2021). Psychometric properties of the persian version of the Overall Anxiety Severity and Impairment Scale (OASIS). *Iranian Journal of Psychiatry and Behavioral Sciences, 14*(4), Article e100674. https://doi.org/10.5812/ijpbs.100674

Garnett, E. O. D., Chow, H. M., Choo, A. L., & Chang, S.-E. (2019). Stuttering severity modulates effects of non-invasive brain stimulation in adults who stutter. *Frontiers in Human Neuroscience, 13*, Article 411. https://doi.org/10.3389/fnhum.2019.00411

Gaudet, I., Hüsser, A., Vannasing, P., & Gallagher, A. (2020). Functional brain connectivity of language functions in children revealed by EEG and MEG: A systematic review. *Frontiers in Human Neuroscience, 14*, Article 62. https://doi.org/10.3389/fnhum.2020.00062

Ghaderi, A. H., Andevari, M. N., & Sowman, P. F. (2018). Evidence for a resting state network abnormality in adults who stutter. *Frontiers in Integrative Neuroscience, 12*, Article 16. https://doi.org/10.3389/fnint.2018.00016

Giacometti, P., Perdue, K. L., & Diamond, S. G. (2014). Algorithm to find high density EEG scalp coordinates and analysis of their correspondence to structural and functional regions of the brain. *Journal of Neuroscience Methods, 229*, 84–96. https://doi.org/10.1016/j.jneumeth.2014.04.020

Giménez, M., Pujol, J., Ortiz, H., Soriano-Mas, C., López-Solà, M., Farré, M., Deus, J., Merlo-Pich, E., & Martín-Santos, R. (2012). Altered brain functional connectivity in relation to perception of scrutiny in social anxiety disorder. *Psychiatry Research: Neuroimaging, 202*(3), 214–223. https://doi.org/10.1016/j.pscychresns.2011.10.008

Ingham, R. J., Fox, P. T., Costello Ingham, J., & Zamarripa, F. (2000). Is overt stuttered speech a prerequisite for the neural activations associated with chronic developmental stuttering? *Brain and Language, 75*(2), 163–194. https://doi.org/10.1006/brln.2000.2351

Jenson, D., Bowers, A. L., Harkrider, A. W., Thornton, D., Cuellar, M., & Saltuklaroglu, T. (2014). Temporal dynamics of sensorimotor integration in speech perception and production: Independent component analysis of EEG data. *Frontiers in Psychology, 5*, Article 656. https://doi.org/10.3389/fpsyg.2014.00656

Jenson, D., Bowers, A. L., Hudock, D., & Saltuklaroglu, T. (2020). The application of EEG mu rhythm measures to neurophysiological research in stuttering. *Frontiers in Human Neuroscience, 13*, Article 458. https://doi.org/10.3389/fnhum.2019.00458

Jenson, D., Reilly, K. J., Harkrider, A. W., Thornton, D., & Saltuklaroglu, T. (2018). Trait related sensorimotor deficits in people who stutter: An EEG investigation of μ rhythm dynamics during spontaneous fluency. *NeuroImage: Clinical, 19*, 690–702. https://doi.org/10.1016/j.nicl.2018.05.026

Jiang, J., Lu, C., Peng, D., Zhu, C., & Howell, P. (2012). Classification of types of stuttering symptoms based on brain activity. *PLoS ONE, 7*(6), Article e39747. https://doi.org/10.1371/journal.pone.0039747

Kaiser, D. A. (2007). What is quantitative EEG? *Journal of Neurotherapy, 10*(4), 37–52. https://doi.org/10.1300/J184v10n04_05

Karsan, Ç., Özdemir, R. S., Bulut, T., & Hanoğlu, L. (2022). The effects of single-session cathodal and bihemispheric tDCS on fluency in stuttering. *Journal of Neurolinguistics, 63*, Article 101064. https://doi.org/10.1016/j.jneuroling.2022.101064

Keizer, A. W. (2019). Standardization and personalized medicine using quantitative EEG in clinical settings. *Clinical EEG and Neuroscience, 52*(2), 82–89. https://doi.org/10.1177/1550059419874945

Kell, C. A., Neumann, K., Behrens, M., von Gudenberg, A. W., & Giraud, A.-L. (2018). Speaking-related changes in cortical functional connectivity associated with assisted and spontaneous recovery from developmental stuttering. *Journal of Fluency Disorders, 55*, 135–144. https://doi.org/10.1016/j.jfludis.2017.02.001

Korzeczek, A., Neef, N. E., Steinmann, I., Paulus, W., & Sommer, M. (2022). Stuttering severity relates to frontotemporal low-beta synchronization during pre-speech preparation. *Clinical Neurophysiology, 138*, 84–96. https://doi.org/10.1016/j.clinph.2022.03.010

Korzeczek, A., Primaßin, A., Wolff von Gudenberg, A., Dechent, P., Paulus, W., Sommer, M., & Neef, N. E. (2021). Fluency shaping increases integration of the command-to-execution and the auditory-to-motor pathways in persistent developmental stuttering. *NeuroImage, 245*, Article 118736. https://doi.org/10.1016/j.neuroimage.2021.118736

Kuremoto, T., Baba, Y., Obayashi, M., Mabu, S., & Kobayashi, K. (2018). Enhancing EEG signals recognition using roc curve. *Journal of Robotics, Networking and Artificial Life, 4*(4), 283–286. https://doi.org/10.2991/jrnal.2018.4.4.5

Kuremoto, T., Baba, Y., Obayashi, M., Mabu, S., & KobayashiI, K. (2017). A method of feature extraction for EEG signals recognition using ROC curve. *Spectrum, 22*(1), 654–657. https://doi.org/10.5954/ICAROB.2017.OS12-2

Lu, C., Chen, C., Ning, N., Ding, G., Guo, T., Peng, D., Yang, Y., Li, K., & Lin, C. (2010). The neural substrates for atypical planning and execution of word production in stuttering. *Experimental Neurology, 221*(1), 146–156. https://doi.org/10.1016/j.expneurol.2009.10.016

Lu, C., Zheng, L., Long, Y., Yan, Q., Ding, G., Liu, L., Peng, D., & Howell, P. (2017). Reorganization of brain function after a short-term behavioral intervention for stuttering. *Brain and Language, 168*, 12–22. https://doi.org/10.1016/j.bandl.2017.01.001

Ma, Y., Gong, A., Nan, W., Ding, P., Wang, F., & Fu, Y. (2023). Personalized brain–computer interface and its applications. *Journal of Personalized Medicine, 13*(1), Article 46. https://doi.org/10.3390/jpm13010046

Mastakouri, A.-A., Weichwald, S., Özdenizci, O., Meyer, T., Schölkopf, B., & Grosse-Wentrup, M. (2017). Personalized brain-computer interface models for motor rehabilitation. *IEEE*

international conference on systems, man, and cybernetics. https://doi.org/10.48550/arXiv.1705.03259

Mersov, A., Cheyne, D., Jobst, C., & De Nil, L. (2018). A preliminary study on the neural oscillatory characteristics of motor preparation prior to dysfluent and fluent utterances in adults who stutter. *Journal of Fluency Disorders, 55*, 145–155. https://doi.org/10.1016/j.jfludis.2017.05.003

Mersov, A.-M., Jobst, C., Cheyne, D. O., & De Nil, L. (2016). Sensorimotor oscillations prior to speech onset reflect altered motor networks in adults who stutter. *Frontiers in Human Neuroscience, 10*, Article 443. https://doi.org/10.3389/fnhum.2016.00443

Miller, B., & Guitar, B. (2009). Long-term outcome of the lidcombe program for early stuttering intervention. *American Journal of Speech-Language Pathology, 18*(1), 42–49. https://doi.org/10.1044/1058-0360(2008/06-0069)

Mizuno, A., Villalobos, M. E., Davies, M. M., Dahl, B. C., & Müller, R.-A. (2006). Partially enhanced thalamocortical functional connectivity in autism. *Brain Research, 1104*(1), 160–174. https://doi.org/10.1016/j.brainres.2006.05.064

Mock, J. R., Foundas, A. L., & Golob, E. J. (2016). Cortical activity during cued picture naming predicts individual differences in stuttering frequency. *Clinical Neurophysiology, 127*(9), 3093–3101. https://doi.org/10.1016/j.clinph.2016.06.005

Moein, N., Mohamadi, R., Rostami, R., Nitsche, M., Zomorrodi, R., & Ostadi, A. (2022). Investigation of the effect of delayed auditory feedback and transcranial direct current stimulation (DAF-tDCS) treatment for the enhancement of speech fluency in adults who stutter: A randomized controlled trial. *Journal of Fluency Disorders, 72*, Article 105907. https://doi.org/10.1016/j.jfludis.2022.105907

Mognon, A., Jovicich, J., Bruzzone, L., & Buiatti, M. (2011). ADJUST: An automatic EEG artifact detector based on the joint use of spatial and temporal features. *Psychophysiology, 48*(2), 229–240. https://doi.org/10.1111/j.1469-8986.2010.01061.x

Neumann, K., Euler, H. A., Kob, M., Wolff von Gudenberg, A., Giraud, A.-L., Weissgerber, T., & Kell, C. A. (2018). Assisted and unassisted recession of functional anomalies associated with dysprosody in adults who stutter. *Journal of Fluency Disorders, 55*, 120–134. https://doi.org/10.1016/j.jfludis.2017.09.003

Olbrich, S., Jödicke, J., Sander, C., Himmerich, H., & Hegerl, U. (2011). ICA-based muscle artefact correction of EEG data: What is muscle and what is brain?: Comment on McMenamin et al. *NeuroImage, 54*(1), 1–3. https://doi.org/10.1016/j.neuroimage.2010.04.256

Oldfield, R. C. (1971). The assessment and analysis of handedness: The Edinburgh inventory. *Neuropsychologia, 9*(1), 97–113. https://doi.org/10.1016/0028-3932(71)90067-4

Onslow, M., Costa, L., Andrews, C., Harrison, E., & Packman, A. (1996). Speech outcomes of a prolonged-speech treatment for stuttering. *Journal of Speech, Language, and Hearing Research, 39*(4), 734–749. https://doi.org/10.1044/jshr.3904.734

Paik, N.-J. (2015). Applications of neuromodulation in neurology and neurorehabilitation. In *Textbook of neuromodulation* (pp. 211–245). Springer.

Paulus, W., Peterchev, A. V., & Ridding, M. (2013). Chapter 27 - Transcranial electric and magnetic stimulation: Technique and paradigms. In A. M. Lozano & M. Hallett (Eds.), *Handbook of clinical neurology* (Vol. 116, pp. 329–342). Elsevier.

Piai, V., & Zheng, X. (2019). Chapter Eight - Speaking waves: Neuronal oscillations in language production. In K. D. Federmeier (Ed.), *Psychology of learning and motivation* (Vol. 71, pp. 265–302). Academic Press.

Popa, L. L., Dragos, H., Pantelemon, C., Rosu, O. V., & Strilciuc, S. (2020). The role of quantitative EEG in the diagnosis of neuropsychiatric disorders. *Journal of Medicine and Life, 13*(1), 8–15. https://doi.org/10.25122/jml-2019-0085

Riley, G. D., & Bakker, K. (2009). *Stuttering severity instrument: SSI-4*. Pro-Ed.

Rimmele, J. M., Gross, J., Molholm, S., & Keitel, A. (2018). Editorial: Brain oscillations in human communication. *Frontiers in Human Neuroscience, 12*, Article 39. https://doi.org/10.3389/fnhum.2018.00039

Saltuklaroglu, T., Harkrider, A. W., Thornton, D., Jenson, D., & Kittilstved, T. (2017). EEG Mu (μ) rhythm spectra and oscillatory activity differentiate stuttering from non-stuttering adults. *NeuroImage, 153*, 232–245. https://doi.org/10.1016/j.neuroimage.2017.04.022

Sengupta, R., & Nasir, S. M. (2016). The predictive roles of neural oscillations in speech motor adaptability. *Journal of Neurophysiology, 115*(5), 2519–2528. https://doi.org/10.1152/jn.00043.2016

Sengupta, R., Shah, S., Loucks, T. M. J., Pelczarski, K., Scott Yaruss, J., Gore, K., & Nasir, S. M. (2017). Cortical dynamics of disfluency in adults who stutter. *Physiological Reports, 5*(9), Article e13194. https://doi.org/10.14814/phy2.13194

Smith, A., & Weber, C. (2016). Childhood stuttering: Where are we and where are we going? *Seminars in Speech and Language, 37*(4), 291–297. https://doi.org/10.1055/s-0036-1587703

Taherifard, M., Saeidmanesh, M., & Azizi, M. (2021). The effectiveness of transcranial direct current stimulation (tDCS) on the anxiety and severity of stuttering in adolescents aged 15 to 18. *Journal of Research in Rehabilitation Sciences, 16*, 224–231. https://doi.org/10.22122/JRRS.V16I0.3605

Tahmasebi, N., Shafie, B., Karimi, H., & Mazaheri, M. (2018). A Persian-version of the stuttering severity instrument-version four (SSI-4): How the new additions to SSI-4 complement its stuttering severity score? *Journal of Communication Disorders, 74*, 1–9. https://doi.org/10.1016/j.jcomdis.2018.04.005

Tezel-Bayraktaroglu, O., Bayraktaroglu, Z., Demirtas-Tatlidede, A., Demiralp, T., & Oge, A. E. (2020). Neuronavigated rTMS inhibition of right pars triangularis anterior in stuttering: Differential effects on reading and speaking. *Brain and Language, 210*, Article 104862. https://doi.org/10.1016/j.bandl.2020.104862

Tian, X., & Poeppel, D. (2010). Mental imagery of speech and movement implicates the dynamics of internal forward models. *Frontiers in Psychology, 1*, Article 166. http://dx.doi.org/10.3389/fpsyg.2010.00166

Tian, X., & Poeppel, D. (2012). Mental imagery of speech: Linking motor and perceptual systems through internal simulation and estimation. *Frontiers in Human Neuroscience, 6*, Article 314. http://dx.doi.org/10.3389/fnhum.2012.00314

Vanhoutte, S., Cosyns, M., van Mierlo, P., Batens, K., Corthals, P., De Letter, M., Van Borsel, J., & Santens, P. (2016). When will a stuttering moment occur? The determining role of speech motor preparation. *Neuropsychologia, 86*, 93–102. https://doi.org/10.1016/j.neuropsychologia.2016.04.018

Wells, B. G., & Moore, W. H., Jr. (1990). EEG alpha asymmetries in stutterers and non-stutterers: Effects of linguistic variables on hemispheric processing and fluency. *Neuropsychologia, 28*(12), 1295–1305. https://doi.org/10.1016/0028-3932(90)90045-p

Woods, A. J., Antal, A., Bikson, M., Boggio, P. S., Brunoni, A. R., Celnik, P., Cohen, L. G., Fregni, F., Herrmann, C. S., Kappenman, E. S., Knotkova, H., Liebetanz, D., Miniussi, C., Miranda, P. C., Paulus, W., Priori, A., Reato, D., Stagg, C., Wenderoth, N., & Nitsche, M. A. (2016). A technical guide to tDCS, and related non-invasive brain stimulation tools. *Clinical Neurophysiology, 127*(2), 1031–1048. https://doi.org/10.1016/j.clinph.2015.11.012

Wymbs, N. F., Ingham, R. J., Ingham, J. C., Paolini, K. E., & Grafton, S. T. (2013). Individual differences in neural regions

functionally related to real and imagined stuttering. *Brain and Language, 124*(2), 153–164. https://doi.org/10.1016/j.bandl.2012.11.013

Yada, Y., Tomisato, S., & Hashimoto, R.-i. (2019). Online cathodal transcranial direct current stimulation to the right homologue of Broca's area improves speech fluency in people who stutter. *Psychiatry and Clinical Neurosciences, 73*(2), 63–69. https://doi.org/10.1111/pcn.12796

Yairi, E., & Carrico, D. M. (1992). Early childhood stuttering. *American Journal of Speech-Language Pathology, 1*(3), 54–62. https://doi.org/10.1044/1058-0360.0103.54

Yaruss, J. S. (2010). Assessing quality of life in stuttering treatment outcomes research. *Journal of Fluency Disorders, 35*(3), 190–202. https://doi.org/10.1016/j.jfludis.2010.05.010

Yordanova, J., Falkenstein, M., Hohnsbein, J., & Kolev, V. (2004). Parallel systems of error processing in the brain. *NeuroImage, 22*(2), 590–602. https://doi.org/10.1016/j.neuroimage.2004.01.040

Yordanova, J., Falkenstein, M., & Kolev, V. (2024). Motor oscillations reveal new correlates of error processing in the human brain. *Scientific Reports, 14*, Article 5624. https://doi.org/10.1038/s41598-024-56223-x

Zhang, N., Yin, Y., Jiang, Y., & Huang, C. (2022). Reinvestigating the neural bases involved in speech production of stutterers: An ALE meta-analysis. *Brain Sciences, 12*(8), Article 1030. https://doi.org/10.3390/brainsci12081030

Received: June 8, 2025
Accepted: July 8, 2025
Published: March 31, 2026

NeuroRegulation

ISNR INTERNATIONAL SOCIETY FOR NEUROREGULATION & RESEARCH

Characterization of Steady-State EEG Responses to Familiar and Unfamiliar Music While Playing a Virtual Reality Rhythm Game

Xander Boit[1*] *and Nathalia Peixoto*[2]

[1]George Mason University, Fairfax, Virginia, USA
[2]University of Sao Paulo, Sao Paulo, Brazil

Abstract

Previous studies have shown that the brain processes familiar and unfamiliar music differently, yet there is a lack of EEG analysis focusing on active rhythm tasks during music listening. Our study aims to address this gap by investigating EEG responses to familiar and unfamiliar music while participants engage in a rhythm game within a virtual reality environment. We utilized a commercially available four-electrode headband to collect EEG data from 10 healthy subjects during experiments. Participants played the rhythm game Beat Saber, using virtual sabers to match the beat of the music. This experiment employed a matched pair design, with each subject serving as their own control in EEG comparisons. EEG data were categorized into delta, theta, alpha, beta, and gamma frequency bands, and power within each band was analyzed to discern patterns across trials. Our findings revealed significant differences in how the brain processed familiar versus unfamiliar music across both audio-only and virtual reality settings. These changes occurred predominantly on the right side of the brain, suggesting hemispheric specialization in music processing. Overall, our study contributes new insights into neural dynamics underlying music perception during active engagement, highlighting distinct EEG responses to familiar and unfamiliar music across sensory contexts.

Keywords: EEG; music familiarity; rhythm game; virtual reality; frequency bands

Citation: Boit, X., & Peixoto, N. (2026). Characterization of steady-state EEG responses to familiar and unfamiliar music while playing a virtual reality rhythm game. *NeuroRegulation, 13*(1), 43–53. https://doi.org/10.15540/nr.13.1.43

***Address correspondence to**: Xander Boit, George Mason University, 4400 University Drive, Fairfax, VA 22030, USA. Email: xboit@gmu.edu

Edited by:
Rex L. Cannon, PhD, Currents, Knoxville, Tennessee, USA

Reviewed by:
Rex L. Cannon, PhD, Currents, Knoxville, Tennessee, USA
Randall Lyle, PhD, Mount Mercy University, Cedar Rapids, Iowa, USA

Introduction

Electroencephalography (EEG) records brain signals from electrodes placed on the scalp surface related to various cognitive states, and these signals can be analyzed to understand human behavior (Kumar & Bhuvaneswari, 2012). One area of focus is how the brain reacts to musical stimuli in various settings. Familiarity with music has been linked to positive emotions and therefore been applied in therapies for Alzheimer's disease, depression, and anxiety patients (Freitas et al., 2018; Hailstone et al., 2009). The familiarity principle is a psychological phenomenon which suggests that the more exposed to something, the more that thing is liked (Zajonc, 1968). The anatomical locations related to this behavior are the left superior frontal gyrus, the ventral lateral nucleus of the left thalamus, and the left medial surface of the superior frontal gyrus for familiar music, whereas the left insula and the right anterior cingulate cortex were activated during unfamiliar music (Freitas et al., 2018). This indicates that different pathways in the brain are activated while processing familiar music and unfamiliar music.

The existing body of research provides little information on the impact of familiar music while the participants complete a task directly related to the music (such as playing an instrument or a rhythm game). This study aims to fill this gap by investigating the impact of unfamiliar and familiar music on a person's brain while completing a rhythm game in a virtual reality (VR) environment. The use

of a VR environment also allows for the control of both the auditorial and visual stimuli, thus allowing for a more controlled experimental design. This has potential applications in future research as VR becomes a more common tool for stimulating the brain in specific contexts or for developing therapeutic systems.

This study evaluated the impact of familiar and unfamiliar music on the brain during a music-related task, which in this case was a VR rhythm game. The data collected in this study enabled the investigation of electrophysiological brain responses to music listening and interaction, which could have significant implications for the music industry. This study also aims to demonstrate the usefulness of VR environments in controlling sensory stimuli during EEG-based research on the brain.

Most prior investigations into the effects of familiar and unfamiliar music on brain behavior have utilized very short portions of songs (1–10 s; Freitas et al., 2018; Jagiello et al., 2019; Malekmohammadi et al., 2023). While this approach can investigate the immediate response to familiar and unfamiliar music, the steady-state response is not able to be properly evaluated. These responses to short stimuli are also usually focused on auditory event-related potentials which are primarily associated with sensation rather than cognitive state. Therefore, this investigation opted to explore longer term responses to familiar and unfamiliar musical stimuli by having participants listen to the entire duration of a song. To help combat participants losing interest with the experimental paradigm or ignoring the stimuli, the VR rhythm game condition was utilized alongside a traditional listening task. Furthermore, the previous studies have little agreement as to the ideal musical stimuli for studies regarding familiarity. Malekmohammadi et al. (2023) and Kumagai et al. (2017) used classical music while Jagiello et al. (2019) utilized popular music from several different genres tailoring the stimuli to each individual participant (Kumagai et al., 2017; Malekmohammadi et al., 2023). There are even examples of studies preparing new musical stimuli specifically for use in their experiment, such as Klostermann et al. (2009). For this study it was determined that using musical stimuli tailored to each individual participant was ideal, as it was a goal of the study to keep the work relevant to the applications as much as possible.

EEG recordings were split into canonical frequency bands for analysis. The delta frequency band has been correlated with cortical plasticity (Malik & Amin, 2017). The theta frequency band has been correlated with learning and memory in EEG recordings (Herweg et al., 2020). The alpha frequency band helps calm down the person when necessary and promote feelings of deep relaxation. If suppressed it can cause anxiety, high stress, and insomnia (Abhang et al., 2016). The beta frequency band correlates with a state of higher awareness and focus (Rakel and Faass, 2006). The gamma frequency is correlated with attention, working memory, and long-term memory processes (Malik & Amin, 2017).

Methods

Participants

The experiment was approved by the Internal Review Board (IRB) at George Mason University (IRB# 1978051-2). Each participant was given a copy of the informed consent document. Before signing the document, each participant was read the entire document and given the opportunity to ask any questions.

Ten participants were recruited for the experiment. Nine of the participants were 21 years old, and the remaining participant was 60 years old. Of the 10 participants, three were male and seven were female. All participants had normal hearing and had normal or corrected-to-normal vision.

Hardware

EEG data were collected using the Muse Monitor 2 (Muse, 2023), a commercially available device chosen for its ease of use and broad accessibility. These features support the potential for this research and its outcomes to be integrated into practical applications. Additionally, the device's small form allows it to fit comfortably beneath the VR headset. The Muse Monitor 2 uses four electrodes placed at TP9, AF7, AF8, and TP10, with a sampling rate of 256 Hz. Electrode placement is illustrated in Figure 1. The VR system used for this study was an HTC Vive.

Figure 1. *a) Muse Monitor 2 Headband b) Electrode Placement – Indicated by Black Circles. FPZ Is Utilized as Ground by the Muse Monitor 2, While the Other Highlighted Electrodes Are Recording Electrodes (Mansi et al., 2021).*

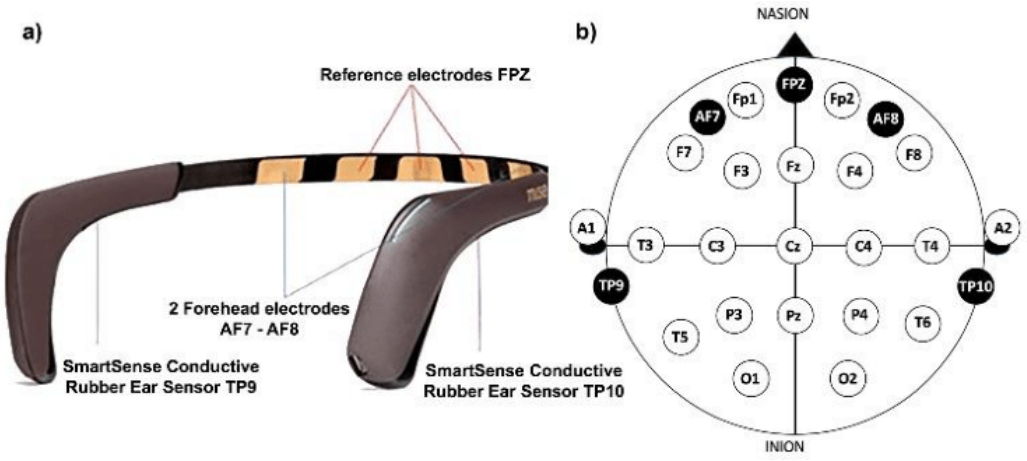

Experimental Task

The VR videogame, Beat Saber, is a rhythm game that involves using imaginary sabers to slash boxes that indicate a specific direction along with the song playing during the game. The saber in each hand are different colors which must match the color of the box that is being slashed (Beat Saber, 2018). For safety purposes, the game was adjusted to only use arm movements (no leg movement). This adjustment also served to reduce motion artifact in the EEG recordings.

Each participant was required to fill out a Google Form when signing up for the experiment. In this form, they were instructed to list five songs that they considered familiar. Four of these songs would be used for the familiar audio and familiar VR scenarios. For the VR scenarios, unfamiliar songs were chosen from the default list in the game. For the audio-only scenarios, unfamiliar songs were chosen from popular bands. The song was selected from unpopular songs from these bands. All participants confirmed that they were not familiar with these songs before recording. See Appendix Table A1 for a list of familiar songs.

Participants first put on the EEG recording device, then the VR headset. Prior to data collection, each participant completed a practice session by playing a randomly selected song in the game. This familiarization period helped them understand the game mechanics, adjust to the recording equipment, and reduce potential confusion during the actual EEG recording. A baseline EEG recording was collected before each experimental section to allow for normalization during data analysis. Participants were also instructed to minimize head movements and blink naturally during EEG recordings. If a prolonged disconnection was observed (10 s), the trial would be stopped, the EEG equipment would be adjusted, and a new recording would be done from the start.

The order of trials and stimuli was randomized for each participant. First, the presentation order of the VR and audio-only sections was randomized. Within each section, the order of familiar and unfamiliar songs was also randomized. EEG responses recorded during the Beat Saber (VR) trials were compared to those from the audio-only recordings, facilitating detection of changes in brain activity during analysis. An example of a possible trial arrangement is shown in Figure 2.

Figure 2. *Example of Randomized Experiment.*

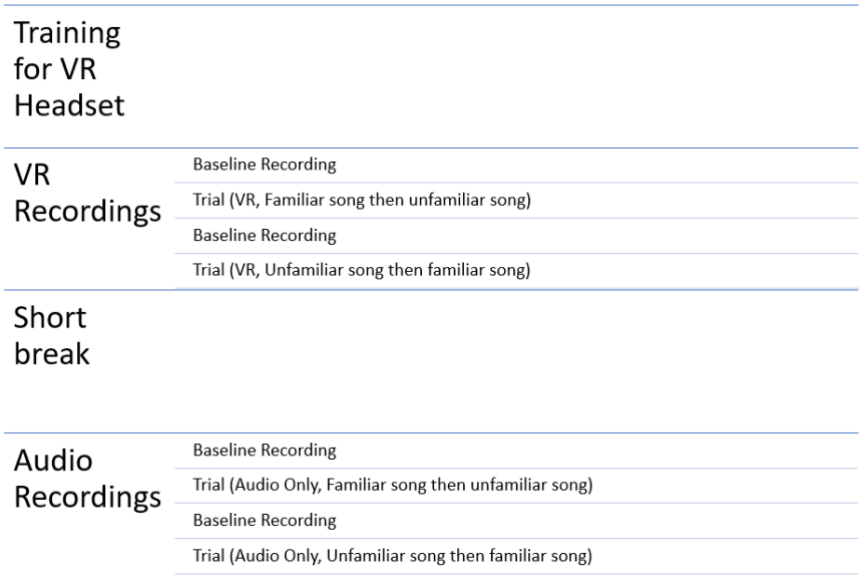

Note. Baseline recordings were 30 s long. the training (approximately 10 min) and short break (approximately 5 min) were determined based off the participant's preference. for each set of trials, the entire song (3 to 4 min) was completed during the recording.

Data Preprocessing

The data preprocessing was performed using MATLAB (Matlab, n.d.). During EEG recordings, several brief disconnections occur during recording. These disconnection artifacts were removed using a Hampel filter (Hampel, n.d.). The Hampel filter was chosen due to its robustness against outliers. EEG signals were segmented into 2-s nonoverlapping epochs. For each channel, artifact rejection was performed by calculating the standard deviation of each epoch. Epochs with a standard deviation exceeding 100 μV were excluded from analysis to remove high-amplitude artifacts. Welch's method was used to extract the power spectral density of the EEG. Following this, data were separated based on the frequency to the appropriate canonical frequency bands: delta (1–4 Hz), theta (4–8 Hz), alpha (8–13 Hz), beta (13–30 Hz), and gamma (30–40 Hz).

After separating the data into canonical frequency bands, the root mean square (RMS) was calculated for each band; for example, one RMS value was 17.6362. This procedure was performed on all baseline and trial recordings for each stimulus type. The RMS values from the trial recordings were then normalized by dividing them by their corresponding baseline values, as shown in Figure 3. These normalized values were saved for subsequent analysis. This procedure was applied to the data of every participant.

Figure 3. *The Data Preprocessing Steps.*

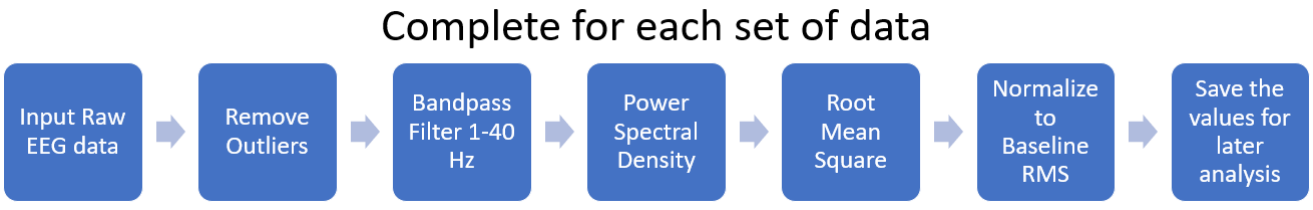

Note. A custom-designed script in MATLAB was used for all steps.

Signal Processing and Statistical Analysis

After preprocessing was completed for all data from all participants, the distributions of RMS values were organized and graphed using boxplots. The data were organized such that each figure created corresponds to one of the canonical frequency bands. In each figure, there are four subplots that correspond to each of the electrodes used on the recording device. In each subplot, there are four separate boxplots that each refer to the four circumstances of recording: familiar audio, unfamiliar audio, familiar VR, and unfamiliar VR. Finally, statistical significance was determined using the Wilcoxon signed rank test. This test determined if there is a statistically significant difference between the baseline value and the median of the corresponding scenario.

Results

The results are organized by frequency band and then further divided by whether the Wilcoxon signed rank test was comparing the power spectral density of the trial to baseline or its paired unfamiliar/familiar trial. If a boxplot was significant, it was highlighted green (significance from baseline) or red (significant between familiar/unfamiliar pair) in the figure for easier viewing. If both significance from baseline and significance between the familiar/unfamiliar pair existed, the boxplot was highlighted blue.

Delta Frequency Results

In Figure 4, only three scenarios showed a difference: unfamiliar audio and familiar VR for the AF8 electrode and familiar audio for the TP10 electrode. There are no significant differences between the familiar and unfamiliar components for the delta frequency.

Theta Frequency Results

In Figure 5, all scenarios show a significant increase in the theta band for the AF8 electrode. Additionally, the familiar audio scenario showed a significant increase in power compared to the baseline in the TP10 electrode. Only one pair of scenarios had a significant difference between each other. The audio-only scenario for the TP10 electrode showed that the familiar audio has more activity than the unfamiliar audio.

Figure 4. *Delta Frequency Results.*

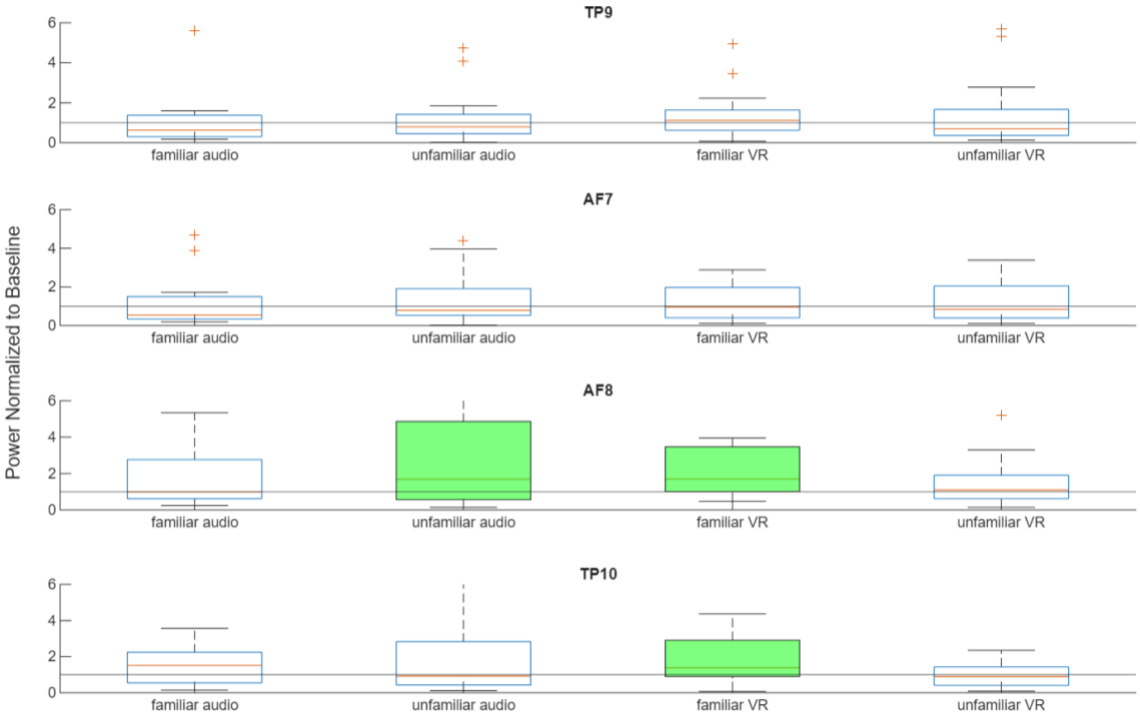

Figure 5. *Theta Frequency Results.*

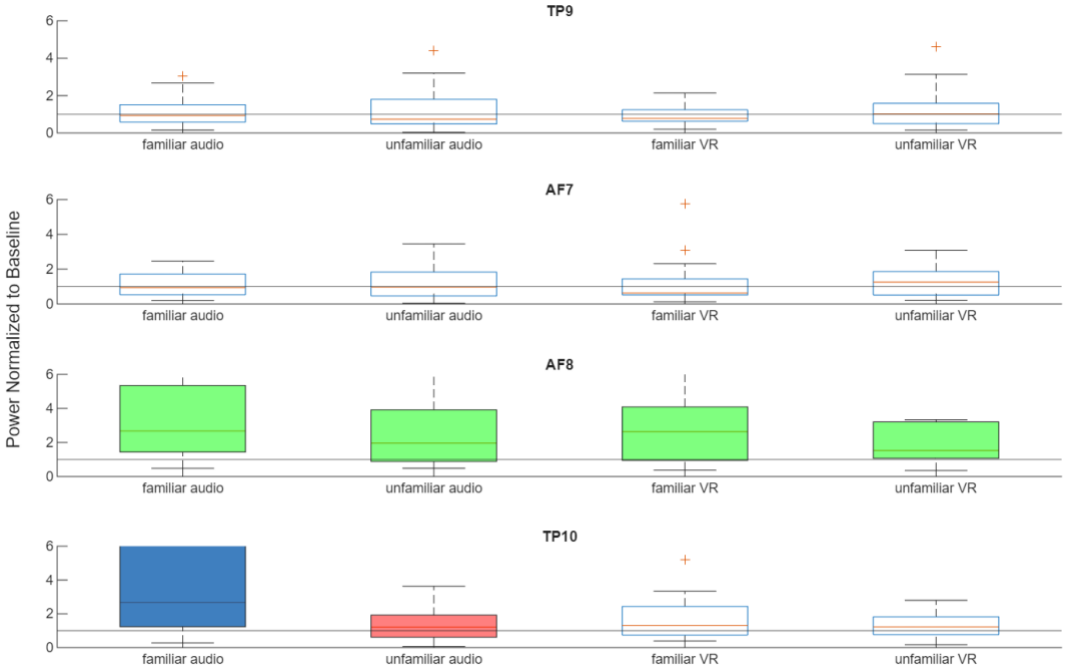

Alpha Frequency Results

In Figure 6, all scenarios show a significant increase in the alpha band for the AF8 electrode. Additionally, the familiar audio scenario showed a significant increase in power compared to the baseline in the TP10 electrode. Only one pair of scenarios had a significant difference between each other. The audio-only scenario for the TP10 electrode showed that the familiar audio has more activity than the unfamiliar audio.

Figure 6. *Alpha Frequency Results.*

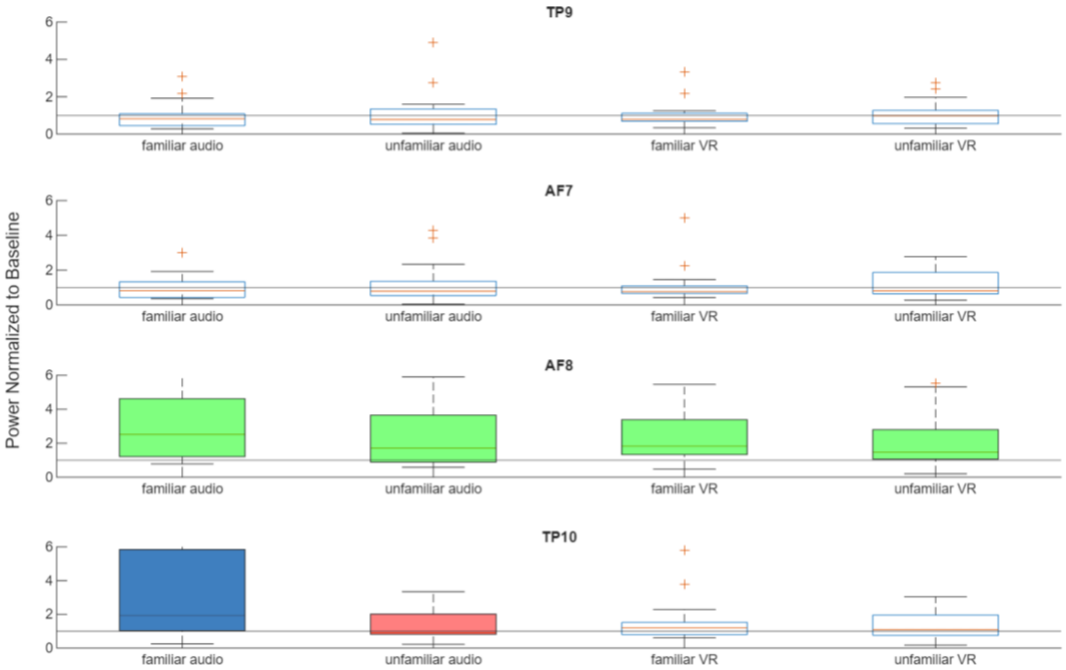

Beta Frequency Results

In Figure 7, there is a significantly lower power compared to baseline for the familiar audio in the AF7 electrode. Across AF8, there is a significant difference between the familiar and unfamiliar scenarios. There is also a significant difference above the baseline for the familiar audio of AF8. For TP10, there is a significant difference between the audio-only scenarios. There is a significant difference below the baseline for the unfamiliar audio of TP10.

Figure 7. *Beta Frequency Results.*

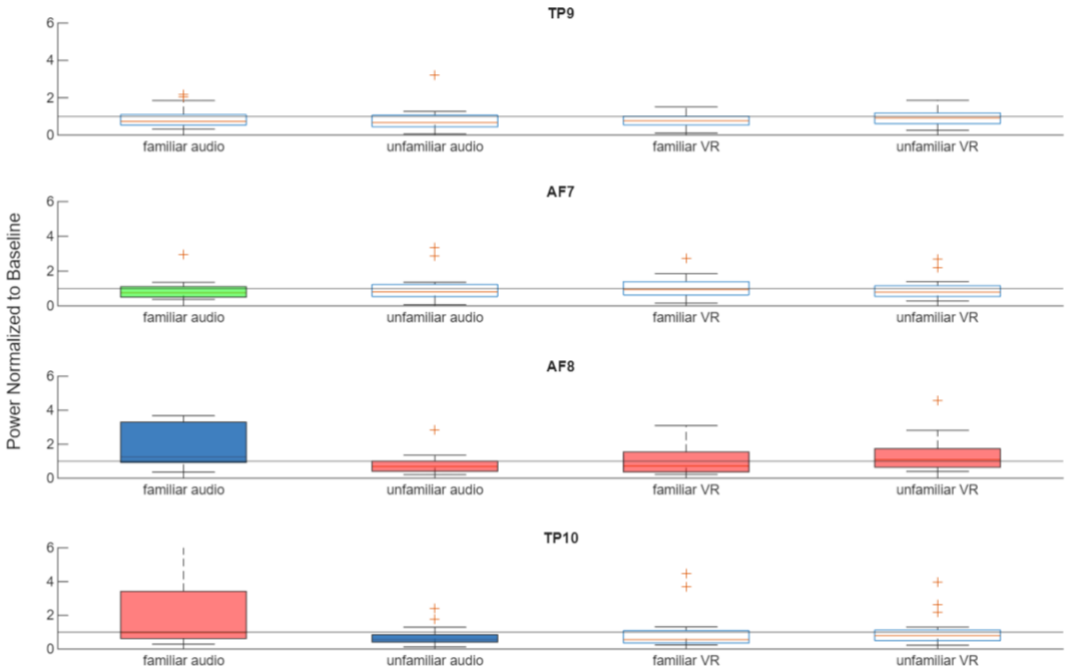

Gamma Frequency Results

In Figure 8, the unfamiliar audio scenario is significantly lower than baseline for the AF8 and TP10 electrode. There are significant differences between the familiar and unfamiliar scenarios for both audio-only and VR sections at the AF8 and TP10 electrodes.

Discussion

Interpreting Results – Significance From Baseline

The delta frequency band results indicate increased activity during two scenarios: unfamiliar audio-only and familiar VR. The AF8 electrode showed increased delta power in both the familiar VR and unfamiliar audio-only conditions, while the TP10 electrode showed increased activity only in the familiar VR condition. These increases in delta activity are likely associated with enhanced cortical plasticity (Malik & Amin, 2017). The difference between the AF8 and TP10 electrodes is likely due to the distinct brain regions they monitor. The AF8 electrode corresponds to the right frontal region, which is partly responsible for spatial awareness and attention (Corbetta & Shulman, 2002). This may explain the increased delta power in the familiar VR condition; however, it is unexpected that the unfamiliar VR condition did not show a similar increase. The TP10 electrode, which corresponds to the right temporal region involved in auditory processing, may reflect increased auditory engagement with familiar music during a music-related task (Hickok & Poeppel, 2007).

The theta frequency band results show increased activity across all scenarios at the AF8 electrode. Additionally, the TP10 electrode exhibited increased activity specifically during the familiar audio-only condition, with a significant difference between the familiar and unfamiliar audio scenarios. Because theta activity is associated with learning and memory, these increases at the AF8 site likely reflect engagement with music-related tasks in the right frontal region of the brain (Herweg et al., 2020).

Figure 8. *Gamma Frequency Results.*

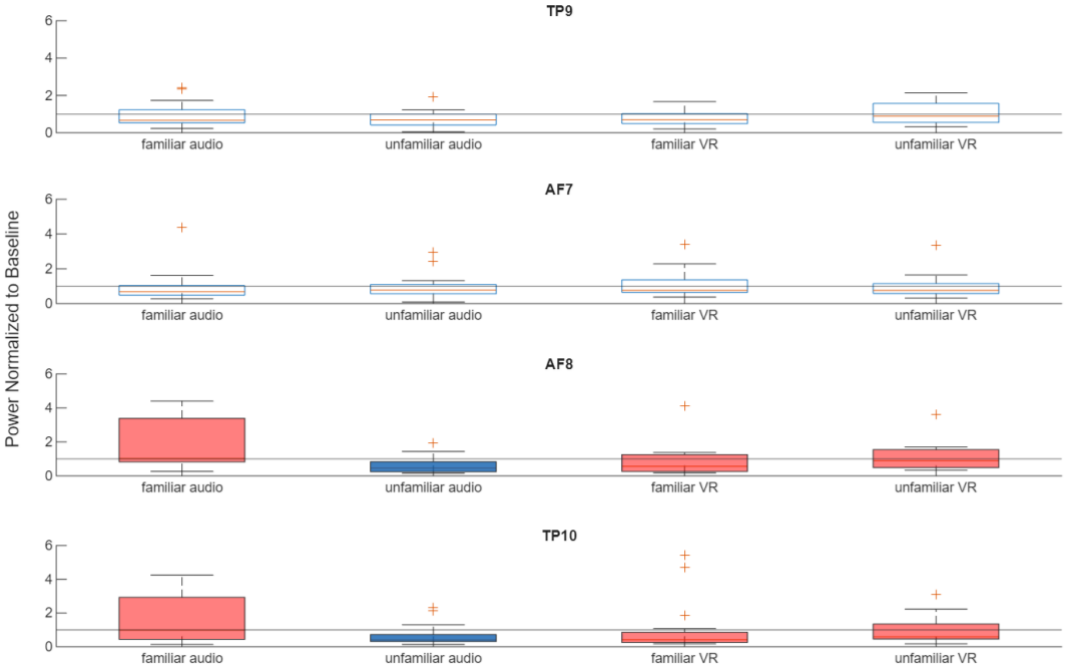

The additional increase at TP10 during familiar audio-only suggests that familiar and unfamiliar music may be processed differently in the right temporal region. This distinction may reflect enhanced memory retrieval or recognition processes associated with familiar auditory stimuli.

The alpha frequency band results mirror the trends observed in the theta band. Specifically, there is increased alpha activity across all scenarios at the AF8 electrode, suggesting greater relaxation in the right frontal region of the brain (Abhang et al., 2016). However, this pattern does not extend to the TP10 electrode. At TP10, increased alpha activity is seen only in the familiar audio condition, with a significant difference compared to the unfamiliar audio condition. This increase is not observed in the familiar VR scenario. These findings may suggest that the brain processes familiar music differently depending on whether it is experienced in a VR environment or through audio-only, particularly in the right temporal region.

The beta frequency band results show significant differences between familiar and unfamiliar scenarios across multiple conditions: audio-only (AF8), VR (AF8), and audio-only (TP10). Notably, the familiar VR condition at AF8 exhibited significantly lower beta activity compared to its unfamiliar counterpart—opposite the trend observed in the other scenarios. In contrast, familiar audio-only at AF8 showed a significant increase from baseline, while unfamiliar audio-only at TP10 showed a significant decrease. For the first time, a significant result was also observed at the AF7 electrode, where familiar audio-only produced a significant decrease in beta activity compared to baseline. Elevated beta activity is typically associated with increased alertness and focus (Rakel & Faass, 2006). Based on this, participants appear to be more focused when listening to familiar songs in the audio-only condition, but this does not hold true for familiar VR scenarios. Similarly, the significant decrease in beta activity during unfamiliar audio-only suggests reduced focus. The result at AF7, showing a decrease during familiar audio-only, contrasts with the increased activity on the right side (AF8), suggesting potential lateralization in how music is processed across the two hemispheres of the brain.

The gamma frequency band results reveal significant differences between familiar and unfamiliar songs in both audio-only and VR scenarios. At the AF8 electrode, unfamiliar audio-only elicited a significant decrease in gamma activity, suggesting reduced attention to unfamiliar music in this condition (Malik & Amin, 2017). A similar pattern was observed at the TP10 electrode. In contrast, the VR scenarios showed the opposite trend; gamma activity was significantly lower in the familiar VR condition compared to the unfamiliar VR

condition. These opposing patterns further highlight a distinction in how the brain processes familiarity in audio-only versus VR environments.

Interpreting Results – Unfamiliar Versus Familiar

The delta frequency band shows no significant differences between familiar and unfamiliar trials. In contrast, the theta, alpha, beta, and gamma bands all show significant differences between familiar and unfamiliar audio-only conditions, with familiar audio eliciting higher power across these bands. For the VR conditions, significant differences appear in the beta and gamma bands, whereas unfamiliar VR scenarios exhibit higher power than their familiar counterparts. These findings suggest distinct patterns of brain activity depend on the context in which music is experienced. Specifically, familiar music evokes stronger neural responses during passive audio-only listening, whereas unfamiliar music elicits greater activity during active engagement in the VR environment. This highlights a fundamental difference in how the brain processes musical familiarity during passive versus immersive tasks.

Limitations

The data collected only used four electrodes, thus limiting how much of the brain's electrical activity can be recorded. It may be possible to see the differences between VR and audio-only scenarios in finer detail if more electrodes were used to record. However, the Muse Monitor 2 allowed for easier recording during VR.

Another complication is that most participants had never used VR or played the game Beat Saber. This adds another element of novelty, since the participant had to learn how to adjust to the virtual environment and understand the game mechanics. It is entirely possible that the differences observed between the audio only and VR scenarios were due to the novelty of their situation instead of the music. Further research will need to be done that removes this issue to declare more certainly that these results are due to the music familiarity and not the experimental paradigm.

An additional limitation is the presence of motion artifacts in the data. While the experiment design attempted to limit the amount of movement occurring by the participant, they still had to move their arms to play the rhythm game, resulting in some motion artifacts being created. A more robust method of motion artifact removal may be necessary for research moving forward.

Conclusions

When comparing the EEG of familiar and unfamiliar music, it appears that there are significant differences between how the brain processes familiar and unfamiliar music in both an audio-only and VR scenario. Significant results almost exclusively occurred on the right side of the brain, indicating that most music-related processing likely occurs on this side of the brain. This makes sense, since this study had participants focus on mainly listening to music, rather than producing music (Peretz & Zatorre, 2005). Overall, it is logical to conclude that there are differences between how the brain processes familiar and unfamiliar music. Additionally, it is concluded that how music is processed in terms of familiarity during a VR game is different than just listening to the music alone. Further research will need to be completed to determine what causes these differences.

Author Acknowledgments

We would like to thank Connor Delaney, a doctoral student at George Mason University, for his contributions and assistance throughout this project.

Author Declaration

George Mason University provided a total of $1500 through the Undergraduate Research Scholars Program (URSP). These funds were used to fund equipment used during the experiment. We have no other financial interest or known conflicts of interest to disclose. AI tools were used solely to assist with rephrasing and improving clarity of the manuscript text. All content was developed by the authors who take full responsibility for the work.

References

Abhang, P. A., Gawali, B. W., & Mehrotra, S. C. (2016). *Introduction to EEG- and speech-based emotion recognition*. Academic Press.

Beat Saber. (2018). *Beat Saber – VR rhythm game* [video game]. Beat Games. https://beatsaber.com/

Corbetta, M., & Shulman, G. L. (2002). Control of goal-directed and stimulus-driven attention in the brain. *Nature Reviews Neuroscience, 3*(3), 201–215. https://doi.org/10.1038/nrn755

Freitas, C., Manzato, E., Burini, A., Taylor, M. J., Lerch, J. P., & Anagnostou, E. (2018). Neural correlates of familiarity in music listening: A systematic review and a neuroimaging meta-analysis. *Frontiers in Neuroscience, 12*, Article 686. https://doi.org/10.3389/fnins.2018.00686

Hailstone, J. C., Omar, R., & Warren, J. D. (2009). Relatively preserved knowledge of music in semantic dementia. *Journal of Neurology, Neurosurgery & Psychiatry, 80*(7), 808–809. https://doi.org/10.1136/jnnp.2008.153130

Hampel. (n.d.). Filter outliers using Hampel identifier – Simulink. *MathWorks*. https://www.mathworks.com/help/dsp/ref/hampelfilter.html

Herweg, N. A., Solomon, E. A., & Kahana, M. J. (2020). Theta oscillations in human memory. *Trends in Cognitive Sciences, 24*(3), 208–227. https://doi.org/10.1016/j.tics.2019.12.006

Hickok, G., & Poeppel, D. (2007). The cortical organization of speech processing. *Nature Reviews Neuroscience, 8*(5), 393–402. https://doi.org/10.1038/nrn2113

Jagiello, R., Pomper, U., Yoneya, M., Zhao, S., & Chait, M. (2019). Rapid brain responses to familiar vs. unfamiliar music – An EEG and pupillometry study. *Scientific Reports, 9*, Article 15570. https://doi.org/10.1038/s41598-019-51759-9

Klostermann, E. C., Loui, P., & Shimamura, A. P. (2009). Activation of right parietal cortex during memory retrieval of nonlinguistic auditory stimuli. *Cognitive, Affective, & Behavioral Neuroscience, 9*(3), 242–248. https://doi.org/10.3758/cabn.9.3.242

Kumagai, Y., Arvaneh, M., & Tanaka, T. (2017). Familiarity affects entrainment of EEG in music listening. *Frontiers in Human Neuroscience, 11*, Article 384. https://doi.org/10.3389/fnhum.2017.00384

Kumar, J. S., & Bhuvaneswari, P. (2012). Analysis of electroencephalography (EEG) signals and its categorization—A study. *Procedia Engineering, 38*, 2525–2536. https://doi.org/10.1016/j.proeng.2012.06.298

Malekmohammadi, A., Ehrlich, S. K., Rauschecker, J. P., & Cheng, G. (2023). Listening to familiar music induces continuous inhibition of alpha and low-beta power. *Journal of Neurophysiology, 129*(6), 1344–1358. https://doi.org/10.1152/jn.00269.2022

Malik, A. S., & Amin, H. U. (2017). *Designing EEG experiments for studying the brain: Design code and example datasets*. Elsevier.

Mansi, S. A., Pigliautile, I., Porcaro, C., Pisello, A. L., & Arnesano, M. (2021). Application of wearable EEG sensors for indoor thermal comfort measurements. *ACTA IMEKO, 10*(4), 214. https://doi.org/10.21014/acta_imeko.v10i4.1180

Matlab. (n.d.). *MathWorks*. https://www.mathworks.com/products/matlab.html

Muse. (2023, March 29). The brain sensing headband store with worldwide shipping: Muse™ EEG-powered meditation & sleep headband. *Muse*. https://choosemuse.com/

Peretz, I., & Zatorre, R. J. (2005). Brain organization for music processing. *Annual Review of Psychology, 56*, 89–114. https://doi.org/10.1146/annurev.psych.56.091103.070225

Rakel, D., & Faass, N. (2006). *Complementary medicine in clinical practice: Integrative practice in American healthcare*. Jones and Bartlett.

Zajonc, R. B. (1968). Attitudinal effects of mere exposure. *Journal of Personality and Social Psychology, 9*(2, Pt. 2), 1–27. https://doi.org/10.1037/h0025848

Received: July 5, 2025
Accepted: August 25, 2025
Published: March 31, 2026

Appendix A

Table A1
Familiar Songs

	Participant 1
Familiar VR 1	Beat It - Michael Jackson
Familiar VR 2	Banana Pie - Lil Darkie
Familiar Audio 1	Radioactive - Imagine Dragons
Familiar Audio 2	Gasolina - Daddy Yankee
	Participant 2
Familiar VR 1	Beat It - Michael Jackson
Familiar VR 2	Shake It Off - Taylor Swift
Familiar Audio 1	Country Roads - John Denver
Familiar Audio 2	Billie Jean - Michael Jackson
	Participant 3
Familiar VR 1	Landslide - Fleetwood Mac
Familiar VR 2	No Roots - Alice Merton
Familiar Audio 1	Waka Waka - Shakira
Familiar Audio 2	Both Sides Now - Joni Mitchell
	Participant 4
Familiar VR 1	Beat It - Michael Jackson
Familiar VR 2	Shake It Off - Taylor Swift
Familiar Audio 1	Untouched - The Veronicas
Familiar Audio 2	Treasure - Bruno Mars
	Participant 5
Familiar VR 1	Mr. Blue Sky - Electric Light Orchestra
Familiar VR 2	Heat Waves - Glass Animals
Familiar Audio 1	Stressed Out - Twenty One Pilots
Familiar Audio 2	Breezeblocks - alt-J
	Participant 6
Familiar VR 1	Shake It Off - Taylor Swift
Familiar VR 2	Never Gonna Give You Up - Rick Astley
Familiar Audio 1	Don't Stop Believin' - Journey
Familiar Audio 2	Forget You - Ceelo Green
	Participant 7
Familiar VR 1	Don't Stop Believin' - Journey
Familiar VR 2	Forget You - Ceelo Green
Familiar Audio 1	Shake It Off - Taylor Swift
Familiar Audio 2	Never Gonna Give You Up - Rick Astley
	Participant 8
Familiar VR 1	Toxic - Britney Spears
Familiar VR 2	I Love It - Icona Pop
Familiar Audio 1	We Didn't Start the Fire - Billy Joel
Familiar Audio 2	Fat Bottomed Girls - Queen
	Participant 9
Familiar VR 1	Star Walkin' - Lil Nas X
Familiar VR 2	Lone Digger - Caravan Palace
Familiar Audio 1	Enemy - Imagine Dragons
Familiar Audio 2	Mic Drop - BTS
	Participant 10
Familiar VR 1	High Hopes - Panic at the Disco
Familiar VR 2	Boulevard of Broken Dream - Green Day
Familiar Audio 1	Radioactive - Imagine Dragons
Familiar Audio 2	Counting Stars - One Republic

NeuroRegulation

ISNR INTERNATIONAL SOCIETY FOR NEUROREGULATION & RESEARCH

Neurological Diagnosis in the AI Era: A Comparative Assessment of ChatGPT 3.5, Google Gemini, Being AI, and Perplexity AI

Muhammad Essa[1], Abdelrhman H. Mohamed[2], Zainullah[3], and Milica Jovanovic[4]*

[1]Neurology Department, BMC Hospital, Quetta, Pakistan
[2]Faculty of Medicine, Luxor University, Luxor, Egypt
[3]Sapienza University of Rome, Rome, Italy
[4]University of Tartu, Tartu, Estonia

Abstract

Background. In neurological diagnostics, where complexity, data volume, and diagnostic urgency present major obstacles, artificial intelligence (AI) systems have the potential to revolutionize the field. Despite widespread use, there is a lack of comparable performance assessments of publicly available AI tools for integrated clinical reasoning in neurology. **Methods.** This cross-sectional study evaluated five AI platforms (ChatGPT 3.5, Google Gemini, Bing AI, Perplexity AI, DeepSeek) utilizing 15 standardized neurological cases from *Case Files: Neurology, Third Edition*. Each platform was given identical prompts imitating clinical consultations. Responses were evaluated (maximum 6 points per case; total 90) in three domains: diagnosis, subsequent diagnostic step, and therapeutic/molecular foundation. Nonparametric statistical methods (Kruskal-Wallis, Chi-square) assessed performance disparities. **Results.** ChatGPT achieved the highest overall score (88/90, 97.8%), followed by DeepSeek (86/90, 95.6%), Perplexity (84/90, 93.3%), Google Gemini (78/90, 86.7%), and Microsoft Copilot (73/90, 81.1%). Therapeutic accuracy was 100% for ChatGPT, DeepSeek, and Gemini, whereas it was 80% for Copilot. Although there were disparities in performance, inferential statistics revealed no significant differences between platforms (Kruskal-Wallis p = .423; Chi-square p = .374). Verbosity showed significant variation: DeepSeek averaged 488 words per response, whereas Copilot and Perplexity averaged 239 to 240 words. **Conclusion.** Popular AI platforms (ChatGPT, DeepSeek) exhibit significant proficiency in neurological diagnosis and treatment planning, but there is a huge difference in the depth and structure of responses across all of the tools. AI should be used as complementary healthcare assistance, with future integration requiring better explainability and real-world validation.

Keywords: artificial intelligence; neurological diagnosis; large language models (LLMs); comparative evaluation; diagnostic accuracy (MeSH)

Citation: Essa, M., Mohamed, A. H., Zainullah, & Jovanovic, M. (2026). Neurological diagnosis in the AI era: A comparative assessment of ChatGPT 3.5, Google Gemini, Being AI, and Perplexity AI. *NeuroRegulation, 13*(1), 54–64. https://doi.org/10.15540/nr.13.1.54

***Address correspondence to**: Dr. Syed Muhammad Essa BMCH Complex. Brewery Road. Quetta, Balochistan. Pakistan, 87300. Email: dressakhan777@gmail.com

Edited by:
Rex L. Cannon, PhD, Currents, Knoxville, Tennessee, USA

Reviewed by:
Rex L. Cannon, PhD, Currents, Knoxville, Tennessee, USA
Randall Lyle, PhD, Mount Mercy University, Cedar Rapids, Iowa, USA

Introduction

In recent years, incorporating artificial intelligence (AI) into different sectors has transformed traditional problem-solving and decision-making methodologies (Nguyen & Vo, 2024; Shokran et al., 2025). AI has shown great promise in helping medical professionals with activities ranging from diagnosis to treatment planning, especially in the field of healthcare (Rashid & Sharma, 2025; Salammagari & Srivastava, 2024; Zeb et al., 2024). The development of more sophisticated AI has the potential to greatly improve neurological care (AbuAlrob & Mesraoua, 2024; Kalani & Anjankar, 2024). This subject is distinguished by its intricacy and dependence on the precise interpretation of complex data. Global healthcare systems have significant challenges with neurological disorders,

including stroke, epilepsy, Parkinson's disease, and Alzheimer's disease (Kandel, 2025; Yang et al., 2025). These conditions are frequently present with a wide range of symptoms and fluctuating rates of progression, which makes diagnosis and treatment extremely difficult. Conventional diagnostic approaches mostly depend on laboratory testing, neuroimaging technologies, and clinical experience, all of which can be laborious and subject to subjective interpretation.

By combining the strength of neural networks, machine learning algorithms, and big data analytics, AI technologies present a paradigm change in neurological diagnostics (Dipankar et al., 2025; Onciul et al., 2025). In order to help doctors diagnose patients accurately and quickly, AI systems have the capacity to evaluate enormous volumes of patient data, including genetic data, clinical records, and medical imaging (Alhejaily, 2025; Li et al., 2024; Oyeniyi & Oluwaseyi, 2024). AI has the potential to enhance human knowledge of neurological diseases by providing machine-driven insights, hence minimizing diagnosis errors and enhancing treatment techniques (Mennella et al., 2024; Valerio et al., 2025).

To determine their practical efficacy and therapeutic value, however, a thorough assessment and comparison are still required amid the expanding field of AI-powered diagnostic tools. This study aims to fill that gap by undertaking a comparative analysis of five major AI platforms in neurological diagnosis. We will specifically assess how well they perform in relation to important parameters like interpretability, scalability, sensitivity, specificity, and diagnostic accuracy. The comparative evaluation also helps researchers and medical professionals find the advantages and disadvantages of various AI systems and decide which ones are most appropriate for particular clinical circumstances or diagnostic tasks. Through meticulous comparison studies, scientists may offer important insights into how AI systems function in various scenarios, supporting the integration of AI technology into clinical practice and supporting evidence-based decision-making. Through thoroughly analyzing each system's advantages and disadvantages, we hope to offer insightful information that can guide clinical judgment and propel neurology forward.

Methodology

This was a cross-sectional comparative study evaluating the diagnostic performance of five publicly available AI platforms—ChatGPT (OpenAI), Microsoft Copilot (Microsoft), DeepSeek, Google Gemini (Google), and Perplexity—in interpreting standardized neurological case scenarios. All responses were generated in April–May 2024.

The four chosen AI platforms—ChatGPT 3.5, Google Gemini, Bing AI, and Perplexity AI—were presented with each case scenario as part of the study design. The following was the typical input prompt for every case: “I'm working on a neurology quiz and will provide you the patient's full medical history, presenting problems, and findings. Behaving like a neurology professor, please provide the most appropriate answer.”

Using a consistent input prompt, the study design presented case scenarios to the AI platforms in an organized manner. This prompt was designed to mimic an actual clinical setting, supplying pertinent findings, the patient’s medical history, and their current problems. Three key questions were used to help AI systems in the task of producing diagnosis theories and therapy recommendations:

1. A diagnosis?
2. What is the next diagnostic action?
3. Next therapeutic step or molecular/genetic basis, ordered by probability.

All AI platforms’ responses were carefully documented and assessed to make sure they answered the questions correctly and comprehensively. Crucially, the AI systems were impartially evaluated for their effectiveness in neurological diagnosis because they were not pretrained with particular command sets or queries.

Ethical Considerations

The study did not require formal ethics committee permission because it was conducted solely using published cases, did not include human individuals, and did not access personal health information. The use of anonymized data and standardized case scenarios guaranteed adherence to ethical rules regarding patient privacy and confidentiality.

Selection of Cases

To undertake a thorough comparative evaluation of AI systems in neurological diagnosis, 15 clinically significant neurological cases were chosen from *Case Files: Neurology, Third Edition* by Eugene C. Toy et al. (2018). These scenarios were selected to

represent a broad spectrum of neurological conditions, such as multiple sclerosis, epilepsy, stroke, Parkinson's disease, Alzheimer's disease, and traumatic brain injury. Every case was thoroughly examined to make sure it depicted a situation that was clinically realistic and had unique diagnostic issues and considerations.

LLM Input-Output Procedures

Every AI platform was given the same input prompt in the form of a chat session for every case scenario. The AI systems were able to produce responses that were well-informed since this input prompt supplied adequate clinical background. Because the AI platforms weren't pretrained with any particular command sets or questions, their responses could be evaluated objectively because they were based only on their natural capabilities.

Scoring System

Accuracy and comprehensiveness in answering the three main questions in the input prompt determined the score for each AI platform's response. This was the scoring system:

(a) 6 points (*excellent*): When all three questions—the diagnosis, the next diagnostic step, the molecular/genetic basis, or the next therapeutic step—were answered correctly.
(b) 4 points (*good*): When two questions were answered accurately.
(c) 2 points (*moderate*): When just one question was answered accurately.
(d) 1 point (*very poor*): When every question was answered wrong.

This grading system allows for a sophisticated evaluation of the AI platforms' performance, taking into account both the accuracy of diagnoses and the comprehensiveness of their responses.

Statistical Analysis

Descriptive statistics were computed for total scores, mean word count, and individual domain accuracy. To assess normality, both Kolmogorov-Smirnov and Shapiro-Wilk tests were applied. Given the nonnormal distribution of scores (as evidenced by significant *p*-values in both tests), nonparametric methods were employed.

Differences in overall performance across AI platforms were analyzed using the Kruskal-Wallis H test, followed by post hoc pairwise comparisons with Bonferroni correction for multiple testing. Word count differences were described descriptively. Exploratory subgroup analyses were planned to evaluate:

- Performance variation by diagnostic category (e.g., movement disorders vs. infectious diseases)
- Correlation between word count and accuracy
- Consistency of responses across repeated prompts

However, due to limited sample size and variability in output structure, these analyses were deemed exploratory and not formally reported in the final results.

Limitations of the Study Design

While efforts were made to maintain standardization, several limitations should be acknowledged:

- AI outputs were influenced by version updates and backend changes during the study period.
- Some models exhibited variability when prompted multiple times, limiting reproducibility.
- No formal external validation dataset was used.
- Human-level comparison (e.g., resident vs. AI) was not included but is recommended for future work.

Results

The basic assessment of AI platform performance was based on a detailed scoring system, with each of the 15 scenarios worth a maximum of 6 points, for a total possible score of 90 points. A thorough synopsis of each AI model's performance metrics is given in Table 1. ChatGPT achieved the highest overall score of 88 points, corresponding to an impressive 97.77% accuracy. DeepSeek closely behind with 86 points (95.55%), signifying strong performance. Perplexity attained third place with 84 points (93.33%). Google Gemini achieved 78 points (86.66%), and Copilot obtained the lowest overall score of 73 points (81.11%; As illustrated in Figure 1).

All AI models exhibited a steady median score of 6.00. This indicates that in at least 50% of the assessed cases, each AI platform was able to deliver an impeccable response by precisely resolving all three essential enquiries: diagnosis, subsequent diagnostic action, and the ensuing therapeutic/molecular/genetic rationale.

Table 1
Performance Metrics by AI Platform

AI Model	Total Score (out of 90)	Percentage (%)	Mean Score	Median	Std. Deviation	Variance	Range	Skewness	Kurtosis
ChatGPT 3.5	88	97.77	5.87	6.00	0.516	0.267	02	−3.873	15.000
DeepSeek AI	86	95.55	5.73	6.00	1.033	1.067	04	−3.873	15.000
Perplexity AI	84	93.33	5.60	6.00	0.828	0.686	02	−1.672	0.897
Google Gemini	78	86.66	5.20	6.00	1.781	3.171	05	−2.098	3.107
Bing Copilot	73	81.11	4.86	6.00	2.066	4.267	05	−1.478	0.392

Figure 1. *Presents a Faceted Dot Plot Comparing the Total Performance Scores and Recommendation Accuracy of Five AI Models.*

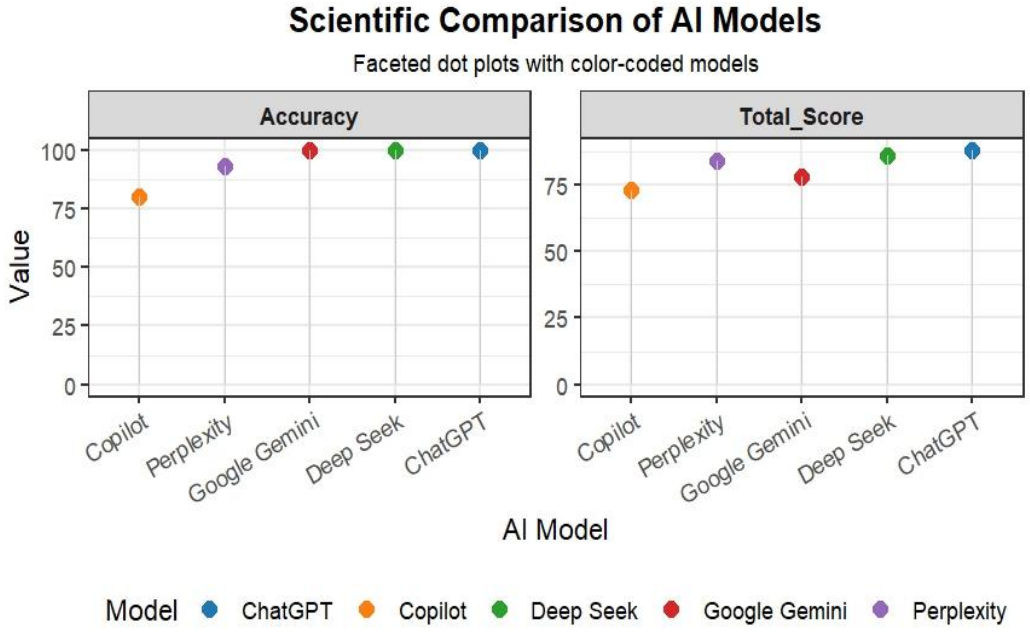

The standard deviations in scores differed, with ChatGPT exhibiting the lowest variability (0.516), signifying highly consistent performance across the scenarios. In contrast, Copilot demonstrated the highest standard deviation (2.066), indicating greater variability in its performance across various neurological conditions. The persistent negative skewness values (from −1.478 for Copilot to −3.873 for ChatGPT and DeepSeek) across all models indicate that the score distribution was biased towards the higher end, suggesting that the AI platforms generally exhibited strong performance, with a greater concentration of scores near the maximum possible value rather than lower scores. The elevated kurtosis values for ChatGPT and DeepSeek (15.000) indicate a sharply peaked distribution with substantial tails, signifying a tendency for scores to cluster around the mean, accompanied by a limited number of extreme outliers (Figure 2).

Figure 2. *The Forest Plot Compares Absolute Skewness and Kurtosis Across AI Models (ChatGPT, Copilot, Etc.), With a Dashed Line at 3 Indicating Severe Deviation. It Highlights Distribution Irregularities, Aiding Model Reliability Assessment.*

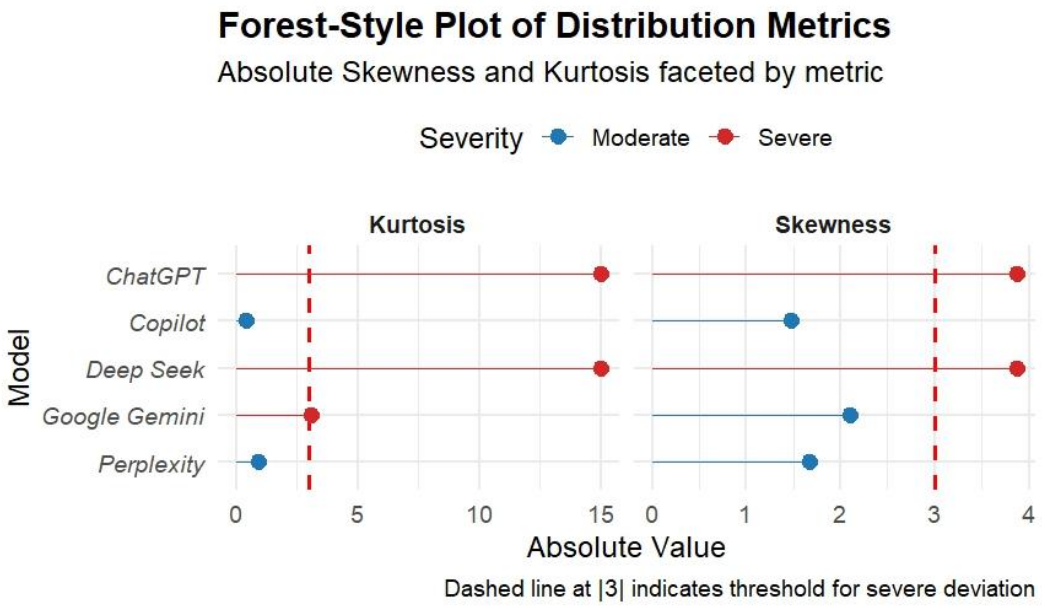

Normality Testing

In order to find the right statistical tests to compare the performance of AI platforms, we used the Kolmogorov-Smirnov and Shapiro-Wilk tests to see if the distribution of the 'Marks' (scores) was normal for each AI platform.

Table 2 demonstrates that both the Kolmogorov-Smirnov and Shapiro-Wilk tests produced significant values (p < .001) for all AI platforms. A p-value below .05 signifies a statistically significant divergence from a normal distribution. Thus, these findings validate that the performance metrics for each AI model exhibited a nonnormal distribution. This discovery is significant as it requires the application of nonparametric statistical methods, such as the Kruskal-Wallis H test, for future comparisons among the AI systems, given that these tests do not presume a normal distribution of the data.

Characteristics of Verbal Output

In addition to accuracy, the study analyzed the characteristics of the verbal output produced by each AI platform. Table 3 presents the aggregate word count and the average word count per response, including their corresponding standard deviations.

DeepSeek AI regularly generated the most extensive responses, averaging 488.4 words each response. ChatGPT ranked as the second most verbose, averaging 429.60 words per response, while Google Gemini produced roughly 379.06 words for each response. Conversely, Copilot and Perplexity offered significantly more short responses, with average word counts of 238.86 and 240.33, respectively. The standard deviation of DeepSeek AI (48.295) signifies a very uniform response length, despite an elevated word count, indicating a methodical approach to thorough responses. Perplexity, albeit generating shorter replies, demonstrated marginally greater variability (59.513) in response length than Copilot. The discrepancies in vocal output may indicate differing degrees of complexity, explanatory depth, or verbosity in the AI's presentation of diagnostic and therapeutic information.

Therapeutic Recommendation Accuracy

Assessing the accuracy of each AI platform's therapeutic advice was a crucial component of the study. Table 5 demonstrates outstanding efficacy in therapeutic recommendations by DeepSeek AI, ChatGPT 3.5, and Google Gemini, each attaining a flawless 100% accuracy rate by delivering 15 accurate recommendations out of 15, without any erroneous suggestions. Perplexity AI exhibited robust performance, attaining a 93.3% accuracy rate

with 14 correct recommendations and merely 1 erroneous one. Copilot exhibited the lowest accuracy in this area, achieving 12 correct and 3 incorrect recommendations, culminating in an 80% accuracy rate (Figure 3). This finding underscores the exceptional reliability of leading AI models in producing precise treatment recommendations, an essential element in clinical neurology.

Table 2
Normality Tests (Kolmogorov–Smirnov and Shapiro–Wilk)

AI Model	KS Stat	KS df	KS Sig.	SW Stat	SW df	SW Sig.
ChatGPT 3.5	0.535	15	.000	0.284	15	.000
DeepSeek AI	0.535	15	.000	0.284	15	.000
Perplexity AI	0.485	15	.000	0.499	15	.000
Google Gemini	0.473	15	.000	0.503	15	.000
Bing Copilot	0.442	15	.000	0.573	15	.000

Table 3
Word Count Summary of AI Responses

AI Model	Total Word Count	Mean Words per Response	Standard Deviation
DeepSeek AI	7326	488.40	48.295
ChatGPT 3.5	6444	429.60	70.632
Google Gemini	5686	379.06	57.231
Perplexity AI	3605	240.33	59.513
Bing Copilot	3583	238.86	40.059

Table 4
Diagnostic Accuracy Overview

AI Model	Correct Answers (out of 45)	Average Score	Incorrect Recommendations
ChatGPT 3.5	44	2.93	01
DeepSeek AI	43	2.86	02
Perplexity AI	42	2.80	03
Google Gemini	38	2.53	07
Bing Copilot	32	2.13	13

Table 5
Therapeutic Recommendation Accuracy

AI Model	Correct Recommendations	Incorrect Recommendations	Accuracy (%)
ChatGPT 3.5	15	0	100%
DeepSeek AI	15	0	100%
Google Gemini	15	0	100%
Perplexity AI	14	1	93.3%
Bing Copilot	12	3	80%

Figure 3. *The Heatmap Shows AI Models' Recommendation Accuracy, With ChatGPT, Gemini, and DeepSeek Scoring Perfectly (15/15 Correct), While Copilot (12/15) and Perplexity (14/15) Had Minor Errors.*

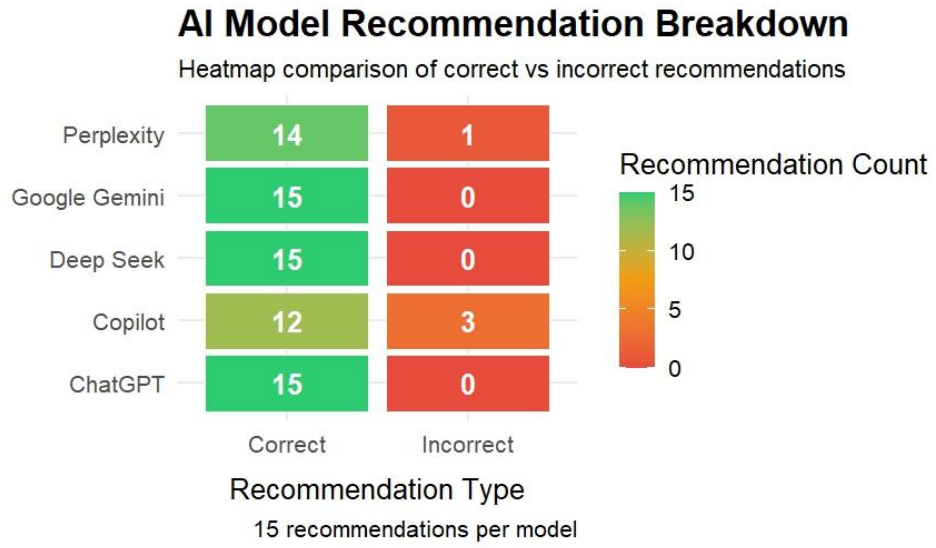

Inferential Statistical Analysis

A Chi-square test of independence and a Kruskal-Wallis H test were performed to thoroughly evaluate the statistical significance or random chance of the observed performance differences across the AI systems.

A Chi-square test of independence was conducted to examine the relationship between the used AI platform and the achieved diagnostic accuracy. The study produced a nonsignificant result, $\chi^2(4, N = 75) = 4.245$, with a *p*-value of .374. Since the *p*-value (.374) is significantly above the traditional significance threshold of $\alpha = .05$, the null hypothesis of no significant relationship between the AI platform and diagnostic accuracy is confirmed. This finding indicates that, statistically, the distribution of diagnostic accuracy does not significantly differ among the various AI platforms assessed in this study.

Additionally, a nonparametric independent-samples Kruskal-Wallis H test was utilized to evaluate the overall performance scores (marks) among the various categories of AI platforms, as the normality tests (Table 2) revealed a nonnormal data distribution. The synopsis of this hypothesis test is defined in Table 6 and Table 7. There was no statistically significant difference in the AI platform performance scores, according to the Kruskal-Wallis H test results (Table 6 and 7), with a $\chi^2(4, N = 75) = 3.875$ and a *p*-value of .423. The *p*-value (.423) above the preestablished significance level of $\alpha = .05$, supporting the null hypothesis that the distribution of marks is consistent across all AI categories. This statistical result indicates that, although there are numerical changes in total scores and percentages (as illustrated in Table 1), these differences are insufficient to be deemed statistically significant. Consequently, the comprehensive statistical analysis indicates that the performance of the assessed AI platforms in aiding neurological diagnosis and suggestions, within the parameters of this study, did not exhibit significant differences (Figure 4). Therefore, in accordance with typical nonparametric analysis protocols, no post hoc pairwise Mann-Whitney U tests were performed due to the nonsignificant overall test outcome.

Table 6

Kruskal-Wallis H Test Summary (Hypothesis Test)

Null Hypothesis	Test Used	*p*-value	Decision
The distribution of marks is the same across AI platforms	Kruskal-Wallis Test	.423	Retain null hypothesis

Table 7
Kruskal-Wallis Detailed Output

Statistic	Value
Total N	75
Test Statistic (χ^2)	3.875
Degrees of Freedom	4
Asymptotic Significance	0.423
Adjusted for ties	Yes
Post hoc comparisons	Not performed

Figure 4. *Parallel Coordinates Plot Comparing the Performance of Five AI Language Models (ChatGPT, Copilot, DeepSeek, Google Gemini, and Perplexity) Across Four Key Metrics: Total Score, Accuracy Percentage, Score Stability (Inverse of Standard Deviation), and Normality (Based on the Shapiro-Wilk Statistic).*

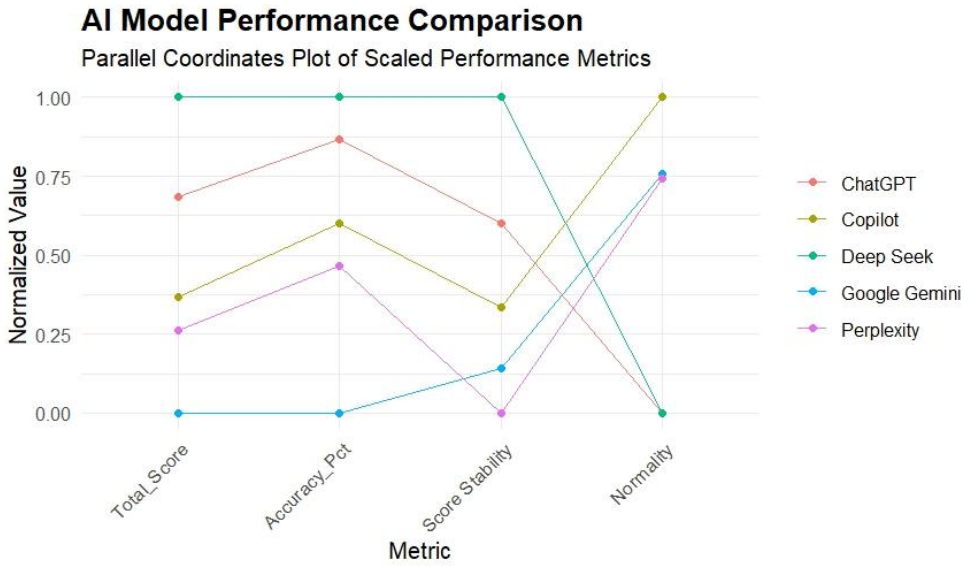

Note. All values are normalized to a 0–1 scale to enable direct comparison across dimensions. This visualization highlights the multidimensional variability in model performance.

Discussion

One of the most exciting developments in contemporary medicine is the incorporation of AI into clinical decision-making. Our side-by-side comparison of five well-liked AI tools—ChatGPT, Microsoft Copilot, DeepSeek, Google Gemini, and Perplexity—demonstrates considerable differences in their capacity for making precise neurological diagnoses, suggesting relevant diagnostic tests, and proposing treatment plans.

Performance Overview

Of the models that were tested, ChatGPT was the most precise with 97.77%, closely followed by DeepSeek with 95.55% and Perplexity with 93.33%. All these models consistently answered the whole of the prompt's three parts: diagnosis, next diagnostic test, and therapeutic or molecular basis. Their high performance indicates that they are adept at mimicking multifaceted clinical reasoning, especially if provided with well-formatted case vignettes from *Case Files: Neurology, Third Edition*.

The responses generated by Google Gemini (86.66%) and Copilot (81.11%) were more inconsistent. Although both models accurately diagnosed numerous instances, they often left out critical diagnostic or therapeutic details, particularly for less well-known conditions such as Creutzfeldt-Jakob disease (CJD), chronic inflammatory demyelinating polyneuropathy (CIDP), and amyotrophic lateral sclerosis (ALS).

The results of this study are in agreement with previous studies that although large language models (LLMs) may have junior resident-level performance in certain diagnostic tasks, their reliability is highly conditional on both the condition's complexity as well as the input question's specificity (Mota et al., 2023; Surianarayanan et al., 2023).

Comparative Strategies Throughout Models

In spite of the variation in accuracy, statistical analysis conducted using the Kruskal-Wallis test showed the absence of a significant difference overall among the AI platforms (p = .423), which meant all the models operated within a fairly comparable range (Sahu et al., 2022). Qualitative analysis of the structure and depth of the responses, however, showed noticeable differences:

Both ChatGPT and DeepSeek gave longer, more explanatory responses, which contributed to higher accuracy but might be daunting for users seeking concise summaries. Perplexity and Gemini favored conciseness, enhancing readability but sometimes at the cost of diagnostic accuracy. Copilot struggled to generate highly structured, evidence-based recommendations, hence exposing potential flaws in its store of medical information. The results emphasize the necessity of achieving a balance between precision and practicality in AI-supported diagnostic processes. Although extensive outputs may enhance accuracy, they must concurrently remain interpretable and actionable for healthcare professionals (Kaur et al., 2020).

Advantages of Artificial Intelligence in Neurological Diagnosis

This research determined the following benefits:

Speed and Efficiency. AI models processed each case in a matter of seconds, enabling quick hypothesis generation and differential narrowing—vital in time-critical neurological emergencies such as subarachnoid hemorrhage or Guillain-Barré syndrome.

Consistency. Unlike human experts who might be impacted by fatigue or cognitive bias, AI provides consistent responses based on available information.

Accessibility. These tools provide high-level information to nonexpert individuals and in resource-poor environments, with the potential to close gaps in global neurology care (Rudie et al., 2019).

Rare Disease Support. AI systems excelled at recognizing patterns for rare diseases, where experience might be sparse (Shen et al., 2019).

Limitations and Ethical Considerations

For all their potential, these AI models have certain limitations:

Lack of Clinical Contextualization. AI lacks in showing bedside manner, expressing empathy, and reading nonverbal cues that are crucial in performing neurological assessments. Excessive dependence on training data results in responses generated from large yet static datasets, which may lack more current diagnostic criteria or treatment protocols.

Regulatory and Liability Issues. The use of AI in clinical decision-making raises unclear questions about validation, oversight, and liability (Segato et al., 2020).

Also, our findings point to human-AI collaboration rather than complete automation. AI will be an additive, complementary tool, augmenting—rather than replacing—the expertise of experienced neurologists (Tyagi & Sharma, 2021).

Comparison With Current Literature

Our results align with prior research showing high diagnostic performance of LLMs in controlled settings (Kaur et al., 2020; Rudie et al., 2019). For instance, Shen et al. (2019) showed that AI models were superior to or as good as doctors across a range of diagnostic domains, including internal medicine and dermatology (World Health Organization, 2023). Similarly, Rudie et al. (2019) highlighted the growing contribution of AI to neuro-oncology, with particular reference to image interpretation and pattern recognition (Mota et al., 2023).

But whereas most of the previous studies concentrated on image-based diagnosis or symptom checkers, our research tested the capacity of AI to integrate multidomain clinical reasoning—a key to

neurology, where syndromic cognition is likely to precede a particular diagnosis.

Future Trajectories

To maximize the potential of AI for neurology, future efforts should concentrate on domain-specific fine-tuning, which involves training models with meticulously chosen medical information and case studies specific to neurological disorders.

- Explainability and Transparency: developing methods to monitor how AI arrives at a diagnosis, engendering trust and aiding clinicians in verifying results.
- Incorporation into Clinical Practices: integration of AI tools into electronic health records (EHRs) and decision support systems allows for their seamless use during patient encounters.
- Human-in-the-loop Systems: creating collaborative interfaces that combine AI efficiency with clinician experience to improve outcomes (Alyami et al., 2024; Rahman et al., 2024).

Conclusion

This comparative evaluation demonstrates that publicly accessible AI platforms, specifically DeepSeek (95.6%) and ChatGPT (97.8%), exhibit high diagnostic accuracy and therapeutic recommendation efficacy in standardized neurological cases, comparable to junior residents. Though there were no statistically significant differences between the platforms (p > .05), there were noticeable qualitative differences. DeepSeek and ChatGPT offered more in-depth explanations in their responses, whereas Perplexity and Copilot prioritized being brief, sometimes at the expense of being completely thorough.

AI models demonstrated exceptional performance in the areas of speed, consistency, and rare-disease recognition. However, they are reliant on immutable training data and lack clinical contextualization, such as empathy and nonverbal assessment. Thus, their function should be supplementary, enhancing rather than replacing the expertise of the clinician.

Author Disclosure

AI tools were used solely for language editing and stylistic refinement of the manuscript. No AI tools were used for study design, data collection, data analysis, or interpretation of results. The authors take full responsibility for the accuracy, integrity, originality, and ethical compliance of the entire manuscript.

References

AbuAlrob, M. A., & Mesraoua, B. (2024). Harnessing artificial intelligence for the diagnosis and treatment of neurological emergencies: A comprehensive review of recent advances and future directions. *Frontiers in Neurology, 15*, Article 1485799. https://doi.org/10.3389/fneur.2024.1485799

Alhejaily, A.-M. G. (2025). Artificial intelligence in healthcare. *Biomedical Reports, 22*(1), Article 11. https://doi.org/10.3892/br.2024.1889

Alyami, M. S. M., Alyami, M. M. M., Al Khuraim, H. A. M., Alsalem, A. M. S., Alrayshan, H. A. M., Albakri, K. A. M., Alsaqran, Q. N., Alyami, H. S., Alzamanan, A. S., Alharbi, F. M., & Alharbi, F. M. (2024). Integrating artificial intelligence across medical clinics: strengthening collaborative efforts for improved patient outcomes. *Journal of Ecohumanism, 3*(7), 2691–2698. https://doi.org/10.62754/joe.v3i7.4668

Dipankar, P., Salazar, D., Dennard, E., Mohiyuddin, S., & Nguyen, Q. C. (2025). Artificial intelligence based advancements in nanomedicine for brain disorder management: An updated narrative review. *Frontiers in Medicine, 12*, Article 1599340. https://doi.org/10.3389/fmed.2025.1599340

Kalani, M., & Anjankar, A. (2024). Revolutionizing neurology: The role of artificial intelligence in advancing diagnosis and treatment. *Cureus, 16*(6), Article e61706. https://doi.org/10.7759/cureus.61706

Kandel, A. (2025). Addressing neurological inequities in developing countries: Challenges and strategic solutions. *Sarvodaya International Journal of Medicine, 1*(1), 1–11. https://doi.org/10.4103/SIJM.SIJM_2_24

Kaur, S., Singla, J., Nkenyereye, L., Jha, S., Prashar, D., Joshi, G. P., El-Sappagh, S., Islam, M. S., & Islam, S. M. R. (2020). Medical diagnostic systems using artificial intelligence (AI) algorithms: Principles and perspectives. *IEEE Access, 8*, 228049–228069. https://doi.org/10.1109/ACCESS.2020.3042273

Li, X., Zhang, L., Yang, J., & Teng, F. (2024). Role of artificial intelligence in medical image analysis: A review of current trends and future directions. *Journal of Medical and Biological Engineering, 44*(2), 231–243. https://doi.org/10.1007/s40846-024-00863-x

Mennella, C., Maniscalco, U., De Pietro, G., & Esposito, M. (2024). Ethical and regulatory challenges of AI technologies in healthcare: A narrative review. *Heliyon, 10*(4), Article e26297. https://doi.org/10.1016/j.heliyon.2024.e26297

Mota, A. L., Ferraciolli, S. F., Ayres, A. S., Polsin, L. L. M., da Costa Leite, C., & Kitamura, F. (2023). AI and big data for intelligent health: Promise and potential. In H. Sakly, K. Yeom, S. Halabi, M. Said, J. Seekins, & M. Tagina (Eds.), *Trends of artificial intelligence and big data for e-health* (pp. 1–14). Springer. https://doi.org/10.1007/978-3-031-11199-0_1

Nguyen, T. V., & Vo, N. (2024). *Using traditional design methods to enhance AI-driven decision making*: IGI Global. https://doi.org/10.4018/979-8-3693-0639-0

Onciul, R., Tataru, C.-I., Dumitru, A. V., Crivoi, C., Serban, M., Covache-Busuioc, R.-A., Radoi, M. P., & Toader, C. (2025). Artificial intelligence and neuroscience: Transformative synergies in brain research and clinical applications. *Journal of Clinical Medicine, 14*(2), 550. https://doi.org/10.3390/jcm14020550

Oyeniyi, J., & Oluwaseyi, P. (2024). Emerging trends in AI-powered medical imaging: Enhancing diagnostic accuracy and treatment decisions. *International Journal of Enhanced Research in Science, Technology & Engineering, 13*(4), 81–94. https://doi.org/10.55948/IJERSTE.2024.0412

Rahman, M. H., Hossan, K. M. R., Uddin, M. K. S., & Hossain, M. D. (2024). Improving collaborative interactions between humans and artificial intelligence to achieve optimal patient

outcomes in the healthcare industry. *SSRN,* Article 5029975. https://doi.org/10.2139/ssrn.5029975

Rashid, M., & Sharma, M. (2025). AI-assisted diagnosis and treatment planning—A discussion of how AI can assist healthcare professionals in making more accurate diagnoses and treatment plans for diseases. In R. Singh, A. Gehlot, N. Rathour, & S. V. Akram (Eds.), *AI in disease detection: Advancements and applications* (pp. 313–336). Wiley-IEEE Press. https://doi.org/10.1002/9781394278695.ch14

Rudie, J. D., Rauschecker, A. M., Bryan, R. N., Davatzikos, C., & Mohan, S. (2019). Emerging applications of artificial intelligence in neuro-oncology. *Radiology, 290*(3), 607–618. https://doi.org/10.1148/radiol.2018181928

Sahu, M., Gupta, R., Ambasta, R. K., & Kumar, P. (2022). Artificial intelligence and machine learning in precision medicine: A paradigm shift in big data analysis. *Progress in Molecular Biology and Translational Science, 190*(1), 57–100. https://doi.org/10.1016/bs.pmbts.2022.03.002

Salammagari, A. R. R., & Srivastava, G. (2024). Artificial intelligence in healthcare: Revolutionizing disease diagnosis and treatment planning. *International Journal of Research in Computer Applications and Information Technology, 7*(1), 41–53.

Segato, A., Marzullo, A., Calimeri, F., & De Momi, E. (2020). Artificial intelligence for brain diseases: A systematic review. *APL Bioengineering, 4*(4), Article 041503. https://doi.org/10.1063/5.0011697

Shen, J., Zhang, C. J., Jiang, B., Chen, J., Song, J., Liu, Z., He, Z., Wong, S. Y., Fang, P.-H., & Ming, W.-K. (2019). Artificial intelligence versus clinicians in disease diagnosis: Systematic review. *JMIR Medical Informatics, 7*(3), Article e10010. https://doi.org/10.2196/10010

Shokran, M., Islam, M. S., & Ferdousi, J. (2025). Harnessing AI adoption in the workforce a pathway to sustainable competitive advantage through intelligent decision-making and skill transformation. *American Journal of Economics and Business Management, 8*(3), 954–976. https://globalresearchnetwork.us/index.php/ajebm/article/view/3355

Surianarayanan, C., Lawrence, J. J., Chelliah, P. R., Prakash, E., & Hewage, C. (2023). Convergence of artificial intelligence and neuroscience towards the diagnosis of neurological disorders—A scoping review. *Sensors, 23*(6), 3062. https://doi.org/10.3390/s23063062

Toy, E. C., Simpson, E. P., Mancias, P., Furr Stimming, E. E. (2018). *Case Files: Neurology, Third Edition*. McGraw Hill.

Tyagi, Y., & Sharma, P. K. (2021). Artificial intelligence: An emerging approach in healthcare. In *Artificial intelligence* (pp. 71–92). CRC Press. https://doi.org/10.3389/fdgth.2025.1644041

Valerio, J. E., Aguirre Vera, G. d. J., Fernandez Gomez, M. P., Zumaeta, J., & Alvarez-Pinzon, A. M. (2025). AI-driven advances in Parkinson's disease neurosurgery: Enhancing patient selection, trial efficiency, and therapeutic outcomes. *Brain Sciences, 15*(5), 494. https://doi.org/10.3390/brainsci15050494

World Health Organization. (2023). *WHO framework for meaningful engagement of people living with noncommunicable diseases, and mental health and neurological conditions*. World Health Organization.

Yang, R., Liu, X., Zhao, Z., Zhao, Y., & Jin, X. (2025). Burden of neurological diseases in Asia, from 1990 to 2021 and its predicted level to 2045: A global burden of disease study. *BMC Public Health, 25*(1), Article 706. https://doi.org/10.1186/s12889-025-21928-9

Zeb, S., Nizamullah, F., Abbasi, N., & Fahad, M. (2024). AI in healthcare: Revolutionizing diagnosis and therapy. *International Journal of Multidisciplinary Sciences and Arts, 3*(3), 118–128. https://doi.org/10.47709/ijmdsa.v3i3.4546

Received: August 3, 2025
Accepted: September 23, 2025
Published: March 31, 2026

NeuroRegulation

ISNR INTERNATIONAL SOCIETY FOR NEUROREGULATION & RESEARCH

Cultural Factors in Neuroregulation: A Review of Evidence and Theoretical Framework

Leslie H. Sherlin[*]

Sherlin Consulting Group, Scottsdale, Arizona, USA
Ottawa University, Surprise, Arizona, USA
Grand Canyon University, Phoenix, Arizona, USA
Sonoran University of Health Sciences, Tempe, Arizona, USA
Fuller Theological Seminary, Phoenix, Arizona, USA
Nova Tech EEG, Inc, Mesa, Arizona, USA

Abstract

Introduction. Despite increasing diversity in patient populations and documented health disparities, the neuroregulation field has given minimal attention to cultural factors influencing treatment access, engagement, and outcomes. **Methods.** This article reviews existing literature examining cultural factors across neuroregulation modalities (neurofeedback, transcranial electrical stimulation, photobiomodulation, peripheral biofeedback) and synthesizes theoretical frameworks from cultural neuroscience, cultural humility, and health disparities research. **Results.** Literature review reveals striking paucity of cultural considerations research across all neuroregulation modalities. While fundamental physiological mechanisms (operant conditioning, neuroplasticity, autonomic regulation) appear universal across human populations, cultural factors profoundly influence treatment perceptions, explanatory models, technology acceptance, and therapeutic relationships. Evidence suggests comparable outcomes across diverse populations when access barriers are addressed. Key disparities stem from structural inequities rather than differential treatment response. **Conclusion.** The neuroregulation field requires systematic integration of cultural considerations while maintaining scientific understanding of universal physiological mechanisms. Distinguishing between invariant biological processes and culturally variable implementation factors provides foundation for developing inclusive, effective interventions across diverse populations.

Keywords: cultural neuroscience; neurofeedback; biofeedback; health disparities; therapeutic alliance; cultural competence

Citation: Sherlin, L. H. (2026). Cultural factors in neuroregulation: A review of evidence and theoretical framework. *NeuroRegulation, 13*(1), 65–76. https://doi.org/10.15540/nr.13.1.65

***Address correspondence to**: Leslie H. Sherlin, PhD, 7272 E. Indian School Rd, Suite 540, Scottsdale, AZ 85251, USA. Email: leslie@drsherlin.com

Edited by:
Rex L. Cannon, PhD, Currents, Knoxville, Tennessee, USA

Reviewed by:
Rex L. Cannon, PhD, Currents, Knoxville, Tennessee, USA
Randall Lyle, PhD, Mount Mercy University, Cedar Rapids, Iowa, USA

Introduction

The field of neuroregulation has evolved substantially over 4 decades, demonstrating efficacy for various neurological and psychological conditions through neurofeedback, biofeedback, and neuromodulation techniques. However, this evolution has occurred with remarkably limited attention to cultural factors that may influence treatment access, engagement, and outcomes. This gap becomes increasingly problematic as practitioners serve more diverse populations while health disparities in neurological and behavioral healthcare persist (Saadi et al., 2017).

The absence of cultural considerations in neuroregulation research and practice is striking. Systematic reviews reveal that over 90% of human neuroimaging publications originate from Western countries (Chiao, 2009). The vast majority of neuroregulation research has been conducted with predominantly white, Western, middle-class populations, raising questions about generalizability of protocols and normative databases. A

comprehensive literature search reveals only a handful of studies explicitly examining cultural factors in neuroregulation interventions.

Recently, Eisenbarth et al. (2025) conducted one of the first systematic investigations of culturally diverse perceptions of electroencephalography (EEG) and neurofeedback research. Their study of 181 participants in New Zealand found significant barriers to participation among diverse populations, including low awareness of these interventions and cultural concerns about electrode placement procedures. Notably, 19.34% of participants indicated that experimenter gender would matter for procedures involving head contact, highlighting intersections of cultural, religious, and gender considerations.

This absence of cultural consideration creates multiple problems. Protocols and normative databases developed with homogeneous populations may not generalize appropriately. Cultural barriers may prevent equitable access to potentially beneficial treatments. Practitioners may inadvertently create cultural mismatches that undermine therapeutic alliance and treatment effectiveness. The lack of culturally responsive approaches perpetuates systemic healthcare inequities. Additionally, the field misses opportunities to learn from diverse cultural perspectives on mind-body relationships, self-regulation, and healing.

This article provides an examination of cultural factors in neuroregulation, reviewing existing evidence across modalities and synthesizing theoretical frameworks to understand how culture influences treatment engagement and outcomes. The analysis distinguishes between universal physiological mechanisms underlying neuroregulation and culturally variable factors affecting implementation. This foundation is essential for developing truly inclusive and effective neuroregulation practices.

Theoretical Foundations

Cultural Humility and Cultural Competence: Complementary Frameworks

Understanding culturally responsive practice in neuroregulation requires integrating two complementary frameworks: cultural humility and cultural competence. These approaches, while distinct, work synergistically to guide practitioners in navigating cultural complexity while maintaining clinical effectiveness.

Cultural humility, introduced by Tervalon and Murray-García (1998), emphasizes an ongoing process rather than an endpoint. Unlike cultural competence, which implies achievable mastery, cultural humility recognizes that cultural learning is never complete. This perspective is particularly relevant for neuroregulation practitioners who must navigate not only general cultural differences in health beliefs but also specific cultural perspectives on brain function, consciousness, technology, and mind-body relationships.

The framework encompasses three core dimensions with direct application to neuroregulation practice. First, lifelong self-evaluation and self-critique require practitioners to continuously examine assumptions about “normal” brain function, treatment compliance, and appropriate goals that may reflect cultural biases. For example, privileging individual symptom reduction over family harmony or spiritual balance reflects Western individualistic values rather than universal treatment priorities.

Second, addressing power imbalances inherent in practitioner-client relationships becomes especially complex in neuroregulation. Practitioners possess specialized technical knowledge about brain function and sophisticated equipment, creating additional distance from clients’ lived experiences. When interpreting EEG patterns or making statements about clients’ internal states based on physiological readings, practitioners wield considerable technical authority. This must be balanced with recognition that clients are experts on their own experiences, cultural contexts, and treatment priorities.

Third, institutional accountability extends beyond individual practitioners. Organizations must examine systemic barriers to culturally responsive care, including why certain populations are underrepresented in research samples, whether clinic locations and hours create access barriers, and how equipment design may inadvertently exclude populations (such as EEG caps incompatible with diverse hair textures or religious head coverings).

While cultural humility provides philosophical grounding, cultural competence offers practical skill development frameworks. Campinha-Bacote’s (2002) model identifies five constructs directly applicable to neuroregulation.

1. Cultural awareness involves recognizing one’s own worldview and biases, including beliefs about consciousness, brain-mind

relationships, technology's role in healing, and what constitutes healthy brain function. Concepts like "self-regulation" and "optimal performance" are culturally constructed with varying meanings across contexts.

2. Cultural knowledge encompasses understanding diverse worldviews and health beliefs, including how cultures conceptualize mental processes, technology acceptability, health locus of control, and traditional practices that might complement or conflict with neuroregulation. For instance, understanding that some Asian cultures express emotional distress through somatic symptoms rather than psychological constructs influences how practitioners explain neurofeedback for anxiety.

3. Cultural skill refers to conducting culturally responsive assessments and interventions, including adapting communication styles, modifying procedures for cultural factors, selecting appropriate feedback displays, and integrating neuroregulation with clients' existing cultural resources. This might include working with interpreters during sessions or adapting protocols for clients who find certain stimuli culturally inappropriate.

4. Cultural encounters involve direct engagement with diverse clients. Research indicates meaningful cross-cultural clinical experiences, accompanied by reflection and supervision, accelerate competence development more effectively than didactic training alone. For neuroregulation practitioners, this means seeking opportunities with diverse populations, community outreach, and engagement with cultural communities.

5. Cultural desire represents genuine motivation to engage in the cultural competence process. This intrinsic motivation sustains ongoing efforts, particularly when facing challenges or mistakes. In neuroregulation, cultural desire manifests as curiosity about diverse populations' experiences, commitment to accessibility, and willingness to adapt established protocols.

The integration of cultural humility and competence provides a robust framework recognizing that practitioners need both foundational knowledge about cultural factors and ongoing process orientation acknowledging knowledge limitations. This synthesis is essential for understanding technical aspects of interventions alongside cultural factors influencing client perceptions and engagement.

Distinguishing Universal Mechanisms From Cultural Variations

A critical consideration in culturally responsive neuroregulation involves distinguishing physiological processes that are universal across human populations from treatment aspects that are culturally influenced. This distinction helps practitioners avoid both assuming everything is culturally relative and ignoring important cultural variations.

Fundamental physiological mechanisms underlying neuroregulation appear universal across human populations. The autonomic nervous system functions similarly across cultures, with sympathetic activation increasing heart rate and parasympathetic activation slowing it (Porges, 2011). Basic neurophysiological processes of operant conditioning underlying neurofeedback, including the ability to modify brain activity through reinforcement, have been demonstrated across diverse populations studied (Sherlin et al., 2011). The physiological stress response, involving hypothalamic-pituitary-adrenal (HPA) axis activation with characteristic changes in heart rate variability (HRV), cortisol release, and EEG patterns, shows remarkable consistency across cultures (McEwen, 2017).

EEG patterns associated with specific neurological conditions demonstrate consistency across populations. The 3 Hz spike-and-wave pattern characteristic of absence seizures appears similar regardless of geographic origin (Betting et al., 2006). Attention-deficit/hyperactivity disorder (ADHD) is associated with elevated theta/beta ratios across diverse populations, though prevalence and symptom expression vary culturally (Arns et al., 2013). Neurophysiological markers of sleep stages remain consistent across cultures, even as sleep practices and beliefs vary widely (Siegel, 2005).

Photobiomodulation mechanisms, involving cytochrome *c* oxidase activation and increased adenosine triphosphate (ATP) production, represent fundamental cellular processes operating similarly across populations (Hamblin, 2016). While skin pigmentation may affect light penetration, basic cellular responses to specific wavelengths appear

universal. Similarly, transcranial electrical stimulation's effects on neuronal excitability through membrane polarization represent basic biophysical processes that should not vary by culture (Nitsche et al., 2008).

However, while fundamental mechanisms may be universal, numerous aspects of neuroregulation are profoundly influenced by culture. Baseline physiological patterns can be shaped by cultural practices and chronic stress exposure. Individuals from cultures experiencing systemic discrimination may show chronically elevated sympathetic arousal and blunted stress reactivity, reflecting allostatic load from chronic stress (Geronimus et al., 2006). Cultural practices such as meditation, prayer, or traditional breathing exercises influence baseline EEG patterns and autonomic tone (Travis & Shear, 2010).

Interpretation and meaning assigned to physiological states vary culturally. Increased heart rate might be interpreted as anxiety in one culture but excitement or spiritual awakening in another. The experience and expression of physiological arousal is filtered through cultural schemas shaping whether sensations are perceived as problematic or normal (Hinton & Good, 2016). These interpretive differences influence whether individuals seek treatment and how they understand treatment goals.

Treatment engagement factors are heavily culturally influenced. The therapeutic alliance, crucial for adherence and outcomes, is shaped by cultural expectations about relationships, communication styles, and power dynamics. Motivation for change may be individually focused in individualistic cultures but family or community focused in collectivistic cultures. Acceptability of different feedback modalities varies based on cultural aesthetics and learning styles.

This understanding has important practice implications. Practitioners can have confidence that fundamental physiological processes targeted by neuroregulation operate similarly across cultures. A neurofeedback protocol increasing sensorimotor rhythm (SMR) and decreasing theta will have similar neurophysiological effects regardless of cultural background. However, how that protocol is explained, what motivates engagement, how progress is measured and celebrated, and how changes are integrated into daily life are all profoundly influenced by culture.

Health Disparities Framework: Understanding Structural Factors

Cultural considerations in neuroregulation cannot be separated from broader health disparities and their underlying mechanisms. Health disparities in neurological and behavioral healthcare are well-documented, with racial and ethnic minorities consistently experiencing lower access, poorer quality care, and worse outcomes (Robbins et al., 2022). These disparities reflect complex interactions of historical, social, economic, and systemic factors rather than cultural differences alone.

Saadi et al. (2017) documented striking disparities in neurological care, finding Black and Hispanic patients had markedly lower rates of outpatient neurology visits compared to White patients, even after controlling for insurance status, education, and income. These disparities were not explained by differences in disease prevalence, suggesting systemic barriers rather than differential need drive inequitable access. For neuroregulation services, often not covered by insurance and requiring specialized providers, these disparities may be even more pronounced.

Structural competency, introduced by Metzl and Hansen (2014), extends cultural competency by focusing on recognizing and addressing upstream social and institutional determinants of health. This framework shifts attention from individual cultural differences to structural factors creating and maintaining health inequities. For neuroregulation practitioners, structural competency involves understanding how insurance coverage limitations, geographic maldistribution of services, transportation barriers, inflexible work schedules, and historical redlining concentrating poverty in certain communities all create access barriers.

Insurance coverage represents a particularly significant structural barrier. Despite decades of research supporting neurofeedback efficacy, most insurance plans classify it as "experimental" without coverage. Medicare and Medicaid, disproportionately serving elderly, disabled, and low-income populations, generally do not cover neurofeedback except for specific conditions. This creates a two-tiered system where neuroregulation is available primarily to those who can afford out-of-pocket payments, typically $1,000–$8,000 per treatment course.

Geographic disparities compound access issues. Neuroregulation services concentrate in urban and suburban areas with higher-income populations,

creating “neurotherapy deserts” in rural areas and lower-income urban neighborhoods. The intersection of geographic and racial disparities is particularly striking in the Southeastern United States, with both the lowest neurologist density per capita and highest proportion of Black residents.

Medical mistrust, rooted in historical and contemporary discrimination and exploitation experiences, significantly affects healthcare engagement among racial and ethnic minorities. Bazargan et al. (2021) found medical mistrust was 73% higher among Black adults and 49% higher among Hispanic adults compared to White adults. This mistrust reflects collective memory of events like the Tuskegee syphilis study, forced sterilizations, and ongoing discrimination experiences in healthcare settings. For brain-based interventions potentially perceived as experimental or manipulative, mistrust may be particularly pronounced.

Therapeutic Alliance as Culturally Mediated Process

The therapeutic alliance, consistently identified as critical for treatment outcomes across interventions, is inherently influenced by cultural factors. In neuroregulation, where treatment extends over many sessions requiring active participation in clinic and home practice, relationship quality may be particularly important for adherence and outcomes.

Cultural values fundamentally shape therapeutic relationship expectations. Clients from hierarchical cultures may expect directive, authoritarian approaches from healthcare providers, viewing practitioners as experts whose recommendations should be followed without question. This expectation may conflict with collaborative approaches common in neurofeedback, where clients provide feedback about experiences and participate in goal setting. Conversely, clients from egalitarian cultures may be uncomfortable with directive approaches, expecting equal partnership in treatment planning.

Communication styles vary significantly across cultures with profound implications for information exchange, rapport building, and treatment planning. Hall’s (1976) distinction between high-context and low-context communication remains relevant. High-context communication, common in many Asian, African, and Latin American cultures, relies heavily on nonverbal cues, implicit understanding, and indirect expression. Low-context communication, typical of Northern European and Anglo-American cultures, emphasizes explicit verbal expression and direct communication.

These differences manifest multiple ways during neuroregulation treatment. Clients from high-context cultures may not directly express disagreement or discomfort with procedures, showing reluctance through nonverbal behavior or missed appointments. They may find direct symptom questions uncomfortable, preferring to communicate distress through somatic complaints or metaphorical language. Practitioners accustomed to low-context communication may misinterpret indirect communication as resistance, poor motivation, or alexithymia.

The technical nature of neuroregulation interventions further complicates therapeutic alliance. Unlike talk therapy where the relationship itself is the primary change vehicle, neuroregulation involves complex equipment, computer interfaces, and physiological measurements potentially diminishing relational aspects. However, research suggests the therapeutic relationship remains crucial. Clients must trust practitioners to attach electrodes, interpret brain patterns, and guide neurological functioning changes, requiring significant vulnerability and trust.

Family involvement represents another culturally variable aspect. Western therapeutic models emphasize individual autonomy, confidentiality, and clear client-family boundaries. However, many cultures view health and healing as communal processes. In collectivist cultures, family members may expect presence during sessions, participation in decisions, and home practice support, creating ethical dilemmas for individually trained practitioners regarding confidentiality and consent.

The active inference model (Constant et al., 2019) provides a useful framework for understanding cultural influences on neuroregulation therapeutic relationships. Alliance building occurs through cooperative communication and mutual prediction, with practitioner and client updating models of each other through interaction. Cultural values shape “priors” or expectations clients bring, influencing interpretation of practitioner behaviors, procedures, and physiological responses during neurofeedback.

Evidence Review: Cultural Factors Across Neuroregulation Modalities

Neurofeedback and EEG Biofeedback

The literature examining cultural factors in neurofeedback reveals a striking paradox: while

practiced globally for over 4 decades, systematic investigation of cultural considerations is virtually absent. This gap is concerning given that EEG patterns, the foundation of neurofeedback assessment and training, may vary across cultural groups. Moss et al. (1985) found differences in EEG asymmetry between Japanese and Western subjects, suggesting Western-developed normative databases may not be universally applicable. Despite this early indication, the field has not pursued systematic investigation of cultural variations in EEG patterns or protocol implications.

However, while cultural practices may influence baseline EEG patterns through neuroplasticity mechanisms, fundamental neurophysiological processes underlying neurofeedback appear universal. The ability to modify brain activity through operant conditioning has been demonstrated across the limited diverse populations studied (Sherlin et al., 2011). Pathological EEG patterns, such as epileptiform activity or elevated theta/beta ratios in ADHD, show consistency across cultures (Arns et al., 2013). This suggests that while cultural factors influence engagement and implementation, core neurofeedback mechanisms operate similarly across populations.

Kelley's (1997) investigation of alpha/theta neurofeedback with a Navajo population for substance abuse treatment remains the most substantial culturally adapted neurofeedback study. This pioneering work with 19 Navajo clients demonstrated cultural adaptation's potential to enhance outcomes. Kelley reported 21% of participants maintained complete abstinence and 63% maintained partial remission at 3-year follow-up. Crucially, the alpha/theta protocol naturally aligned with traditional Navajo medicine-ways and spiritual practices. Deep states induced by training resembled traditional healing ceremonies, with emerging visual imagery interpreted through Navajo spiritual frameworks. Participants reported neurofeedback helped reconnect with traditional values and spiritual practices supporting sobriety.

This study's significance extends beyond positive outcomes, demonstrating neurofeedback need not be positioned as Western technological intervention incompatible with traditional healing but can integrate with Indigenous worldviews. The study also highlights missed opportunities, with no published replication or extension with Native American or other Indigenous populations in subsequent decades, despite high trauma and substance abuse rates potentially benefiting from culturally adapted neurofeedback.

Eisenbarth et al. (2025) conducted the first systematic study of culturally diverse perceptions of EEG and neurofeedback research. Their mixed-methods study with 181 New Zealand participants revealed multiple barriers among diverse populations. Low awareness of EEG and neurofeedback methods was nearly universal among non-Western participants, with many expressing surprise that brain activity could be measured noninvasively or voluntarily modified. Electrode placement concerns were multifaceted, including hair disturbance worries (particularly among those with textured hair requiring significant styling), religious or cultural head-touching concerns, and gender-matched researcher preferences.

Particularly revealing were qualitative findings about emotion regulation skepticism. Some participants viewed emotions as fundamentally human experiences that shouldn't be technologically manipulated. Others worried that changing brain patterns might alter personality or cultural identity. These concerns highlight needs for careful explanation of neurofeedback capabilities and limitations, with attention to cultural values about authenticity, identity, and emotional experience nature.

Fleischman (2022) provided valuable evidence about neurofeedback effectiveness with underserved populations, though cultural factors weren't the primary focus. Their infra-low frequency neurofeedback study with over 300 clients across 20+ community agency sites demonstrated that when access barriers were addressed, diverse clients with complex presentations showed substantial improvements. The population was characterized by high trauma rates (average ACE scores of 6), multiple co-occurring disorders (average 5 diagnoses), and socioeconomic disadvantage.

Several findings have cultural implications. The remarkably low no-show rate (2% vs. typical 25–45%) suggests high engagement when services are accessible and responsive. Clients rated neurofeedback more helpful than counseling or medication, possibly because it offered nonstigmatizing, nonverbal intervention not requiring trauma discussion or cultural conflict exploration. Dramatic reductions in self-harm (79%) and arrests (70%) suggest neurofeedback addresses dysregulation patterns common among marginalized

populations experiencing chronic stress. These outcomes indicate fundamental neurofeedback mechanisms operate across diverse populations when cultural barriers are addressed.

Transcranial Electrical Stimulation

Research on cultural factors in transcranial electrical stimulation (transcranial direct current stimulation [tDCS] and transcranial alternating current stimulation [tACS]) is even more limited, with only one identified study explicitly examining cross-cultural differences. This gap is concerning given rapid tDCS research expansion and increasing home-based application interest potentially reaching diverse populations.

Martin et al. (2019) conducted groundbreaking research examining cultural influences on tDCS effects. Their study with 104 young adults (52 Southeast Asian Singaporeans and 52 Caucasian Australians) found cultural background significantly influenced both baseline social cognition and high-definition (HD)-tDCS responses. Targeting dorsomedial prefrontal cortex and right temporoparietal junction regions involved in self-other processing, baseline differences showed Southeast Asians had greater self-other integration than Caucasians, consistent with collectivistic versus individualistic cultural self-construal differences. Remarkably, anodal HD-tDCS resulted in Caucasians performing more similarly to Southeast Asians, suggesting stimulation could temporarily shift culturally influenced cognitive patterns.

These findings have profound implications for tDCS application across diverse populations. If cultural background influences baseline neural processing in targeted regions, optimal stimulation parameters may differ across groups. Protocols developed for Western populations might have different or opposite effects in populations with different baseline patterns. The study raises ethical questions about using brain stimulation to alter culturally influenced cognitive styles.

However, fundamental tDCS mechanisms involving neuronal membrane polarization and excitability changes represent basic biophysical processes operating similarly across populations (Nitsche et al., 2008). Electrical current effects on neural tissue follow universal physical laws. What varies culturally is the baseline state being modulated and resulting change interpretation. This distinction is crucial: while technology works through universal mechanisms, application must consider cultural variations in baseline neural organization and treatment goals.

The absence of cultural acceptability research is problematic given the intervention's intimate nature. For example, tDCS involves applying electrical current through the skull to alter brain activity, potentially raising unique cultural and religious concerns. Some may view external brain activity manipulation as violating personal autonomy or spiritual integrity. Others may have specific concerns about electrical devices near the head based on consciousness, soul, or life force beliefs. tDCS equipment similarity to electroconvulsive therapy devices may evoke particular concerns among populations with psychiatric abuse or coercive treatment histories.

Photobiomodulation

The photobiomodulation literature shows rapid recent growth but reveals significant gaps addressing cultural and ethnic diversity. Recent systematic reviews and meta-analyses demonstrate efficacy for depression, cognitive enhancement, and pain management, but none examine cultural, racial, or ethnic factors potentially influencing treatment response or acceptability.

Fundamental photobiomodulation mechanisms represent universal cellular processes. Specific light wavelength interaction with cytochrome *c* oxidase, leading to increased ATP production and reactive oxygen species modulation, occurs in all human cells regardless of cultural background (Hamblin, 2016). Transcription factor activation and subsequent gene expression changes represent fundamental biological processes conserved across populations.

However, absence of cultural considerations is concerning given potential treatment parameter variations. Melanin content, varying significantly across racial and ethnic groups, absorbs light and could theoretically influence photobiomodulation penetration and biological effects. Despite this obvious consideration, no published studies examine whether optimal wavelengths, power densities, or treatment durations should be adjusted based on skin type or melanin content. The biphasic dose response suggests too little light has no effect while too much inhibits desired responses. If tissue optical properties vary by ethnicity, therapeutic windows might differ across populations.

Cultural acceptability remains unexplored. Light application to the head for therapeutic purposes

might be viewed differently across cultural contexts. Some cultures may be more accepting due to traditional sunlight or colored light healing practices. Others might be skeptical of claims that light penetrates the skull influencing brain function. Typical photobiomodulation device appearance often resembling LED array helmets might evoke different cultural associations.

Peripheral Biofeedback

The peripheral biofeedback literature provides somewhat more cultural factors evidence, though significant gaps remain. The modality's focus on teaching conscious autonomic control intersects with diverse mind-body practice traditions, potentially increasing acceptability for populations familiar with yoga, qigong, meditation, or contemplative practices.

Physiological processes underlying peripheral biofeedback are universal. The autonomic nervous system functions identically regardless of cultural background, with sympathetic activation increasing heart rate, peripheral vasoconstriction, and electrodermal activity, while parasympathetic activation produces opposite effects (Porges, 2011). Baroreflex, respiratory sinus arrhythmia, and other cardiorespiratory coupling mechanisms operate through conserved pathways. Gaining voluntary control over typically involuntary processes through feedback represents fundamental human nervous system learning capacity.

Feldman et al. (2016) conducted the most comprehensive culturally adapted biofeedback study, examining cognitive-behavioral psychophysiological therapy (CBPT) with HRV biofeedback for Latino adults with comorbid asthma and panic disorder. Their randomized controlled trial with 53 participants incorporated cultural adaptations including Spanish language sessions, family involvement, culturally relevant examples, addressing cultural asthma beliefs, and incorporating culturally resonant stress concepts. Both adapted CBPT and music relaxation showed improvements, with CBPT showing medication adherence advantages. Nelson et al. (2020) found HRV and end-tidal CO_2 changes partially mediated treatment effects, indicating targeted physiological mechanisms operated similarly across cultural groups despite requiring culturally adapted engagement pathways.

Beltrán-Velasco et al. (2020) documented cultural differences in psychophysiological stress responses with biofeedback protocol implications. Comparing Spanish and Colombian students revealed significant subjective and objective stress response differences. While fundamental stress mechanisms are universal, chronic cultural and environmental factors shape baseline patterns and reactivity influencing biofeedback training. However, the ability to modify patterns through training appears consistent.

Population-Specific Patterns and Considerations

While recognizing tremendous diversity within any cultural group and avoiding stereotypes, research identifies barrier and facilitator patterns affecting different populations' neuroregulation access and engagement. These patterns reflect complex historical, cultural, social, and economic factor interactions creating unique community challenges. Importantly, these barriers affect access and engagement but don't alter fundamental physiological mechanisms.

Racial and Ethnic Minorities

Racial and ethnic minorities' healthcare experiences in the United States are profoundly shaped by historical and ongoing discrimination. Multiple disparity layers compound creating significant neuroregulation access barriers. Saadi et al. (2017) documented Black patients had 30% lower odds and Hispanic patients 40% lower odds of receiving outpatient neurology care compared to White patients, controlling for insurance, education, and income. Given neuroregulation often requires neurologist referral or collaboration, specialty care disparities create upstream barriers.

Medical mistrust among communities of color reflects ongoing discrimination experiences. Studies document Black patients receive less pain medication, are less likely referred for advanced treatments, and report frequent provider disrespect and bias. For potentially experimental or unfamiliar neuroregulation interventions, mistrust creates additional barriers. Technical neurofeedback and neurostimulation nature may seem particularly foreign or threatening to those experiencing medical exploitation.

However, when barriers are addressed and trust established, evidence suggests neuroregulation interventions are equally effective across racial and ethnic groups. Neuroplasticity, operant conditioning, and autonomic regulation mechanisms operate identically regardless of race or ethnicity. Fleischman's (2022) work with predominantly minority, low-income populations demonstrated

robust outcomes when services were accessible and culturally responsive, indicating outcome disparities often reflect access and engagement disparities rather than differential treatment effectiveness.

Language barriers significantly impact care access and quality for many ethnic minorities. While Spanish-language services have expanded, neuroregulation rarely has bilingual providers or translated materials. Technical vocabulary for explaining neurofeedback or neurostimulation is complex even in English; conveying concepts through interpreters unfamiliar with neuroscience terminology presents challenges. Many languages lack equivalent terms for *biofeedback* or *neurostimulation*, requiring creative translation.

Cultural symptom presentation and help-seeking variations influence engagement. Asian Americans tend toward somatic complaints and may avoid mental health services due to stigma and emotional restraint values. This could paradoxically make biofeedback more acceptable than psychotherapy, focusing on physiological rather than emotional processes. Without culturally informed outreach, these populations may never learn about options.

Indigenous Communities

Indigenous peoples globally face unique challenges accessing culturally appropriate healthcare, including neuroregulation services. Challenges reflect colonization, forced assimilation, and medical exploitation histories creating deep-seated Western medical intervention mistrust. The highly technological neuroregulation nature may seem particularly foreign, representing potential colonial intrusion.

Traditional Indigenous worldviews often conceptualize health fundamentally differently from biomedical models underlying neuroregulation. Many Indigenous cultures view health as physical, mental, emotional, and spiritual balance, with illness reflecting disrupted relationships with family, community, ancestors, and nature. Most neuroregulation protocols' individualistic focus may seem incomplete from relational worldviews.

However, Kelley's (1997) Navajo work suggests successful integration when approached with cultural humility and genuine collaboration. Neurophysiological changes from neurofeedback, including arousal, attention, and state regulation shifts, align with many traditional practice goals though conceptualized differently. Alpha/theta states may resemble traditional ceremony altered consciousness states, providing technology bridges. Nonverbal neurofeedback nature may suit cultures with different communication styles or difficult-to-verbalize trauma.

Sovereignty and self-determination are critical Indigenous community considerations, recognizing tribal nations' inherent self-governance rights including health services. Practitioners should understand relevant tribal governance, health systems, and cultural protocols, potentially involving tribal council permission, traditional healer collaboration, or service adaptation to tribal priorities.

International and Immigrant Populations

International neuroregulation approach diversity reveals significant acceptance, regulation, and healthcare integration variations. While well-established in some countries (particularly Europe and parts of Asia), they remain unknown elsewhere. Immigrants may arrive from mainstream or completely unfamiliar contexts, creating varying baseline knowledge and acceptance.

Despite familiarity and acceptance differences, underlying physiological mechanisms remain constant. Stress response, autonomic regulation, and neuroplasticity operate through identical biological pathways regardless of origin. Immigrant population research shows biofeedback and neurofeedback effectiveness when language barriers are addressed and cultural adaptations enhance engagement (Feldman et al., 2016). Physiological mechanism universality means interventions developed in one country can successfully apply elsewhere with culturally adapted delivery.

Acculturation stress and immigration trauma create unique mental health needs neuroregulation might address, yet multiple barriers prevent access. Recent immigrants face practical barriers including insurance lack, limited English, healthcare system unfamiliarity, and basic needs prioritization over specialized services. Undocumented immigrants may avoid any healthcare due to deportation fear.

Socioeconomic Factors

Socioeconomic factors create perhaps the most pervasive access barriers, intersecting with race, ethnicity, and geography compounding disparities. High neuroregulation costs ($50–$200 per session, 20–40 sessions required) place interventions beyond low-income reach. Even with sliding scales,

total cost and time commitment may be prohibitive for those working multiple jobs or lacking paid leave.

However, socioeconomic status doesn't alter fundamental physiological processes. Learning control over physiological processes through feedback is basic human capacity operating regardless of income or education. When financial barriers are removed, as in Medicaid programs or free services, outcomes compare to affluent populations (Fleischman, 2022). This underscores that disparities are structural rather than biological, reflecting differential access rather than benefit capacity.

Insurance disparities significantly impact access. While some private plans may cover biofeedback for specific conditions, Medicaid and Medicare coverage is extremely limited. This creates paradoxical situations where populations with the highest trauma and stress-related conditions rates have the least intervention access. Neurofeedback classification as "experimental," despite decades of research, perpetuates disparities.

Synthesis and Implications

The evidence review reveals both concerning gaps and important insights about cultural factors in neuroregulation. The paucity of research across all modalities after decades of clinical practice represents a critical limitation undermining the field's inclusivity and effectiveness. However, available evidence combined with theoretical frameworks provides foundation for understanding how culture influences neuroregulation while maintaining scientific grounding in universal physiological mechanisms.

A crucial insight is distinguishing between invariant physiological processes and culturally variable implementation factors. Fundamental mechanisms including operant conditioning, neuroplasticity, autonomic regulation, and cellular photobiomodulation responses operate identically across human populations. This universality provides confidence that neuroregulation can be effective across diverse populations when cultural barriers are addressed.

However, numerous factors influencing treatment access, engagement, and outcomes are culturally shaped. These include illness explanatory models, technology comfort, communication preferences, therapeutic relationship expectations, and structural care barriers. The limited evidence available suggests that when these factors are addressed through culturally responsive approaches, diverse populations achieve comparable outcomes.

The intersection of cultural factors with structural inequities creates compounded barriers for many populations. Medical mistrust rooted in historical and ongoing discrimination, combined with language barriers, insurance limitations, and geographic access issues, creates multiple obstacles to neuroregulation access. These structural factors require systemic solutions beyond individual practitioner cultural competence.

The therapeutic alliance emerges as a critical culturally mediated factor influencing engagement and outcomes. Cultural values shape expectations about practitioner relationships, communication styles, family involvement, and treatment goals. The technical nature of neuroregulation doesn't diminish relational importance but adds complexity to building trust across cultural differences.

Conclusion

This comprehensive examination of cultural factors in neuroregulation reveals both significant knowledge gaps and important foundations for developing culturally responsive practice. The striking absence of cultural considerations research across all neuroregulation modalities represents a critical field limitation requiring urgent attention. After decades of clinical practice, the lack of systematic investigation into how culture influences treatment engagement and outcomes undermines scientific validity and perpetuates healthcare inequities.

The theoretical frameworks presented provide essential grounding for understanding cultural influences on neuroregulation. Cultural humility's emphasis on ongoing self-reflection and power dynamic awareness, combined with cultural competence's practical knowledge and skills, creates a robust approach foundation. The health disparities framework reveals how structural inequities compound cultural factors creating multilevel access barriers. Understanding therapeutic alliance as culturally mediated process highlights relationship importance even in technically oriented interventions.

Distinguishing universal physiological mechanisms from culturally variable factors provides crucial clarity. Fundamental processes underlying neuroregulation operate consistently across human populations, offering confidence in intervention

effectiveness potential across diverse groups. However, how these mechanisms are accessed, understood, and integrated into lives varies profoundly by culture. This distinction guides practitioners in maintaining scientific integrity while adapting delivery for cultural responsiveness.

The limited available evidence suggests promising outcomes when cultural barriers are addressed. Studies with diverse populations show engagement and effectiveness comparable to majority populations when services are accessible and culturally adapted. This indicates disparities stem primarily from structural barriers rather than differential treatment response, highlighting the importance of systemic change alongside individual practitioner development.

Future research must prioritize systematic investigation of cultural factors across all neuroregulation modalities. This includes developing diverse normative databases, testing cultural adaptation effectiveness, examining implementation in community settings, and understanding how traditional healing practices might complement neuroregulation. Research must distinguish between universal mechanisms requiring preservation and variable factors requiring adaptation.

The path forward requires coordinated action across multiple levels. Individual practitioners must commit to ongoing cultural competence development while deepening understanding of physiological mechanisms. Organizations must implement equity-promoting policies and practices. Professional associations must establish cultural competence standards and support workforce diversity. Researchers must prioritize diverse population inclusion and cultural factors investigation. Policy makers must address systemic barriers through insurance reform and support for culturally responsive models.

The ultimate goal extends beyond adapting existing interventions for diverse populations to transforming the field to be inherently inclusive and culturally responsive while maintaining scientific rigor. The universality of underlying mechanisms provides foundation for inclusivity, while attention to cultural factors ensures effective access and utilization by all populations.

As neuroregulation continues evolving, cultural considerations must be central rather than peripheral. This article provides foundation for that integration, but much work remains. Through systematic research, thoughtful practice development, and commitment to equity, the field can ensure neuroregulation benefits are available to all who might benefit, regardless of cultural background, race, ethnicity, language, or socioeconomic status.

Author Declarations

The author declares no grant support, financial interests, or conflicts of interest relevant to this submission. Artificial intelligence (AI) tools were used exclusively for technical manuscript preparation (proofreading and formatting) in this work. No AI was used for content generation, analysis, or intellectual contributions. The author assumes full responsibility for all scientific content and conclusions presented.

References

Arns, M., Heinrich, H., & Strehl, U. (2013). Evaluation of neurofeedback in ADHD: The long and winding road. *Biological Psychology, 95*, 108–115. https://doi.org/10.1016/j.biopsycho.2013.11.013

Bazargan, M., Cobb, S., & Assari, S. (2021). Discrimination and medical mistrust in a racially and ethnically diverse sample of California adults. *Annals of Family Medicine, 19*(1), 4–15. https://doi.org/10.1370/afm.2632

Beltrán-Velasco, A. I., Bellido-Esteban, A., Ruisoto-Palomera, P., & Clemente-Suárez, V. J. (2020). The effect of cultural differences in psychophysiological stress response in high education context: A pilot study. *Applied Psychophysiology and Biofeedback, 45*(1), 23–29. https://doi.org/10.1007/s10484-019-09452-0

Betting, L. E., Mory, S. B., Lopes-Cendes, I., Li, L. M., Guerreiro, M. M., Guerreiro, C. A., & Cendes, F. (2006). EEG features in idiopathic generalized epilepsy: Clues to diagnosis. *Epilepsia, 47*(3), 523–528. https://doi.org/10.1111/j.1528-1167.2006.00462.x

Campinha-Bacote, J. (2002). The process of cultural competence in the delivery of healthcare services: A model of care. *Journal of Transcultural Nursing, 13*(3), 181–184. https://doi.org/10.1177/10459602013003003

Chiao, J. Y. (Ed.). (2009). *Cultural neuroscience: Cultural influences on brain function*. Elsevier.

Constant, A., Ramstead, M. J., Veissière, S. P., & Friston, K. (2019). Regimes of expectations: An active inference model of social conformity and human decision making. *Frontiers in Psychology, 10*, Article 679. https://doi.org/10.3389/fpsyg.2019.00679

Eisenbarth, H., D'Cruz, C., Bulbulia, J. A., & Thanni, B. (2025). Culturally diverse perceptions of EEG and neurofeedback research and how to address them to reduce sampling bias. *Psychophysiology, 62*(6), Article e70077. https://doi.org/10.1111/psyp.70077

Feldman, J. M., Matte, L., Interian, A., Lehrer, P. M., Lu, S. E., Scheckner, B., Steinberg, D. M., Oken, T., Kotay, A., Sinha, S., & Shim, C. (2016). Psychological treatment of comorbid asthma and panic disorder in Latino adults: Results from a randomized controlled trial. *Behaviour Research and Therapy, 87*, 142–154. https://doi.org/10.1016/j.brat.2016.09.007

Fleischman, M. J. (2022). Documenting the impact of infra low frequency neurofeedback on underserved populations with complex clinical presentations. *Frontiers in Human*

Neuroscience, 16, Article 921491. https://doi.org/10.3389/fnhum.2022.921491

Geronimus, A. T., Hicken, M., Keene, D., & Bound, J. (2006). "Weathering" and age patterns of allostatic load scores among blacks and whites in the United States. *American Journal of Public Health, 96*(5), 826–833. https://doi.org/10.2105/ajph.2004.060749

Hall, E. T. (1976). *Beyond culture*. Anchor Books.

Hamblin, M. R. (2016). Shining light on the head: Photobiomodulation for brain disorders. *BBA Clinical, 6*, 113–124. https://doi.org/10.1016/j.bbacli.2016.09.002

Hinton, D. E., & Good, B. J. (Eds.). (2016). *Culture and PTSD: Trauma in global and historical perspective*. University of Pennsylvania Press.

Kelley, M. J. (1997). Native Americans, neurofeedback, and substance abuse theory: Three year outcome of alpha/theta neurofeedback training in the treatment of problem drinking among Dine' (Navajo) people. *Journal of Neurotherapy, 2*(3), 24–60. https://doi.org/10.1300/J184v02n03_03

Martin, A. K., Su, P., & Meinzer, M. (2019). Common and unique effects of HD-tDCS to the social brain across cultural groups. *Neuropsychologia, 133*, Article 107170. https://doi.org/10.1016/j.neuropsychologia.2019.107170

McEwen, B. S. (2017). Neurobiological and systemic effects of chronic stress. *Chronic Stress, 1*, Article 2470547017692328. https://doi.org/10.1177/2470547017692328

Metzl, J. M., & Hansen, H. (2014). Structural competency: Theorizing a new medical engagement with stigma and inequality. *Social Science & Medicine, 103*, 126–133. https://doi.org/10.1016/j.socscimed.2013.06.032

Moss, E. M., Davidson, R. J., & Saron, C. (1985). Cross-cultural differences in hemisphericity: EEG asymmetry discriminates between Japanese and Westerners. *Neuropsychologia, 23*(1), 131–135. https://doi.org/10.1016/0028-3932(85)90054-5

Nelson, K. L., Matte-Landry, A., Feldman, J. M., & Lehrer, P. M. (2020). Further exploration of treatment response in Latinos with comorbid asthma and panic disorder: A brief report of HRV and ETCO2 as potential mediators of treatment response. *Applied Psychophysiology and Biofeedback, 45*(2), 67–75. https://doi.org/10.1007/s10484-020-09454-3

Nitsche, M. A., Cohen, L. G., Wassermann, E. M., Priori, A., Lang, N., Antal, A., Paulus, W., Hummel, F., Boggio, P. S., Fregni, F., & Pascual-Leone, A. (2008). Transcranial direct current stimulation: State of the art 2008. *Brain Stimulation, 1*(3), 206–223. https://doi.org/10.1016/j.brs.2008.06.004

Porges, S. W. (2011). *The polyvagal theory: Neurophysiological foundations of emotions, attachment, communication, and self-regulation*. Norton.

Robbins, N. M., Charleston, L. IV, Saadi, A., Thayer, Z., Codrington, W. U. III, Landry, A., Bernat, J. L., & Hamilton, R. (2022). Black patients matter in neurology: Race, racism, and race-based neurodisparities. *Neurology, 99*(3), 106–114. https://doi.org/10.1212/WNL.0000000000200830

Saadi, A., Himmelstein, D. U., Woolhandler, S., & Mejia, N. I. (2017). Racial disparities in neurologic health care access and utilization in the United States. *Neurology, 88*(24), 2268–2275. https://doi.org/10.1212/WNL.0000000000004025

Sherlin, L. H., Arns, M., Lubar, J., Heinrich, H., Kerson, C., Strehl, U., & Sterman, M. B. (2011). Neurofeedback and basic learning theory: Implications for research and practice. *Journal of Neurotherapy, 15*(4), 292–304. https://doi.org/10.1080/10874208.2011.623089

Siegel, J. M. (2005). Clues to the functions of mammalian sleep. *Nature, 437*(7063), 1264–1271. https://doi.org/10.1038/nature04285

Tervalon, M., & Murray-García, J. (1998). Cultural humility versus cultural competence: A critical distinction in defining physician training outcomes in multicultural education. *Journal of Health Care for the Poor and Underserved, 9*(2), 117–125. https://doi.org/10.1353/hpu.2010.0233

Travis, F., & Shear, J. (2010). Focused attention, open monitoring and automatic self-transcending: Categories to organize meditations from Vedic, Buddhist and Chinese traditions. *Consciousness and Cognition, 19*(4), 1110–1118. https://doi.org/10.1016/j.concog.2010.01.007

Received: October 6, 2025
Accepted: October 26, 2025
Published: March 31, 2026

NeuroRegulation

ISNR INTERNATIONAL SOCIETY FOR NEUROREGULATION & RESEARCH

A Novel Neurofeedback Paradigm: First Implementation of Cordance-Based Training for Anxiety and Mood Recovery

Rubén Pérez-Elvira[1,2], Javier Oltra-Cucarella[3], María Agudo Juan[2], Raúl Juárez Vela[4], and Alfonso Salgado-Ruiz[1]*

[1]Pontifical University of Salamanca, Salamanca, Spain
[2]Neuropsychophysiology Lab, NEPSA Rehabilitación Neurológica, Salamanca, Spain
[3]Miguel Hernández University, Elche, Spain
[4]University of La Rioja, Logroño, Spain

Abstract

This study presents the first implementation of a neurofeedback (NF) protocol based on cordance targeting mood and anxiety disorders. Cordance, a multivariate measure of brain activity, integrates both power within frequency bands and interfrequency relationships, providing a unique perspective on neural synchronization and connectivity. Using a single-case design, a 44-year-old male patient with anxiety, depression, and insomnia was selected based on left frontal discordance. Seven NF sessions were conducted, reinforcing increases in cordance in the left anterior quadrant. The results showed significant improvements in psychometric measures, including reductions in depression, anxiety, and insomnia scores, alongside a marked shift in cordance values toward normative levels. This study introduces cordance-based NF as a potential tool for mood and anxiety regulation, offering promising preliminary evidence for its efficacy. Future research should explore larger sample sizes and longer follow-ups to confirm these findings and expand the clinical applications of cordance-based interventions.

Keywords: concordance; neurofeedback; anxiety; depression

Citation: Pérez-Elvira, R., Oltra-Cucarella, J., Agudo Juan, M., Juárez Vela, R., & Salgado-Ruiz, A. (2026). A novel neurofeedback paradigm: First implementation of cordance-based training for anxiety and mood recovery. *NeuroRegulation, 13*(1), 77–90. https://doi.org/10.15540/nr.13.1.77

***Address correspondence to**: Rubén Pérez-Elvira, Dept. of Psychobiology, Faculty of Psychology, Pontifical University of Salamanca; Calle de la Compañía nº5, 37002 Salamanca, Spain. Email: rperezel@upsa.es

Edited by:
Rex L. Cannon, PhD, Currents, Knoxville, Tennessee, USA

Reviewed by:
Rex L. Cannon, PhD, Currents, Knoxville, Tennessee, USA
Tanya Morosoli, MSc: 1) Clínica de Neuropsicología Diagnóstica y Terapéutica, Mexico City, Mexico; 2) PPCR, ECPE, Harvard T. H. Chan School of Public Health, Boston, Massachusetts, USA

Introduction

The analysis of electroencephalography (EEG) and quantitative electroencephalography (qEEG) has become a powerful tool in brain function research and in clinical practice for diagnosing various neurological and psychiatric disorders (Babiloni et al., 2020; Chiarenza, 2021; Höller & Nardone, 2021; Niedermeyer & Lopes da Silva, 2005; Schomer & Lopes da Silva, 2017). However, traditional approaches based on univariate analyses of EEG or qEEG have shown significant limitations in consistently and accurately detecting pathologies or in identifying specific therapeutic targets at the physiological level (Livint Popa et al., 2020; McVoy et al., 2019). These methods, which often focus on univariate measures such as the amplitude of frequencies, coherence, or spectral power across different frequency bands, may not adequately capture the complexity of the neurophysiological mechanisms underlying the clinical alterations (Cohen, 2014; Dede et al., 2023; Faiman et al., 2023; Thatcher, 2016). Univariate markers, though informative, are insufficient to fully reflect the complex and multidimensional organization of the human brain. This highlights the need for more robust and sophisticated analytical approaches for identifying specific pathological markers.

This raises the possibility that a more sophisticated approach, such as the use of multivariate analyses or nonlinear methods, could provide a more

comprehensive and representative view of the patient's neurophysiological state. Multivariate analyses allow for the exploration of interactions and activation patterns involving multiple brain regions and various frequency bands, thereby facilitating a more holistic assessment of functional connectivity and brain dynamics in pathological states (Bassett & Sporns, 2017; Friston, 2009; Medaglia et al., 2015; Michel & Murray, 2012). For example, techniques such as complex network analysis, functional connectivity, and multichannel synchronization have proven useful in uncovering interaction patterns that would remain invisible with a univariate approach (Bastos & Schoffelen, 2016; Rubinov & Sporns, 2010).

One of the multivariate measures developed for brain activity analysis is cordance, a complex measure in EEG analysis (Leuchter et al., 1999; Leuchter, Cook, Lufkin, et al., 1994; Leuchter, Cook, Mena, et al., 1994). Unlike simple linear measures, such as amplitude or spectral power, which examine a single feature of the signal, cordance combines multiple aspects of brain activity to provide an integrated view. Specifically, cordance evaluates both the absolute power within a frequency band and its relationship to total power over a broader range, allowing for interpretation of synchronization status and the relative change between different frequencies and brain areas. By combining these elements, cordance provides a perspective on neural connectivity and synchronization that cannot be captured with isolated linear measures such as correlation or power spectral analysis, which assume direct, proportional relationships between variables, making it particularly useful in complex clinical contexts where integrated and robust indicators of brain activity are needed. Cordance has been used as a biomarker of pathology, primarily for depression (Tas et al., 2015) but also for other conditions as Alzheimer's disease, multi-infarct dementia, multiple sclerosis, or frontal lobe degeneration (Cook & Leuchter, 1996; Leuchter, Cook, Lufkin, et al., 1994), as a marker of response to psychopharmacological treatment in depression (Adamczyk et al., 2015; Broadway et al., 2012; Hunter et al., 2006) and also as a marker of response to neuromodulation techniques (Erguzel et al., 2015; Hunter et al., 2018).

Neurofeedback (NF) is a neuroregulation technique that enables individuals to regulate their brain activity through real-time feedback, typically obtained from EEG (Carrobles, 2016). Positioned among nonpharmacological interventions, NF differs from other methods by focusing on the direct training of specific patterns of brain activity, facilitating self-regulation of neural processes. In most cases, NF targets univariate variables, such as power in different frequency bands, to guide training. This technique has demonstrated utility in managing disorders such as anxiety and depression (Hammond, 2005), obsessive compulsive disorder (Sürmeli & Ertem, 2011), attention-deficit/hyperactivity disorder (Arns et al., 2009; Bakhshayesh et al., 2011; Pérez-Elvira et al., 2020), insomnia (Hammer et al., 2011; Pérez-Elvira et al., 2019), fibromyalgia (Kayiran et al., 2007; Pérez-Elvira & Jiménez Gómez, 2020), and epilepsy (Walker, 2005), among others, offering an alternative or complement to conventional pharmacological interventions.

Given that cordance has never before been used as a dependent variable or target for change in NF interventions, the aim of this study is to explore the implementation and efficacy of an NF protocol specifically designed to train cordance, applied in this case to a patient with mood and anxiety difficulties. This experimental protocol seeks to evaluate changes in EEG cordance metrics associated with targeted training, in order to provide preliminary evidence of the feasibility and clinical utility of cordance training as an intervention. To the best of our knowledge, this research represents the first application of a cordance-based training approach, thereby laying the groundwork for future studies in broader clinical contexts.

Methods

Participant

A 44-year-old male patient presented to the neuropsychophysiology clinic with emotional and cognitive complaints. He reported that, after the 2020 pandemic, he had experienced a marked increase in feelings of anxiety and unease, accompanied by persistent fatigue and significant mood fluctuations. These episodes included periods of emotional downturn alternating with moments of greater stability. Overall, he described a constant sense of restlessness and lack of motivation. Over the past year, these symptoms had intensified, affecting his ability to concentrate and sleep. Additionally, he had experienced episodes of insomnia, further exacerbating his fatigue. For anxiety management, he had been prescribed rescue anxiolytic medication, though he reported using it only during critical moments. His medical history also included a previous diagnosis of migraine with aura, which had first appeared during his university years, although these episodes had

been sporadic and were not part of the patient's current primary concerns. We selected this patient based on his cordance profile (left frontal discordance) and the presence of a conventional qEEG with *Z*-scores within the normal range. This selection was made for two main reasons: first, the discordance suggested a potential responsiveness to cordance-based NF, which was the novel intervention being tested; and second, the lack of other abnormal findings in the conventional qEEG minimized the likelihood that any observed improvements could be attributed to unrelated or uncontrolled variables. This made the patient an appropriate candidate to isolate and evaluate the specific effects of the cordance training protocol.

The patient provided written informed consent for the intervention and the publication of this study, which was undertaken at NEPSA Rehabilitación Neurológica, a neurologic rehabilitation clinic authorized by the Regional Department of Health (Castilla y León, Spain. Authorization Code: 37-C24-0216). The Regional Department of Health provided approval for this kind of intervention.

Psychometric Assessment

Beck Depression Inventory-II (BDI-II). The BDI-II (Beck et al., 1996; Sanz et al., 2003) is a self-administered questionnaire designed to assess the severity of depressive symptoms. Some items were updated by Beck et al. (1996) to better align with the DSM-IV diagnostic criteria for major depressive disorder. It consists of 21 items covering both emotional and physical symptoms of depression such as sadness, loss of interest, changes in appetite, fatigue, and feelings of guilt. Each item is rated on a 0 to 3 Likert-type scale, with higher scores indicating greater severity of depressive symptoms. Total scores range from 0 to 63 and are categorized into ranges to determine the level of depression: 0–13 indicates *minimal* depression, 14–19 *mild* depression, 20–28 *moderate* depression, and 29–63 *severe* depression (Beck et al., 1996). It is widely used in both clinical and research settings due to its high reliability and validity in measuring depression severity (Kendall et al., 1987; Sanz & García-Vera, 2013).

Hamilton Anxiety Rating Scale (HARS). The HARS (Hamilton, 1959; Lobo et al., 2002) is one of the most widely used tools in clinical and research settings designed to assess the severity of anxiety symptoms. It consists of 14 items covering both psychological and somatic symptoms. Each item is rated on a 0 to 4 Likert-type scale, with higher scores indicating greater symptom severity. Total scores range from 0 to 56, and results can be classified into mild, moderate, or severe levels of anxiety. A total score of 0–17 indicates *mild* anxiety, 18–24 *moderate* severity, and 25–56 *severe* anxiety (Hamilton, 1959; Lobo et al., 2002). The HARS is a reliable and valid instrument, widely used in clinical studies and in assessing the efficacy of treatments for anxiety (Bech, 2009; Maier et al., 1988; Sugarman et al., 2014; Thompson, 2015).

Athens Insomnia Scale (AIS). The AIS (Gómez-Benito et al., 2011; Soldatos et al., 2000, 2003) is a self-administered questionnaire designed to assess the severity of insomnia based on the criteria of the International Classification of Sleep Disorders (Sateia, 2014). The questionnaire consists of eight items, each rated on a 0 to 3 Likert-type scale, with a total score ranging from 0 to 24 and higher scores indicating greater insomnia severity. A total score of 6 or higher is considered indicative of clinically relevant insomnia problems (Shahid et al., 2011).

Neuropsychophysiological Assessment (qEEG)

EEG Acquisition and Preprocessing. For the collection of the EEGs the patient was fitted with an EEG cap, Electro-Cap (Electro-cap International) with 19 channels located according to International System 10–20 (Fp1, Fp2, F7, F3, Fz, F4, F8, T3, C3, Cz, C4, T4, T5, P3, Pz, P4, T6, O1, and O2) and using a Linked Ears montage. For 5 min, EEG signals from all 19 channels were simultaneously obtained and collected using a Discovery24 amplifier from BrainMaster Technologies, Inc. Impedances of less than 5 kΩ were maintained, and a constant temperature and humidity of less than 25°C and 50%, respectively, were maintained in the laboratory. EEG recordings were made in the closed-eye state with the use of Brain Avatar 4.6.4 software (BrainMaster Technologies, Inc.). The EEG signal preprocessing was performed using MNE-Python (version 1.8.0). The signal was band-pass filtered between 1 and 40 Hz, and artifacts were handled using Artifact Subspace Reconstruction (Blum et al., 2019; Kothe & Jung, 2016).

EEG Analysis and Processing. All EEG data processing were performed using Python (version 3.12.1) and the MNE-Python package (1.8.0; Gramfort et al., 2014). These tools were used for signal processing, cordance computation, and graphical representation. Additionally, data visualization and the generation of Microsoft Excel tables with the numerical cordance data were accomplished using SciPy (Virtanen et al., 2020), NumPy (Harris et al., 2020), and Pandas (The

Pandas Development Team, 2024). EEG recordings were processed using Linked Ears montage.

Cordance Calculation.

1. Hjorth Power Calculation of the Alpha Band. Hjorth power was calculated in the alpha band (8–13 Hz), a frequency band frequently studied in EEG due to its association with resting activity and cognitive functions (Başar et al., 2001). A filter between 8 and 13 Hz was applied to the EEG data using MNE-Python's filtering tools, ensuring the extraction of information specific to the alpha band.

Hjorth power in each channel was obtained by calculating the mean square of the alpha-filtered signal, according to the following equation:

$$Hjorth\ power_i = \frac{1}{N}\sum_{t=1}^{N} x_{i,t}^2$$

where:

N is the number of samples,

$x_{i,t}^2$ represents the amplitude at time *t* in channel *i*, and

$Hjorth\ power_i$ corresponds to the alpha band power for channel *i*.

This quadratic power is a common measure to assess the intensity of activity within a specific band, providing an approximation of the signal power in the selected frequency range (Teplan, 2002).

2. Calculation of Total Broadband Power (1–30 Hz). To normalize the power values in the alpha band, the total power in the range of 1–30 Hz was calculated for each channel, encompassing low-frequency components (1 Hz) up to the upper limit of the beta band (30 Hz). This approach follows established practices in EEG quantification, where total power serves as a reference for relative power analyses and normalization (Nunez & Srinivasan, 2006).

Total power was calculated as the mean square of the signal filtered in the 1–30 Hz range:

$$Total\ power_i = \frac{1}{N}\sum_{t=1}^{N} k_{i,t}^2$$

Where $Total\ power_i$ represents the power of the signal for channel *i* across the full frequency range, and $k_{i,t}^2$ represents the amplitude at time *t* in channel *i*.

3. Normalization of Alpha Hjorth Power and Calculation of Relative Power. Two normalization indices were used to assess cordance in each channel, based on the comparison of power in the alpha band with total power.

Alpha normalization (a_{norm}): The Hjorth power of each channel in the alpha band was normalized by dividing it by the maximum Hjorth power value across all channels, as shown in the following formula:

$$a_{norm,i} = \frac{Hjorth\ power_i}{max(Hjorth\ power)}$$

Normalized relative power (r_{norm}): The relative power in the alpha band was defined as the ratio between Hjorth power and total power in each channel, subsequently normalized by dividing it by the maximum relative power value across channels:

$$r_{norm,i} = \frac{\frac{Hjorth\ power_i}{Total\ power_i}}{max\left(\frac{Hjorth\ power}{Total\ power}\right)}$$

This normalization allows for consistent comparison of power levels across channels, regardless of absolute intensity differences (Cohen, 2014).

4. Cordance Classification. To classify cordance, three main categories were established based on the normalized values of a_{norm} and r_{norm}, following the approach proposed in previous studies (Leuchter, Cook, Lufkin, et al., 1994; Leuchter, Cook, Mena, et al., 1994; Kappenman & Luck, 2010):

Discordant: channels where a_{norm} <0.5 and r_{norm} >0.5

Concordant: channels where a_{norm} >0.5 and r_{norm} >0.5

Neutral: channels that do not meet any of the above conditions

This classification was implemented using logical comparisons and allowed categorization of each channel's states based on cordance, providing a three-level objective interpretation of the alignment

between normalized power and relative power in each channel.

5. Cordance Magnitude Calculation. Finally, cordance magnitude was calculated to quantify the degree of concordance or discordance in each channel. This value reflects the degree of deviation of each channel from a reference value of 0.5 in both normalizations, using the following formula:

$$\text{Cordance Magnitude}_i = \left(\left|a_{\text{norm,i}} - 0.5\right| + \left|r_{\text{norm},i} - 0.5\right|\right) \times 100$$

For graphical representation, and by convention (Leuchter, Cook, Lufkin, et al., 1994), discordance values are transformed to negative values, and concordance values to positive values. This cordance analysis was implemented in Python using the MNE-Python library (Gramfort et al., 2013) for EEG signal processing and filtering, whilst NumPy (Harris et al., 2020) was used for mathematical operations and data normalization.

Generation of Comparison Data for Cordance Comparison. To develop a reference database for cordance interpretation, data from 10 EEGs were used from the database: resting-state EEG data before and after cognitive activity across the adult lifespan and a 5-year follow-up, version 1.9.0 (Wascher et al., 2024). The selected EEGs belonged to subjects with characteristics similar to the study subject, allowing for a meaningful comparison in terms of physiological variability and demographic characteristics. Each EEG file, in EDF format, was imported and analyzed in Python using the MNE-Python library (Gramfort et al., 2013). Cordance variables were calculated using the same procedure explained above. The normality of the produced data was checked and organized in a tabular format using Pandas (The Pandas Development Team, 2024). The variables that did not follow an approximate normal distribution (Table 4) were subjected to a logarithmic transformation $X' = log_{10}(x)+1$ to approximate normality and stabilize variance (Bland & Altman, 1996). The addition of 1 was applied to avoid negative values in the transformed data, especially when dealing with original values smaller than 1, for which logarithms yield negative results. Subsequently, the same logarithmic transformation was applied to the subject's data that were to be compared with the comparison database, thereby ensuring homogeneity in the measurement scale. This strategy enabled the derivation of *Z*-scores, facilitating a direct comparison between individual values and the parameters of the comparison database.

Intervention. For the implementation of the NF protocol, the BrainAvatar software (Collura, 2012) was used, which was specifically configured in its Event Wizard to calculate and provide real-time feedback based on cordance parameters. This setup included the creation of bipolar virtual channels, ensuring a montage consistent with Hjorth's (1975) online transformation of EEG potentials into orthogonal source derivations and employed by Leuchter, Cook, Mena, et al. (1994) in cordance calculation.

The cordance calculation procedures were applied using the previously defined metrics, which involve the assessment of Hjorth power in the alpha band (8–13 Hz) and total power in the range of 1–30 Hz. These calculations were conducted according to the methods established in previous studies (Leuchter et al., 1999; Leuchter, Cook, Lufkin, et al., 1994; Leuchter, Cook, Mena, et al., 1994), thus ensuring the consistency and validity of the approach.

The selection of the intervention area was based on cordance measurements. Rather than defining a specific location, an entire quadrant was designated. The quadrant chosen for intervention was determined upon the initial assessment prior to the intervention by comparing the subject's cordance values with those of the comparison database. Specifically, the quadrant that exhibited the greatest average deviation from the normative values, expressed in terms of *Z*-scores and indicating a more pronounced alteration, was selected for intervention (Tables 2, 3, and 4).

The software was set up to integrate the results of the cordance calculations into the feedback provided to the patient, thereby facilitating a real-time training process that responded to variations in brain activity. The setup NF protocol provided reinforcement to the patient each time their current cordance magnitude increased compared to the average of the previous 10 s. This is represented as follow:

$$Reinforcement = \begin{cases} 1, if\ Cordance_{current} > Average\left(Cordance_{prev\ 10}\right) \\ 0, otherwise \end{cases}$$

where:

$Cordance_{current}$ is the current cordance magnitude, and

$Average\left(Cordance_{prev\ 10}\right)$ is the average cordance magnitude over the previous 10 s.

A value of 1 indicates reinforcement is provided, while 0 indicates no reinforcement. The reinforcer was given to the patient every time the cordance value exceeded a preset threshold. Movies selected by the patient were used as reinforcement, ensuring they were engaging enough to sustain attention. This approach was based on evidence suggesting that self-chosen and personally satisfying reinforcers are optimal for facilitating learning through NF (Pérez-Elvira et al., 2021). A dimmer was applied to the movies, which increased in opacity (obscuring the screen) when the patient failed to meet the criterion and became more transparent (allowing the movie to be visible) when the criterion was met. Seven 30-min sessions were conducted, twice per week, following this procedure. This decision to use seven sessions, as opposed to the 10 sessions employed in our previous studies (Pérez-Elvira et al., 2020, 2021), was made to minimize the number of sessions required, thereby avoiding unnecessary burden on the patient within the context of this purely experimental procedure.

Statistical Analysis. To evaluate changes in the scores of the psychological tests administered, the reliable change index (RCI) of Jacobson and Truax (1991) was used.

The RCI is calculated using the following formula:

$$RCI = \frac{X_2 - X_1}{S_{diff}}$$

where:

X_1 is the score obtained in the posttreatment assessment,

X_2 is the score obtained in the pretreatment assessment, and

S_{diff} is the standard error of the difference between the two scores and is calculated as:

$$S_{diff} = \sqrt{2\ x\ SE}$$

The SE or standard error of measurement is obtained using the following formula:

$$SE = SD\ x\ \sqrt{1 - r}$$

where:

SD is the standard deviation of the test scores in the reference population (Gómez-Benito et al., 2011; Lobo et al., 2002; Sanz et al., 2003), and

r is the reliability of the test (such as the test-retest reliability coefficient or Cronbach's alpha).

To interpret the RCI, if the value is greater than 1.96 or less than −1.96, the change is considered statistically significant at the 95% confidence level. If the value is between −1.96 and 1.96, the change is not considered significant.

To apply a paired samples *t*-test and study changes in cordance, a similar approach to that expressed by Thatcher (2021) was used. A sliding window approach was employed to segment the EEG data into overlapping chunks. Chunks of 30 s were generated. A window of the specified length was set and slid across the entire EEG recording, advancing 1 s for each new segment. Specifically, the first segment included data from $t = 1$ to $t = n$, where t represents the time points of the segment and n is the theoretical upper limit of the segment interval. The second segment would then encompass data from $t = 2$ to $t = n + 1$, and so on, covering the entire dataset.

Mathematically, for the EEG time series $X(t)$, where $t = 1, 2, \ldots, T$ represents the time points in the EEG recording, each segment S_i is defined as:

$$S_i = X(i{:}\ i + \omega - 1),\ i = 1, 2, \ldots, T - \omega + 1$$

where:

S_i represents the i-th segment,

$X(i{:}\ i + \omega - 1)$ denotes the subset of the EEG signal from the time point i up to $i + \omega - 1$,

ω is the length of the window, and

T is the total number of time points in the EEG recording.

Both EEGs (pre and post) had the same recording duration but different edited durations. The first had an artifact-free duration of 1 min and 20 s, while the second had an artifact-free duration of 1 min and 2 s. Thus, 51 samples were generated for the pre-EEG and 33 for the post-EEG. To match the comparisons and avoid issues with the different number of samples, the number of samples for the shorter EEG was selected, meaning that 33 samples were used for both measurements.

For the analyses, which involved multiple comparisons, we applied Storey's *q*-value method (Storey, 2002), which estimates the proportion of true null hypotheses (π_0) and provides adjusted *p*-values (*q*-values) that control the false discovery rate. The λ parameter was set to 0.5 for π_0 estimation. Statistical significance was set at α = .05 for all analyses, with results considered significant when $q < .05$ after correction.

Results

Baseline Psychometric Assessment

In the baseline psychometric assessment of this subject, scores indicative of psychological distress and insomnia were found (Table 1).

Specifically, regarding mood assessment, a BDI-II score of 28 points was obtained, suggesting the presence of clinical depression symptoms such as low mood, feelings of hopelessness, and decreased interest in activities. Regarding anxiety symptoms, the total score of 23 suggested moderate levels of anxiety. On the AIS, the subject scored 12 points, suggesting a moderate intensity of insomnia.

Posttreatment Psychometric Changes

The subject's scores for each scale, as well as the results of their statistical analysis, are shown in the table (Table 1).

Table 1
Psychometric Assessment

Test	X_1	X_2	*r*	*SD*	RCI
BDI-II	28	15	.91	10.9	−2.81
HARS	23	14	.92	9.45	−2.38
AIS	12	6	.90	3.24	−4.14

Note. BDI-II**:** Beck Depression Inventory-II; HARS: Hamilton Anxiety Rating Scale; AIS: Athens insomnia scale; X_1: Pretreatment assessment; X_2: Posttreatment assessment; *r*: reliability coefficient; *SD*: standard deviation; RCI: Reliable Change Index.

Cordance Baseline

In Table 5, the pretreatment cordance calculated and its associated magnitude can be found. In Table 2, the average magnitude of the cordance can be observed in a classification by quadrants (Gazzaniga, 2000; Hammond, 2005).

Quadrant A was selected for intervention as it had the highest average *Z*-score, deviated the most from the comparison values, and therefore exhibited the least optimal functioning (Northoff & Tumati, 2019), in addition to its connection with the patient's symptoms (Grimm et al., 2008; Thibodeau et al., 2006), the left anterior quadrant, particularly the FP1, F3, and F7 electrodes, is associated with emotional regulation and has been linked to mood and anxiety disorders. Altered alpha and theta activity in this region reflect impaired emotion processing, with studies showing reduced cortical activity in individuals with depression and anxiety disorders (Pokorny et al., 2024; Wutzl et al., 2024).

Table 2
Average Cordance by Quadrant

	Quadrant A	Quadrant B	Quadrant C	Quadrant D
Pre	−40.27	−29.56	−12.95	13.17
Post	−20.90	−6.71	27.15	48.80

Note. Quadrant A: Fp1, F7, F3, Fz, C3; Quadrant B: Fp2, F8, F4, Fz, C4; Quadrant C: C3, P3, T5, Pz, O1; Quadrant D: C4, P4, Pz, T6, O2.

Table 3
Average Pre-Post Z Scores by Quadrant

	Pre	Post
Quadrant 1	−0.795	−0.475
Quadrant 2	−0.652	−0.395
Quadrant 3	−0.407	0.212
Quadrant 4	0.247	0.296

Note. Although the subject's *Z*-scores fall within the statistically normal range (±1.98 *SD*), when analyzed categorically (the only prior criterion available for cordance), the majority were discordant, with negative scores as shown in Table 2. In contrast, in the control group, almost all values were neutral or positive, approaching zero.

Posttreatment Cordance

Table 5 presents the changes in cordance scores pre- and postintervention, as well as the statistical significance of these changes. Overall, an increase in cordance values was observed across all channels compared to the pretreatment measurement (Figure 1). Table 3 shows the change in the average *Z*-scores for each quadrant. All quadrants exhibited a noticeable trend toward the mean, except for Quadrant 4, which, however, was the closest to the mean in the pretreatment phase (Table 3).

Figure 1. *Pre- and Posttreatment, Difference Pre-Post Cordance Topomaps and P-Values Topomap.*

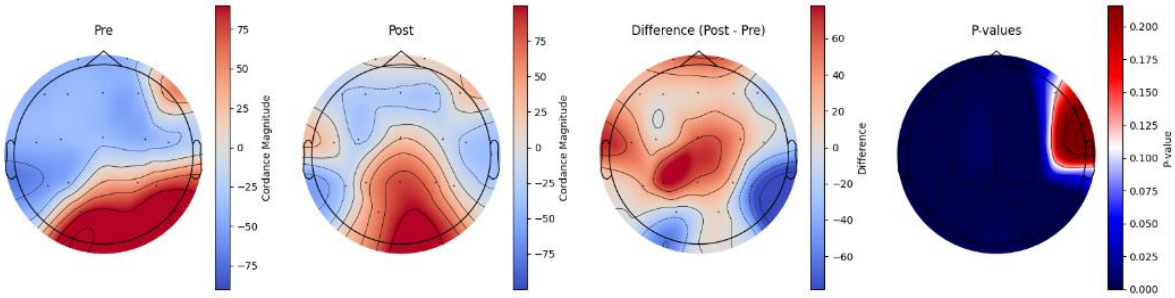

Table 4

Comparison Database Statistics and Individual Cordance Scores (Log-Transformed Values)

		FP1	FP2	F3*	F4*	C3	C4*	P3	P4*	O1*	O2*	F7	F8	T3	T4	T5	T6*	Fz*	Cz*	Pz*
Group	*M*	11.77	8.29	0.35	−0.02	−10.00	−0.01	−7.94	−0.29	1.52	1.47	19.91	−2.39	2.56	2.62	38.64	1.48	0.36	0.68	−0.66
	SD	44.59	51.19	1.75	1.84	55.30	1.83	52.08	1.74	1.16	1.14	47.20	48.70	41.30	45.21	56.30	1.16	1.87	1.73	1.62
Subject	*Pre X*	−42.67	−43.60	−1.61	−1.63	−43.60	−1.69	−45.00	1.63	1.88	1.98	39.27	39.04	−44.80	−37.02	−57.36	1.84	−1.67	−1.62	1.63
	Pre Z	−1.22	−1.01	−1.12	−0.88	−0.61	−0.91	−0.71	1.10	0.31	0.44	0.41	0.85	−1.15	−0.88	−1.71	0.31	−1.09	−1.33	1.42
	Post X	25.06	28.36	−1.47	−1.49	28.36	−1.46	41.28	1.74	1.85	2.00	−28.93	28.43	−30.09	−34.84	−43.23	1.68	−1.47	1.59	1.93
	Post Z	0.30	0.39	−1.04	−0.80	0.69	−0.79	0.95	1.16	0.28	0.46	−1.03	0.63	−0.79	−0.83	−1.45	0.17	−0.98	0.53	1.60

Note. *M*: Group mean, *SD*: group standard deviation, Pre *X*: subject´s pretreatment cordance direct value, Pre *Z*: subject´s pretreatment cordance *Z*-Score, Post *X*: subject´s posttreatment cordance direct value, Post *Z*: subject´s posttreament cordance *Z*-Score. The values obtained from the channels marked with * did not follow a normal distribution, and a logarithmic transformation was applied to both the group data and the individual subject data.

Table 5

Statistical Comparison of Pre- and Postcordance Values Based on 33 EEG Subsamples

Channel	Cordance magnitude Pre (*SD*)	Cordance magnitude Post (*SD*)	Diff. (Post-Pre)	*t*-statistic	*p*-value	*q*-value BH
C3	−38.58 (2.63)	−29.24 (1.12)	9.34	−21.49	.010	**.0173**
C4	−44.30 (1.68)	−7.79 (28.88)	36.51	−8.09	.010	**.0173**
Cz	−36.51 (2.16)	22.51 (31.80)	59.02	−11.68	.010	**.0112**
F3	−37.43 (1.94)	−29.53 (1.33)	7.90	−21.40	.010	**.0173**
F4	−38.91 (2.05)	−28.90 (9.08)	10.01	−6.69	.010	**.0173**
F7	−41.78 (1.04)	−24.90 (14.48)	16.87	−7.68	.010	**.0173**
F8	29.56 (25.92)	17.41 (33.03)	−12.15	1.62	.112	.1182
Fp1	−42.13 (1.45)	8.17 (32.20)	50.30	−10.49	.010	**.0173**
Fp2	−42.00 (1.44)	14.76 (33.18)	56.76	−11.20	.010	**.0173**
Fz	−41.43 (2.02)	−29.03 (1.44)	12.40	−29.68	.010	**.0112**
O1	81.02 (6.26)	64.33 (13.26)	−16.69	5.89	.010	**.0173**
O2	90.13 (1.41)	99.97 (0.22)	9.84	−42.60	.010	**.0173**
P3	−38.87 (11.79)	39.38 (8.49)	78.25	−31.50	.010	**.0173**
P4	40.95 (7.02)	54.32 (6.31)	13.36	−7.32	.010	**.0173**
Pz	29.69 (22.84)	83.56 (6.49)	53.87	−12.91	.010	**.0112**
T3	−42.12 (1.43)	9.97 (31.03)	52.08	−10.95	.010	**.0158**
T4	−33.70 (1.79)	−31.04 (13.69)	2.66	−1.26	.216	.2160
T5	−54.09 (2.27)	−22.25 (39.66)	31.84	−5.08	.010	**.0112**
T6	71.65 (3.60)	13.96 (46.67)	−57.69	7.93	.010	**.0112**

Note. *DE* = Standard Deviation; Diff. = Post-Pre; BH *q*-value = *p*-value adjusted using the Benjamini-Hochberg False Discovery Rate method; Significant: BH *q*-value < .05. The values with a significant *q*-value have been highlighted in bold.

Discussion

In this study we aimed to analyze the utility of a new NF paradigm—cordance-based NF—for alleviating anxious and depressive symptoms. Notably, to the best of our knowledge, this is the first time that real-time cordance calculation has been implemented and applied in NF.

To implement the NF protocol based on concordance, we selected a patient with anxiety, mood disturbances, and insomnia. This patient also met the requirement of exhibiting left frontal discordance (Bench et al., 1992; Leuchter, Cook, Mena, et al., 1994; Videbech, 2000) and did not exhibit any other relevant abnormalities in their qEEG expressed in *Z*-scores. The patient was evaluated psychometrically, with results consistent with mood disturbances, anxiety, and insomnia. Additionally, as previously mentioned, the patient underwent neurometric assessment, which revealed no significant findings in the commonly measured qEEG parameters. Cordance was calculated for the patient's EEG and divided by quadrants. The patient exhibited marked discordance (low concordance) in the left anterior quadrant. A NF protocol was designed to reinforce the patient every time cordance increased. Seven sessions of this protocol were applied, and it was found that there was a general increase in cordance, resulting in a statistically significant change across all regions except for the right frontotemporal region, which already exhibited positive concordance during the pretreatment phase. This change was accompanied by a significant shift in the desired direction in the psychometric variables, with improvements in depression (from *moderate* to *mild*), anxiety (from *moderate* to *mild*) and insomnia (reduced to half of the initial score; Gómez-Benito et al., 2011; Lobo et al., 2002; Sanz & García-Vera, 2013).

Cordance has been shown to correlate significantly with cerebral perfusion and metabolism. In his seminal study, Leuchter et al. (1999) demonstrated that cordance values, particularly in frontal regions, were highly correlated with regional cerebral blood flow measured by SPECT. This suggests that cordance may serve as a noninvasive electrophysiological proxy for assessing metabolic activity in the brain, providing a valuable tool for neuropsychiatric research and clinical monitoring.

In this regard, our results suggest that NF based on cordance may be an effective intervention for patients with mood and anxiety disorders and are consistent with previous research identifying patterns of hypoperfusion and hypometabolism in the left frontal region among individuals with affective disorders (Bench et al., 1992; Drevets et al., 2008; Videbech, 2000). Mayberg et al. (2000, 2005) reported on a correlation between left frontal metabolic activity and depressive symptoms, showing that normalization of activity in the left dorsolateral prefrontal cortex is strongly associated with clinical remission. Their studies using positron emission tomography (PET) revealed that increases in glucose metabolism and cerebral blood flow in these regions are significantly correlated with reductions in depression scores, as measured by standardized instruments such as the Hamilton Depression Rating Scale (Hamilton, 1960). In this regard, Cook et al. (2002) reported that prefrontal cordance may serve as a useful biomarker for predicting treatment response in depression. Cook et al. (2002) observed that changes in prefrontal cordance preceded clinical improvement in patients with depression treated with psychotropic medications. Our approach, compared to theirs, differs in that we employed NF to directly modify cordance, rather than merely observing it as a passive biomarker.

Regarding the number of sessions required for improvement to appear, our results align with those highlighted by Baker (2023), who applied passive infrared hemoencephalography (pIR HEG) to a sample of individuals with mental health conditions, primarily emotional and anxiety-related issues, finding positive results around the fifth session. The pIR HEG reflects underlying cerebral blood flow and metabolic activity (Carmen, 2004; Coben & Padolsky, 2007) and focuses on enhancing prefrontal cortex function through noninvasive NF, measuring changes in thermal activity as a byproduct of cerebral blood flow. Both techniques, pIR HEG and cordance, assess brain function but approach the analysis from different angles. Cordance not only offers a more detailed frequency-based view of brain activity but also provides greater versatility in terms of the regions and structures that can be evaluated. In any case, the number of sessions appears significantly lower than the typical number reported in the scientific literature using conventional amplitude NF (Hammond, 2005; Marzbani et al., 2016) or other modalities such as slow cortical potentials (Sitaram et al., 2017).

This study presents limitations that must be considered when interpreting its results. First, as it employs a single-case design, the generalizability of the findings to a broader population is limited. In

addition, the reduced number of sessions, may restrict the long-term efficacy of the intervention when compared with conventional amplitude-based NF protocols. Therefore, future research is recommended to include larger samples, follow-up assessment, and a comparison intervention to confirm and expand these preliminary findings and to examine their long-term maintenance. Our data analysis was based on statistical changes, which might fail to appraise clinically meaningful changes for smaller effect sizes than the one reported in the present work. Additional research using more sophisticated statistical methods than the RCI (McAleavey, 2024) is needed.

The present work introduces an innovative NF paradigm based on real-time cordance calculation. To our knowledge, this is the first application of this methodology. The results obtained suggest that this technique can effectively modulate brain activity, which is associated with improvements in symptoms of anxiety and depression. Despite the inherent limitations of the single-case design, this contribution opens new perspectives for the clinical application of this type of NF and lays the groundwork for future investigations.

Author Disclosure

The authors declare that they have not used AI during the writing of this paper.

References

Adamczyk, M., Gazea, M., Wollweber, B., Holsboer, F., Dresler, M., Steiger, A., & Pawlowski, M. (2015). Cordance derived from REM sleep EEG as a biomarker for treatment response in depression – A naturalistic study after antidepressant medication. *Journal of Psychiatric Research, 63*, 97–104. https://doi.org/10.1016/j.jpsychires.2015.02.007

Arns, M., de Ridder, S., Strehl, U., Breteler, M., & Coenen, A. (2009). Efficacy of neurofeedback treatment in ADHD: The effects on inattention, impulsivity and hyperactivity: A meta-analysis. *Clinical EEG and Neuroscience, 40*(3), 180–189. https://doi.org/10.1177/155005940904000311

Babiloni, C., Blinowska, K., Bonanni, L., Cichocki, A., De Haan, W., Del Percio, C., Dubois, B., Escudero, J., Fernández, A., Frisoni, G., Guntekin, B., Hajos, M., Hampel, H., Ifeachor, E., Kilborn, K., Kumar, S., Johnsen, K., Johannsson, M., Jeong, J., … Randall, F. (2020). What electrophysiology tells us about Alzheimer's disease: A window into the synchronization and connectivity of brain neurons. *Neurobiology of Aging, 85*, 58–73. https://doi.org/10.1016/j.neurobiolaging.2019.09.008

Baker, C. T. (2023). Documenting the effects of noninvasive prefrontal pIR HEG neurofeedback in the treatment of common mental health problems. *NeuroRegulation, 10*(3), 207–218. https://doi.org/10.15540/nr.10.3.207

Bakhshayesh, A. R., Hänsch, S., Wyschkon, A., Rezai, M. J., & Esser, G. (2011). Neurofeedback in ADHD: A single-blind randomized controlled trial. *European Child & Adolescent Psychiatry, 20*(9), 481–491. https://doi.org/10.1007/s00787-011-0208-y

Başar, E., Başar-Eroglu, C., Karakaş, S., & Schürmann, M. (2001). Gamma, alpha, delta, and theta oscillations govern cognitive processes. *International Journal of Psychophysiology, 39*(2–3), 241–248. https://doi.org/10.1016/s0167-8760(00)00145-8

Bassett, D. S., & Sporns, O. (2017). Network neuroscience. *Nature Neuroscience, 20*(3), 353–364. https://doi.org/10.1038/nn.4502

Bastos, A. M., & Schoffelen, J.-M. (2016). A tutorial review of functional connectivity analysis methods and their interpretational pitfalls. *Frontiers in Systems Neuroscience*, *9*, Article 175. https://doi.org/10.3389/fnsys.2015.00175

Bech, P. (2009). Fifty years with the Hamilton scales for anxiety and depression. *Psychotherapy and Psychosomatics, 78*(4), 202–211. https://doi.org/10.1159/000214441

Beck, A. T., Steer, R. A., & Brown, G. K. (1996). *BDI-II, Beck Depression Inventory: Manual*. Psychological Corporation.

Bench, C. J., Friston, K. J., Brown, R. G., Scott, L. C., Frackowiak, R. S. J., & Dolan, R. J. (1992). The anatomy of melancholia – Focal abnormalities of cerebral blood flow in major depression. *Psychological Medicine, 22*(3), 607–615. https://doi.org/10.1017/S003329170003806X

Bland, J. M., & Altman, D. G. (1996). Statistics notes: Transforming data. *BMJ, 312*(7033), 770–770. https://doi.org/10.1136/bmj.312.7033.770

Blum, S., Jacobsen, N. S. J., Bleichner, M. G., & Debener, S. (2019). A Riemannian modification of artifact subspace reconstruction for EEG artifact handling. *Frontiers in Human Neuroscience, 13*, Article 141. https://doi.org/10.3389/fnhum.2019.00141

Broadway, J. M., Holtzheimer, P. E., Hilimire, M. R., Parks, N. A., DeVylder, J. E., Mayberg, H. S., & Corballis, P. M. (2012). Frontal theta cordance predicts 6-month antidepressant response to subcallosal cingulate deep brain stimulation for treatment-resistant depression: A pilot study. *Neuropsychopharmacology, 37*(7), 1764–1772. https://doi.org/10.1038/npp.2012.23

Carmen, J. A. (2004). Passive infrared hemoencephalography: Four years and 100 migraines. *Journal of Neurotherapy, 8*(3), 23–51. https://doi.org/10.1300/J184v08n03_03

Carrobles Isabel, J. A. (2016). Bio/neurofeedback. *Clínica y Salud, 27*(3), 125–131. https://doi.org/10.1016/j.clysa.2016.09.003

Chiarenza, G. A. (2021). Quantitative EEG in childhood attention deficit hyperactivity disorder and learning disabilities. *Clinical EEG and Neuroscience, 52*(2), 144–155. https://doi.org/10.1177/1550059420962343

Coben, R., & Padolsky, I. (2007). Infrared imaging and neurofeedback: Initial reliability and validity. *Journal of Neurotherapy, 11*(3), 3–13. https://doi.org/10.1080/10874200802126100

Cohen, M. X. (2014). *Analyzing neural time series data: Theory and practice*. The MIT Press. https://doi.org/10.7551/mitpress/9609.001.0001

Collura, T. (2012). BrainAvatar: Integrated brain imaging, neurofeedback, and reference database system. *NeuroConnections Summer*, 31–36.

Cook, I. A., & Leuchter, A. F. (1996). Synaptic dysfunction in Alzheimer's disease: Clinical assessment using quantitative EEG. *Behavioural Brain Research, 78*(1), 15–23. https://doi.org/10.1016/0166-4328(95)00214-6

Cook, I. A., Leuchter, A. F., Morgan, M., Witte, E., Stubbeman, W. F., Abrams, M., Rosenberg, S., and Uijtdehaage, S. H. J. (2002). Early changes in prefrontal activity characterize clinical responders to antidepressants. *Neuropsychopharmacology, 27*(1), 120–131. https://doi.org/10.1016/S0893-133X(02)00294-4

Dede, A. J. O., Xiao, W., Vaci, N., Cohen, M. X., & Milne, E. (2023). Lack of univariate, clinically-relevant biomarkers of

autism in resting state EEG: A study of 776 participants. *medRxiv*. https://doi.org/10.1101/2023.05.21.23290300

Drevets, W. C., Price, J. L., & Furey, M. L. (2008). Brain structural and functional abnormalities in mood disorders: Implications for neurocircuitry models of depression. *Brain Structure & Function, 213*(1–2), 93–118. https://doi.org/10.1007/s00429-008-0189-x

Erguzel, T. T., Ozekes, S., Gultekin, S., Tarhan, N., Hizli Sayar, G., & Bayram, A. (2015). Neural network based response prediction of rTMS in major depressive disorder using QEEG cordance. *Psychiatry Investigation, 12*(1), 61–65. https://doi.org/10.4306/pi.2015.12.1.61

Faiman, I., Sparks, R., Winston, J. S., Brunnhuber, F., Ciulini, N., Young, A. H., & Shotbolt, P. (2023). Limited clinical validity of univariate resting-state EEG markers for classifying seizure disorders. *Brain Communications, 5*(6), Article fcad330. https://doi.org/10.1093/braincomms/fcad330

Friston, K. (2009). Causal modelling and brain connectivity in functional magnetic resonance imaging. *PLoS Biology, 7*(2), Article e1000033. https://doi.org/10.1371/journal.pbio.1000033

Gazzaniga, M. S. (2000). Cerebral specialization and interhemispheric communication: Does the corpus callosum enable the human condition? *Brain, 123*(7), 1293–1326. https://doi.org/10.1093/brain/123.7.1293

Gómez-Benito, J., Ruiz, C., & Guilera, G. (2011). A Spanish version of the Athens insomnia scale. *Quality of Life Research, 20*(6), 931–937. https://doi.org/10.1007/s11136-010-9827-x

Gramfort, A., Luessi, M., Larson, E., Engemann, D. A., Strohmeier, D., Brodbeck, C., Goj, R., Jas, M., Brooks, T., Parkkonen, L., & Hämäläinen, M. (2013). MEG and EEG data analysis with MNE-Python. *Frontiers in Neuroscience, 7*, Article 267. https://doi.org/10.3389/fnins.2013.00267

Grimm, S., Beck, J., Schuepbach, D., Hell, D., Boesiger, P., Bermpohl, F., Niehaus, L., Boeker, H., & Northoff, G. (2008). Imbalance between left and right dorsolateral prefrontal cortex in major depression is linked to negative emotional judgment: An fMRI study in severe major depressive disorder. *Biological Psychiatry, 63*(4), 369–376. https://doi.org/10.1016/j.biopsych.2007.05.033

Hamilton, M. (1959). The assessment of anxiety states by rating. *British Journal of Medical Psychology, 32*(1), 50–55. https://doi.org/10.1111/j.2044-8341.1959.tb00467.x

Hamilton, M. (1960). A rating scale for depression. *Journal of Neurology, Neurosurgery & Psychiatry, 23*(1), 56–62. https://doi.org/10.1136/jnnp.23.1.56

Hammer, B. U., Colbert, A. P., Brown, K. A., & Ilioi, E. C. (2011). Neurofeedback for insomnia: A pilot study of Z-Score SMR and individualized protocols. *Applied Psychophysiology and Biofeedback*, *36*(4), 251–264. https://doi.org/10.1007/s10484-011-9165-y

Hammond, D. C. (2005). Neurofeedback treatment of depression and anxiety. *Journal of Adult Development, 12*(2–3), 131–137. https://doi.org/10.1007/s10804-005-7029-5

Harris, C. R., Millman, K. J., Van Der Walt, S. J., Gommers, R., Virtanen, P., Cournapeau, D., Wieser, E., Taylor, J., Berg, S., Smith, N. J., Kern, R., Picus, M., Hoyer, S., Van Kerkwijk, M. H., Brett, M., Haldane, A., Del Río, J. F., Wiebe, M., Peterson, P., … Oliphant, T. E. (2020). Array programming with NumPy. *Nature, 585*(7825), 357–362. https://doi.org/10.1038/s41586-020-2649-2

Hjorth, B. (1975). An on-line transformation of EEG scalp potentials into orthogonal source derivations. *Electroencephalography and Clinical Neurophysiology, 39*(5), 526–530. https://doi.org/10.1016/0013-4694(75)90056-5

Höller, Y., & Nardone, R. (2021). Quantitative EEG biomarkers for epilepsy and their relation to chemical biomarkers. In G. S. Makowsi (Ed.), *Advances in clinical chemistry* (Vol. 102, pp. 271–336). Elsevier. https://doi.org/10.1016/bs.acc.2020.08.004

Hunter, A. M., Leuchter, A. F., Morgan, M. L., & Cook, I. A. (2006). Changes in brain function (quantitative EEG cordance) during placebo lead-in and treatment outcomes in clinical trials for major depression. *The American Journal of Psychiatry, 163*(8), 1426–1432. https://doi.org/10.1176/ajp.2006.163.8.1426

Hunter, A. M., Nghiem, T. X., Cook, I. A., Krantz, D. E., Minzenberg, M. J., & Leuchter, A. F. (2018). Change in quantitative EEG theta cordance as a potential predictor of repetitive transcranial magnetic stimulation clinical outcome in major depressive disorder. *Clinical EEG and Neuroscience, 49*(5), 306–315. https://doi.org/10.1177/1550059417746212

Jacobson, N. S., & Truax, P. (1991). Clinical significance: A statistical approach to defining meaningful change in psychotherapy research. *Journal of Consulting and Clinical Psychology, 59*(1), 12–19. https://doi.org/10.1037/0022-006X.59.1.12

Kappenman, E. S., & Luck, S. J. (2010). The effects of electrode impedance on data quality and statistical significance in ERP recordings. *Psychophysiology, 47*(5), 888–904. https://doi.org/10.1111/j.1469-8986.2010.01009.x

Kayiran, S., Dursun, E., Ermutlu, N., Dursun, N., & Karamürsel, S. (2007). Neurofeedback in fibromyalgia syndrome. *Agri: Agri (Algoloji) Dernegi'nin Yayin Organidir = The Journal of the Turkish Society of Algology, 19*(3), 47–53.

Kendall, P. C., Hollon, S. D., Beck, A. T., Hammen, C. L., & Ingram, R. E. (1987). Issues and recommendations regarding use of the Beck Depression Inventory. *Cognitive Therapy and Research, 11*(3), 289–299. https://doi.org/10.1007/BF01186280

Kothe, C. A., & Jung, T.-P. (2016). *Artifact removal techniques with signal reconstruction* (Patent No. US20160113587A1).

Leuchter, A. F., Uijtdehaage, S. H., Cook, I. A., O'Hara, R., & Mandelkern, M. (1999). Relationship between brain electrical activity and cortical perfusion in normal subjects. *Psychiatry Research: Neuroimaging, 90*(2), 125–140. https://doi.org/10.1016/S0925-4927(99)00006-2

Leuchter, A. F., Cook, I. A., Lufkin, R. B., Dunkin, J., Newton, T. F., Cummings, J. L., Mackey, J. K., & Walter, D. O. (1994). Cordance: A new method for assessment of cerebral perfusion and metabolism using quantitative electroencephalography. *NeuroImage*, *1*(3), 208–219. https://doi.org/10.1006/nimg.1994.1006

Leuchter, A. F., Cook, I. A., Mena, I., Dunkin, J. J., Cummings, J. L., Newton, T. F., Migneco, O., Lufkin, R. B., Walter, D. O., & Lachenbruch, P. A. (1994). Assessment of cerebral perfusion using quantitative EEG cordance. *Psychiatry Research: Neuroimaging, 55*(3), 141–152. https://doi.org/10.1016/0925-4927(94)90022-1

Livint Popa, L., Dragos, H., Pantelemon, C., Verisezan Rosu, O., & Strilciuc, S. (2020). The role of quantitative EEG in the diagnosis of neuropsychiatric disorders. *Journal of Medicine and Life, 13*(1), 8–15. https://doi.org/10.25122/jml-2019-0085

Lobo, A., Chamorro, L., Luque, A., Dal-Ré, R., Badia, X., Baró, E. & Grupo de Validación en Español de Escalas Psicométricas (GVEEP) (2002). Validación de las versiones en español de la Montgomery-Asberg Depression Rating Scale y la Hamilton Anxiety Rating Scale para la evaluación de la depresión y de la ansiedad [Validation of the Spanish versions of the Montgomery-Asberg Depression and Hamilton Anxiety rating scales]. *Medicina Clínica, 118*(13), 493–499. https://doi.org/10.1016/S0025-7753(02)72429-9

Maier, W., Buller, R., Philipp, M., & Heuser, I. (1988). The Hamilton anxiety scale: Reliability, validity and sensitivity to change in anxiety and depressive disorders. *Journal of Affective Disorders, 14*(1), 61–68. https://doi.org/10.1016/0165-0327(88)90072-9

Marzbani, H., Marateb, H., & Mansourian, M. (2016). Methodological note: Neurofeedback: A comprehensive review on system design, methodology and clinical applications. *Basic and Clinical Neuroscience Journal, 7*(2), 143–158. https://doi.org/10.15412/J.BCN.03070208

Mayberg, H. S., Brannan, S. K., Tekell, J. L., Silva, J. A., Mahurin, R. K., McGinnis, S., & Jerabek, P. A. (2000). Regional metabolic effects of fluoxetine in major depression: Serial changes and relationship to clinical response. *Biological Psychiatry, 48*(8), 830–843. https://doi.org/10.1016/s0006-3223(00)01036-2

Mayberg, H. S., Lozano, A. M., Voon, V., McNeely, H. E., Seminowicz, D., Hamani, C., Schwalb, J. M., & Kennedy, S. H. (2005). Deep brain stimulation for treatment-resistant depression. *Neuron, 45*(5), 651–660. https://doi.org/10.1016/j.neuron.2005.02.014

McAleavey, A. A. (2024). When (not) to rely on the reliable change index: A critical appraisal and alternatives to consider in clinical psychology. *Clinical Psychology: Science and Practice, 31*(3), 351–366. https://doi.org/10.1037/cps0000203

McVoy, M., Lytle, S., Fulchiero, E., Aebi, M. E., Adeleye, O., & Sajatovic, M. (2019). A systematic review of quantitative EEG as a possible biomarker in child psychiatric disorders. *Psychiatry Research, 279*, 331–344. https://doi.org/10.1016/j.psychres.2019.07.004

Medaglia, J. D., Lynall, M.-E., & Bassett, D. S. (2015). Cognitive network neuroscience. *Journal of Cognitive Neuroscience, 27*(8), 1471–1491. https://doi.org/10.1162/jocn_a_00810

Michel, C. M., & Murray, M. M. (2012). Towards the utilization of EEG as a brain imaging tool. *NeuroImage, 61*(2), 371–385. https://doi.org/10.1016/j.neuroimage.2011.12.039

Niedermeyer, E., & Lopes da Silva, F. H. (2005). *Electroencephalography: Basic principles, clinical applications, and related fields* (5th ed.). Lippincott Williams & Wilkins.

Northoff, G., & Tumati, S. (2019). "Average is good, extremes are bad" – Non-linear inverted U-shaped relationship between neural mechanisms and functionality of mental features. *Neuroscience & Biobehavioral Reviews, 104*, 11–25. https://doi.org/10.1016/j.neubiorev.2019.06.030

Nunez, P. L., & Srinivasan, R. (2006). A theoretical basis for standing and traveling brain waves measured with human EEG with implications for an integrated consciousness. *Clinical Neurophysiology, 117*(11), 2424–2435. https://doi.org/10.1016/j.clinph.2006.06.754

Pérez-Elvira, R., Carrobles, J., López Bote, D., & Oltra-Cucarella, J. (2019). Efficacy of live z-score neurofeedback training for chronic insomnia: A single-case study. *NeuroRegulation*, *6*(2), 93–101. https://doi.org/10.15540/nr.6.2.93

Pérez-Elvira, R., & Jiménez Gómez, A. (2020). sLORETA neurofeedback in fibromyalgia. *Neuroscience Research Notes, 3*(1), 1–10. https://doi.org/10.31117/neuroscirn.v3i1.40

Pérez-Elvira, R., Oltra-Cucarella, J., & Carrobles, J. (2020). Comparing live z-score training and theta/beta protocol to reduce theta-to-beta ratio: A pilot study. *NeuroRegulation, 7*(2), 58–63. https://doi.org/10.15540/nr.7.2.58

Pérez-Elvira, R., Oltra-Cucarella, J., & Carrobles, J. A. (2021). Effects of quantitative electroencephalogram normalization using 4-channel live z-score training neurofeedback for children with learning disabilities: Preliminary data. *Behavioral Psychology/Psicología Conductual, 29*(1), 191–206. https://doi.org/10.51668/bp.8321110n

Pokorny, L., Biermann, L., Breitinger, E., Jarczok, T. A., Wagner, D., Vöckel, J., & Bender, S. (2024). Young adults with anxiety disorders show reduced inhibition in the dorsolateral prefrontal cortex at higher trait anxiety levels: A TMS-EEG study. *Depression and Anxiety, 2024*, Article 2758522. https://doi.org/10.1155/2024/2758522

Rubinov, M., & Sporns, O. (2010). Complex network measures of brain connectivity: Uses and interpretations. *NeuroImage, 52*(3), 1059–1069. https://doi.org/10.1016/j.neuroimage.2009.10.003

Sanz, J., & García-Vera, M. P. (2013). Rendimiento diagnóstico y estructura factorial del Inventario para la Depresión de Beck–Segunda edición (BDI-II) en pacientes españoles con trastornos psicológicos [Diagnostic performance and factorial structure of the Beck Depression Inventory–Second edition (BDI-II)]. *Anales de Psicología, 29*(1), 66–75. https://doi.org/10.6018/analesps.29.1.130532

Sanz, J., Perdigó, L. A., & Vázquez, C. (2003). Adaptación española del Inventario para la depresión de Beck-II (BDI-II): 2. Propiedades psicométricas en población general [The Spanish adaptation of Beck's Depression Inventory-II (BDI-II): 2. Psychometric properties in the general population]. *Clínica y Salud, 14*(3), 249–280.

Sateia, M. J. (2014). International classification of sleep disorders-third edition. *Chest, 146*(5), 1387–1394. https://doi.org/10.1378/chest.14-0970

Schomer, D. L., & Lopes da Silva, F. H. (Eds.). (2017). *Niedermeyer's electroencephalography* (Vol. 1). Oxford University Press. https://doi.org/10.1093/med/9780190228484.001.0001

Shahid, A., Wilkinson, K., Marcu, S., & Shapiro, C. M. (2011). Athens Insomnia Scale (AIS). In A. Shahid, K. Wilkinson, S. Marcu, & C. M. Shapiro (Eds.), *STOP, THAT and one hundred other sleep scales* (pp. 53–54). Springer New York. https://doi.org/10.1007/978-1-4419-9893-4_5

Sitaram, R., Ros, T., Stoeckel, L., Haller, S., Scharnowski, F., Lewis-Peacock, J., Weiskopf, N., Blefari, M. L., Rana, M., Oblak, E., Birbaumer, N., & Sulzer, J. (2017). Closed-loop brain training: The science of neurofeedback. *Nature Reviews Neuroscience, 18*(2), 86–100. https://doi.org/10.1038/nrn.2016.164

Soldatos, C. R., Dikeos, D. G., & Paparrigopoulos, T. J. (2000). Athens insomnia scale: Validation of an instrument based on ICD-10 criteria. *Journal of Psychosomatic Research, 48*(6), 555–560. https://doi.org/10.1016/S0022-3999(00)00095-7

Soldatos, C. R., Dikeos, D. G., & Paparrigopoulos, T. J. (2003). The diagnostic validity of the Athens insomnia scale. *Journal of Psychosomatic Research, 55*(3), 263–267. https://doi.org/10.1016/S0022-3999(02)00604-9

Storey, J. D. (2002). A direct approach to false discovery rates. *Journal of the Royal Statistical Society Series B: Statistical Methodology, 64*(3), 479–498. https://doi.org/10.1111/1467-9868.00346

Sugarman, M. A., Loree, A. M., Baltes, B. B., Grekin, E. R., & Kirsch, I. (2014). The efficacy of paroxetine and placebo in treating anxiety and depression: A meta-analysis of change on the Hamilton rating scales. *PLoS ONE, 9*(8), Article e106337. https://doi.org/10.1371/journal.pone.0106337

Sürmeli, T., & Ertem, A. (2011). Obsessive compulsive disorder and the efficacy of qEEG-guided neurofeedback treatment: A case series. *Clinical EEG and Neuroscience, 42*(3), 195–201. https://doi.org/10.1177/155005941104200310

Tas, C., Cebi, M., Tan, O., Hızlı-Sayar, G., Tarhan, N., & Brown, E. C. (2015). EEG power, cordance and coherence differences between unipolar and bipolar depression. *Journal of Affective Disorders, 172*, 184–190. https://doi.org/10.1016/j.jad.2014.10.001

Teplan, M. (2002). Fundamentals of EEG measurement. *Measurement Science Review, 2*(2), 1–11. https://www.measurement.sk/2002/S2/Teplan.pdf

Thatcher, R. W. (2016). *Handbook of quantitative electroencephalography and EEG biofeedback* (2nd ed.). Anipublishing.

Thatcher, R. W. (2021). *NeuroGuide manual*. Applied Neuroscience, Inc.

The Pandas Development Team. (2024). *Pandas-dev/pandas: Pandas* (Versión v2.2.3) [Software]. Zenodo. https://doi.org/10.5281/ZENODO.3509134

Thibodeau, R., Jorgensen, R. S., & Kim, S. (2006). Depression, anxiety, and resting frontal EEG asymmetry: A meta-analytic review. *Journal of Abnormal Psychology, 115*(4), 715–729. https://doi.org/10.1037/0021-843X.115.4.715

Thompson, E. (2015). Hamilton rating scale for anxiety (HAM-A). *Occupational Medicine, 65*(7), 601. https://doi.org/10.1093/occmed/kqv054

Videbech, P. (2000). PET measurements of brain glucose metabolism and blood flow in major depressive disorder: A critical review. *Acta Psychiatrica Scandinavica, 101*(1), 11–20. https://doi.org/10.1034/j.1600-0447.2000.101001011.x

Virtanen, P., Gommers, R., Oliphant, T. E., Haberland, M., Reddy, T., Cournapeau, D., Burovski, E., Peterson, P., Weckesser, W., Bright, J., Van Der Walt, S. J., Brett, M., Wilson, J., Millman, K. J., Mayorov, N., Nelson, A. R. J., Jones, E., Kern, R., Larson, E., … Vázquez-Baeza, Y. (2020). SciPy 1.0: Fundamental algorithms for scientific computing in Python. *Nature Methods, 17*(3), 261–272. https://doi.org/10.1038/s41592-019-0686-2

Walker, J. (2005). Neurofeedback treatment of epilepsy. *Child and Adolescent Psychiatric Clinics of North America, 14*(1), 163–176. https://doi.org/10.1016/j.chc.2004.07.009

Wascher, E., Schneider, D., Gajewski, P. D., & Getzmann, S. (2024). *Resting-state EEG data before and after cognitive activity across the adult lifespan and a 5-year follow-up* [Dataset]. Openneuro. https://doi.org/10.18112/OPENNEURO.DS005385.V1.0.2

Wutzl, B., Leibnitz, K., & Murata, M. (2024). An analysis of the correlation between the asymmetry of different EEG-sensor locations in diverse frequency bands and short-term subjective well-being changes. *Brain Sciences, 14*(3), Article 267. https://doi.org/10.3390/brainsci14030267

Received: May 26, 2025
Accepted: July 8, 2025
Published: March 31, 2026

NeuroRegulation

ISNR INTERNATIONAL SOCIETY FOR NEUROREGULATION & RESEARCH

Decoding Self-Regulation in Substance Use Disorders: Machine Learning and LORETA Neurofeedback at Precuneus

Rex L. Cannon[*]

Currents, Knoxville, Tennessee, USA

Abstract

Substance use disorders (SUD) remain among the most treatment-resistant conditions, particularly in incarcerated populations. Despite decades of neuropsychological models, few approaches capture the dynamic, network-level self-regulation deficits observed in SUD. In this study, 63 incarcerated individuals completed 20 sessions of LORETA neurofeedback targeting alpha (8–13 Hz) at the left precuneus. Pre–post EEG current source density (CSD) and Personality Assessment Inventory (PAI) scores were analyzed. A Random Forest classifier was trained on spectral CSD features and behavioral deltas, with Shapley Additive Explanation (SHAP) values used to interpret model contributions. Results showed significant alpha increases at the trained ROI, accompanied by posterior-to-frontal energy redistribution and functional asymmetry. Notably, both alpha synchronization and desynchronization predicted behavioral improvement, with an overall PAI effect size of d = 0.85. Regression and PCA confirmed directional reorganization and subgroup differentiation. Cohen's d analysis revealed frequency-specific effects in alpha and low beta bands. Machine learning (ML) revealed that changes in posterior and frontal regions of interest (ROI) were differentially predictive of treatment response, and Reliable Change Index (RCI) identified responders with physiological and behavioral concordance. These findings challenge static trait-based models of addiction and suggest that rhythmic neurofeedback and ML interpretation can uncover emergent regulatory subtypes. This work proposes a shift from amplitude-based training to network-informed modulation as a foundation for scalable, individualized SUD interventions.

Keywords: EEG; neurofeedback; machine learning; artificial intelligence; learning; substance use disorders

Citation: Cannon, R. L. (2026). Decoding self-regulation in substance use disorders: Machine learning and LORETA neurofeedback at precuneus. *NeuroRegulation, 13*(1), 91–116. https://doi.org/10.15540/nr.13.1.91

***Address correspondence to**: Rex L. Cannon, PhD, BCN, Currents, LLC, 214 South Peters Rd., Ste 102, Knoxville, TN 37923, USA. Email: rcannonphd@gmail.com

Edited by:
Randall Lyle, PhD, Mount Mercy University, Cedar Rapids, Iowa, USA

Reviewed by:
John Davis, PhD, McMaster University, Hamilton, Ontario, Canada
Tanya Morosoli, MSc: 1) Clínica de Neuropsicología Diagnóstica y Terapéutica, Mexico City, Mexico; 2) PPCR, ECPE, Harvard T. H. Chan School of Public Health, Boston, Massachusetts, USA

Introduction

Substance use disorder (SUD) continues to represent one of the most costly and treatment-resistant conditions in public health, particularly in incarcerated populations (Belenko & Peugh, 2005; Mumola & Karberg, 2006). Despite decades of clinical observation, pseudostandardized treatment protocols, and policy reform, the majority of justice-involved individuals, as well as general populations in treatment settings for SUD experience high relapse rates and recidivism (Mericle et al., 2010). These outcomes suggest that our models of addiction, and especially our attempts to intervene, may be built on fundamentally incomplete understanding of brain function.

The prevailing neuropsychological models of addiction rely heavily on correlational designs, linear assumptions, and aggregate behavioral markers. Cognitive and affective dysfunctions are described primarily as trait-based deficits, to be managed or compensated for through pharmacology or behavioral methods. In more recent years, trauma

has been posited as a causative agent of addictive behaviors. Yet these models often fail to account for the dynamism of the human brain as a self-organizing system (Friston, 2010), and they offer little explanatory power for the variability observed in real-world treatment outcomes. The problem is not merely one of statistical power or sample size; it is a conceptual failure to understand the brain as a dynamic, temporally structured, and context-responsive network. In this paper, we propose a fundamentally different approach, one that integrates EEG-based current source density (CSD), machine learning (ML), and nonlinear dynamics, to uncover a replicable neurophenotype of self-regulation in incarcerated individuals with SUD.

The historical dominance of null hypothesis significance testing (NHST) in psychology and neuroscience has inadvertently constrained discovery. Most clinical studies have been bound by the $p < .05$ rule, which restricts interpretation to predefined relationships and excludes high-dimensional interactions between brain regions, frequency bands, and learning mechanisms (Cannon, 2009; Gigerenzer, 2004). This has created an illusion of empirical rigor while simultaneously filtering out critical insights that emerge from nonlinear, network-level behavior (Bassett & Sporns, 2017). As a result, the past 50 years of neuroscience research has produced thousands of "confirmed" findings, but little in the way of real predictive power for who will benefit from which interventions—or why. Although, the data in this paper has met the typical $p < .05$ rule in pre and post neurophysiological, psychometric and regression matrices, as well as rearrest rates (Cannon et al., 2025), questions remain regarding how this translates to self-regulating networks and interactions between frequencies, regions of interest (ROI) and behavioral states. ML and artificial intelligence (AI) may be methods to discover these unknowns and inspire new directions of study.

Electroencephalographic rhythms reflect more than background activity; they are intrinsic signals of regulatory processing in the central nervous system. Among these, theta (4–8 Hz) and alpha (8–13 Hz) oscillations have long been linked to core learning and self-regulatory functions (Başar et al., 2001; Klimesch, 1999). Theta is widely understood to support encoding, working memory, and attentional engagement, particularly during task-related learning and motivational conflict (Cavanagh & Frank, 2014; Mitchell et al., 2008). Meanwhile, alpha oscillations regulate cortical inhibition, sensory gating, and the timing of attentional shifts, acting as a control signal for prioritizing information streams (Jensen & Mazaheri, 2010).

Importantly, these rhythms are not confined to task states. In both resting-state and default mode network (DMN) configurations, alpha and theta jointly coordinate internally-focused processing, including emotional regulation, autobiographical memory, and self-referential thought (Knyazev, 2013; Scheeringa et al., 2008). Alterations in either rhythm have been observed across a range of psychiatric conditions, including depression, anxiety, attention-deficit/hyperactivity disorder (ADHD), and SUD (Bazanova & Vernon, 2014). In particular, disrupted theta–alpha interactions may indicate a failure to integrate affective and cognitive control mechanisms, leaving individuals vulnerable to impulsive decision-making, poor error monitoring, and dysregulated emotion.

Asymmetries in alpha and theta power across hemispheres further suggest specialized vulnerabilities in affective and regulatory processing. Left frontal regions, particularly in the alpha band, have been repeatedly implicated in the neural basis of mood, motivation, and self-directed action. Reduced alpha power in the left hemisphere (reflecting increased cortical activation) is commonly associated with approach-related tendencies, impulsivity, and risk-taking behaviors, whereas increased left alpha (relative hypoactivity) has been linked to depression, anhedonia, and withdrawal (Coan & Allen, 2004; Davidson, 2004). These asymmetries may converge with SUD pathways through mechanisms shaped by trauma, affective blunting, social disconnection, or disrupted neurodevelopment. Of particular concern is the potential compounding effect of prenatal drug exposure (PDE), which may alter the establishment of these frontal-limbic asymmetries early in life, setting the stage for later difficulties in mood regulation, attentional shifting, and behavioral inhibition. Future studies should directly examine whether alpha and theta asymmetry patterns in PDE-affected children parallel those found in SUD populations, offering a possible early biomarker of self-regulatory vulnerability (Koponen, et al., 2020).

Together, these rhythmic patterns participate in the oscillatory infrastructure of self-regulation. Our approach to neurofeedback and its ML-based analysis, is grounded in the idea that meaningful change must occur within these rhythms, not apart

from them. They are not background noise, but the signal of the self in time.

Alpha Regulation and the Central Role of BA 19

Among the most studied rhythms in electroencephalography (EEG), the alpha band (8–13 Hz) has consistently emerged as a key indicator of cognitive idling, attention, and internally directed states (Barry et al., 2007; Klimesch, 1999). However, newer models suggest that alpha power, and especially its modulation, is far more than a passive index. Alpha rhythm serves as an active gatekeeper of information flow, particularly in posterior midline regions where the precuneus, posterior cingulate, and adjacent visual-parietal cortices coordinate internal simulation, self-referential thought, and attentional switching (Buckner et al., 2008; Cavanna & Trimble, 2006) as well as its interactions and involvement with the default network of the brain.

Within this network, Brodmann area 19 (BA 19), located in the medial occipital cortex, serves as a relay between visual-spatial processing and self-representational systems, especially under conditions requiring inhibitory control or internal reflection (Gusnard & Raichle, 2001). Prior work by Cannon (2009), Cannon et al. (2012, 2014, 2025), and Baldwin et al. (2011) demonstrated that this region shows significant modulation during LORETA neurofeedback (LNFB) aimed at enhancing self-regulation. Furthermore, alpha activity in BA 19 is functionally tied to posterior cingulate cortex (PCC) dynamics and medial prefrontal engagement, forming a posterior-frontal loop that we argue is essential for adaptive regulation and may be deficient in SUD populations.

Although traditionally mapped as part of the medial occipital lobe and associated with visual-spatial processing, the precuneus, especially its ventral and posterior segments, is now understood to be a key integrative hub in the DMN and a primary contributor to episodic memory, self-referential processing, and contextual awareness (Cavanna & Trimble, 2006; Leech & Sharp, 2014). Its anatomical and functional position allows it to relay and integrate sensory, cognitive, and affective information from both posterior and frontal structures. The precuneus maintains strong reciprocal connections with the PCC, which monitors self-related stimuli; the medial prefrontal cortex (mPFC), which is closely involved with value attribution, mentalizing, and emotional decision-making; the hippocampus, which supports episodic encoding; and lateral temporal and parietal regions involved in perceptual integration and social narrative continuity.

This connectivity supports what might be described as the episodic context of self, a scene-setting function that locates the self in time, space, and social position, even in the absence of external tasks. Disruptions in this region have been observed in conditions involving depersonalization, trauma, psychosis, and SUD, often presenting with unstable self-awareness, memory and identity fragmentation, or emotional disconnection (Brewer et al., 2013; Cannon et al., 2004; Northoff et al., 2006). In the context of SUD, these are not peripheral symptoms; they are core deficits. Individuals frequently experience an unstable, impoverished and fragmented self-concept, difficulty linking emotional events to behavior, and diminished access to autobiographical continuity. The precuneus may serve as a critical neural substrate for restoring a stabilized and embodied sense of self, particularly when targeted by interventions that operate within its native rhythmic domain.

Within this framework, targeting alpha modulation in the left precuneus via neurofeedback is not merely an intervention on the visual cortex, it is an intentional engagement of the brain's energetic signature of the self. This region supports contextual integration, autobiographical memory, and the temporal scaffolding of awareness. Rhythmic entrainment here may allow for reorganization of attentional control and internal coherence, offering a rare opportunity to modify the physiological substrates of self-regulation at their core. The rationale for selecting the precuneus as a neurofeedback target in previous studies with SUD subjects was twofold: first, its extensive involvement across psychiatric disorders and self-referential disturbances; and second, a more fundamental hypothesis that the DMN anchors the experience of "self." As this network rose to scientific prominence in the late 2000s, investigations of SUD in the present author's laboratory returned to a simple question: What is more default than the self? If the self holds no regulatory or reward value, then no external reinforcement will suffice. While intuitive rather than theoretical, this premise became the catalyst for a decade of work. Importantly, this line of reasoning may hold relevance for individuals with early adversity or PDE, where disruptions to the formation of self-regulatory and default network architecture have been documented well into adolescence and early adulthood (Kelley et al., 2019; Koponen et al., 2020).

In the current dataset, described below, the BA 19/precuneus pathway within the DMN was trained directly using LNFB, targeting a three-voxel cluster centered at Talairach coordinates (−31, −81, 22), corresponding to the left ventral precuneus (Cannon et al., 2014). The left precuneus was selected as the primary training target based on extensive research demonstrating its role in self-referential processing, episodic and perceptual encoding of experience, and its dense connectivity with angular and Wernicke's areas within the left parietal receptive language network, as well as its broader integration within the DMN (Buckner et al., 2008; Northoff et al., 2006).

In contrast, the right precuneus has been implicated in different functional contexts, including attentional shifts and visuospatial processing. As a precaution, particularly in populations with SUD, PTSD, and related clinical issues, we targeted the left precuneus to leverage its well-characterized role in internal mentation and language-linked integration. This choice was further supported by early alpha/theta neurofeedback work by Peniston and Kulkosky (1989), who trained at electrode site O1 and observed significant changes on Minnesota Multiphasic Personality Inventory (MMPI) scales, as well as by pilot training data demonstrating consistent modulation patterns across CSD measures, Personality Assessment Inventory (PAI) scores, and other behavioral indices when the left precuneus was trained.

What Linear Models Leave Lacking, and What Machine Learning Reveals

Traditional linear regression models assume independent, additive contributions of predictors toward a singular outcome. While these methods have served psychology and neuroscience for decades, they are inherently mismatched to the brain's recursive, interacting, and nonstationary nature (Friston, 2010). In reality, frequencies do not act in isolation, nor do regions contribute independently; rather, the brain operates as a system of rhythmic interactions that reconfigure across time and state. For neurofeedback data, especially with spatially resolved CSD features, these interactions matter far more than any single coefficient.

This is where ML offers a profound shift. Rather than testing predefined hypotheses, ML allows the data itself to reveal predictive structure. Models such as Random Forests (Breiman, 2001) are especially suited to EEG-CSD data due to their ability to handle high-dimensional, collinear, and nonlinear feature spaces. In our approach, CSD values across all ROI and alpha subbands have been used as inputs to train a classifier that could distinguish pre- from posttraining patterns or predict reliable change on an individual basis.

To interpret these models, we employed Shapley Additive Explanation (SHAP) values, a modern implementation of cooperative game theory that attributes importance scores to each input feature (Lundberg & Lee, 2017). SHAP identifies not only which regions and frequencies contribute to model predictions but also the strength and direction of these contributions. This enables us to "open the black box" of ML and clarify which aspects of neurofeedback training meaningfully drive self-regulation (Cannon, 2025).

Notably, these analytic strategies build on methods the author has used long before "machine learning" became a standard framework. Early applications included differentiating networks of executive attention in the anterior cingulate gyrus and dorsolateral prefrontal cortices (Cannon, 2009); dissertation work examining EEG sources associated with self-referential processes (Cannon, 2009); analyses of ROI-level CSD and network dynamics associated with attention task performance in ADHD (Cannon et al., 2014); and investigations of white matter connectivity disruptions between the posterior cingulate and hippocampi in Alzheimer's disease using diffusion tensor imaging (DTI) to probe episodic memory impairments (Zhou et al., 2008).

At that time, advanced statistical techniques such as logistic regression, ROC analyses, and partial correlations were employed to isolate network-level relationships, but computational and visualization workflows were slow and largely manual, often requiring image construction in PowerPoint. Contemporary SHAP-based interpretability dramatically accelerates and clarifies these kinds of multivariate network insights, allowing us to model learning dynamics at scale with far greater precision. Together, SHAP and network modeling offer a generative lens: we are not confirming theories but generating new ones from real-world change data. This is what neuroscience has long lacked, not stronger *p*-values, but stronger tools for listening to the brain as it adapts and learns.

Toward a Model of Rhythmic Self-Regulation: The Cycle of Error

Alpha activity, particularly in the posterior midline, is not simply a marker of attention or "rest." It is a

rhythmic expression of the self-regulatory system in action with an energetic signature indicating where awareness is focused, how inhibition is organized, and whether internal versus external information is being prioritized (Jensen & Mazaheri, 2010). Strikingly, few models of dopaminergic function acknowledge its role in stillness or motor inhibition, despite dopamine's well-established involvement in movement regulation (Grace, 1991). The emphasis on dopamine as a reward or drive signal has overshadowed its fundamental role in modulating motor readiness, inhibition, and behavioral gating. In this light, our approach to neurofeedback is not merely about increasing alpha, but about training the brain to flexibly shift and regulate its internal dynamics across changing contexts.

Building on previous work (Cannon et al., 2012, 2014), we conceptualize this process as a recursive cycle of error: Self-regulation often fails not because of a single discrete deficit, but through a repeating loop in which perceptual, affective, and behavioral responses mutually reinforce dysregulated states. For justice-involved individuals with SUD, this cycle of error is frequently neurodevelopmental in origin, shaped by factors such as early trauma, prenatal and perinatal substance exposure, and disrupted attachment experiences (e.g., Cannon, 2025; Cavanna & Trimble, 2006; Northoff et al., 2006). Over time, these repeating patterns become physiologically embedded through chronic enactment, leading to stable but maladaptive rhythmic and network dynamics.

The alpha system, particularly BA 19 and its cortical projections within the posterior DMN, provides a biological foothold for intervention on this repetitive cycle. By modulating rhythmic activity in the left ventral precuneus, it is possible to interrupt episodic redundancy, the brain's tendency to recycle maladaptive perceptual-affective patterns, thereby enabling the development of the scaffolding and experiential encoding necessary for a stable sense of self and improved self-regulation (Buckner et al., 2008; Cannon, 2009; Cannon et al., 2025; Zhou et al., 2008).

By identifying and targeting the energetic patterns that underlie impairments or dysregulated self-regulation, we propose that neural rhythms can be reshaped toward stability. Our use of ML is central to this goal: rather than manually categorizing responders or cherry-picking outcomes, we train models to identify the structure of learning itself. SHAP values help reveal which regions participate most meaningfully. Also crucial to our work is the use of Principal Components Analysis (PCA), described below, which shows how group-level change emerges, and Reliable Change Index (RCI) which quantifies whether these shifts are clinically and statistically meaningful on the individual level (Jacobson & Truax, 1991).

Importantly, prior observations and theoretical considerations suggest that increased alpha activity is not uniformly beneficial. In some individuals, reliable alpha desynchronization has been associated with positive behavioral change, reflecting the possibility that neural downregulation and disengagement from maladaptive patterns may be a necessary prelude to stabilization. If so, ML methods may help clarify these response profiles, revealing when and for whom up- or downregulation of rhythmic activity supports adaptive self-regulation. Such flexibility challenges earlier neurofeedback models that often treated "more power is better" as an implicit assumption, rather than a tested principle.

Study Aims

In this paper, we present a dataset of 63 incarcerated individuals with SUD who completed LNFB training at the left precuneus (BA 19), alongside pre–post PAI measures and voxel-wise CSD data (Cannon et al., 2025). We use Random Forests to model self-regulation outcomes and SHAP values to interpret model dynamics. We present new network evidence of posterior-to-frontal alpha redistribution and confirm reliable changes through both RCI classification and PCA.

Our overarching aim is to demonstrate that ML-driven neurofeedback can (a) uncover meaningful regulatory subtypes, (b) detect both synchronization and desynchronization learning profiles, and (c) support a dynamic model of rhythmic self-regulation in vulnerable clinical populations. Crucially, these approaches move beyond linear pre–post comparisons and toward modeling network-level change, capturing the distributed, nonlinear, and state-dependent dynamics of brain adaptation (Sitaram et al., 2017). We argue that ML and AI are not only valuable for analyzing LORETA-based protocols but essential for advancing the entire field of neurofeedback. Surface-level protocols such as SMR or alpha-theta training have long demonstrated behavioral and clinical impact yet lack corresponding cortical models that explain how or where these changes occur (Haugg et al., 2020). While MRI and EEG studies have revealed connectivity changes following surface neurofeedback, these findings remain difficult to translate into individualized

treatment models. Yet in much contemporary brain research, even when statistically significant group effects are reported, we rarely ask a critical question: What magnitude of power or connectivity change actually constitutes a meaningful effect on system-wide or behavioral outcomes? This gap has become especially urgent in light of the broader replication crisis, which has shown that many statistically significant findings fail to replicate or translate into real-world contexts (Ioannidis, 2018; Open Science Collaboration, 2015).

Our approach, employing individualized neurofeedback training, CSD metrics, and ML, is designed to help bridge this gap, shifting emphasis from abstract statistical significance toward measurable, reproducible neural change that corresponds with behavioral outcomes.

Without robust tools to decode the functional architecture behind training, much of neurofeedback has remained protocol-driven rather than network-driven. ML and AI now offer the opportunity to reverse this, allowing us to detect, predict, and ultimately prescribe training protocols based on meaningful neurophysiological features. This study represents one step in that direction, anchoring protocol design in rhythm, region, and recovery, not just in surface targets or statistical significance.

Methods

Participants

This case grouping includes 63 individuals (19 female) with a mean age of 37.11 (*SD* = 9.69), 58 of whom were right-handed. The initial participant count was 110, with 64.5% completing the protocol and 35.5% dropping out. Only those who completed all sessions, as well as post-LNFB baseline and PAI measures, were included in the final analysis. Inclusion criteria included a history of substance-related legal offenses and willingness to participate in a 20-session neurofeedback training protocol. All participants completed pre- and posttraining psychometrics and EEG recordings from (Cannon et al., 2025).

Neurofeedback Protocol

Participants underwent 20 consecutive sessions of alpha uptraining, and their brain activity was measured via CSD extracted from LORETA source space. CSD offers an anatomically constrained estimate of energy dynamics in microamps per square centimeter (μA/cm²), allowing for precise, frequency-specific insights at both the voxel and region level (Pascual-Marqui et al., 1994, 2002). LNFB training sessions were composed of six 5-min rounds and were conducted five times per week for 20 consecutive weekdays. For each session ~3-min presession eyes-opened baselines were collected. Each session required ~50 min to complete. In the preliminary session, the participants were instructed to control tongue and eye movements, blinks, and muscle activity in forehead, neck, and jaws. This enabled the subjects to minimize the production of extracranial artifacts, in electromyography (EMG), electro-oculogram (EOG), etc., during the sessions. During the preliminary session shaping was induced to set thresholds such that each participant could meet the reward criteria of 20 points per minute at a minimum (e.g., generate the desired response at a minimal rate), and participants were informed of the inhibitory and reward aspects of the training. Standardized thresholds listed below were then set and maintained for each participant (Cannon, 2014; Cannon et al., 2014, Cannon et al., 2025). Participants were able to choose from a selection of 25 games for the sessions. The participants were provided visual and auditory feedback, and points were achieved when they were able to simultaneously increase alpha CSD (8–13 Hz) at the, left precuneus while minimizing EMG (35–55 Hz) and EOG (1–3 Hz) in linear combinations of channels: EMG: T3, T4, T5, T6, O1, and O2; EOG: FP1, FP2, F3, F4, F7, and F8. These criteria had to be maintained for .75 s to achieve 1 point. The auditory stimuli provided feedback with a pleasant tone when the criteria were met. Similarly, the visual stimuli were activated when the criteria were met (e.g., a car or a spaceship driving faster and straighter). Alternatively, slower speed of the car, driving in the wrong lane, or the spaceship flying slowly and crookedly were seen when the criteria were not met (Deymed Diagnostics). The score for meeting the criteria was also seen by the participants in a small window of the game screen. Additionally, the visual stimuli contained a signal for rewards and inhibits relative to a threshold level, and a bar graph illustrating reward, EOG and EMG. After completing at least 10 sessions without missing any sessions without a valid excuse (illness, court, etc.), inmates were permitted to use DVD movies for the A/V feedback mechanism. The DVD covaries with the inhibit and reward features by the sound diminishing or the screen being blurred or noise added when the criteria are not met.

EEG Recording and CSD Extraction

EEG was recorded using a 21-channel gel-based cap (10–20 system) with a sampling rate of 256 Hz. Channels included Fpz, Fp1/2, F3/4, C3/4, P3/4, O1/2, and midline sites (Fz, Cz, Pz). Reference was

set to linked ears, and impedance was maintained below 15 kΩ.

In contrast with studies utilizing traditional neurofeedback, the whole-head EEG data with 19 electrodes were continuously stored during the sessions. In addition, the participants in this study were encouraged to keep a written journal of sleep patterns, mood, overall cognitive and attention processes, and to note specifically any odd occurrences. EEG data for all participants were analyzed at premeasures and across each session with NeuroGuide (Applied Neuroscience, Tampa, FL) and contrasted to normative samples in the lifespan database to examine power metrics and connectivity across sessions during training However, for pre- and postcontrasts NeuroGuide was employed for the automatic artifact identification procedures that were utilized for gross artifact contamination, then EEG data were converted to Lexicor format and edited with EureKa!3 software by NovaTech EEG (Mesa, AZ). All EEG data were processed with particular attention given to the frontal and temporal leads. All episodic blinks, eye movements, teeth clenching, jaw tension, body movements, and possible electrocardiogram (EKG) were removed from the EEG stream by visual inspection. For all included sessions, power spectra were computed using fast Fourier transform (FFT) over 75% overlapping 4-s epochs, and log-transformed spectral densities were obtained prior to modeling. The 10 ROI were selected based on prior findings (Cannon, 2009; Cannon et al., 2012) and potential hubs of the self-regulation network. A full list of coordinates and anatomical labels is presented in Table 1. These cross-spectral matrices constitute the input for LORETA estimation in the frequency domain. CSD was then computed using standardized LORETA (Pascual-Marqui, 2002; Pascual-Marqui et al., 1994) at each of 10 predefined cortical ROI. Spectral CSD estimates were averaged within six frequency bands: delta (1–4 Hz), theta (4–8 Hz), alpha1 (8–10 Hz), alpha2 (10–13 Hz), beta1 (13–21 Hz), and beta2 (21–40 Hz). ROI-level averages were used as input features for ML and statistical analysis.

Psychological Assessment

The PAI (Morey, 1991) was administered pre- and posttraining. The PAI is an objective inventory of adult personality characteristics that assesses psychopathological syndromes and provides information relevant for clinical diagnosis, treatment planning, and screening for psychopathology. This assessment contains 344 items that constitute 22 nonoverlapping scales covering the constructs most relevant to a broad-based assessment of mental disorders: four validity scales, 11 clinical scales, five treatment scales, and two interpersonal scales. To facilitate interpretation and to cover the full range of complex clinical constructs, 10 scales contain conceptually derived subscales. The scales (with subscales in parentheses) listed in the table are somatic (conversion, somatization, health concerns); anxiety (cognitive, affective, physiological); anxiety related disorders (obsessive-compulsive, phobias, traumatic stress); depression (cognitive, affective, physiological); mania (activity level, grandiosity, irritability); paranoia (resentment, hypervigilance, persecution); schizophrenia (psychotic experiences, social detachment, thought disorder); borderline features (affective instability, identity problems, negative relations, self-harm); antisocial features (antisocial behaviors, egocentricity,

Table 1

Regions of Interest for Analytics and Machine Learning Procedures

x	*y*	*z*	Region	Label	BA	#
5	0	35	Limbic Lobe	Cingulate Gyrus	BA 24	ROI 9
15	−85	0	Occipital Lobe	Lingual Gyrus	BA 17	ROI 8
40	−5	10	Sub-lobar	Insula	BA 13	ROI 7
25	55	5	Frontal Lobe	Superior Frontal Gyrus	BA 10	ROI 6
−10	−50	30	Parietal Lobe	Precuneus	BA 31	ROI 5
−15	−60	5	Limbic Lobe	Posterior Cingulate	BA 30	ROI 4
−5	0	35	Limbic Lobe	Cingulate Gyrus	BA 24	ROI 3
−15	−85	0	Occipital Lobe	Lingual Gyrus	BA 17	ROI 2
−30	30	35	Frontal Lobe	Middle Frontal Gyrus	BA 9	ROI 1
−25	−75	10	Occipital Lobe	Cuneus	BA 30	ROI 0

Note. In the SHAP images and tables ROI 0 = ROI 1 and ROI 9 = ROI 10.

stimulus-seeking); aggression (aggressive attitude, verbal aggression, physical aggression). Delta scores (post–pre) were computed for all clinical subscales, entered into ML models, and used to interpret state change.

RCI Derivation and Application

To determine whether observed changes in neurophysiological signals following LNFB training represented meaningful effects beyond measurement error, we applied the RCI framework (Jacobson & Truax, 1991). The RCI is a well-established method for distinguishing true change from statistical noise. However, due to the absence of normative CSD baselines in substance-using populations and across specific Brodmann area–defined ROI, standard reliability-adjusted formulas could not be universally applied.

Log-transformed CSD values were used in all RCI computations to normalize amplitude distributions and reduce outlier distortion. Empirical mean and *SD* were calculated per ROI using the pre- and posttraining eyes-opened baseline data for all completers. While normative test–retest databases for CSD remain limited in SUD populations, our choice of internal standardization mirrors recent RCI applications in small-sample biobehavioral research.

Instead, the RCI was derived using empirical means and standard deviations from our study sample, following a simplified but validated approach:

$$RCI = \frac{X_{post} - X_{pre}}{SD_{pre}}$$

Where:

- X_{pre} = log-transformed CSD value at baseline
- X_{post} = log-transformed CSD value posttraining
- SD_{pre} = standard deviation of pretraining values across participants for that ROI

This method is supported by prior research demonstrating high test–retest reliability of log-transformed CSD values. Specifically, Cannon et al. (2012) reported reliability coefficients exceeding .90 for current density at both the precuneus and anterior cingulate cortex over a 30-day interval, confirming the temporal stability of these signals in nonclinical populations. These findings support the use of within-sample variance estimates when external normative data are unavailable.

We adopted a bidirectional threshold of |RCI| > 1.96 |RCI| denoting change at or beyond the 95% confidence interval. This threshold was used to classify participants as “increase responders,” “decrease responders,” or “nonresponders” at each ROI, capturing both synchronization and desynchronization effects across training.

This empirical RCI framework may also offer a generalizable approach for evaluating signal-level change in other neurophysiological or biochemical measures where normative or test–retest data are sparse. By grounding change metrics in sample-derived variance, researchers can apply this method across small-sample or early-phase interventions, including EEG, fMRI, heart rate variability, or inflammatory markers—domains where pre–post comparison is often the most feasible index of treatment response. As such, the present model contributes to a broader push for rigorous, individualized metrics of change in applied neuroscience and biobehavioral research.

Machine Learning Workflow

A Random Forest classifier (Breiman, 2001) was trained to predict reliable alpha change using input features derived from pre- and posttraining CSD values and PAI deltas. Data were preprocessed using Python 3.11 and Scikit-learn v1.4.1. Log-transformed CSD values were computed for 10 ROI at alpha and theta frequencies. Delta PAI scores (post–pre) were included as behavioral features, and RCI group labels were used as binary or multiclass outcomes depending on the model. Model training was conducted in Python using Scikit-learn with default hyperparameters (n_estimators = 100, max_depth = auto). Accuracy and feature importance were evaluated using cross-validation.

SHAP values (Lundberg & Lee, 2017) were used to interpret model output and estimate the relative contribution of each ROI and frequency band. SHAP values were averaged across trees to produce global feature importance scores and visualized via summary plots.

To mitigate overfitting and ensure generalizability, we implemented several key safeguards throughout our ML workflow. First, ROI-level CSD data were log-transformed prior to model input to reduce skew and minimize the influence of outliers or inflated amplitude values. Second, feature dimensionality

was constrained by using region-averaged CSD within specific frequency bands rather than voxel-wise inputs, reducing noise and multicollinearity. Third, we employed a Random Forest classifier, chosen for its resilience to collinearity and capacity for internal feature selection (Breiman, 2001). Fourth, cross-validation was applied across training folds to prevent overfitting and evaluate model stability. Finally, SHAP values were used to interpret feature importance and verify that biologically plausible effects—not artifacts—were driving model predictions. These combined steps provide strong assurance that our findings reflect robust, generalizable signal rather than overfit noise or conflated variance.

Principal Component Analysis (PCA)

To examine clustering and dimensional compression, PCA was applied to the full matrix of alpha band CSD values (pre- and posttraining) across all subjects. The first two principal components (PC1 and PC2) were retained for visualization. Subjects were color-coded based on RCI classification and plotted to examine response-based grouping.

All preprocessing, classification, and visualization code was developed in Python 3.11.8 using open-source packages. Analytic notebooks and deidentified data matrices are available upon request for academic replication. A reproducible pipeline for CSD transformation, RCI classification, and Random Forest modeling is currently being prepared for public release.

Results

CSD Network Patterns and Posterior–Frontal Shift

Posttraining CSD values revealed consistent energy redistribution across posterior and frontal ROI. Figures 2 and 3 show the results for paired contrasts with significant alpha1 and alpha2 increases at the target ROI ($p < .05$), with secondary modulation observed in left anterior cingulate (ROI 3) and midline posterior cingulate (ROI 4) regions. A regression-weighted network diagram (Figure 4) illustrates a posterior to frontal shift in spectral alpha activity, interpreted as enhanced engagement of top-down regulatory networks.

Figure 2. *Deltas for CSD Levels in Posterior/Frontal Regions Linked to Precuneus Training Region.*

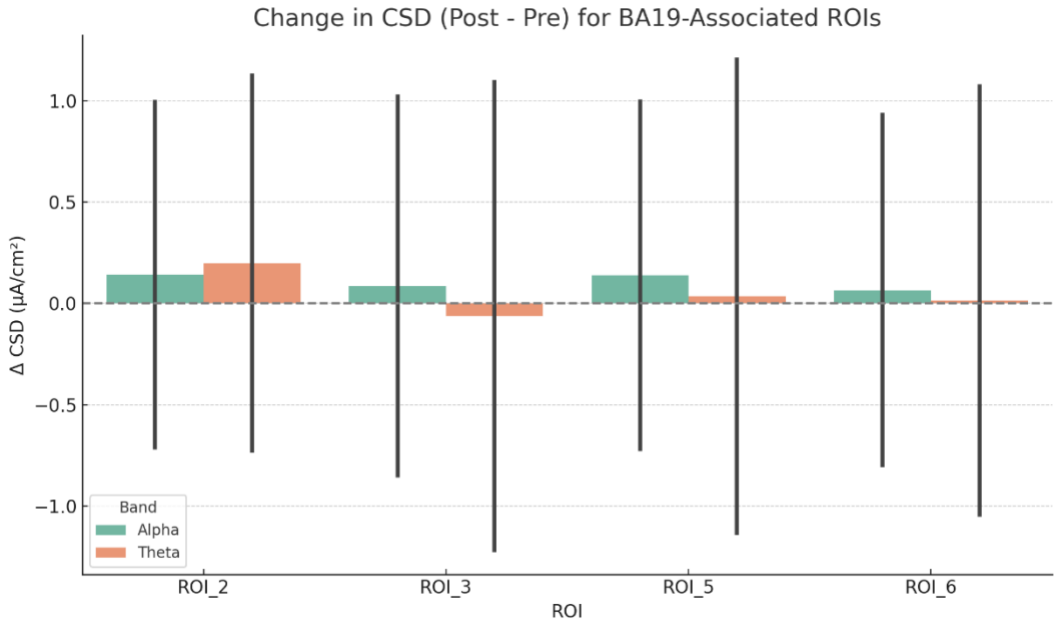

Figure 3. *Deltas for CSD in Frontal Regions Tied to SR and Posterior Regions.*

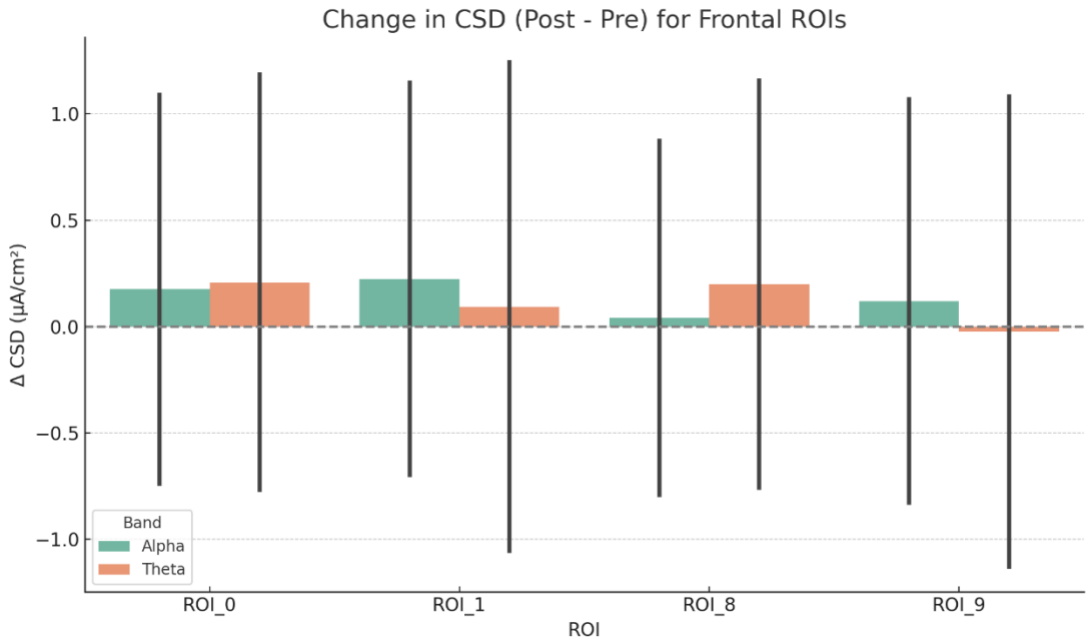

Figure 4. *Directed Posterior → Frontal Network Based on ΔAlpha CSD Regression Paths (N = 63).*

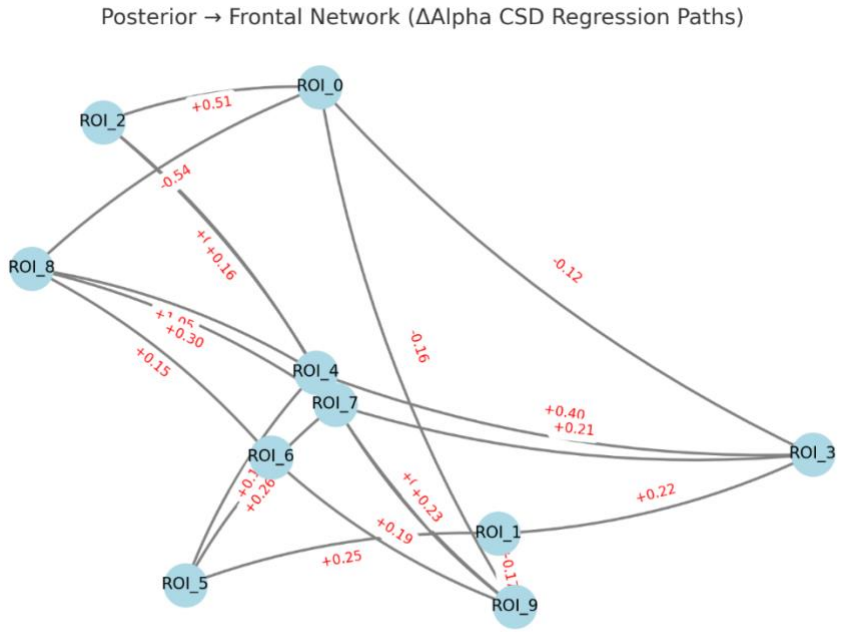

Note. Line sizes indicate significant directional relationships (|β| > 0.10) from posterior to frontal ROI. Node labels represent ROI indices. Edge labels within the figure reflect standardized beta coefficients (Table 2) derived from multiple linear regressions using posterior ROI predictors.

Network-level correlation analysis revealed a structured set of associations between alpha-band CSD shifts and changes in PAI symptom domains (Figure 5). Notably, ROI_4 (Posterior Cingulate) and ROI_2 (Lingual Gyrus) emerged as central hubs, showing multiple strong positive correlations (red) with clinical deltas—especially for somatic complaints, paranoia, and antisocial traits. Negative associations (blue) were more prevalent, consistent with symptom reduction accompanying increased alpha power in key posterior ROI. This pattern further supports the model that alpha synchronization within posterior visual-parietal areas contributes to broad symptom stabilization, particularly within self-perceptual and threat-related domains.

Compared to the alpha-based network, the theta-band model (Figure 6) exhibited a broader and denser matrix of negative associations between neural and clinical change. Posterior cingulate/precuneus (ROI_5) and lingual gyrus (ROI_4) remained active hubs, while ROI_2, a ventral occipital/BA19 contributor, also emerged as highly connected. The majority of associations were negatively signed, suggesting that increased theta synchronization was linked with symptom reductions —especially in scales indexing somatic, depressive, and paranoid ideation. These results imply that theta dynamics may reflect a regulatory substrate, enabling attenuation of maladaptive internal states and ruminative traits.

The composite network (Figure 7) illustrates a convergent and distributed structure linking CSD changes at posterior ROI with improvements across diverse symptom domains. Notably, purple edges (shared alpha and theta) clustered around aggression (agga_d), somatic complaints (somc_d), and perceptual disturbance (sczt_d), confirming that both frequency bands engage shared regulatory circuits. Theta-specific (orange) associations dominated paranoia, mania, and anxiety subscales, while alpha-specific (green) links concentrated around cognitive and interpersonal traits. These patterns support a dual-frequency model of neuroplastic change, with alpha coordinating internal sensory regulation and theta modulating affective-cognitive integration.

Figure 5. *Alpha-Band ROI-to-PAI Delta Network Showing Significant Correlations Between Alpha-Band CSD Changes at Selected ROI and Changes in PAI Symptom Scores (|r| ≥ 0.20).*

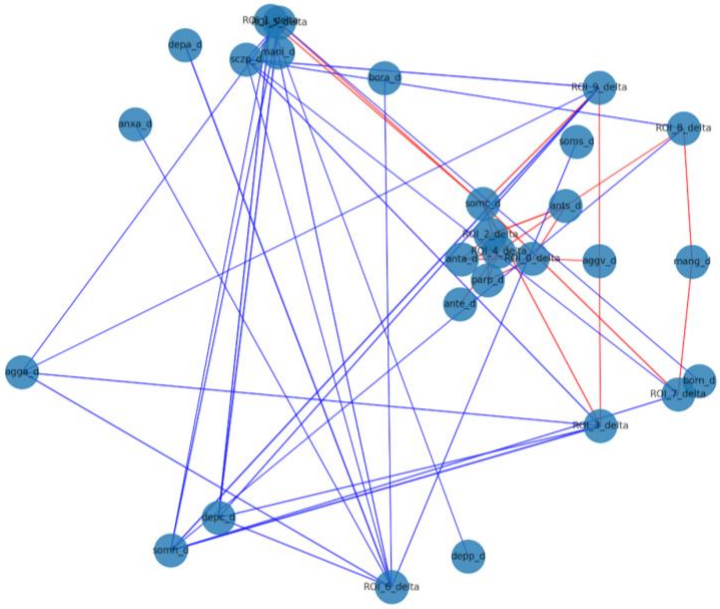

Note. Nodes represent either a PAI subscale delta (e.g., somc_d) or an ROI delta (e.g., ROI_4_delta). Blue edges indicate negative correlations; red edges indicate positive correlations. Edge thickness reflects the strength of association. Central nodes include ROI_2, ROI_4, and somc_d, highlighting convergence between posterior alpha modulation and somatic/cognitive symptom resolution.

Figure 6. *Theta-Band ROI-to-PAI Delta Network Showing Significant Correlations (|r| ≥ 0.20) Between Theta CSD Changes Across ROI and PAI Symptom Change Scores.*

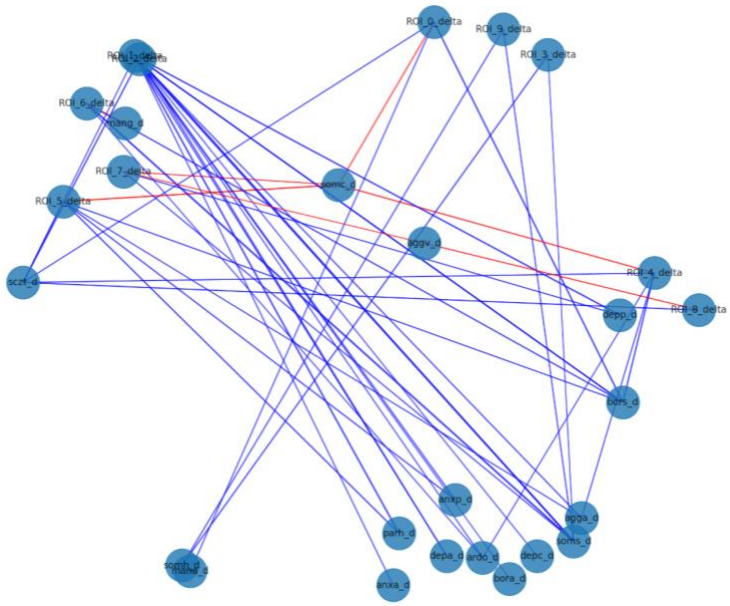

Note. Blue edges represent negative correlations (improvement associated with increased theta CSD); red edges indicate positive correlations. Several posterior ROI (e.g., ROI_4, ROI_5, ROI_0) demonstrate high degree centrality, linking with changes in diverse PAI subscales including aggression, somatic complaints, and depression.

SHAP Interpretation of Predictive Features

SHAP summary values in Figure 4 revealed that posterior (ROI 2, ROI 5) and left frontal (ROI 3) alpha bands contributed most to the model's predictions. Alpha2 (10–13 Hz) in ROI 2 and alpha1 (8–10 Hz) in ROI 3 had the highest positive impact on model output, aligning with the observed functional connectivity pathway. Notably, desynchronization responders showed SHAP profiles with inverse contributions in ROI 4, suggesting differential strategies in regulation. SHAP summary plots were generated using the TreeExplainer module from the SHAP package (v0.41.0), with line size by frequency and ROI for interpretability. Table 2 shows the region, target ROI and beta coefficients for the model. Dependence plots were also used to probe nonlinear effects and ROI–frequency interactions.

Alpha CSD Change and RCI Classification

Because ROI 5 (left ventral precuneus, BA 19) and frontal midline regions, primarily anterior cingulate cortex (ACC; BA 24/32) and mPFC (BA 10/11), are key nodes within the self-regulation network, we classified participants based on reliable alpha modulation (|RCI| > 1.96) observed at these posterior and frontal sites. Participants were categorized as dual responders when reliable modulation occurred at both ROI 5 and the frontal ROI, frontal-only or precuneus-only responders when change was isolated to one region, and nonresponders when neither site met the threshold.

Out of the 63 participants, 21 individuals (33.3%) demonstrated reliable alpha modulation at both the precuneus and frontal ROI, qualifying them as dual responders. Another 10 participants (15.9%) exhibited reliable change only at the frontal ROI, while 8 participants (12.7%) showed reliable modulation exclusively at the trained precuneus site. The remaining 24 participants (38.1%) did not meet the threshold for reliable change at either site and were classified as nonresponders.

Figure 7. *Combined Alpha and Theta Band ROI-to-PAI Delta Network Showing All Correlations ≥ 0.20.*

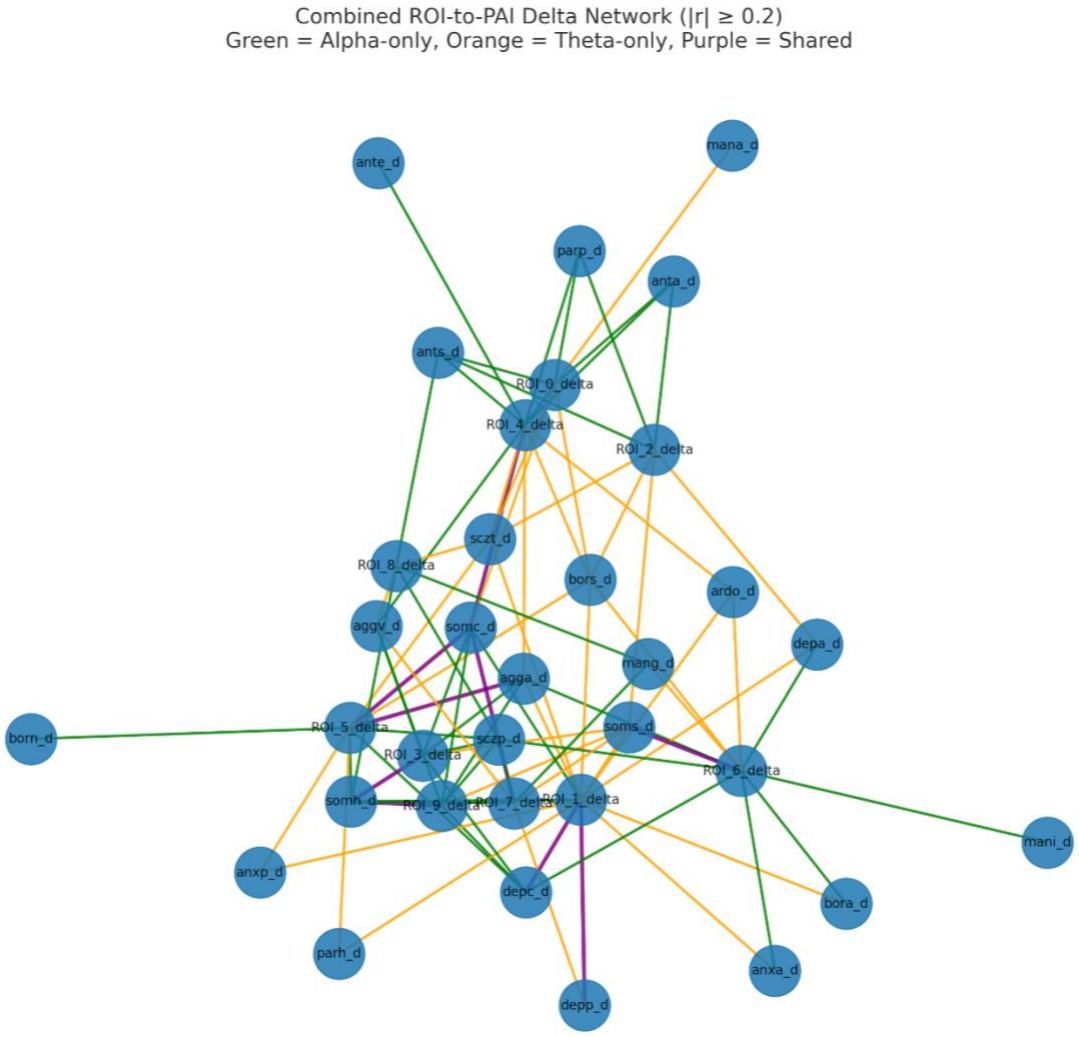

Note. Green edges represent alpha-only associations; orange edges indicate theta-only associations; and purple edges indicate correlations observed in both bands. Nodes represent ROI or PAI symptom delta variables. Shared associations (purple) highlight cross-frequency contributions to key symptom changes, particularly somatic complaints, aggression, and thought disorders.

Table 2

Regression Path Coefficients for Directed Posterior → Frontal ROI Network (ΔAlpha CSD)

Source Region (ROI)	Target Region (ROI)	Standardized Beta
Cuneus (ROI_0)	Cingulate Gyrus BA24 (ROI_3)	−0.12
Lingual Gyrus (ROI_1)	Cingulate Gyrus BA24 (ROI_3)	+0.22
Lingual Gyrus (ROI_4)	Cingulate Gyrus BA24 (ROI_3)	+0.21
Posterior Cingulate (ROI_6)	Cingulate Gyrus BA24 (ROI_5)	+0.19
Precuneus (ROI_7)	Cingulate Gyrus BA24 (ROI_5)	+0.26
Lingual Gyrus (ROI_1)	Insula (ROI_9)	−0.17
Precuneus (ROI_7)	Insula (ROI_9)	+0.25
Cuneus (ROI_0)	Middle Frontal Gyrus (ROI_2)	+0.51
Lingual Gyrus (ROI_4)	Middle Frontal Gyrus (ROI_2)	+0.16
Cuneus (ROI_0)	Superior Frontal Gyrus (ROI_8)	+0.54
Lingual Gyrus (ROI_4)	Superior Frontal Gyrus (ROI_8)	+0.30
Posterior Cingulate (ROI_6)	Superior Frontal Gyrus (ROI_8)	+0.15
Precuneus (ROI_7)	Superior Frontal Gyrus (ROI_8)	+1.05

Note. Standardized beta coefficients for each significant regression path (|β| > 0.10) from posterior to frontal regions of interest (ROI) based on change in alpha band current source density (ΔCSD). ROI codes correspond to the functional-anatomical areas introduced in Table 1.

This distribution reveals that more than 60% of participants demonstrated physiologically meaningful change across one or both targeted regions, with a substantial portion engaging both posterior and frontal self-regulatory structures. These outcomes further support the idea that neurofeedback training at the precuneus initiates broader network-level reorganization. The distribution of response types is presented in Figure 8.

Analysis of PAI delta scores revealed clear and distinct patterns of change across Alpha RCI-defined responder types. Figure 9 illustrates the 15 PAI subscales with the greatest between-group variation. Individuals classified as precuneus-only responders demonstrated the most robust and consistent positive changes across several clinically meaningful subscales, including features related to paranoia (parp_d; paranoia), borderline (bori_d; identity), aggression (aggp_d; physical aggression), and anxiety (anxa_d; affective).

Dual responders showed moderate improvements across many domains, including (anxc_d; cognitive), schizophrenia (sczp_d; psychotic), and somatic complaints (somc_d; conversion). In contrast, Frontal-only responders displayed more selective change, particularly in cognitive-related domains such as schizophrenia-thought disorder (sczt_d; thought disorder) and antisocial traits (anta_d; antisocial behaviors), while nonresponders consistently exhibited the least overall delta and narrower variability across all subscales.

Frontal-only responders demonstrated a marked and unexpected increase on the Mania grandiosity subscale (mang_d; grandiosity), with an average delta of nearly +15 points, which is substantially higher than any other group. This isolated elevation may reflect superficial cognitive compensation or defensive restructuring, potentially triggered by early-stage frontal activation in the absence of deeper self-referential integration. Without concurrent modulation of posterior regions such as the precuneus, these frontal changes may lack grounding in experiential processing or introspective awareness. This finding underscores the importance of whole-network training approaches for producing balanced and enduring psychological change.

Figure 8. *Classification of RCI Response Types in the SUD Participant Group (N = 63), Using Absolute RCI Threshold of |1.96|.*

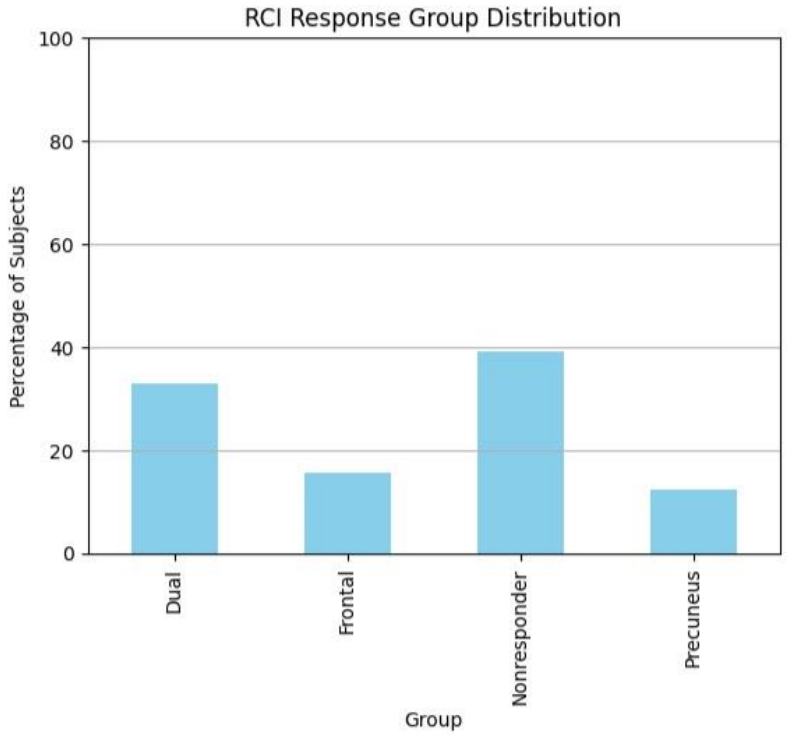

Note. Subjects were grouped into four categories: Dual Responder (alpha change at both frontal and precuneus ROI), Precuneus Only, Frontal Only, and Nonresponder. This classification reflects clinically meaningful alpha modulation regardless of direction, supporting functional interpretation of both increase and desynchronization responses.

Figure 9. *Mean PAI Delta Scores Showing the Greatest Between-Group Differences Across Alpha RCI-Defined Response Types (SUD Group, N = 63).*

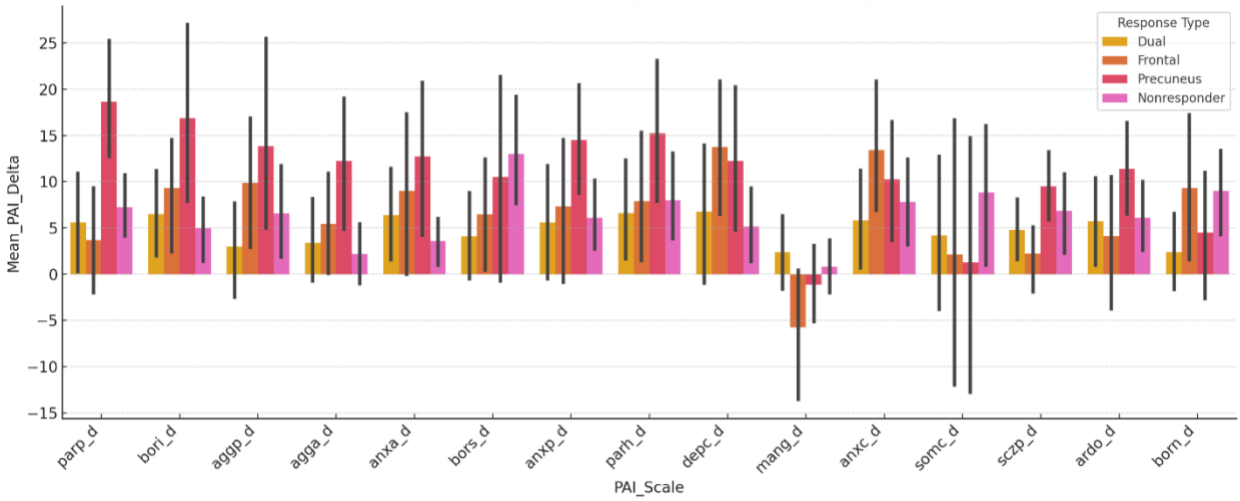

Note. Groups include dual responders (change at both frontal and posterior alpha ROI), frontal-only responders, precuneus-only responders, and nonresponders. Bars represent mean change scores from pre- to posttraining, with error bars denoting standard error of the mean. The subscales reflect clinical domains such as paranoia persecution, aggression physical, anxiety affective, and schizophrenia thought disorder. Precuneus responders exhibited the strongest improvements across multiple domains.

PAI Delta Scores and Behavioral Change

Group-level PAI deltas indicated consistent reductions in subscales of aggression (AGG) related to somatic issues, cognitive and affective components, and to the affective instability subscale of the borderline scale (BOR) across all RCI groups. Both increase and desynchronization responders showed greater magnitude of change compared to nonresponders. Exploratory analysis showed that desynchronization responders exhibited larger reductions in somatic and aggressiveness subscales, even during incarceration, potentially reflecting a deactivation of maladaptive frontal overdrive.

SHAP analysis was performed to identify which brain regions and frequency bands most strongly predicted changes in personality symptomatology (PAI delta scores) following LNFB. Figure 10 illustrates the most significant ROI for both alpha and theta frequency bands, based on mean SHAP values from the trained Random Forest model.

The most significant alpha predictor was ROI 8 (left occipital/lingual gyrus), which yielded a mean SHAP value approaching 4.0, indicating a substantial role in forecasting PAI score improvement. This was followed by ROI 6 (superior frontal) and ROI 1 (middle frontal), both of which contributed meaningfully to model predictions. Theta-band predictors were led by ROI 5 (posterior cingulate/precuneus), which showed the highest SHAP value across all theta features, followed by ROI 6 and ROI 9 (right ACC).

The distinct frequency-specific ranking underscores the complementary roles of alpha and theta rhythms in shaping individual psychological trajectories. Alpha dynamics were particularly influential in frontal and parietal regions associated with regulation, attention, and cognitive control. Theta contributions were more prominent in limbic and midline structures, suggesting involvement in emotional reactivity and internal narrative modulation.

Together, these findings support the idea that the integration of both alpha and theta rhythms is important in modeling personality change, reinforcing the view that multiple frequency-specific mechanisms underpin neurofeedback-related improvement in complex clinical populations.

PCA Visualization of Learning Clusters

PCA was conducted on the full matrix of alpha and theta CSD change scores across all ROI to examine the dimensional structure of training-related brain dynamics. The first two principal components (PC1 and PC2) captured the majority of shared variance across subjects and frequency bands, providing a compressed representation of network-level change. The alpha/theta PCA model achieved an R^2 of approximately 0.72 with a correspondingly low RMSE (~0.0019), indicating strong model fit without evidence of overfitting. Given that this represents an initial stage of ML/AI implementation on a novel dataset and analytic pipeline, these values are expected to improve with larger samples and more sophisticated model tuning, thereby enhancing the predictive power of the framework. As shown in Figure 11, PCA revealed partially overlapping but distinct distributions of alpha and theta responses. While both frequency bands occupied a shared low-dimensional space, their relative spread suggests differential encoding of treatment effects. Theta-band CSD changes were more laterally distributed along PC1, whereas alpha responses tended to separate vertically along PC2. This divergence implies that the two bands contribute complementary information: theta may reflect broader network synchrony or state-related variability, while alpha appears more associated with targeted regulation and intra-individual modulation.

To examine the spectral and spatial precision of neurofeedback effects, Cohen's d was computed for post–pre differences in CSD amplitude across 20 frequency bins for four BA 19-associated ROI including frontal ROI (ROI 2, ROI 3, ROI 5, ROI 6).

As shown in Figure 12, the largest effect sizes clustered in the alpha band (8–13 Hz) and its neighboring bins, confirming the specificity of modulation to the trained frequency range. These effects were most prominent in ROI 3 and ROI 5, supporting both the SHAP-derived frontal importance and the posterior–frontal redistribution observed in network-level modeling.

Frequency-resolved effect size mapping revealed ROI- and bin-specific patterns of CSD modulation. ROI6 (Superior frontal gyrus) exhibited a peak positive effect in the highest frequency bin (Bin_20), reflecting increased gamma-range CSD, while also showing consistent modulation across alpha and beta ranges. Conversely, ROI3 (anterior cingulate) demonstrated notable suppression in low-frequency bins (Bins 3–5), consistent with desynchronization in theta during neurofeedback.

Figure 10. *ROI of Greatest Significance for Predicting PAI Delta Scores, Derived From SHAP Values in Random Forest Models Using Alpha and Theta Band CSD as Input Features.*

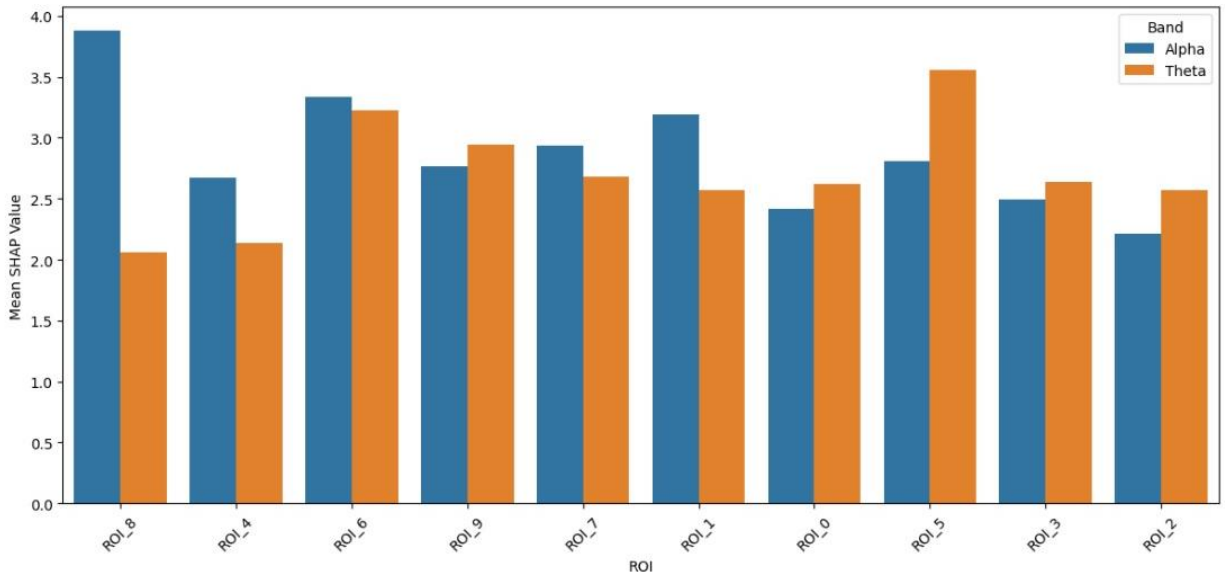

Note. ROI are sorted by overall contribution, with separate bars for alpha (blue) and theta (orange). ROI 8 (left frontal cortex) showed the highest SHAP value for alpha, while ROI 5 (posterior cingulate) was the most predictive in the theta band. This suggests frequency- and region-specific contributions to personality change following neurofeedback.

Figure 11. *PCA of Total CSD Change Across All ROI, Separated by Frequency Band.*

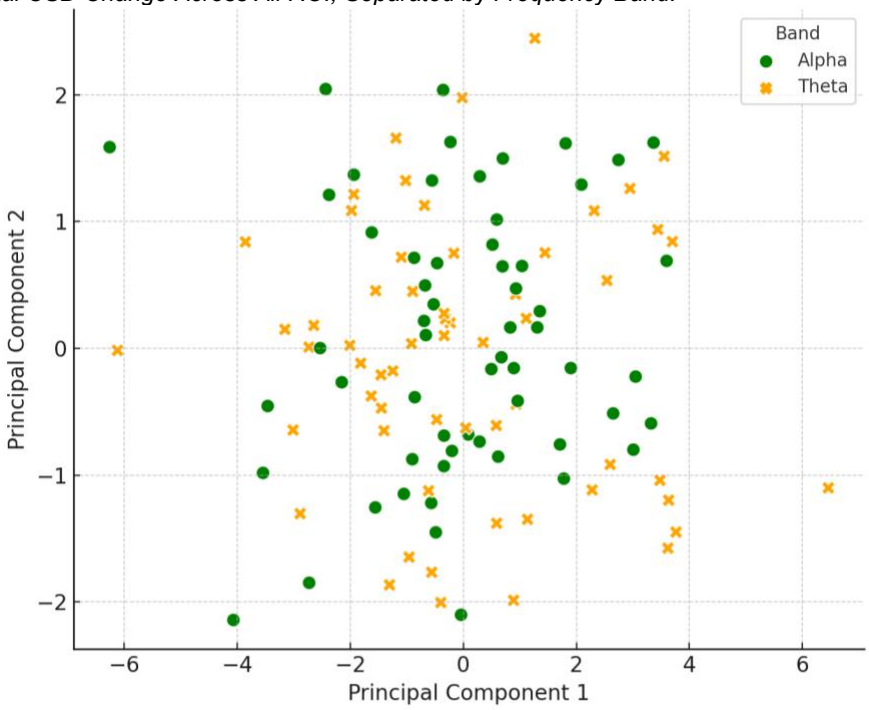

Note. Each point represents a subject's CSD change profile projected into 2D PCA space for the alpha (green) or theta (orange) band. Principal components reflect major axes of variance in neurophysiological change patterns. Overlap in distributions suggests shared underlying structure, while band-specific dispersion may indicate distinct frequency-resolved response characteristics.

Figure 12. *Effect Sizes (Cohen's d) for CSD Change From Pre- to Posttraining Across Four BA 19-Related ROI and 20 Frequency Bins (Each Spanning 2 Hz From 1–40 Hz).*

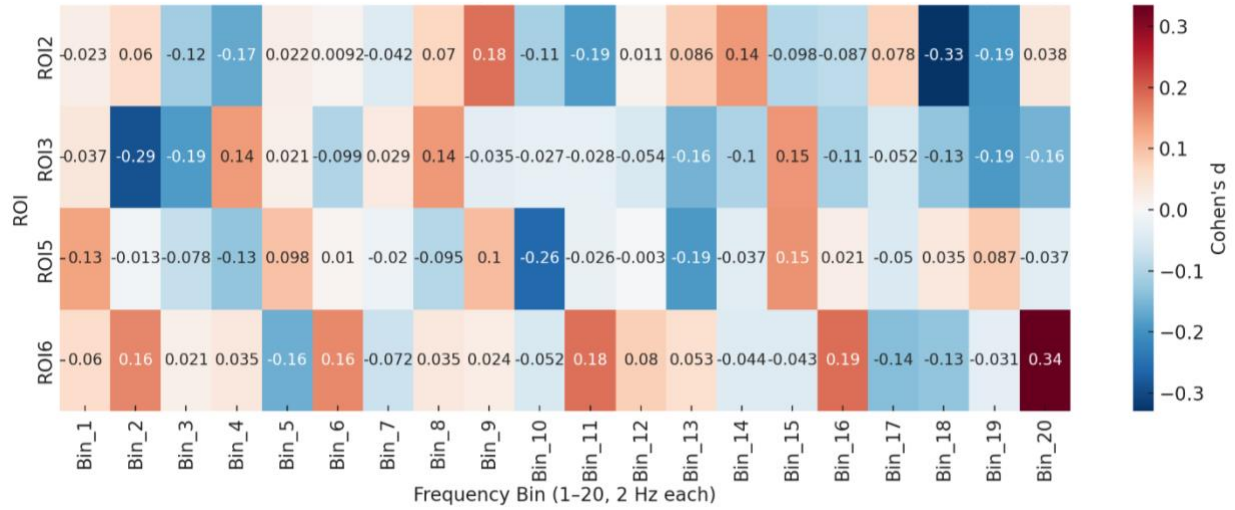

Note. Positive values (red) indicate increased posttraining CSD; negative values (blue) indicate reduced CSD. ROI labels reflect Brodmann area 19 subregions (e.g., ROI2: Cuneus; ROI3: Lingual Gyrus; ROI5: Posterior Cingulate; ROI6: Precuneus). ROI6 (Precuneus) showed the strongest increase in the 39–40 Hz bin, while ROI3 exhibited consistent suppression across low-mid frequencies.

Discussion

This study was not designed to validate or disprove theoretical models, nor to retest hypotheses already well-established in linear EEG or clinical outcome literature. Those studies have been done and often leave more questions than answers when applied to real-world, high-risk populations. Instead, we approached this analysis with a simple but essential question: What, if anything, is changing in the brain of someone with a SUD when they undergo targeted LNFB at the precuneus? And to inform regarding the questioning of neurofeedback training in general—what specific effects are shown from neurofeedback training?

Rather than neat linear changes or isolated effects, the data revealed distributed, nonlinear, and frequency-specific dynamics that challenged traditional expectations. What emerged was a picture of neuroplastic recovery far more dynamic than previously reported, and perhaps one that redefined what "improvement" looks like in EEG-based regulation.

These findings build on early work by Cannon (2009), which utilized LORETA-based current density connectivity to identify self-regulatory cortical hubs. That study anticipated many of the now-standard ML and network approaches used in this field. In our current work, alpha and theta rhythms did not simply increase or decrease; rather, they reconfigured across individuals in heterogeneous yet functionally meaningful ways. These shifts reflected both successful and unsuccessful attempts at self-regulation, forming distributed networks rather than isolated regional effects. CSD changes were not random. They aligned with functional topographies of attention, inhibition, and mood regulation, particularly involving posterior hubs and left hemisphere integration.

To further examine the specificity of alpha-related changes, correlations between alpha-band CSD shifts and PAI symptom change were evaluated within the SUD group. As shown in Table 3, alpha-specific CSD changes demonstrated stronger and more consistent associations with reductions in aggression and depression than average power measures, particularly in precuneus and posterior cingulate regions, supporting a frequency- and location-specific mechanism of change.

Table 3
Alpha-Band Correlation with PAI Symptom Change (SUD Group)

ROI	PAI Target	*r* (Alpha Δ CSD)	*r* (Avg CSD Δ)
ROI2 (Lingual Gyrus)	Depression	−0.17	−0.00
ROI2	Aggression	**−0.45**	+0.02
ROI3 (Anterior cingulate)	Depression	−0.26	−0.10
ROI3	Aggression	−0.29	+0.23
ROI4 (Post. Cingulate)	Depression	+0.16	−0.09
ROI4	Aggression	−0.11	+0.24
ROI5 (Precuneus)	Aggression	−0.34	+0.11
ROI6 (Superior frontal gyrus)	Aggression	**−0.57**	**+0.27**

Note. Shows that alpha-specific CSD changes (especially in precuneus and posterior cingulate) track better with behavioral improvement (aggression, depression) than general power shifts. Negative correlations indicate symptom reduction is associated with increased alpha CSD. ROI 6 shows divergent patterns across alpha-specific vs. average power changes. This demonstrates increased coordination between alpha sub-bands, especially in precuneus, suggesting functional network integration posttraining.

The RCI allowed classification of participants into valid subgroups, each showing distinct neural response profiles. Both alpha synchronizers and desynchronizers exhibited meaningful clinical improvement, suggesting that adaptive self-regulation may proceed along different neural routes for different recipients of neurofeedback. This finding directly challenges the long-standing assumption that increased alpha is always the goal of training.

Differential response patterns across RCI-defined groups were further characterized by examining the most influential ROI–frequency–PAI relationships. As shown in Table 4, alpha and theta CSD changes in posterior cingulate, precuneus, anterior cingulate, and insular regions were consistently associated with somatic and anxiety-related subscales, supporting a network-level interpretation of responder classification.

ML analyses helped unpack complexity. SHAP values revealed nonlinear contributions across regions and frequencies, while PCA revealed structured learning profiles not visible through traditional statistics. These results strengthen the case for posterior alpha modulation as a core mechanism for rebalancing dysfunctional self-regulation, especially in individuals with high rates of trauma, psychiatric comorbidity, and motivational deficits (Cannon, 2025; Cannon et al., 2025). The effect size findings confirm regionally specific and frequency-sensitive plasticity in response to training, particularly within BA 19 components of the posterior self-regulation network. To further characterize frequency-specific changes within BA 19–related regions, effect sizes (Cohen's *d*) were computed across the full 1–40 Hz spectrum. As shown in Figure 12, distinct patterns of frequency-dependent modulation emerged, with the precuneus (ROI 6) demonstrating the strongest increases at higher frequencies, while the lingual gyrus (ROI 3) showed consistent suppression across low- to mid-frequency bands. Notably, while most effect sizes fell in the small-to-moderate range, they were accompanied by robust behavioral improvements, with group-level PAI deltas reaching a large effect size of $d = 0.85$ (Cannon et al., 2025). This dissociation illustrates a key point: even modest, frequency-specific neural changes can produce substantial clinical gains, particularly when training is anatomically constrained and behaviorally reinforced. These findings reinforce the precision of spectral targeting in LNFB and suggest that network-level reorganization, rather than bulk amplitude change, underlies clinically relevant improvement in individuals with SUD.

Rethinking SUD: From Trait to Developmental Trajectory

This study also contributes to a broader reframing of SUD, from fixed trait models to developmental, neuroplastic trajectories. Heritability estimates for addiction remain modest, and genome-wide studies have yet to identify stable predictors of risk (Kendler et al., 2003). More compelling evidence points to a convergence of early attachment disruption, social instability, trauma, and intrauterine substance exposure as key factors shaping the SUD phenotype. These factors often interact through the nervous system's regulatory architecture, not merely through learned behavior or moral failing.

Table 4
Summarizes the Mean and Standard Deviation of Delta Values for the 15 Most Significant Subscales Across Each RCI Group

Band	ROI (Region)	PAI Subscale	Mean SHAP
Alpha	ROI_4 (Posterior Cingulate)	somc_d	4.63
Alpha	ROI_6 (Superior Frontal Gyrus)	somc_d	3.9
Alpha	ROI_8 (Lingual Gyrus)	somc_d	2.93
Alpha	ROI_9 (Anterior Cingulate)	somd_d	2.65
Alpha	ROI_7 (Insula)	somd_d	2.5
Alpha	ROI_1 (Middle Frontal Gyrus)	somh_d	2.24
Alpha	ROI_4 (Posterior Cingulate)	somh_d	1.86
Alpha	ROI_9 (Anterior Cingulate)	somh_d	0.92
Alpha	ROI_4 (Posterior Cingulate)	anxc_d	2.77
Alpha	ROI_0 (Cuneus)	anxa_d	1.57
Alpha	ROI_5 (Precuneus)	anxa_d	2.21
Alpha	ROI_2 (Lingual Gyrus)	anxa_d	2.16
Theta	ROI_4 (Posterior Cingulate)	somc_d	4.86
Theta	ROI_7 (Insula)	somc_d	3.4
Theta	ROI_5 (Precuneus)	somc_d	3.15
Theta	ROI_6 (Superior Frontal Gyrus)	somd_d	4.74
Theta	ROI_1 (Middle Frontal Gyrus)	somd_d	1.6
Theta	ROI_8 (Lingual Gyrus)	somd_d	1.24
Theta	ROI_5 (Precuneus)	somh_d	4.56
Theta	ROI_1 (Middle Frontal Gyrus)	somh_d	1.82
Theta	ROI_2 (Lingual Gyrus)	somh_d	1.15
Theta	ROI_9 (Anterior Cingulate)	anxc_d	4.01
Theta	ROI_5 (Precuneus)	anxc_d	2.4
Theta	ROI_3 (Anterior Cingulate)	anxc_d	2.08
Theta	ROI_8 (Lingual Gyrus)	anxa_d	2.24
Theta	ROI_2 Lingual Gyrus)	anxa_d	2.05

Note. The differential response patterns align with the underlying neurophysiological distinctions derived from CSD shifts, providing convergent validity for the RCI-based responder classification.

Many substance abuse clients are diagnosed shortly after detoxification, yet their brains often struggle to restructure social, emotional, and physiological stability, even after 2 weeks to 5 months of abstinence (Nixon & Lewis, 2020). Moreover, SUD histories frequently overlap with prenatal exposures, when parents-to-be conceive while under the influence of substances or ‘safe’ psychiatric medications. For example, prenatal selective serotonin reuptake inhibitors (SSRI) exposure may lead to subtle but persistent disruptions in neurodevelopment, especially in domains of attention, emotion regulation, and executive function (Koc et al., 2023). Thus, SUD and PDE may be better understood as sequential dysregulation spanning generations. Critically, many individuals with SUD histories go on to conceive children under the influence of alcohol, nicotine, cannabis, opioids, or prescribed psychiatric medications. Even when deemed “safe,” such exposures, particularly to SSRIs, may contribute to subtle but durable neurodevelopmental disruptions in the child, particularly in domains related to attention, emotion regulation, and executive control (Croen et al., 2011; Gentile, 2010; Oberlander et al., 2007). As such, SUD and PDE may be viewed not as separate conditions, but as sequential iterations of dysregulation, echoing across generations. This

reframing implies that interventions aimed at restoring rhythms and self-regulation in SUD patients may have cascading effects beyond the individual. By improving brain network integrity and adaptive function, neurofeedback may serve as both a therapeutic and preventative tool.

Implications for Clinical Neurofeedback

The current findings support the use of individualized, voxel-level neurofeedback protocols guided by ML. Both responders and nonresponders showed meaningful information patterns in their CSD changes, with responders exhibiting both increases and decreases in alpha power, depending on baseline state. Importantly, desynchronization should not be seen as a failure, but as a viable pathway to regulation. This challenges a foundational bias in the neurofeedback field, that amplitude increases are inherently good (Bell et al., 2019; Riha, 2021).

Consistent with prior work on lateralized function, left frontal and left posterior ROI emerged as major contributors to regulation and behavioral improvement. ROI 2 (posterior parietal cortex) and ROI 3 (anterior cingulate cortex) were repeatedly flagged in SHAP analyses, and are known to support attentional reorientation, emotional regulation, and inhibition, core deficits in many SUD populations. SUD individuals in recovery tend to struggle with social, emotional and adaptive skills development, and often experience the self and world in unfavorable ways (Cannon et al., 2008). A further consideration is the perceived “threat” of neurofeedback to traditional mental health practice. It is critical to emphasize that EEG or neuroimaging techniques are not at a stage where data can simply be programmed into the brain. Neurofeedback does not implant skills, values, or social knowledge; rather, it facilitates the brain’s intrinsic capacity for self-regulation by promoting adaptive oscillatory states and functional connectivity. Translating these neurophysiological gains into meaningful life changes still requires social learning, cognitive restructuring, and therapeutic engagement. In other words, neurofeedback primes the neural architecture for regulation, but clients must still be taught how to apply these capacities in real-world contexts—social, emotional, and adaptive—through structured, purposeful, and insight-oriented interventions. Thus, neurofeedback should not be regarded as a replacement for psychotherapy or education but as a complementary method that enhances their efficacy by stabilizing the neural foundations upon which skills are built (Hammond, 2011; Micoulaud-Franchi & Fovet, 2016).

More broadly, the findings align with literature implicating left-hemisphere hypoactivity in mood and affective disorders (Davidson, 2004). In particular, left posterior structures such as the precuneus and temporoparietal junction (TPJ) appear essential to internal narrative, self-related thought, and receptive language. Disruption in these areas may impair the scaffolding of identity and hinder access to autobiographical memory, a pattern commonly observed in addiction, trauma, and depression (Gibson et al., 2022; Zhang et al, 2025).

The spectral distribution of training-related cortical change revealed frequency- and region-specific modulation across BA 19 ROI. Alpha-band frequencies (8–13 Hz) showed the strongest training effects in ROI 2 (lingual gyrus), ROI 3 (precuneus), and ROI 5 (anterior cingulate), with moderate effect sizes (Cohen’s d = 0.29–0.33). ROI 6 (superior frontal gyrus) showed selective low beta modulation (~30–34 Hz), indicating dynamic plasticity across multiple bands. Importantly, these modest physiological effects were accompanied by a significant group-level PAI improvement (d = 0.85), highlighting the power of frequency-specific modulation to induce meaningful behavioral shifts across heterogenous populations (Cannon et al., 2025).

The posterior-to-frontal shift observed in regression-weighted networks and PCA loading vectors suggests that regulation is not about isolated activation, but dynamic redistribution. Effective self-regulation appears to require a realignment of attentional control and default mode systems, a process that may be visible only through network-level, multivariate models like those used here.

One of the clearest outcomes of this study is the confirmation that frequency-specific modulation, interregional coordination, and network-level reorganization do occur because of neurofeedback, particularly when guided by LORETA-based CSD training. While many traditional neurofeedback models have reported localized amplitude changes, the present findings provide direct evidence that training can induce structured, nonlinear alterations in frequency distribution (e.g., alpha desynchronization or redistribution), comodulation across cortical hubs, and emergent connectivity patterns indicative of restored regulatory function.

These outcomes were not inferred from surface amplitudes or visual inspection but derived from anatomically constrained, voxel-wise data

interpreted using multivariate ML models. Such models, especially when paired with SHAP analysis and PCA, identified nonlinear and distributed changes that would be invisible to univariate statistics or visual EEG review. The emergent pattern of posterior-to-frontal redistribution, frequency-specific ROI involvement, and group-stratified regulatory profiles represents a compelling case for network-based, frequency-sensitive neurofeedback analytics.

The network visualization in Figure 7 highlights a rare but critically important phenomenon: not only do cortical regions demonstrate posttraining changes in alpha and theta oscillatory dynamics, but these neural shifts are meaningfully linked to validated subscales of psychological symptoms and experiential processes. The presence of both alpha-only (green) and theta-only (orange) connections underscores frequency-specific contributions to regulation, while the purple "shared" links reveal overlapping spectral signatures of symptom-related variance. Such associations extend beyond simple electrophysiological modulation, suggesting that certain ROI–PAI relationships may constitute neural "flags" of disorder phenotypes, marking enduring vulnerabilities in attention, affect regulation, and self-related processing. This bridging of EEG source dynamics with psychometric measures is seldom achieved in neurofeedback research, where electrophysiological changes are often reported without concurrent demonstration of clinical or personality correlates. Importantly, the appearance of left posterior (precuneus, parietal) and left middle frontal and anterior cingulate regions within these networks is consistent with prior work identifying these loci as hubs of self-regulation and inhibitory control, both of which are disrupted in substance use and related disorders (Enriquez-Geppert et al., 2017). Moreover, the convergence of ROI-based alpha and theta connectivity with subscales reflecting mood, somatization, paranoia, and substance-related experiences parallels broader evidence that cross-frequency coupling within default mode and executive networks underpins vulnerability across psychiatric dimensions (Huster et al., 2013; Menon, 2011). Thus, the present findings suggest that individualized neurofeedback training does not merely shift oscillatory power in isolation but also reshapes functional couplings that map onto clinically relevant psychological dimensions, supporting the promise of voxel-level, ML-guided approaches for uncovering network-level biomarkers of both disorder and recovery.

Together, these observations lay the groundwork for a new generation of interventions: systems that adapt to individual learning rhythms, map actual neural engagement, and evolve through feedback-informed AI rather than static protocols. Current effect sizes and lack of truly standardized procedures beg for a system that can do what humans to date have failed to accomplish, understand and then treat substance abuse problems. In order for AI and ML to function meaningfully in brain research, regardless of the method employed, standardized procedures and protocols are essential. Without consistency in data acquisition, preprocessing, and labeling, even the most advanced models will amplify noise rather than extract signal. The application of ML and AI to EEG and other physiological modalities holds enormous promise but only if those methods are grounded in structured, standardized acquisition and analysis procedures. Unlike exploratory hypothesis testing, which may tolerate variability, ML depends on coherent, repeatable input. Without clearly defined protocols for data collection, preprocessing, feature selection, and target labeling, even the most powerful algorithms will simply mirror noise. In the neurofeedback literature, as well as in fMRI, qEEG, and other imaging domains, inconsistent methods have led to conflicting outcomes and questionable reproducibility. For AI to function as a generative tool in neuroscience, capable of detecting patterns, predicting response, and refining treatment, its foundation must be stability. That means using physiologically valid models, reliable data pipelines, and rigorous documentation at every step. The brain is already a noisy and dynamic system; when experimental variability is added on top of that, the result is analytical confusion rather than insight. Structure enables signal to emerge, and in the absence of that structure, AI will only mirror our uncertainty.

Future research is needed to apply similar modeling and analytic frameworks to more traditional surface-based neurofeedback approaches, including SMR, theta/beta, and *Z*-score protocols. Without comparable data and structure, direct comparisons remain difficult. However, the present findings suggest that current source-guided neurofeedback may offer a more reliable and physiologically grounded means of accessing and modulating core self-regulatory networks with particular focus in clinical populations with complex, distributed dysregulation such as those with SUD.

Limitations and Future Directions

This study has several limitations. The sample, while well-characterized, was drawn entirely from incarcerated adults, limiting generalizability to community-based or adolescent SUD populations. While CSD offers improved spatial resolution over surface EEG, it still lacks the precision of fMRI or magnetoencephalography (MEG) source analysis. Future work should include longitudinal studies, additional neuroimaging modalities, and developmental extensions to better understand intergenerational effects of rhythm-based dysregulation.

Moreover, although our ML models offered interpretable and accurate classifications, they are ultimately constrained by the quality of input data. As any practitioner outside of tightly controlled laboratory settings recognizes, artifact-free EEG baselines are virtually unattainable in real-world clinical and forensic settings. This challenge is amplified when contrasting surface EEG with CSD approaches. While surface recordings are more vulnerable to volume conduction, reference contamination, and peripheral artifacts, CSD estimation attenuates many of these issues by enhancing spatial resolution and isolating cortical generators. Nonetheless, even CSD methods depend on the integrity of the raw recordings, requiring careful artifact management, standardized protocols for baselines, training and preprocessing pipelines, and clear target definitions. The generalizability of our findings therefore hinges on methodological alignment across laboratories and practitioners. Without such convergence, neurofeedback will remain heterogeneous, and the translational promise of AI-driven insights will be limited (Kayser & Tenke, 2015; Ros et al., 2020).

Despite over 6 decades of progress in neuroscience and diagnostic psychiatry, the field has yet to isolate a single, biologically valid “disorder” in the brain. This does not necessarily imply that mental disorders are fictitious but rather that our current definitions and diagnostic frameworks may be misaligned with the biological realities they intend to capture. The greatest challenge and perhaps the greatest promise of AI and ML lies in their potential to clarify and deconstruct this diagnostic ambiguity. At present, psychiatric classifications remain largely syndromal, relying on subjective criteria rather than objective neural signatures (Insel et al., 2010). Disorders such as depression, ADHD, or schizophrenia have shown high internal heterogeneity and poor predictive utility, even when examined through decades of neuroimaging and genetics research (Elliott et al., 2018; Kapur et al., 2012). Advanced ML tools provide an opportunity to move beyond symptom clusters and instead characterize disorders by measurable, network-based features that evolve over time and context.

For example, work by Drysdale et al. (2017) used resting-state fMRI and ML to identify four distinct neurophysiological subtypes of depression, each with unique connectivity patterns and treatment responses. Similarly, Dwyer et al. (2018) demonstrated that ML approaches can outperform traditional methods in identifying functional brain patterns in schizophrenia, patterns that cross diagnostic boundaries and reveal unexpected dimensions of psychopathology. These studies highlight the urgent need to rethink disorder classifications, not as fixed categories, but as dynamic profiles embedded in the structure of brain networks. Until such models are widely adopted, misclassification and treatment mismatch will remain significant barriers to progress. We have much work to do in this regard, but the tools now exist to do it.

Conclusion

In this study, we did not aim to prove a theory, but to interrogate a reality: What changes, and how, when a brain with SUD undergoes neurofeedback at a known self-regulatory hub? Using ML tools to decode EEG-derived current density and behavior, we found robust and interpretable patterns of network reorganization, tied to individual learning profiles and behavioral outcomes. These findings support a shift in how we view addiction, not as a moral failure or fixed trait, but as a dynamic, frequency-sensitive disruption in regulatory function.

This reframing, grounded in real-world data and validated by nonlinear models, sets the stage for a more precise and humane understanding of SUD. AI will not solve addiction, but it may finally allow us to ask the right questions and listen to what the brain is trying to say.

The present work represents a first step in decoding self-regulation in SUD using CSD-informed neurofeedback and ML. Moving forward, we will extend this framework to children with in utero drug exposure (IUDE), as well as normative and heterogeneous adolescent and adult samples, to clarify developmental trajectories of rhythmic self-regulation and identify potential early biomarkers of risk. Parallel to this research agenda, we have developed stand-alone software capable of delivering the current LNFB protocol, along with

additional source-based protocols, across a range of EEG devices. This platform is designed for flexible implementation in diverse clinical and research settings. Beyond local delivery, we are building cloud-based infrastructure for automated artifact detection, ROI extraction, and large-scale data integration. These advances will allow for scalable, reproducible, and standardized neurofeedback across populations, creating the possibility of real-time precision interventions that bridge neuroscience, clinical practice, and AI-driven analytics.

Importantly, the future of this work must also emphasize equity and access. Neurofeedback informed by ML and source-space modeling should not remain limited to specialized or privileged contexts. Our goal is to ensure that these tools are available to all in-need populations, including children, incarcerated individuals, and communities historically underserved by mental health systems, and to the professionals who work alongside them. By building accessible, strict, evidence-based platforms, we aim to extend the benefits of rhythmic self-regulation beyond the laboratory and into the settings where they are needed most.

Author Declarations

The author thanks the developers and maintainers of open-source scientific software libraries that made this work possible, including NumPy, pandas, SciPy, scikit-learn, UMAP-learn, and Matplotlib. Portions of the data processing, analysis, and manuscript drafting were supported by the use of large language models as a writing and code-assistance tool. All analytic decisions, interpretations, and conclusions are solely the responsibility of the author. A provisional patent application has been filed related to the methods and systems described in this study, including the LNFB training architecture and ML model for CSD classification.

References

Baldwin, D. R., Cannon, R., Fischer, S., & Kivisto, K. (2011). The inverse of psychopathology: A Loreta EEG and cortisol examination. *Journal of Neurotherapy, 15*(4), 374–388. https://doi.org/10.1080/10874208.2011.623095

Barry, R. J., Clarke, A. R., Johnstone, S. J., Magee, C. A., & Rushby, J. A. (2007). EEG differences between eyes-closed and eyes-open resting conditions. *Clinical Neurophysiology, 118*(12), 2765–2773. https://doi.org/10.1016/j.clinph.2007.07.028

Başar, E., Başar-Eroglu, C., Karakaş, S., & Schürmann, M. (2001). Gamma, alpha, delta, and theta oscillations govern cognitive processes. *International Journal of Psychophysiology, 39*(2–3), 241–248. https://doi.org/10.1016/s0167-8760(00)00145-8

Bassett, D. S., & Sporns, O. (2017). Network neuroscience. *Nature Neuroscience, 20*(3), 353–364. https://doi.org/10.1038/nn.4502

Bazanova, O. M., & Vernon, D. (2014). Interpreting EEG alpha activity. *Neuroscience & Biobehavioral Reviews, 44*, 94–110. https://doi.org/10.1016/j.neubiorev.2013.05.007

Belenko, S., & Peugh, J. (2005). Estimating drug treatment needs among state prison inmates. *Drug and Alcohol Dependence, 77*(3), 269–281. https://doi.org/10.1016/j.drugalcdep.2004.08.023

Bell, A. N., Moss, D., & Kallmeyer, R. J. (2019). Healing the neurophysiological roots of trauma: A controlled study examining LORETA *z*-score neurofeedback and HRV biofeedback for chronic PTSD. *NeuroRegulation, 6*(2), 54–70. https://doi.org/10.15540/nr.6.2.54

Breiman, L. (2001). Random forests. *Machine Learning, 45*(1), 5–32. https://doi.org/10.1023/A:1010933404324

Brewer, J. A., Garrison, K. A., & Whitfield-Gabrieli, S. (2013). What about the "self" is processed in the posterior cingulate cortex? *Frontiers in Human Neuroscience, 7*, Article 647. https://doi.org/10.3389/fnhum.2013.00647

Buckner, R. L., Andrews-Hanna, J. R., & Schacter, D. L. (2008). The brain's default network. *Annals of the New York Academy of Sciences, 1124*(1), 1–38. https://doi.org/10.1196/annals.1440.011

Cannon, R. L. (2009). *Functional connectivity of EEG LORETA in cortical core components of the self and the default network (DNt) of the brain*. [PhD dissertation, University of Tennessee]. https://trace.tennessee.edu/utk_graddiss/571

Cannon, R. L. (2014). Parietal foci for attention-deficit/hyperactivity disorder: Targets for LORETA neurofeedback with outcomes. *Biofeedback, 42*(2), 47–57. https://doi.org/10.5298/1081-5937-42.2.01

Cannon, R. L. (2025). Quantifying self-regulation: Neuroevolutionary insights from precuneus alpha modulation via LORETA neurofeedback. *NeuroRegulation, 12*(2), 65–81. https://doi.org/10.15540/nr.12.2.65

Cannon, R. L., Baldwin, D. R., Diloreto, D. J., Phillips, S. T., Shaw, T. L., & Levy, J. J. (2014). LORETA neurofeedback in the precuneus: Operant conditioning in basic mechanisms of self-regulation. *Clinical EEG and Neuroscience, 45*(4), 238–248. https://doi.org/10.1177/1550059413512796

Cannon, R. L., Baldwin, D. R., Shaw, T. L., Diloreto, D. J., Phillips, S. M., Scruggs, A. M., & Riechel, B. D. (2012). Reliability of quantitative EEG (qEEG) measures and LORETA current source density at 30 days. *Neuroscience Letters, 518*(1), 27–31. https://doi.org/10.1016/j.neulet.2012.04.035

Cannon, R., Lubar, J., & Baldwin, D. (2008). Self-perception and experiential schemata in the addicted brain. *Applied and Psychophysiology Biofeedback, 33*(4), 223–238. https://doi.org/10.1007/s10484-008-9067-9

Cannon, R., Lubar, J., Thornton, K., Wilson, S., & Congedo, M. (2004). Limbic beta activation and LORETA: Can hippocampal and related limbic activity be recorded and changes visualized using LORETA in an affective memory condition? *Journal of Neurotherapy, 8*(4), 5–24. https://doi.org/10.1300/J184v08n04_02

Cannon, R. L., Mills, C., Geroux, M., Zhart, L. A., Boluyt, K., Webber, R., & Cook, D. (2025). LORETA neurofeedback at precuneus: A standard approach for use in incarcerated populations with substance use problems. *NeuroRegulation, 12*(3), 213–233. https://doi.org/10.15540/nr.12.3.213

Cavanagh, J. F., & Frank, M. J. (2014). Frontal theta as a mechanism for cognitive control. *Trends in Cognitive Sciences, 18*(8), 414–421. https://doi.org/10.1016/j.tics.2014.04.012

Cavanna, A. E., & Trimble, M. R. (2006). The precuneus: A review of its functional anatomy and behavioural correlates. *Brain, 129*(3), 564–583. https://doi.org/10.1093/brain/awl004

Coan, J. A., & Allen, J. J. B. (2004). Frontal EEG asymmetry as a moderator and mediator of emotion. *Biological Psychology, 67*(1–2), 7–50. https://doi.org/10.1016/j.biopsycho.2004.03.002

Croen, L. A., Grether, J. K., Yoshida, C. K., Odouli, R., & Hendrick, V. (2011). Antidepressant use during pregnancy and childhood autism spectrum disorders. *Archives of General Psychiatry, 68*(11), 1104–1112. https://doi.org/10.1001/archgenpsychiatry.2011.73

Davidson, R. J. (2004). What does the prefrontal cortex "do" in affect: Perspectives on frontal EEG asymmetry research. *Biological Psychology, 67*(1–2), 219–233. https://doi.org/10.1016/j.biopsycho.2004.03.008

Drysdale, A. T., Grosenick, L., Downar, J., Dunlop, K., Mansouri, F., Meng, Y., Fetcho, R. N., Zebley, B., Oathes, D. J., Etkin, A., Schatzberg, A. F., Sudheimer, K., Keller, J., Mayberg, H. S., Gunning, F. M., Alexopoulos, G. S., Fox, M. D., Pascual-Leone, A., Voss, H. U. ... & Liston, C. (2017). Resting-state connectivity biomarkers define neurophysiological subtypes of depression. *Nature Medicine, 23*(1), 28–38. https://doi.org/10.1038/nm.4246

Dwyer, D. B., Falkai, P., & Koutsouleris, N. (2018). Machine learning approaches for clinical psychology and psychiatry. *Annual Review of Clinical Psychology, 14*, 91–118. https://doi.org/10.1146/annurev-clinpsy-032816-045037

Enriquez-Geppert, S., Huster, R. J., & Herrmann, C. S. (2017). EEG-neurofeedback as a tool to modulate cognition and behavior: A review tutorial. *Frontiers in Human Neuroscience, 11*, Article 51. https://doi.org/10.3389/fnhum.2017.00051

Elliott, M. L., Romer, A., Knodt, A. R., & Hariri, A. R. (2018). A connectome-wide functional signature of transdiagnostic risk for mental illness. *Biological Psychiatry, 84*(6), 452–459. https://doi.org/10.1016/j.biopsych.2018.03.012

Friston, K. (2010). The free-energy principle: A unified brain theory? *Nature Reviews Neuroscience, 11*(2), 127–138. https://doi.org/10.1038/nrn2787

Gentile, S. (2010). Neurodevelopmental effects of prenatal exposure to psychotropic medications. *Depression and Anxiety, 27*(7), 675–686. https://doi.org/10.1002/da.20706

Gibson, B. C., Vakhtin, A., Clark, V. P., Abbott, C. C., & Quinn, D. K. (2022). Revisiting hemispheric asymmetry in mood regulation: Implications for rTMS for major depressive disorder. *Brain Sciences, 12*(1), Article 112. https://doi.org/10.3390/brainsci12010112

Gigerenzer, G. (2004). Mindless statistics. *The Journal of Socio-Economics, 33*(5), 587–606. https://doi.org/10.1016/j.socec.2004.09.033

Grace, A. A. (1991). Phasic versus tonic dopamine release and the modulation of dopamine system responsivity: A hypothesis for the etiology of schizophrenia. *Neuroscience, 41*(1), 1–24. https://doi.org/10.1016/0306-4522(91)90196-U

Gusnard, D. A., & Raichle, M. E. (2001). Searching for a baseline: Functional imaging and the resting human brain. *Nature Reviews Neuroscience, 2*(10), 685–694. https://doi.org/10.1038/35094500

Hammond, D. C. (2011). What is neurofeedback: An update. *Journal of Neurotherapy, 15*(4), 305–336. https://doi.org/10.1080/10874208.2011.623090

Haugg, A., Sladky, R., Skouras, S., McDonald, A., Craddock, C., Kirschner, M., Herdener, M., Koush, Y., Papoutsi, M., Keynan, J. N., Hendler, T., Cohen Kadosh, K., Zich, C., MacInnes, J., Adcock, R. A., Dickerson, K., Chen, N. K., Young, K., Bodurka, J., Yao, S., … Scharnowski, F. (2020). Can we predict real-time fMRI neurofeedback learning success from pretraining brain activity? *Human Brain Mapping, 41*(14), 3839–3854. https://doi.org/10.1002/hbm.25089

Huster, R. J., Enriquez-Geppert, S., Lavallee, C. F., Falkenstein, M., & Herrmann, C. S. (2013). Electroencephalography of response inhibition tasks: Functional networks and cognitive contributions. *International Journal of Psychophysiology, 87*(3), 217–233. https://doi.org/10.1016/j.ijpsycho.2012.08.001

Insel, T. R., Cuthbert, B. N., Garvey, M., Heinssen, R., Pine, D. S., Quinn, K., Sanislow, C., & Wang, P. (2010). Research domain criteria (RDoC): Toward a new classification framework for research on mental disorders. *American Journal of Psychiatry, 167*(7), 748–751. https://doi.org/10.1176/appi.ajp.2010.09091379

Ioannidis, J. P. A. (2018). The challenge of reforming nutritional epidemiologic research. *JAMA, 320*(10), 969–970. https://doi.org/10.1001/jama.2018.11025

Jacobson, N. S., & Truax, P. (1991). Clinical significance: A statistical approach to defining meaningful change in psychotherapy research. *Journal of Consulting and Clinical Psychology, 59*(1), 12–19. https://doi.org/10.1037/0022-006X.59.1.12

Jensen, O., & Mazaheri, A. (2010). Shaping functional architecture by oscillatory alpha activity: Gating by inhibition. *Frontiers in Human Neuroscience*, *4*, Article 186. https://doi.org/10.3389/fnhum.2010.00186

Kapur, S., Phillips, A. G., & Insel, T. R. (2012). Why has it taken so long for biological psychiatry to develop clinical tests and what to do about it? *Molecular Psychiatry, 17*(12), 1174–1179. https://doi.org/10.1038/mp.2012.105

Kayser, J., & Tenke, C. E. (2015). Issues and considerations for using the scalp surface Laplacian in EEG/ERP research: A tutorial review. *International Journal of Psychophysiology, 97*(3), 189–209. https://doi.org/10.1016/j.ijpsycho.2015.04.012

Kelley, L., Strunk, W., Cannon, R., & Leighton, J. (2019). EEG source localization and attention differences between children exposed to drugs in utero and those with attention-deficit/hyperactivity disorder: A pilot study. *NeuroRegulation, 6*(1), 23–37. https://doi.org/10.15540/nr.6.1.23

Kendler, K. S., Jacobson, K. C., Prescott, C. A., & Neale, M. C. (2003). Specificity of genetic and environmental risk factors for use and abuse/dependence of cannabis, cocaine, hallucinogens, sedatives, stimulants, and opiates. *American Journal of Psychiatry, 160*(4), 687–695. https://doi.org/10.1176/appi.ajp.160.4.687

Koc, D., Tiemeier, H., Stricker, B. H., Muetzel, R. L., Hillegers, M., & El Marroun, H. (2023). Prenatal antidepressant exposure and offspring brain morphologic trajectory. *JAMA Psychiatry, 80*(12), 1208–1217. https://doi.org/10.1001/jamapsychiatry.2023.3161

Koponen, A. M., Nissinen, N.-M., Gissler, M., Autti-Rämö, I., Sarkola, T., & Kahila, H. (2020). Prenatal substance exposure, adverse childhood experiences and diagnosed mental and behavioral disorders – A longitudinal register-based matched cohort study in Finland. *SSM - Population Health, 11*, Article 100625. https://doi.org/10.1016/j.ssmph.2020.100625

Klimesch, W. (1999). EEG alpha and theta oscillations reflect cognitive and memory performance: A review and analysis. *Brain Research Reviews, 29*(2–3), 169–195. https://doi.org/10.1016/S0165-0173(98)00056-3

Knyazev, G. G. (2013). EEG correlates of self-referential processing. *Frontiers in Human Neuroscience, 7*, Article 264. https://doi.org/10.3389/fnhum.2013.00264

Leech, R., & Sharp, D. J. (2014). The role of the posterior cingulate cortex in cognition and disease. *Brain, 137*(1), 12–32. https://doi.org/10.1093/brain/awt162

Lundberg, S. M., & Lee, S.-I. (2017). A unified approach to interpreting model predictions. In *Advances in neural information processing systems* (Vol. 30). https://doi.org/10.48550/arXiv.1705.07874

Menon, V. (2011). Large-scale brain networks and psychopathology: A unifying triple network model. *Trends in*

Cognitive Sciences, 15(10), 483–506. https://doi.org/10.1016/j.tics.2011.08.003

Mericle, A. A., Casaletto, K., Knoblach, D., Brooks, A. C., & Carise, D. (2010). Drug policy by popular sovereignty. *Journal of Drug Issues, 40*(4), 819–839. https://doi.org/10.1177/002204261004000404

Micoulaud-Franchi, J. A., & Fovet, T. (2016). Neurofeedback: Time needed for a promising non-pharmacological therapeutic method. *The Lancet Psychiatry, 3*(9), Article e16. https://doi.org/10.1016/S2215-0366(16)30189-4

Mitchell, D. J., McNaughton, N., Flanagan, D., & Kirk, I. J. (2008). Frontal-midline theta from the perspective of hippocampal "theta." *Progress in Neurobiology, 86*(3), 156–185. https://doi.org/10.1016/j.pneurobio.2008.09.005

Morey, L. C. (1991). *Personality Assessment Inventory: Professional manual*. Psychological Assessment Resources.

Mumola, C. J., & Karberg, J. C. (2006). *Drug use and dependence, state and federal prisoners, 2004* (NCJ 213530). U.S. Department of Justice, Bureau of Justice Statistics.

Nixon, S. J., & Lewis, B. (2020). Brain structure and function in recovery. *Alcohol Research: Current Reviews, 40*(3), Article 04. https://doi.org/10.35946/arcr.v40.3.04

Northoff, G., Heinzel, A., de Greck, M., Bermpohl, F., Dobrowolny, H., & Panksepp, J. (2006). Self-referential processing in our brain—A meta-analysis of imaging studies on the self. *NeuroImage, 31*(1), 440–457. https://doi.org/10.1016/j.neuroimage.2005.12.002

Oberlander, T. F., Reebye, P., Misri, S., Papsdorf, M., Kim, J., & Grunau, R. E. (2007). Externalizing and attentional behaviors in children of depressed mothers treated with a selective serotonin reuptake inhibitor antidepressant during pregnancy. *Archives of Pediatrics & Adolescent Medicine, 161*(1), 22–29. https://doi.org/10.1001/archpedi.161.1.22

Open Science Collaboration. (2015). Estimating the reproducibility of psychological science. *Science, 349*(6251), Article aac4716. https://doi.org/10.1126/science.aac4716

Pascual-Marqui, R. D., Michel, C. M., & Lehmann, D. (1994). Low resolution electromagnetic tomography: A new method for localizing electrical activity in the brain. *International Journal of Psychophysiology, 18*(1), 49–65. https://doi.org/10.1016/0167-8760(84)90014-x

Pascual-Marqui, R. D. (2002). Standardized low-resolution brain electromagnetic tomography (sLORETA): Technical details. *Methods and Findings in Experimental and Clinical Pharmacology, 24*(Suppl D), 5–12.

Pascual-Marqui, R. D., Esslen, M., Kochi, K., & Lehmann, D. (2002). Functional imaging with low-resolution brain electromagnetic tomography (LORETA): A review. *Methods and Findings in Experimental and Clinical Pharmacology, 24* (Suppl C), 91–95.

Peniston, E. G., & Kulkosky, P. J. (1989). Alpha–theta brainwave training and beta-endorphin levels in alcoholics. *Alcoholism: Clinical and Experimental Research, 13*(2), 271–279. https://doi.org/10.1111/j.1530-0277.1989.tb00325.x

Riha, C. (2021). *Developing individual neurofeedback: Latent class modeling of responder trajectories in alpha-band training* [Doctoral dissertation]. University of Zurich.

Ros, T., Enriquez-Geppert, S., Zotev, V., Young, K. D., Wood, G., Whitfield-Gabrieli, S., Wan, F., Vuilleumier, P., Vialatte, F., Van De Ville, D., Todder, D., Surmeli, T., Sulzer, J. S., Strehl, U., Sterman, M. B., Steiner, N. J., Sorger, B., Soekadar, S. R., Sitaram, R., … Thibault, R. T. (2020). Consensus on the reporting and experimental design of clinical and cognitive-behavioural neurofeedback studies (CRED-nf checklist). *Brain, 143*(6), 1674–1685. https://doi.org/10.1093/brain/awaa009

Scheeringa, R., Petersson, K. M., Oostenveld, R., Norris, D. G., Hagoort, P., & Bastiaansen, M. C. M. (2008). Trial-by-trial coupling between EEG and BOLD identifies networks related to alpha and theta EEG power increases during working memory maintenance. *NeuroImage, 44*(3), 1224–1238. https://doi.org/10.1016/j.neuroimage.2008.08.041

Sitaram, R., Ros, T., Stoeckel, L., Haller, S., Scharnowski, F., Lewis-Peacock, J., Weiskopf, N., Blefari, M. L., Rana, M., Oblak, E., Birbaumer, N., & Sulzer, J. (2017). Closed-loop brain training: The science of neurofeedback. *Nature Reviews Neuroscience, 18*(2), 86–100. https://doi.org/10.1038/nrn.2016.164

Zhang, L., Qin, K., Pan, N., Xu, H., & Gong, Q. (2025). Shared and distinct patterns of default mode network in major depressive disorder and bipolar disorder: A comparative meta-analysis. *Journal of Affective Disorders, 368*, 23–32. https://doi.org/10.1016/j.jad.2024.09.021

Zhou, Y., Dougherty, J. H. Jr., Hubner, K. F., Bai, B., Cannon, R. L., & Hutson, R. K. (2008). Abnormal connectivity in the posterior cingulate and hippocampus in early Alzheimer's disease and mild cognitive impairment. *Alzheimer's & Dementia, 4*(4), 265–270. https://doi.org/10.1016/j.jalz.2008.04.006

Received: August 26, 2025
Accepted: October 1, 2025
Published: March 31, 2026